



Technical Support Document

Photochemical Modeling for the Louisiana 8-Hour Ozone State Implementation Plan

Prepared for:
Air Permits Division
Louisiana Department of Environmental Quality
602 North Fifth Street
Baton Rouge, Louisiana 70802

Prepared by:
ENVIRON International Corporation
773 San Marin Drive, Suite 2115
Novato, California, 94998

and

Eastern Research Group, Inc.
10860 Gold Center Drive, Suite 275
Rancho Cordova, CA 95670

August 2013
06-26427



CONTENTS

EXECUTIVE SUMMARY	1
Overview of Modeling Approach	1
Modeled Attainment Test Results	3
1.0 INTRODUCTION	7
1.1 Study Background.....	7
1.1.1 The Ozone NAAQS	7
1.1.2 Recent Ozone History in Louisiana	8
1.2 Overview of Modeling Approach	9
2.0 EPISODE SELECTION	12
2.1 Decadal Trends Analysis	13
2.2 2008 Ozone Season	15
2.3 2009 Ozone Season	19
2.4 2010 Ozone Season	22
2.5 Final Consideration and Selection	26
3.0 METEOROLOGICAL MODELING EVALUATION.....	28
3.1 Wind speed.....	29
3.2 Wind Direction.....	35
3.3 Temperature.....	39
3.4 Precipitation	43
3.5 Summary.....	46
4.0 PHOTOCHEMICAL MODEL INPUTS	47
4.1 Meteorology	47
4.2 Landuse.....	50
4.3 Albedo-Haze-Ozone.....	55
4.4 Clear-Sky Photolysis Rates.....	55
4.5 Initial and Boundary Conditions	55
5.0 DEVELOPMENT OF 2010 BASE YEAR EMISSIONS	56
5.1 Introduction.....	56
5.2 Emissions in Louisiana	56

5.2.1	Area Sources	59
5.2.2	On-Road Mobile Sources	60
5.2.3	Off-Road Sources	67
5.2.4	Commercial Marine Vessels: Shipping Channels and Ports.....	68
5.2.5	Port Fourchon	70
5.2.6	Haynesville Shale	71
5.3	Gulf Sources.....	72
5.4	Anthropogenic Emissions Outside of Louisiana	73
5.5	Biogenic Emissions	74
5.5.1	MEGAN Processing.....	74
5.5.2	BEIS Processing	75
5.6	Wildland, Agricultural, and Prescribed Fires.....	76
5.7	Summary of 2010 Louisiana Emissions	76
6.0	BASE YEAR MODEL PERFORMANCE EVALUATION	82
6.1	Overview and Context	82
6.1.1	Evaluation Datasets	83
6.1.2	Model Configuration.....	83
6.2	Initial CAMx Run	84
6.3	Diagnostic Sensitivity Testing (Phase 1)	98
6.4	Evaluation of Ozone Precursors	99
6.5	Additional Sensitivity Testing (Phase 2)	107
6.6	Final Base Year CAMx Run.....	111
6.6.1	Regional Ozone Performance	121
7.0	2017 FUTURE YEAR OZONE PROJECTION	125
7.1	Development of Future Year Emissions	125
7.1.1	Emissions in Louisiana.....	125
7.1.2	Gulf Sources	130
7.1.3	Future Emissions Outside of Louisiana	131
7.1.4	2017 Emissions Summary	131
7.2	Ozone Modeling and Attainment Test	137
7.2.1	Summary of the MATS Technique	137
7.2.2	2017 DV Projection Results.....	139
7.2.3	2017 Sensitivity Tests.....	139

8.0 REFERENCES 146
TABLES

Table S-1. Base year DM8O ₃ design values at each active monitoring site in Louisiana for the 2010-2012 average and the 2017 projection. Values exceeding the current 75 ppb ozone NAAQS are highlighted in red. Blank entries indicate insufficient data from which to calculate the base year DV.....	5
Table 2-1. 2008 ozone observation statistics.	18
Table 2-2. Total number of 75 ppb exceedances in 2008 by region.	18
Table 2-3. 2009 ozone observation statistics.	22
Table 2-4. Total number of 75 ppb exceedances in 2009 by region.	22
Table 2-5. 2010 ozone observation statistics.	25
Table 2-6. Total number of 75 ppb exceedances in 2010 by region.	25
Table 2-7. August-October 2010 ozone observation statistics.....	25
Table 2-8. Total number of 75 ppb exceedances in August-October 2010 by region.....	26
Table 2-9. Summary of the number of 75 ppb exceedances during four potential modeling periods, by region (extracted from Tables 1 through 8).....	26
Table 2-10. Summary of number of days during five potential modeling periods when daily 8-hour ozone exceeded 60, 65, 70, and 75 ppb at each monitoring site in the Baton Rouge nonattainment area.....	27
Table 4-1. CAMx and WRF vertical layer structures.	49
Table 4-2. CAMx landuse categories for the Zhang dry deposition scheme.	51
Table 4-3. NALC LULC classification.	52
Table 4-4. LULC mapping between the 29 NALC categories and the 26 CAMx categories.	53
Table 5-1. Spatial surrogate codes developed for Louisiana emissions processing.....	58
Table 5-2. Representative Louisiana parish groups for MOVES model runs.....	61
Table 5-3. Spatial surrogates used in CONCEPT MV processing.....	63
Table 5-4. Louisiana average vehicle speeds.	65
Table 5-5. Parishes assigned 7.8 RVP for episode days September 1- 15, 2010.	67
Table 5-6. Principal Ports Commodity Tonnage by year.....	69

Table 5-7. Summary of 2010 Louisiana emissions (tons/day) for typical September weekday.	78
Table 6-1. Phase 1 diagnostic sensitivity tests performed on the CAMx 2010 base year simulation.....	98
Table 6-2. September and October averages of 6-9 AM observed and simulated NO _x , VOC, and VOC:NO _x ratio at four PAMS sites in Baton Rouge. VOC:NO _x ratios are colored according to VOC-limited (blue), NO _x -limited (red), and transition (purple) conditions.	104
Table 6-3. Phase 2 diagnostic sensitivity tests performed on the CAMx 2010 base year simulation.....	108
Table 7-1. Louisiana 2015 CAIR Program annual NO _x allocations.....	126
Table 7-2. Louisiana Regional Labor Market Areas (RLMAs)	128
Table 7-3. Summary of 2017 Louisiana emissions (tons/day) for typical September weekday.	132
Table 7-4. Percent change in Louisiana emissions from 2010 to 2017. Empty entries indicate no emissions were reported or estimated in 2010 and 2017.....	134
Table 7-5. Base year DM8O ₃ design values at each active monitoring site in Louisiana for the 2010-2012 average and the 2017 projection. Values exceeding the current 75 ppb ozone NAAQS are highlighted in red. Blank entries indicate insufficient data from which to calculate the base year DV.....	140
Table 7-6. Base year DM8O ₃ design values at each active monitoring site in Louisiana for the 2010-2012 average and the 2017 projection in response to an additional 30% across-the-board anthropogenic NO _x reduction in Louisiana. Values exceeding the current 75 ppb ozone NAAQS are highlighted in red. Blank entries indicate insufficient data from which to calculate the base year DV.	142
Table 7-7. Base year DM8O ₃ design values at each active monitoring site in Louisiana for the 2010-2012 average and the 2017 projection in response to an additional 30% across-the-board anthropogenic VOC reduction in Louisiana. Values exceeding the current 75 ppb ozone NAAQS are highlighted in red. Blank entries indicate insufficient data from which to calculate the base year DV.	144

FIGURES

Figure S-1. MATS-derived 2017 DM8O₃ design value projection from the 2010-2012 average design value for un-monitored areas in Louisiana.....6

Figure 1-1. Ranked monitor design values in Louisiana based on 2010-2012 measurement data.....9

Figure 2-1. Location of ozone monitoring sites in Louisiana, color coded by region.....13

Figure 2-2. Decadal trends (2000-2011) in site-peak and site-average annual 4th highest 8-hour ozone concentration in Baton Rouge, Lake Charles, Shreveport, and New Orleans.14

Figure 2-3. Decadal trends (2000-2011) in annual 4th highest 8-hour ozone concentration at five individual sites throughout Louisiana.15

Figure 2-4. Time series of the highest observed 8-hour ozone (top) and number of ozone sites above selected thresholds (bottom) in Louisiana in 2008.....16

Figure 2-5. Time series of the highest observed 8-hour ozone (top) and number of ozone sites above selected thresholds (bottom) in Baton Rouge in 2008.....17

Figure 2-6. Time series of the highest observed 8-hour ozone (top) and number of ozone sites above selected thresholds (bottom) in Louisiana in 2009.....20

Figure 2-7. Time series of the highest observed 8-hour ozone (top) and number of ozone sites above selected thresholds (bottom) in Baton Rouge in 2009.....21

Figure 2-8. Time series of the highest observed 8-hour ozone (top) and number of ozone sites above selected thresholds (bottom) in Louisiana in 2010.....23

Figure 2-9. Time series of the highest observed 8-hour ozone (top) and number of ozone sites above selected thresholds (bottom) in Baton Rouge in 2010.....24

Figure 3-1. Meteorology stations in Louisiana with the north and south sites colored in blue and red, respectively.....28

Figure 3-2. Hourly predicted (blue) and observed (black) wind speed averaged over all sites in northern Louisiana for August (top), September (middle) and October (bottom).29

Figure 3-3. Hourly wind speed bias over all sites in northern Louisiana for August (top), September (middle) and October (bottom).....30

Figure 3-4. Time series of hourly predicted (red) and observed (black) wind speeds averaged over all sites in southern Louisiana for August (top), September (middle) and October (bottom).....31

Figure 3-5. Time series of hourly wind speed bias over all sites in southern Louisiana for August (top), September (middle) and October (bottom).....32

Figure 3-6. Scatter plots of hourly predicted and observed wind speeds on high ozone dates during September (left) and October (right) for northern Louisiana (top) and southern Louisiana (bottom). Red circles represent daytime hours (8 AM – 6 PM CST), blue represents nighttime hours (7 PM to 7 AM). The solid black diagonal line is the 1:1 perfect correlation line; the two black dashed lines represent the ± 2 m/s bias envelope. Statistics show the regression line and the fraction of hours when the bias is between ± 0.5 , 1, and 2 m/s.33

Figure 3-7. Soccer goal plot of daily wind speed statistics. Red circles highlight the high ozone dates.34

Figure 3-8. Hourly predicted (blue) and observed (black) wind direction averaged over all sites in northern Louisiana for August (top), September (middle) and October (bottom).....35

Figure 3-9. Hourly predicted (red) and observed (black) wind direction averaged over all sites in southern Louisiana for August (top), September (middle) and October (bottom).....36

Figure 3-10. Scatter plots of hourly predicted and observed wind direction on high ozone dates during September (left) and October (right) for northern Louisiana (top) and southern Louisiana (bottom). Red circles represent daytime hours (8 AM – 6 PM CST), blue represents nighttime hours (7 PM to 7 AM). The solid black diagonal line is the 1:1 perfect correlation line; the two black dashed lines represent the ± 30 degree bias envelope. Statistics show the regression line and the fraction of hours when the bias is between ± 10 , 20, and 30 degrees.....37

Figure 3-11. Soccer goal plots of daily wind direction statistics. Red circles highlight the high ozone dates.38

Figure 3-12. Hourly predicted (blue) and observed (black) temperature averaged over all sites in northern Louisiana for August (top), September (middle) and October (bottom).....39

Figure 3-13. Hourly predicted (red) and observed (black) temperature averaged over all sites in southern Louisiana for August (top), September (middle) and October (bottom).....40

Figure 3-14. Scatter plots of hourly predicted and observed temperature on high ozone dates during September (left) and October (right) for northern Louisiana (top) and southern Louisiana (bottom). Red circles represent daytime hours (8 AM – 6 PM CST), blue represents nighttime hours (7 PM to 7 AM). The solid black diagonal line is the

1:1 perfect correlation line; the two black dashed lines represent the ± 2 K bias envelope. Statistics show the regression line and the fraction of hours when the bias is between ± 0.5 , 1, and 2 K.41

Figure 3-15. Soccer goal plots of daily temperature bias and error. Red circles highlight the high ozone dates.42

Figure 3-16. Observed (left) and predicted (right) 24-hour precipitation ending at 6 AM CST on September 13 (top) and 14 (bottom).43

Figure 3-17. Observed (left) and predicted (right) 24-hour precipitation ending at 6 AM CST on September 16 (top) and 17 (bottom).44

Figure 3-18. Daily observed (left) and predicted (right) precipitation on selected episode dates (October 24, 27, and 28).45

Figure 4-1. Map of CAMx and WRF modeling domains.48

Figure 4-2. Dominant landuse type in each grid cell of the 4 km CAMx domain.54

Figure 5-1. Monthly temporal profiles by roadway type.64

Figure 5-2. Day of week temporal profiles by roadway type.64

Figure 5-3. Hourly temporal profiles for all roadways on weekdays and weekends.65

Figure 5-4. Louisiana on-road NO emissions (mol/h) during 8-9 AM LST September 1, 2010.66

Figure 5-5. Louisiana on-road alkane (PAR) emissions (mol/h) during 8-9 AM LST September 1, 2010.66

Figure 5-6. 24-hour commercial marine shipping NOx emissions at Louisiana deep draft ports and along RSV shipping lanes.70

Figure 5-7. Table 2.1 from the Port Fourchon Ozone Day Port-Related Emissions Inventory Study (Starcrest and LSU, 2010).71

Figure 5-8. Port Fourchon with 4 km grid overlay.71

Figure 5-9. FINN-based fire NOx emissions for September and October 2010.77

Figure 5-10. Spatial distribution of total (anthropogenic and biogenic) weekday surface NOx emissions (tons/day) in 2010.80

Figure 5-11. Spatial distribution of total weekday surface CO emissions (tons/day) in 2010.80

Figure 5-12. Spatial distribution of total (anthropogenic and biogenic) weekday surface VOC emissions (tons/day) in 2010.81

Figure 6-1. Spatial distribution of predicted MDA8 ozone (ppb) from the initial base year run on days exceeding the 2008 ozone NAAQS in Louisiana. Plots are shown for the entire 4 km modeling grid (left) and for south-

central Louisiana focusing on Baton Rouge, with observed MDA8
ozone overlaid at monitor locations (right).85

Figure 6-1 (continued).86

Figure 6-1 (continued).87

Figure 6-1 (continued).88

Figure 6-1 (concluded).89

Figure 6-2. Daily statistical performance for the initial base year run at all Baton
Rouge monitoring sites and for all hours when observed ozone was
greater than 40 ppb, for September (left) and October (right), 2010.
Top row: maximum daily peak 1-hour observed ozone (red) and paired
simulated peak at the same site (blue). Middle row: daily mean
normalized bias (bars) with $\pm 15\%$ bias highlighted (red lines). Bottom
row: daily mean normalized gross error (bars) with 35% error
highlighted (red lines).90

Figure 6-3. “Goal” plots of daily normalized bias and error from the initial base year
run in Baton Rouge for September (left) and October (right). The blue
goal denotes statistics within the 1-hour performance benchmarks.
Red points are the high ozone days shown in Figure 6-1.91

Figure 6-4. “Goal” plots of daily normalized bias and error from the initial base year
run in New Orleans for September (left) and October (right). The blue
goal denotes statistics within the 1-hour performance benchmarks.
Red points are the high ozone days.91

Figure 6-5. “Goal” plots of daily normalized bias and error from the initial base year
run in Shreveport for September (left) and October (right). The blue
goal denotes statistics within the 1-hour performance benchmarks.
Red points are the high ozone days.92

Figure 6-6. “Goal” plots of daily normalized bias and error from the initial base year
run in Lake Charles for September (left) and October (right). The blue
goal denotes statistics within the 1-hour performance benchmarks.
Red points are the high ozone days.92

Figure 6-7. Hourly time series of observed (blue dots) and predicted (solid line)
ozone at the LSU monitoring site during September (top) and October
(bottom). Grey shading indicates the range of predicted ozone among
the nine grid cells surrounding the monitor.94

Figure 6-8. Hourly time series of observed (blue dots) and predicted (solid line) NOx
at the LSU monitoring site during September (top) and October
(bottom). Grey shading indicates the range of predicted NOx among
the nine grid cells surrounding the monitor.94

Figure 6-9. Hourly time series of observed (blue dots) and predicted (solid line) ozone at the Dutchtown monitoring site during September (top) and October (bottom). Grey shading indicates the range of predicted ozone among the nine grid cells surrounding the monitor.95

Figure 6-10. Hourly time series of observed (blue dots) and predicted (solid line) NOx at the Dutchtown monitoring site during September (top) and October (bottom). Grey shading indicates the range of predicted NOx among the nine grid cells surrounding the monitor.95

Figure 6-11. Hourly time series of observed (blue dots) and predicted (solid line) ozone at the Pride monitoring site during September (top) and October (bottom). Grey shading indicates the range of predicted ozone among the nine grid cells surrounding the monitor.96

Figure 6-12. Hourly time series of observed (blue dots) and predicted (solid line) NOx at the Pride monitoring site during September (top) and October (bottom). Grey shading indicates the range of predicted NOx among the nine grid cells surrounding the monitor.96

Figure 6-13. WRF performance for wind direction against observations in southern Louisiana in September (left) and October (right). Figure is duplicated from Figure 3-10.....97

Figure 6-14. WRF performance for temperature against observations in southern Louisiana in September (left) and October (right). Figure is duplicated from Figure 3-14.....97

Figure 6-15. Top row: Spatial distribution of predicted MDA8 ozone (ppb) from Run 10 on September 14. Plots are shown for the entire 4 km modeling grid (left) and for south-central Louisiana focusing on Baton Rouge, with observed MDA8 ozone overlaid at monitor locations (right). Bottom row: Spatial distribution of differences (Run 10 – Run 1) in MDA8 on the 4 km modeling grid (left) and over south-central Louisiana (right).....100

Figure 6-16. “Goal” plots of daily normalized bias and error from Run 10 in Baton Rouge for September (left) and October (right). The blue goal denotes statistics within the 1-hour performance benchmarks. Red points are the high ozone days shown in Figure 6-1.....101

Figure 6-17. “Goal” plots of daily normalized bias and error from Run 10 in New Orleans for September (left) and October (right). The blue goal denotes statistics within the 1-hour performance benchmarks. Red points are the high ozone days shown in Figure 6-1.101

Figure 6-18. “Goal” plots of daily normalized bias and error from Run 10 in Shreveport for September (left) and October (right). The blue goal

denotes statistics within the 1-hour performance benchmarks. Red points are the high ozone days shown in Figure 6-1.102

Figure 6-19. “Goal” plots of daily normalized bias and error from Run 10 in Lake Charles for September (left) and October (right). The blue goal denotes statistics within the 1-hour performance benchmarks. Red points are the high ozone days shown in Figure 6-1.102

Figure 6-20. Location of AQS monitoring sites in the Baton Rouge area (stars). Highlighted are four co-located PAMS sites measuring 3-hour VOC samples every few days.103

Figure 6-21. Comparison of 6-9 AM observed (blue) and simulated (red) CB05 VOCs at four PAMS sites in Baton Rouge on September 14, 2010. Plots are annotated with 6-9 AM observed/predicted NOx and VOC:NOx ratio.105

Figure 6-22. Comparison of 6-9 AM observed (blue) and simulated (red) relative contributions of CB05 VOCs to total VOC at four PAMS sites in Baton Rouge on September 14, 2010.....105

Figure 6-23. Comparison of 6-9 AM observed (blue) and simulated (red) CB05 VOCs at four PAMS sites in Baton Rouge on October 23, 2010. Plots are annotated with 6-9 AM observed/predicted NOx and VOC:NOx ratio.106

Figure 6-24. Comparison of 6-9 AM observed (blue) and simulated (red) relative contributions of CB05 VOCs to total VOC at four PAMS sites in Baton Rouge on October 23, 2010.106

Figure 6-25. Midday (12-3 PM) observed and predicted (Run 10) isoprene concentrations at the Capitol PAMS site on sampling days throughout September and October 2010.....108

Figure 6-26. Daily total isoprene emissions across the entire 4 km modeling grid estimated by MEGAN and BEIS for each day of August through October 2010.....109

Figure 6-27. Top row: Spatial distribution of predicted MDA8 ozone (ppb) from Run 11 on September 14. Plots are shown for the entire 4 km modeling grid (left) and for south-central Louisiana focusing on Baton Rouge, with observed MDA8 ozone overlaid at monitor locations (right). Bottom row: Spatial distribution of differences (Run 11 – Run 10) in MDA8 on the 4 km modeling grid (left) and over south-central Louisiana (right).....110

Figure 6-28. Top row: Spatial distribution of predicted MDA8 ozone (ppb) from Run 15 on September 14. Plots are shown for the entire 4 km modeling grid (left) and for south-central Louisiana focusing on Baton Rouge, with observed MDA8 ozone overlaid at monitor locations (right). Bottom row: Spatial distribution of differences (Run 15 – Run 11) in

MDA8 on the 4 km modeling grid (left) and over south-central Louisiana (right).....111

Figure 6-29. Spatial distribution of predicted MDA8 ozone (ppb) from the final base year run on days exceeding the 2008 ozone NAAQS in Louisiana. Plots are shown for the entire 4 km modeling grid (left) and for south-central Louisiana focusing on Baton Rouge, with observed MDA8 ozone overlaid at monitor locations (right).113

Figure 6-29 (continued).114

Figure 6-29 (continued).115

Figure 6-29 (continued).116

Figure 6-29 (concluded).117

Figure 6-30. Daily statistical performance for the final base year run at all Baton Rouge monitoring sites and for all hours when observed ozone was greater than 40 ppb, for September (left) and October (right), 2010. Top row: maximum daily peak 1-hour observed ozone (red) and paired simulated peak at the same site (blue). Middle row: daily mean normalized bias (bars) with $\pm 15\%$ bias highlighted (red lines). Bottom row: daily mean normalized gross error (bars) with 35% error highlighted (red lines).118

Figure 6-31. “Goal” plots of daily normalized bias and error from the final base year run in Baton Rouge for September (left) and October (right). The blue goal denotes statistics within the 1-hour performance benchmarks. Red points are the high ozone days shown in Figure 6-1.119

Figure 6-32. “Goal” plots of daily normalized bias and error from the final base year run in New Orleans for September (left) and October (right). The blue goal denotes statistics within the 1-hour performance benchmarks. Red points are the high ozone days.119

Figure 6-33. “Goal” plots of daily normalized bias and error from the final base year run in Shreveport for September (left) and October (right). The blue goal denotes statistics within the 1-hour performance benchmarks. Red points are the high ozone days.120

Figure 6-34. “Goal” plots of daily normalized bias and error from the final base year run in Lake Charles for September (left) and October (right). The blue goal denotes statistics within the 1-hour performance benchmarks. Red points are the high ozone days.120

Figure 6-35. Hourly time series of observed (blue dots) and predicted (solid red line) ozone from the final base year run at the LSU monitoring site during September (top) and October (bottom).122

Figure 6-36. Hourly time series of observed (blue dots) and predicted (solid red line) ozone from the final base year run at the Dutchtown monitoring site during September (top) and October (bottom).122

Figure 6-37. Hourly time series of observed (blue dots) and predicted (solid red line) ozone from the final base year run at the Pride monitoring site during September (top) and October (bottom).123

Figure 6-38. Locations of regional monitoring sites in areas surrounding Louisiana, relative to the CAMx modeling grid system.....123

Figure 6-39. Daily statistical performance for the final base year run at all western regional monitoring sites and for all hours when observed ozone was greater than 40 ppb, for September (left) and October (right), 2010. Top row: daily mean normalized bias (bars) with $\pm 15\%$ bias highlighted (red lines). Bottom row: daily mean normalized gross error (bars) with 35% error highlighted (red lines).124

Figure 6-40. As in Figure 6-42, but at all northern regional monitoring sites.124

Figure 6-41. As in Figure 6-42, but at all eastern regional monitoring sites.124

Figure 7-1. Spatial distribution of 2017 total (anthropogenic and biogenic) surface NO_x emissions (tons/day).136

Figure 7-2. Spatial distribution of 2017 total surface CO emissions (tons/day).....136

Figure 7-3. Spatial distribution of 2017 total (anthropogenic and biogenic) surface VOC emissions (tons/day).137

Figure 7-4. MATS-derived 2017 DM8O₃ design value projection from the 2010-2012 average design value for un-monitored areas in Louisiana.141

Figure 7-5. MATS-derived 2017 DM8O₃ design value projection from the 2010-2012 average design value for un-monitored areas in Louisiana; response to an additional 30% across-the-board anthropogenic NO_x reduction in Louisiana.....143

Figure 7-6. MATS-derived 2017 DM8O₃ design value projection from the 2010-2012 average design value for un-monitored areas in Louisiana; response to an additional 30% across-the-board anthropogenic VOC reduction in Louisiana.....145

EXECUTIVE SUMMARY

This Technical Support Document (TSD) describes the photochemical modeling conducted to support an attainment demonstration of the 2008 8-hour ozone National Ambient Air Quality Standard (NAAQS) in the Baton Rouge nonattainment area and other areas of Louisiana. The attainment demonstration is a central component of the Louisiana State Implementation Plan (SIP) that will specifically establish strategies to attain the 2008 ozone standard. The modeling program was directed by the Louisiana Department of Environmental Quality (LDEQ), Office of Environmental Services, Air Permits Division. The technical work was conducted by the contractor team of ENVIRON International Corporation (ENVIRON) and Eastern Research Group, Inc. (ERG). The US Environmental Protection Agency (EPA), Region 6, is responsible for reviewing and approving all SIPs submitted by the State of Louisiana.

The goal of this study was to develop the photochemical modeling tools and related databases needed to reliably simulate the complex interplay between meteorology, emissions, and ambient photochemistry during a recent 8-hour ozone exceedance period in the Baton Rouge area, to project those conditions to a future year, and to evaluate emissions reductions needed to reach attainment of the current ozone NAAQS. For nonattainment areas that are classified as “moderate”, the modeled attainment demonstration must show that 8-hour ozone design values at all monitoring sites in the nonattainment area are projected to be below the 2008 standard of 75 ppb by the end of 2018.

Several EPA-accepted modeling platforms and datasets were applied to address episodic-to-seasonal meteorology, emissions, and air quality during the selected modeling period of September-October 2010. Significant effort was directed towards the inclusion of the latest Louisiana state-wide emission inventories, and the leveraging of nationwide emission databases developed by the EPA, the National Center for Atmospheric Research (NCAR), and the Bureau of Ocean Energy and Management (BOEM). A modeling protocol document was developed previously (ENVIRON and ERG, 2012) following the latest modeling guidance published by the EPA related to 8-hour ozone attainment demonstrations (EPA, 2007).

Overview of Modeling Approach

This study has built from previous attainment demonstration modeling conducted for the same area that addressed the requirements of the 1997 ozone NAAQS, but included appropriate deviations to account for new episodes, updated datasets, new modeling tools, and other recently identified issues. For continuity, the modeling system employed many of the same emissions and photochemical model components as the previous modeling effort. However, some newer state-of-the-science components were used. The modeling system included:

- The Weather Research and Forecasting (WRF) meteorological model;
- The Emissions Processing System, version 3 (EPS3);
- The Sparse Matrix Operating Kernel Emissions (SMOKE) processor, version 3.1;

- The Consolidated Community Emissions Processing Tool (CONCEPT) combined with the EPA Motor Vehicle Emissions Simulator (MOVES) emission factor model for on-road sources;
- EPA's National Mobile Inventory Model (NMIM) for non-road sources;
- The Model of Emissions of Gases and Aerosols from Nature (MEGAN) for biogenic emissions;
- EPA's Biogenic Emissions Inventory System (BEIS);
- The Fire Inventory from NCAR (FINN) for wildfires, and agricultural/prescribed burning;
- The Comprehensive Air quality Model with extensions (CAMx).

This modeling system was employed for an extended period during September and October 2010 when elevated ozone was monitored throughout Louisiana. The modeling domain consists of a two-way interactive nested grid system employing three grids with 36, 12, and 4 km grid resolution, similarly to the previous modeling. However, the projection parameters were changed to align with the standard projection defined by the regional planning organizations (RPOs), and the 36 km grid was expanded to match the RPO continental US (CONUS) domain. This maximized portability of previously or concurrently developed emission inventories and other datasets into this project. The CAMx vertical grid structure was defined on a subset of the WRF meteorological grid structure, extending from the surface to about 11 km altitude.

Other agencies and groups contributed to the datasets employed in this study. The Louisiana Department of Transportation and Development (LDOTD) and the Capitol Region Planning Commission (CRPC) provided datasets necessary for the development of Baton Rouge and State-wide on-road emission estimates. All meteorological modeling, biogenic modeling with BEIS, and processing of EPA anthropogenic emission datasets outside of Louisiana and the Gulf of Mexico were externally performed by Alpine Geophysics, LLC (Alpine), who operated under contract to the local industry coalition.

The WRF meteorological model was supplied with several terrestrial and meteorological databases available from NCAR. Standard meteorological analyses were used to define initial/boundary conditions and to provide for analysis nudging as part of WRF's Four Dimensional Data Assimilation (FDDA) package. Meteorological modeling was conducted on the 36/12/4 km nested grid system for the duration of the modeling period. Details of the WRF configuration and application are provided in a separate report prepared by Alpine (2012). ENVIRON performed a focused evaluation of WRF's accuracy in replicating episodic weather conditions in the State of Louisiana.

Base year (2010) and projected future year (2017) model-ready emissions of ozone precursors were developed for all three modeling domains spanning the entire modeling period. The EPS3 and CONCEPT/MOVES emissions processors/models were used to translate raw stationary, non-road, and on-road emission inventories for the State of Louisiana to temporally allocated, speciated, spatially allocated input files in formats compatible with CAMx. The latest data for Louisiana stationary source emissions (from LDEQ) and on-road mobile source activity, fleet

activity, and fuel parameters (from LDOTD/CRPC) were accessed. Several datasets were used to generate CAMx-ready emissions outside of Louisiana: (1) anthropogenic inventories for the US, Canada, and Mexico developed by the EPA (processed by Alpine); (2) Gulf-wide oil and gas development and commercial shipping inventories developed by the BOEM; and (3) wildland, agricultural and prescribed fire emissions developed by NCAR. The MEGAN biogenic model was initially used to generate biogenic emissions on all three modeling grids using common North American vegetative distribution datasets. In response to model performance issues indicating over predictions of isoprene leading to over predictions of ozone, we ultimately switched to biogenic emissions generated by the EPA's BEIS model (processed by Alpine Geophysics) for final base and all future year modeling. Future year projections of US emissions considered growth, emission controls already on the books, and various other factors influencing emission rates to the extent possible. Natural emissions (biogenic and fires) were held constant between the base and future year scenarios.

Ancillary photochemical modeling inputs such as initial/boundary conditions, landuse, and photolysis rates were developed using appropriate contemporary data and techniques. Chemical boundary conditions were generated from archived 2010 global modeling products from NCAR, and used for both base and future year CAMx simulations. The latest version of CAMx was run for the entire modeling period using the Carbon Bond 6 (CB6) photochemical mechanism and several new state-of-the-science algorithms. Modifications to the initial configuration were made according to the model performance evaluation process and sensitivity testing. Final base and all future year modeling employed the Carbon Bond 2005 (CB05) photochemical mechanism.

An extensive model performance evaluation of the base year modeling was conducted for ozone and precursor predictions, to the extent possible given available ambient observational data. Graphical and statistical performance was gauged for ozone, NO_x, and VOC using several techniques following EPA guidance. Diagnostic and sensitivity testing were conducted to understand model sensitivity and to obtain the best performance possible for the correct reasons. Eighteen different CAMx simulations were conducted with various emission inputs, vertical mixing characterization, chemistry mechanisms and inputs, and deposition rates. These tests culminated in improved model performance in replicating measurements throughout Louisiana, with the final CAMx base year run achieving statistical benchmarks for a well-performing model.

Future year modeling was conducted for the year 2017, to establish projections one year prior to the attainment year. The EPA model attainment test procedures were utilized to determine if the future year predictions attain the 2008 8-hour ozone standard. Future emission sensitivity tests were modeled and processed through the attainment test methodology to evaluate ozone response.

Modeled Attainment Test Results

CAMx was run for the September-October 2010 modeling period using the final base year model configuration, but exchanging the 2010 emissions with projected 2017 future year

emissions. Predicted daily maximum 8-hour ozone (DM8O_3) concentrations throughout the September-October modeling period were extracted from the CAMx results. These modeled concentrations were supplied to the EPA Modeled Attainment Test Software (MATS) tool, which tabulated the change in DM8O_3 at each site, determined site-specific relative response factors (RRF) averaged over all high ozone days during the modeling period, and applied the RRFs to current design values (DV) to estimate the 2017 DV at each site. MATS was also used to perform an “unmonitored area analysis” by extrapolating site-specific future year DVs to the entire modeling grid using modeled spatial gradients to help form the resulting DV surface. Following EPA (2007) guidance, we used MATS to calculate projections from the 2010-2012 average DV.

Table S-1 presents the base year 2010-2012 average DVs at each active monitoring site in Louisiana and the corresponding 2017 future year DVs projected by MATS. Missing values in the table indicate insufficient observation data from which to calculate a valid base year DV. All DVs are projected to be below the 75 ppb ozone NAAQS in 2017.

Figure S-1 displays the 2017 unmonitored area calculation (projected from the 2010-2012 average DV) for the portion of the 4 km grid covering the State of Louisiana. DVs are projected to be below the 75 ppb NAAQS throughout the State. Areas contoured in white show locations where DVs are either estimated to be below 40 ppb, or are missing because they could not be extrapolated by MATS.

Two emission sensitivity tests were run for the 2017 future year to quantify effects from simple across-the-board reductions in Louisiana anthropogenic NO_x and VOC emissions. An arbitrary reduction of 30% was applied first to NO_x (no change to VOC) and then to VOC (no change to NO_x). All 2017 model-ready anthropogenic emissions in grid cells covering the State were scaled downward, including all low-level (gridded) sources and point sources. Emissions outside the State were not affected, nor were biogenic and fire sources throughout the 4 km grid.

These sensitivity tests indicated further ozone reductions by up to 10 ppb throughout the State. While both NO_x and VOC reductions are shown to be effective in reducing ozone throughout the State, ozone tends to be somewhat more responsive to NO_x reductions by typically 2-3 ppb. This effect could be more quantitatively analyzed through the use of CAMx probing tools, such as the Ozone Source Apportionment Tool (OSAT) or the Decoupled Direct Method (DDM) of sensitivity analysis.

Table S-1. Base year DM8O₃ design values at each active monitoring site in Louisiana for the 2010-2012 average and the 2017 projection. Values exceeding the current 75 ppb ozone NAAQS are highlighted in red. Blank entries indicate insufficient data from which to calculate the base year DV.

AIRS Site ID	Parish	Base Year	Future Year
		2010-12 DV	2017 DV
220050004	Ascension	76	70
220110002	Beauregard		
220150008	Bossier	77	68
220170001	Caddo	74	70
220190002	Calcasieu	74	68
220190008	Calcasieu	66	61
220190009	Calcasieu	73	67
220330003	E Baton Rouge	79	73
220330009	E Baton Rouge	75	69
220330013	E Baton Rouge	72	66
220331001	E Baton Rouge	72	66
220430001	Grant		
220470007	Iberville	71	64
220470009	Iberville	74	67
220470012	Iberville	75	68
220511001	Jefferson	75	68
220550005	Lafayette		
220550007	Lafayette	72	64
220570004	Lafourche	72	66
220630002	Livingston	75	69
220710012	Orleans	70	63
220730004	Ouachita	64	58
220770001	Pointe Coupee	75	70
220870002	St. Bernard		
220870009	St. Bernard	69	63
220890003	St. Charles	71	65
220930002	St. James	68	64
220950002	St. J. Baptist	74	69
221010003	St. Mary		
221030002	St. Tammany	74	65
221210001	W Baton Rouge	71	65

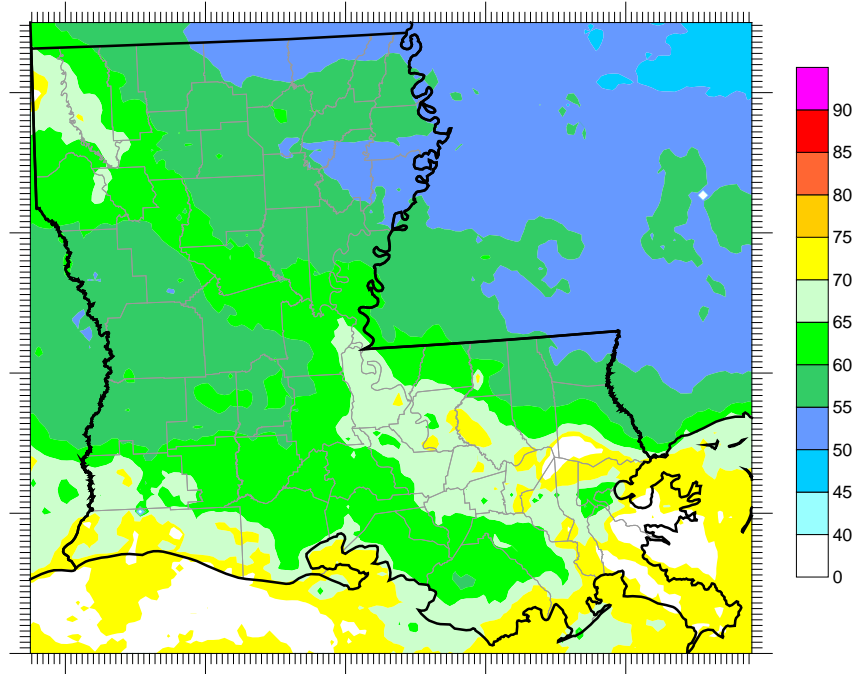


Figure S-1. MATS-derived 2017 DM8O₃ design value projection from the 2010-2012 average design value for un-monitored areas in Louisiana.

1.0 INTRODUCTION

This Technical Support Document (TSD) describes the photochemical modeling conducted to support an attainment demonstration of the 2008 8-hour ozone National Ambient Air Quality Standard (NAAQS) in the Baton Rouge nonattainment area and other areas of Louisiana. The attainment demonstration is a central component of the Louisiana State Implementation Plan (SIP) that will specifically establish strategies to attain the 2008 ozone standard. The modeling program was directed by the Louisiana Department of Environmental Quality (LDEQ), Office of Environmental Services, Air Permits Division. The technical work was conducted by the contractor team of ENVIRON International Corporation (ENVIRON) and Eastern Research Group, Inc. (ERG). The US Environmental Protection Agency (EPA), Region 6, is responsible for reviewing and approving all SIPs submitted by the State of Louisiana.

The goal of this study was to develop the photochemical modeling tools and related databases needed to reliably simulate the complex interplay between meteorology, emissions, and ambient photochemistry during a recent 8-hour ozone exceedance period in the Baton Rouge area, to project those conditions to a future year, and to evaluate emissions reductions needed to reach attainment of the current ozone NAAQS. For nonattainment areas that are classified as “moderate”, the modeled attainment demonstration must show that 8-hour ozone design values at all monitoring sites in the nonattainment area are projected to be below the 2008 standard of 75 ppb by the end of 2018.

Several EPA-accepted modeling platforms and datasets were applied to address episodic-to-seasonal meteorology, emissions, and air quality during the selected modeling period of September-October 2010. Significant effort was directed towards the inclusion of the latest Louisiana state-wide emission inventories, and the leveraging of nationwide emission databases developed by the EPA, the National Center for Atmospheric Research (NCAR), and the Bureau of Ocean Energy and Management (BOEM). A modeling protocol document was developed previously (ENVIRON and ERG, 2012) following the latest modeling guidance published by the EPA related to 8-hour ozone attainment demonstrations (EPA, 2007).

1.1 Study Background

1.1.1 The Ozone NAAQS

The EPA is required to consider revisions to the NAAQS every five years. The standard for each criteria pollutant comprises a primary value designed to protect public health, and a secondary value designed to protect public welfare. EPA promulgated the first 8-hour ozone NAAQS in 1997. The form of the standard is the three year running average of the annual fourth highest daily maximum 8-hour ozone concentration. This form establishes the yearly ozone “design value” (DV) for each individual monitor in the State. Design values exceeding the standard at any monitor result in a nonattainment designation for the area; the degree to which a monitor exceeds the standard determines the area’s classification (e.g., Marginal, Moderate, Serious, Severe, or Extreme). The 1997 primary and secondary 8-hour ozone standards were set at 0.08 ppm.

In March 2008, EPA lowered the 8-hour primary and secondary ozone NAAQS to 0.075 ppm. In January 2010, EPA announced that they were reconsidering a further reduction of the 2008 primary standard to within 0.060 – 0.070 ppm, while instituting a new secondary standard in the form of a seasonal (3 month) accumulation of ozone during daylight hours (8 AM – 8 PM) within 7-15 ppm-hrs. In September 2011, the Obama Administration directed EPA to withdraw the reconsideration and so the 2008 8-hour primary and secondary ozone NAAQS remains at 0.075 ppm.

The implementation schedule for the 2008 NAAQS calls for nonattainment area designations by mid-2012 based on monitoring data recorded in 2008-2010. The attainment year for marginal areas (Louisiana's highest nonattainment classification) is 2015. Marginal areas are not required to conduct modeling to demonstrate attainment, since EPA expects these areas to be able to attain the ozone NAAQS within three years of designation. During this time EPA is continuing to develop and implement federal rules that will reduce emissions from utilities, mobile sources, oil and gas source, and boilers/incinerators throughout the US. However, if nonattainment areas do not attain the ozone NAAQS by 2015 they will be bumped up to the moderate classification. In that case, modeling must be performed to demonstrate attainment by 2018.

In 2010 EPA initiated their next round of ozone NAAQS review. This is expected to result in a proposed new set of ozone NAAQS in 2014: a primary 8-hour ozone standard in the range of 0.060 – 0.070 ppm; and a secondary seasonal accumulated ozone standard of 7-15 ppm-hrs.

1.1.2 Recent Ozone History in Louisiana

Based on measured ozone data from 2001-2003, the EPA designated the five parishes comprising greater Baton Rouge (East Baton Rouge, West Baton Rouge, Livingston, Ascension, and Iberville) as a Marginal nonattainment area according to the 1997 8-hour ozone NAAQS. However, Baton Rouge experienced high ozone conditions as late as 2006 and therefore did not attain the 1997 standard by the Marginal attainment date of June 15, 2007. In response, EPA reclassified Baton Rouge as a Moderate nonattainment area with an attainment date of June 15, 2010.

Between 2007-2009, the LDEQ and its contractors developed a photochemical modeling system to support the attainment demonstration for the Baton Rouge Moderate-area ozone SIP. This modeling and related corroborative analyses showed that the area would reach attainment of the 1997 standard by the 2010 attainment date. Monitoring in Baton Rouge since 2006 has exhibited no exceedances of the 1997 standard, and thus in 2010 the LDEQ submitted an attainment reclassification request and maintenance plan to EPA Region 6 that included a TSD detailing the modeling demonstration (ENVIRON and ERG, 2009). On November 30, 2011, EPA took final action to redesignate Baton Rouge to attainment of the 1997 standard (Federal Register, 2011).

Based on a recent three year period of measured ozone data from 2008-2010, which constitutes the official period from which EPA has designated final nonattainment areas, only

one parish (East Baton Rouge) exceeded the 2008 standard of 75 ppb at the Marginal level (out of 18 monitored parishes in Louisiana). Figure 1-1 shows ranked design values from the most recent official three year data period (2010-2012).

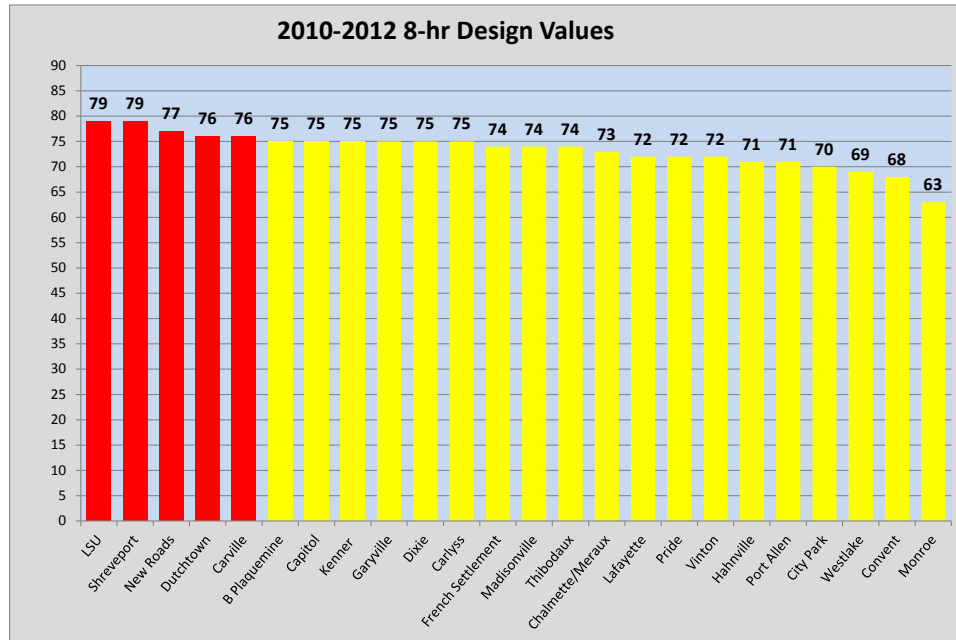


Figure 1-1. Ranked monitor design values in Louisiana based on 2010-2012 measurement data.

1.2 Overview of Modeling Approach

The goal of this study was to develop the photochemical modeling data bases and associated analysis tools needed to reliably simulate the processes responsible for ozone exceedances in the Baton Rouge nonattainment area and other areas throughout the State. It will culminate in the ozone attainment demonstration for the next 8-hour ozone SIP due in 2015. This study has built from previous attainment demonstration modeling conducted for the same area that addressed the requirements of the 1997 standard, but with appropriate deviations to account for new episodes, updated datasets, new modeling tools, and other recently identified issues.

The ENVIRON/ERG modeling team developed a Modeling Protocol document detailing the data, models, configurations, and analysis techniques to be employed in this project (ENVIRON and ERG, 2012). In particular, the Protocol outlined the rationale for model selection and grid configuration, and established the procedures for episode selection; such information is not repeated in this TSD. This section summarizes the technical approach and later chapters of this TSD provide further details.

For continuity, the modeling system employed many of the same emissions and photochemical model components documented in the 2009 TSD. However, some newer state-of-the-science components were used. The modeling system included:

- The Weather Research and Forecasting (WRF) meteorological model;
- The Emissions Processing System, version 3 (EPS3);
- The Sparse Matrix Operating Kernel Emissions (SMOKE) processor, version 3.1;
- The Consolidated Community Emissions Processing Tool (CONCEPT) combined with the EPA Motor Vehicle Emissions Simulator (MOVES) emission factor model for on-road sources;
- EPA's National Mobile Inventory Model (NMIM) for non-road sources;
- The Model of Emissions of Gases and Aerosols from Nature (MEGAN) for biogenic emissions;
- EPA's Biogenic Emissions Inventory System (BEIS);
- The Fire Inventory from NCAR (FINN) for wildfires, and agricultural/prescribed burning;
- The Comprehensive Air quality Model with extensions (CAMx).

This modeling system was employed for an extended period during September and October 2010 when elevated ozone was monitored throughout Louisiana. The modeling domain consists of a two-way interactive nested grid system employing three grids with 36, 12, and 4 km grid resolution, similarly to the previous modeling. However, the projection parameters were changed to align with the standard projection defined by the regional planning organizations (RPOs), and the 36 km grid was expanded to match the RPO continental US (CONUS) domain. This maximized portability of previously or concurrently developed emission inventories and other datasets into this project. The CAMx vertical grid structure was defined on a subset of the WRF meteorological grid structure, extending from the surface to about 11 km altitude.

Other agencies and groups contributed to the datasets employed in this study. The Louisiana Department of Transportation and Development (LDOTD) and the Capitol Region Planning Commission (CRPC) provided datasets necessary for the development of Baton Rouge and State-wide on-road emission estimates. All meteorological modeling, biogenic modeling with BEIS, and processing of EPA anthropogenic emission datasets outside of Louisiana and the Gulf of Mexico were externally performed by Alpine Geophysics, LLC (Alpine), who operated under contract to the local industry coalition.

The WRF meteorological model was supplied with several terrestrial and meteorological databases available from NCAR. Standard meteorological analyses were used to define initial/boundary conditions and to provide for analysis nudging as part of WRF's Four Dimensional Data Assimilation (FDDA) package. Meteorological modeling was conducted on the 36/12/4 km nested grid system for the duration of the modeling period. Details of the WRF configuration and application are provided in a separate report prepared by Alpine (2012).

ENVIRON performed a focused evaluation of WRF's accuracy in replicating episodic weather conditions in the State of Louisiana.

Base year (2010) and projected future year (2017) model-ready emissions of ozone precursors were developed for all three modeling domains spanning the entire modeling period. The EPS3 and CONCEPT/MOVES emissions processors/models were used to translate raw stationary, non-road, and on-road emission inventories for the State of Louisiana to temporally allocated, speciated, spatially allocated input files in formats compatible with CAMx. The latest data for Louisiana stationary source emissions (from LDEQ) and on-road mobile source activity, fleet activity, and fuel parameters (from LDOTD/CRPC) were accessed. Several datasets were used to generate CAMx-ready emissions outside of Louisiana: (1) anthropogenic inventories for the US, Canada, and Mexico developed by the EPA (processed by Alpine); (2) Gulf-wide oil and gas development and commercial shipping inventories developed by the BOEM; and (3) wildland, agricultural and prescribed fire emissions developed by NCAR. The MEGAN biogenic model was initially used to generate biogenic emissions on all three modeling grids using common North American vegetative distribution datasets. In response to model performance issues indicating over predictions of isoprene, we ultimately switched to biogenic emissions generated by the EPA's BEIS model (processed by Alpine Geophysics) for final base and all future year modeling. Future year projections of US emissions considered growth, emission controls already on the books, and various other factors influencing emission rates to the extent possible. Natural emissions were held constant between the base and future year scenarios.

Ancillary photochemical modeling inputs such as initial/boundary conditions, landuse, and photolysis rates were developed using appropriate contemporary data and techniques. Chemical boundary conditions were generated from archived 2010 global modeling products from NCAR, and used for both base and future year CAMx simulations.. The latest version of CAMx was run for the entire modeling period using the Carbon Bond 6 (CB6) photochemical mechanism and several new state-of-the-science algorithms. Modifications to the initial configuration were made according to the model performance evaluation process and sensitivity testing. Final base and all future year modeling employed the Carbon Bond 2005 (CB05) photochemical mechanism.

An extensive model performance evaluation of the base year modeling was conducted for ozone and precursor predictions, to the extent possible given available ambient observational data. Graphical and statistical performance was gauged using several techniques following EPA guidance. Diagnostic and sensitivity testing were conducted to understand model sensitivity and to obtain the best performance possible for the correct reasons.

Future year modeling was conducted for the year 2017, to establish projections one year prior to the attainment year. The EPA model attainment test procedures were utilized to determine if the future year predictions attain the 2008 8-hour ozone standard. Future emission sensitivity tests were modeled and processed through the attainment test methodology to evaluate ozone response.

2.0 EPISODE SELECTION

This section presents an evaluation of statewide ozone data between 2008 and 2010 from which to select a representative episode for photochemical modeling. Figure 2-1 shows the locations of the 26 observation sites in Louisiana, color-coded by region.

EPA (2007) has identified four primary episode selection criteria when choosing an episode for ozone SIP modeling:

- A variety of meteorological conditions should be covered, especially the types of meteorological conditions that produce 8-hour ozone exceedances in the area of interest;
- Choose episodes having days with monitored 8-hour daily maximum ozone concentrations close to the monitors' design values (DV);
- To the extent possible, the modeling database should include days for which extensive measurement data (i.e. beyond routine aerometric and emissions monitoring) are available; and
- Sufficient days should be available such that relative response factors (RRF) can be based on several (i.e., > 10) days, with at least 5 days being the absolute minimum.

Four secondary criteria should also be considered:

- Choose periods that have already been modeled;
- Choose periods that are drawn from the years upon which the current design values are based;
- Include weekend days among those chosen; and
- Choose modeling periods that meet as many episode selection criteria as possible in the maximum number of nonattainment areas as possible.

Ozone data were examined for three ozone seasons (April to October) between 2008 and 2010, from which new ozone attainment designations were established by EPA. If an entire ozone season were modeled, all of the criteria should be fulfilled as long as the season contained several 8-hour ozone exceedance events. The following conditions were considered to select the best period to model:

- The period from which the nonattainment designations are defined;
- A large number of exceedance days at all (or most) monitoring locations;
- A representative (non-extreme) spectrum of meteorological conditions that represent a range of transport patterns, high ozone periods, and clean out days;
- A representative (usual) pattern of anthropogenic activities not impacted by major planned or accidental events that effect population, traffic, or industrial/commercial activity.

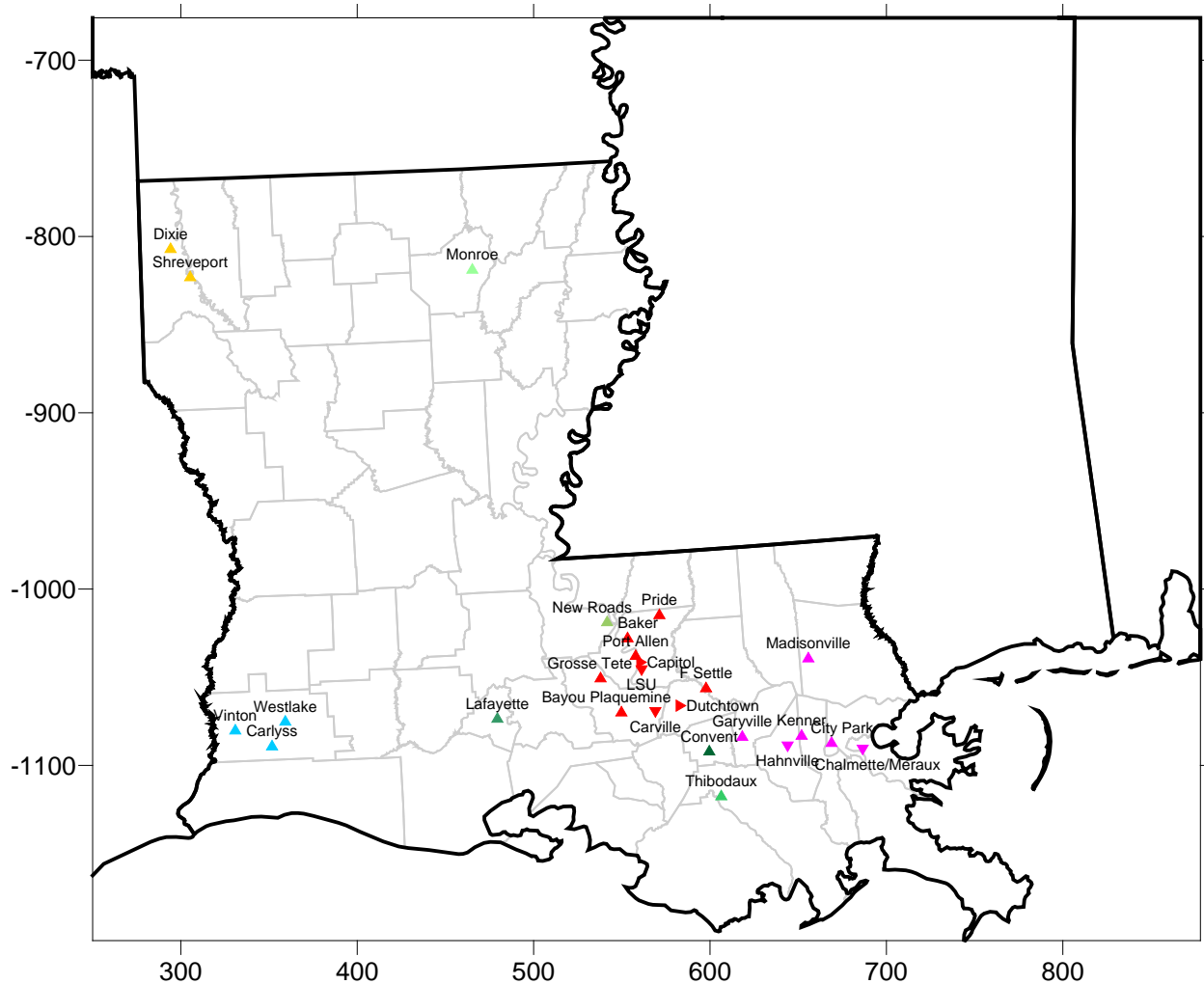


Figure 2-1. Location of ozone monitoring sites in Louisiana, color coded by region.

2.1 Decadal Trends Analysis

Figure 2-2 presents the 2000-2011 trends in annual 4th highest 8-hour ozone in the four regions of Louisiana with multiple monitoring sites (Baton Rouge, New Orleans, Shreveport, and Lake Charles). The figures present the trends for the peak site and for an average over all sites; a simple linear regression fit is also shown for both. In all four regions, the 4th highest ozone is trending downward at rates between -0.5 ppb/year (Shreveport) and -1.3 ppb/year (Baton Rouge). However, the most recent years show an uptick in peak ozone concentrations that reduce the gains seen between 2000 and 2008, especially in Shreveport.

Similar plots are shown in Figure 2-3, but for regions with just a single monitoring site. Four of five of these sites show similar and generally stronger downward trends, ranging from -0.8 ppb/year (Convent) to -1.7 ppb/year (Monroe). The site “New Roads” suggests a positive trend in peak ozone. Given that this site is just north of Baton Rouge (usually a downwind direction

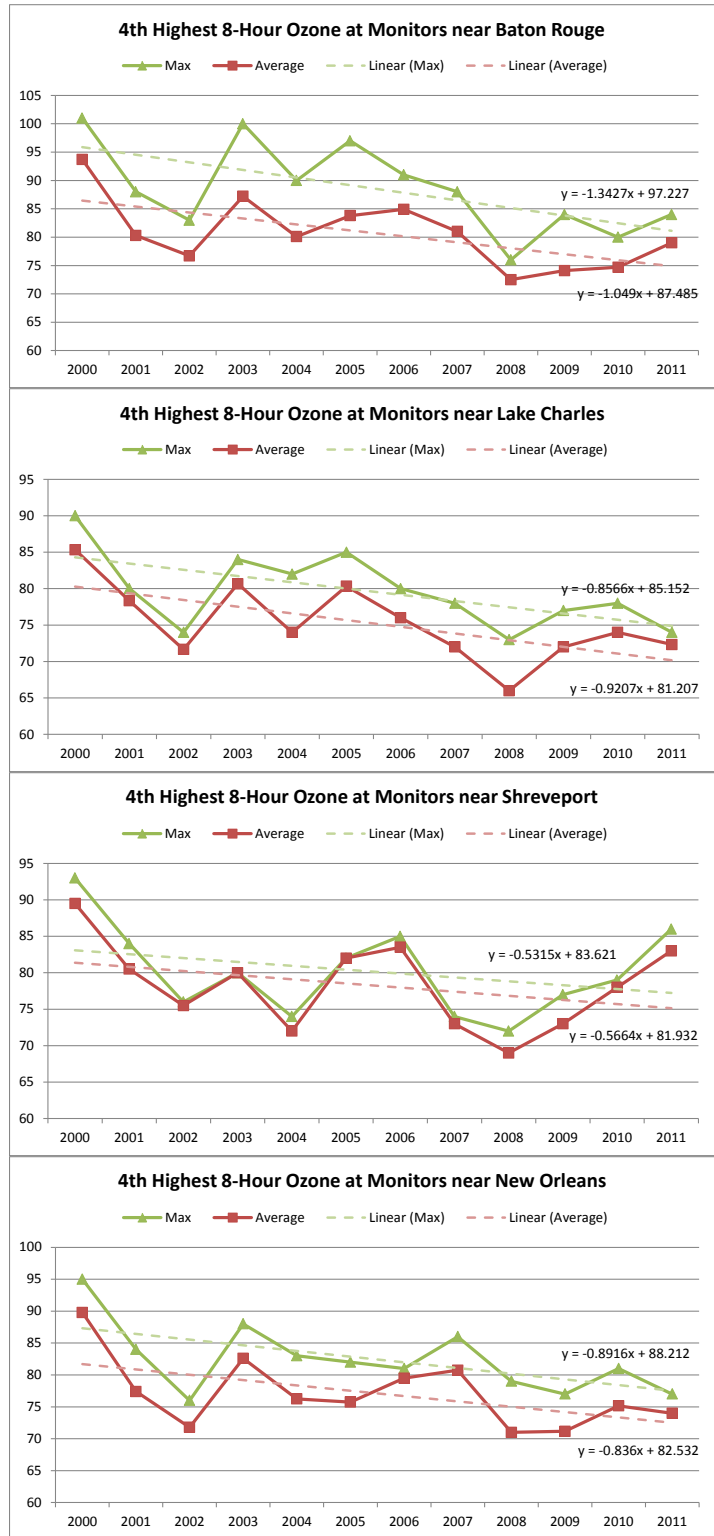


Figure 2-2. Decadal trends (2000-2011) in site-peak and site-average annual 4th highest 8-hour ozone concentration in Baton Rouge, Lake Charles, Shreveport, and New Orleans.



Figure 2-3. Decadal trends (2000-2011) in annual 4th highest 8-hour ozone concentration at five individual sites throughout Louisiana.

according to ozone episode climatology), it is possible that this site is measuring an increase in downwind ozone production from precursors originating in Baton Rouge. Larger reductions of industrial VOC emissions relative to urban NOx emissions would serve to slow urban ozone production, reduce peak ozone concentrations near Baton Rouge, and raise peak concentrations downwind.

2.2 2008 Ozone Season

In 2008 there were 24 active ozone monitors across Louisiana. Two time series are shown in Figure 2-4. The top displays the highest daily observed 8-hour ozone at any monitor in Louisiana for each date from April to October 2008. The dashed red line at 75 ppb denotes the current 8-hour ozone standard. The bottom plot shows the number of monitoring sites measuring at least 75, 70, 65, and 60 ppb on each date. Figure 2-5 shows similar time series for just the monitors in Baton Rouge. Table 2-1 summarizes the number of days and site-days when 8-hour ozone was above the same four thresholds throughout Louisiana and specifically

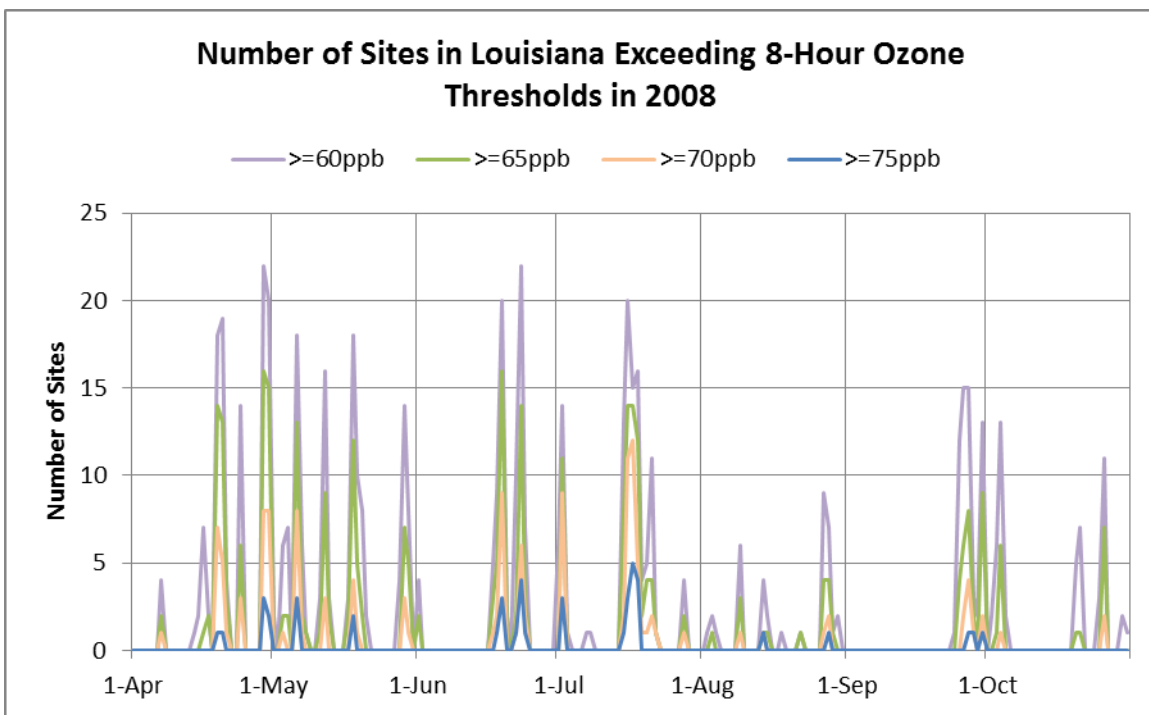
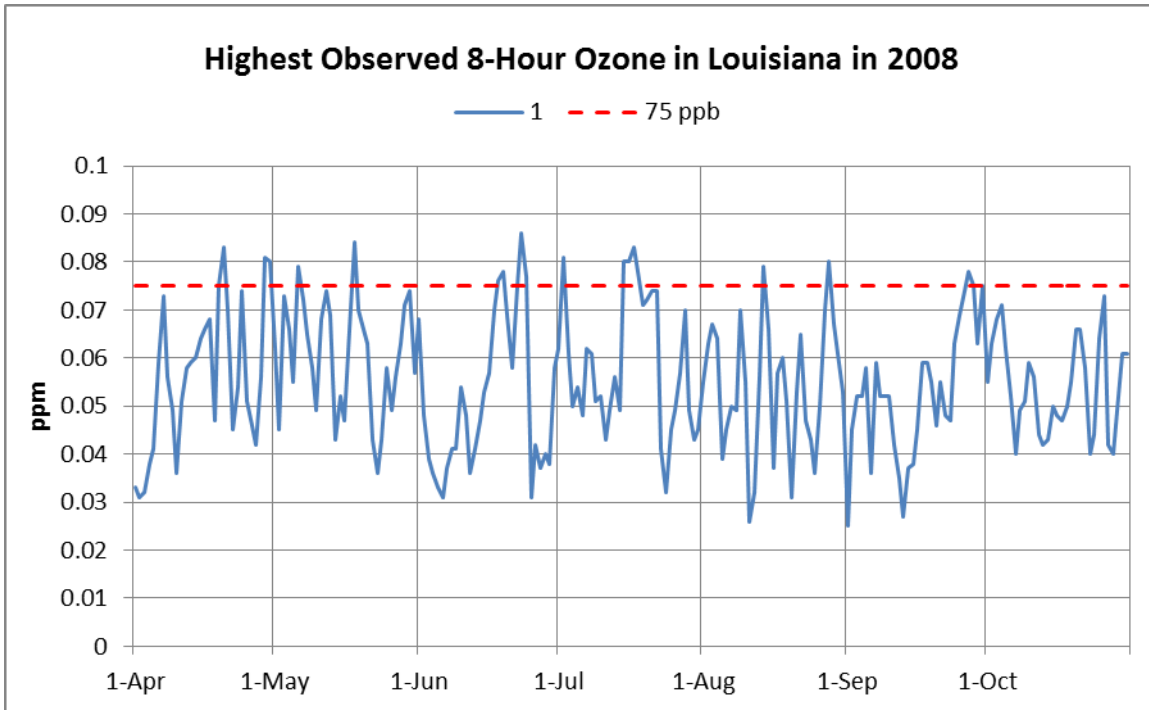


Figure 2-4. Time series of the highest observed 8-hour ozone (top) and number of ozone sites above selected thresholds (bottom) in Louisiana in 2008.

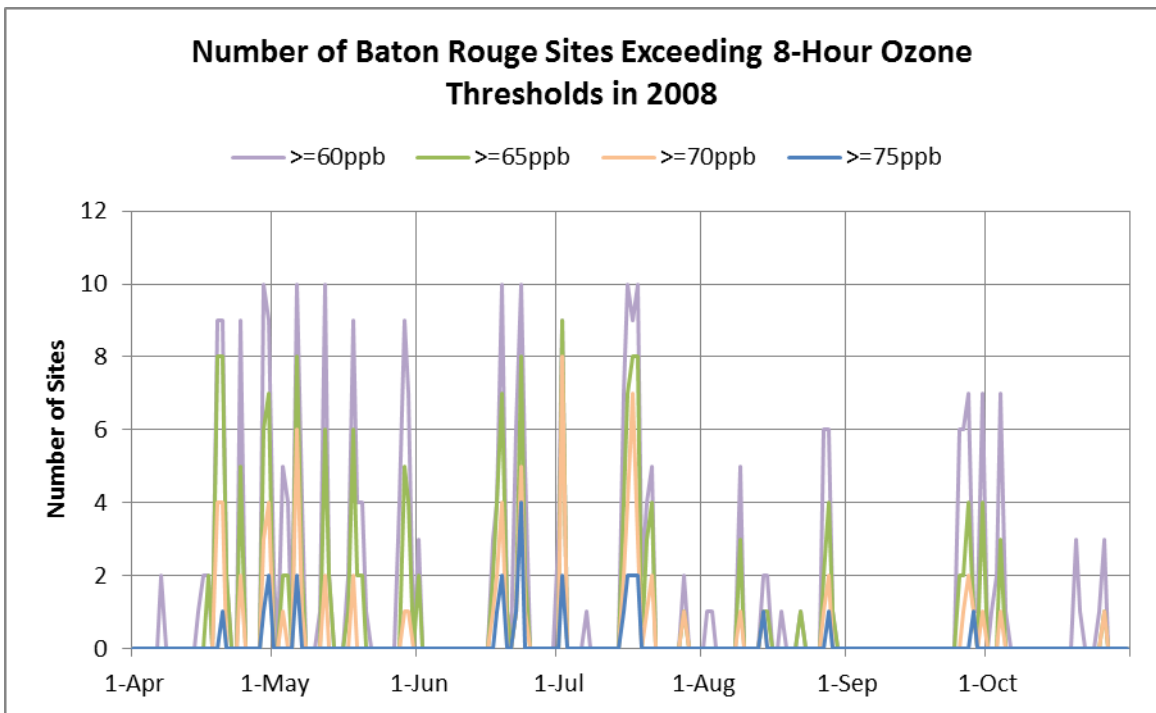
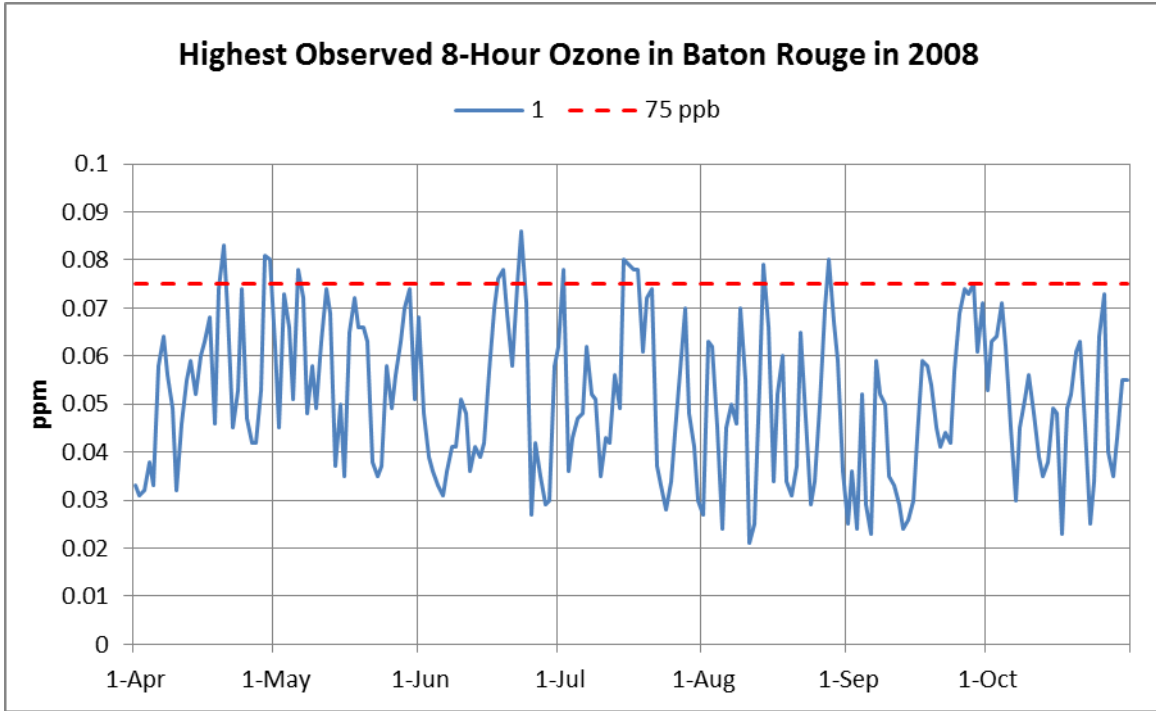


Figure 2-5. Time series of the highest observed 8-hour ozone (top) and number of ozone sites above selected thresholds (bottom) in Baton Rouge in 2008.

Table 2-1. 2008 ozone observation statistics.

Ozone threshold (ppb)	All Louisiana monitors		Baton Rouge monitors	
	Number of days	Number of site-days	Number of days	Number of site-days
≥ 75 ppb	21	43	16	26
≥ 70 ppb	41	138	36	85
≥ 65 ppb	59	316	49	181
≥ 60 ppb	79	583	69	310

in Baton Rouge; the number of site-days represents the total number of exceedances from all sites and all dates.

Ozone exceeded 75 ppb on 43 occasions during 21 dates across Louisiana. Most were 1 or 2 day episodes with peaks only slightly above the 75 ppb standard. There were never more than 5 sites exceeding 75 ppb ozone on the same date in 2008. Six of the 24 monitors never exceeded 75 ppb on any date in 2008. Baton Rouge accounted for more than half (26 out of 43) of all exceedances in the state, where 9 of the 10 monitors exceeded 75 ppb on at least one date in 2008. Ozone was greater than or equal to 75 ppb from at least one site in Baton Rouge on 16 days in 2008.

Table 2-2 lists the number of days and number of exceedances greater than or equal to 75 ppb in four areas of Louisiana (Baton Rouge, New Orleans, Lake Charles, and Shreveport), based on the monitor groupings shown in Figure 2-1. In New Orleans, Lake Charles, and Shreveport, each region had no more than 2 days and no more than 3 site-days of 8-hour ozone exceeding 75 ppb. These would not qualify as a sufficient number of exceedance days for ozone SIP modeling.

Table 2-2. Total number of 75 ppb exceedances in 2008 by region.

Region	Number of days	Number of site-days
Baton Rouge	16	26
New Orleans	1	1
Shreveport	2	3
Lake Charles	2	2

Ozone patterns in 2008 were characterized by occasional, localized, low to moderate exceedance episodes during the spring and summer. It was an active year for tropical weather in Louisiana. The state was impacted by Hurricane Gustav on September 1 and by Hurricane Ike from September 10-13, both of which most likely disrupted typical activities across the state. In addition, Tropical Storm Edouard and Tropical Depression Fay were in the vicinity on August 5 and August 24-25, respectively, helping mix out the air pollutants on those dates. No atypical anthropogenic activity patterns were apparent in 2008. The low number of exceedance days, low number of exceeding sites, low peak concentrations, and the active tropical season made this year atypically clean, and thus it is not an ideal year for ozone SIP modeling.

2.3 2009 Ozone Season

Figures 2-6 and 2-7 are parallel to Figures 2-4 and 2-5, showing time series of the highest observed 8-hour ozone at any monitor, and the frequency of sites exceeding various thresholds on each date in 2009 throughout Louisiana and in Baton Rouge, respectively. Data were available for 25 ozone monitors in 2009, but the statistics for the number of days and site-days exceeding thresholds in Tables 2-3 and 2-4 only consider the exceedances from the 24 monitors common to all three years.

Most ozone exceedances took place between June and August, with some of the highest 8-hour ozone levels in the 3-year period. Peaks reached 94, 96, and 96 ppb in Baton Rouge, Shreveport, and Lake Charles, respectively. But while the number of days when at least one monitor in Louisiana exceeded the 75, 70, 65, or 60 ppb thresholds was the lowest among the three ozone seasons, there were more ozone monitors that measured at least 75 ppb on at least one date in 2009 than in 2008 (21 sites vs. 18 sites); 2009 also had more site exceedances than in 2008 (68 site-days vs. 43 site-days). Baton Rouge showed similar trends, with the fewest number of days (14 days) at or over 75 ppb of all three years, but with more sites (10 out of 10) and more site-days (35) over 75 ppb than in 2008.

Table 2-4 separates the total number of observed 2009 exceedances into 4 regions of Louisiana. There were more exceedances in 2009 than in 2008 in all four regions. Shreveport, with only 2 ozone monitors, had 6 exceedance site-days; the other regions all had at least 10. All regions had at least 5 exceedance days in 2009.

Ozone patterns in 2009 were characterized by a few intense, widespread exceedance events during the summer. Tropical storm activity was relatively quiet near Louisiana. June was hot and dry as Baton Rouge recorded the third warmest June and fourth driest June on record. Conversely, October was very wet; Baton Rouge reported 21 rain days and the second wettest October on record, which was reflected by the fact that 8-hour ozone never exceeded 60 ppb at any monitor in Louisiana after October 1. The near-record heat in June could be considered an extreme meteorological condition, but ozone was only high at the beginning and end of the month, and was swept clean during the middle of the month. No atypical anthropogenic activity patterns were apparent in 2009, except that the year marked the low point in the US economic recession. However, the LDEQ believes that Louisiana was not impacted by the recession to the extent experienced in other regions of the US. The inactive tropical season and higher number of site exceedances in all four regions of Louisiana makes 2009 a better ozone season to model than 2008.

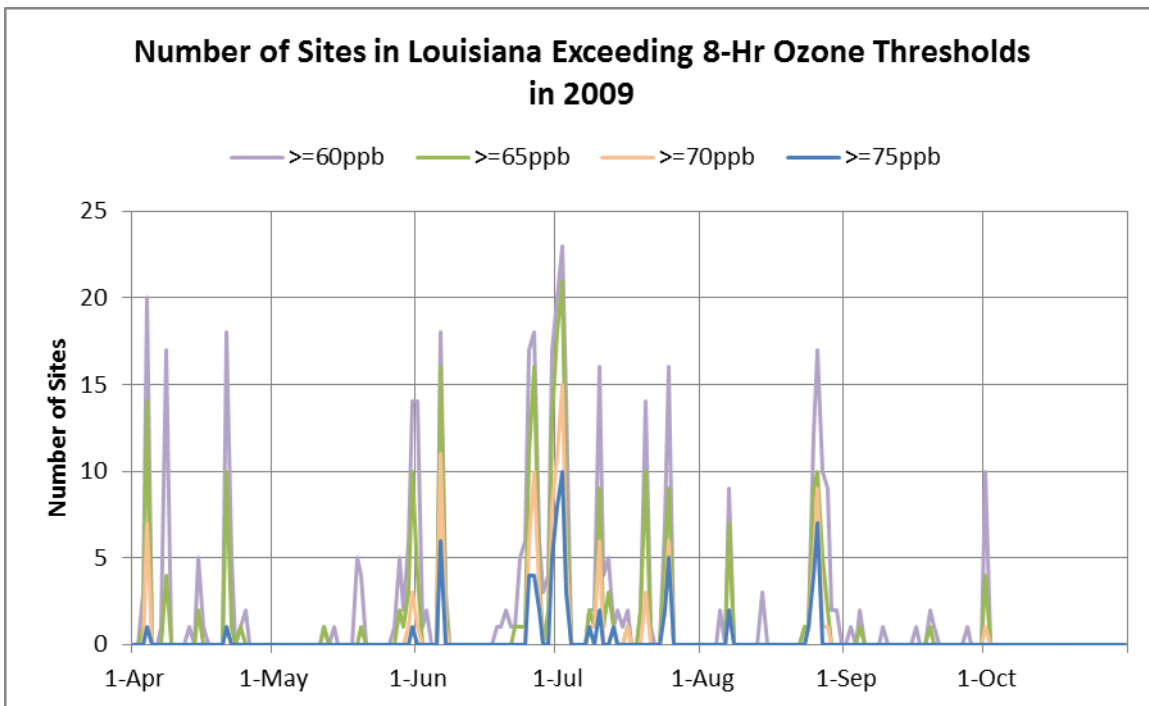
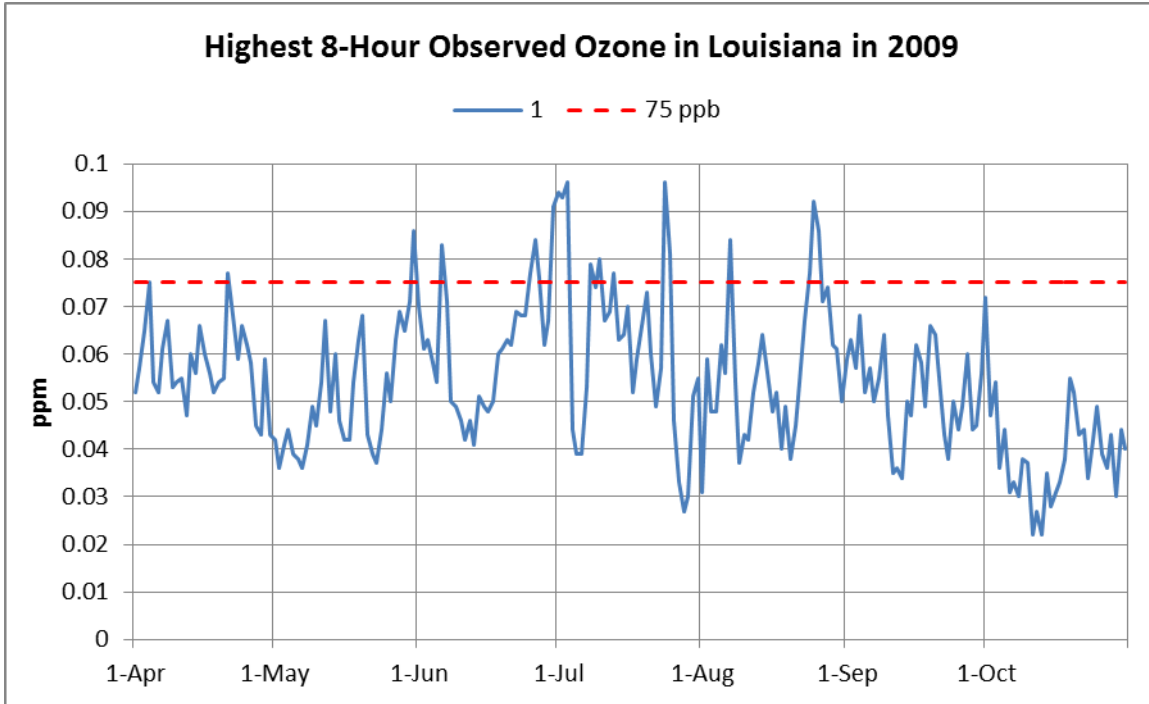


Figure 2-6. Time series of the highest observed 8-hour ozone (top) and number of ozone sites above selected thresholds (bottom) in Louisiana in 2009.

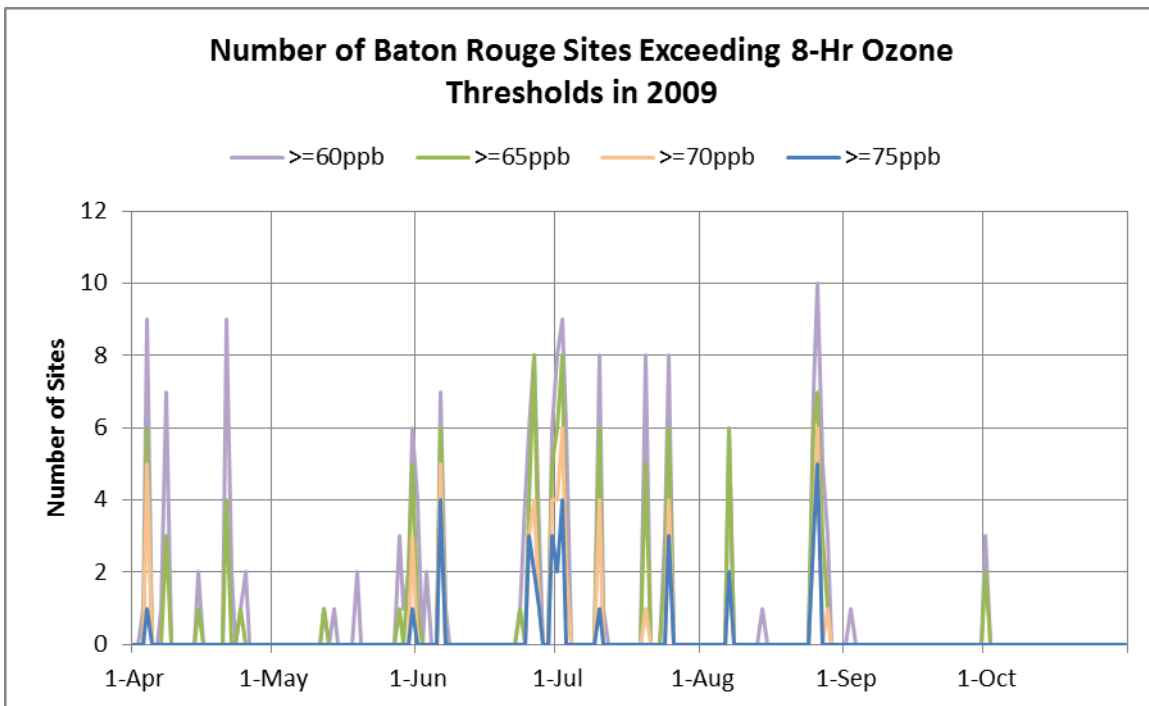
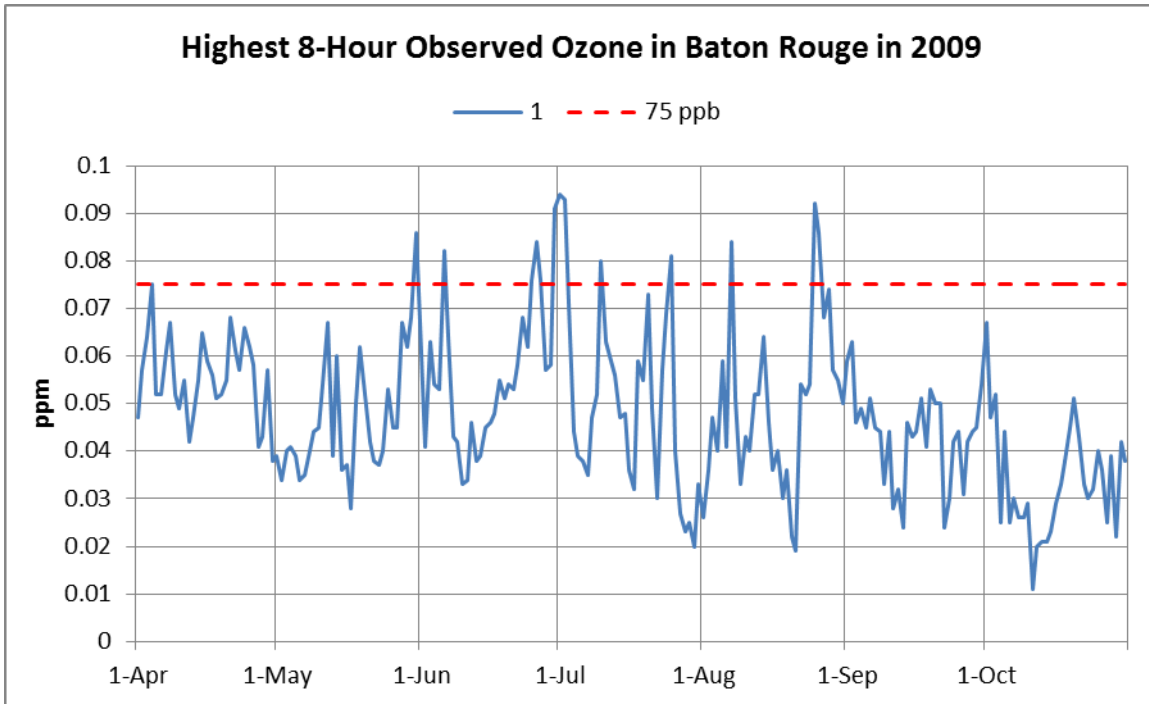


Figure 2-7. Time series of the highest observed 8-hour ozone (top) and number of ozone sites above selected thresholds (bottom) in Baton Rouge in 2009.

Table 2-3. 2009 ozone observation statistics.

Ozone threshold (ppb)	All Louisiana monitors		Baton Rouge monitors	
	Number of days	Number of site-days	Number of days	Number of site-days
≥ 75 ppb	20	68	14	35
≥ 70 ppb	27	119	17	58
≥ 65 ppb	46	241	29	110
≥ 60 ppb	71	428	42	179

Table 2-4. Total number of 75 ppb exceedances in 2009 by region.

Region	Number of days	Number of site-days
Baton Rouge	14	35
New Orleans	5 (5) ¹	10 (12) ¹
Shreveport	5	6
Lake Charles	8	11

¹when including 1 additional site not available in 2008

2.4 2010 Ozone Season

Figures 2-8 and 2-9 show similar sets of time series based on 2010 ozone data from the Louisiana and Baton Rouge monitors, respectively. Table 2-5 summarizes the number of days and site-days in 2010 that exceed the four thresholds in Louisiana and Baton Rouge. Table 2-6 breaks down the statistics at the 75 ppb cutoff for four regions in Louisiana.

The 2010 ozone season had the most number of days (27) during which at least one monitor recorded an exceedance, the most number of exceeding sites (22 out of the 24 sites common to all 3 years), and the most number of site-day exceedances (88 – twice as many as in 2008). This was true both statewide and in the Baton Rouge non-attainment area. Lake Charles was the only area that did not experience more exceedances than 2009.

Ozone patterns in 2010 were characterized by a variety of low to intense, localized and widespread exceedance events during the spring and late summer/fall. Tropical storms were minimal in 2010 except for tropical depression 5, which produced copious amounts of precipitation in Louisiana, resulting in the third wettest August on record in Baton Rouge. This was followed by a very dry September.

Overall, the higher number and variety of exceedance events would make the April to October, 2010 episode the ideal modeling period. However, the BP Deepwater Horizon oil production platform exploded on April 20, 2010, resulting in a massive oil spill in the outer Louisiana coastal waters. Cleanup efforts lasted for months as oil threatened to wash up onto the beaches, and fishing in the Gulf was suspended. This obviously represents an atypical activity and emissions pattern for the Gulf coast region. The EPA installed additional air quality sensors on the Louisiana coast to monitor for emissions from the spill, but no significant impacts to air quality were detected. According to the LDEQ, the oil spill also did not impact Louisiana's

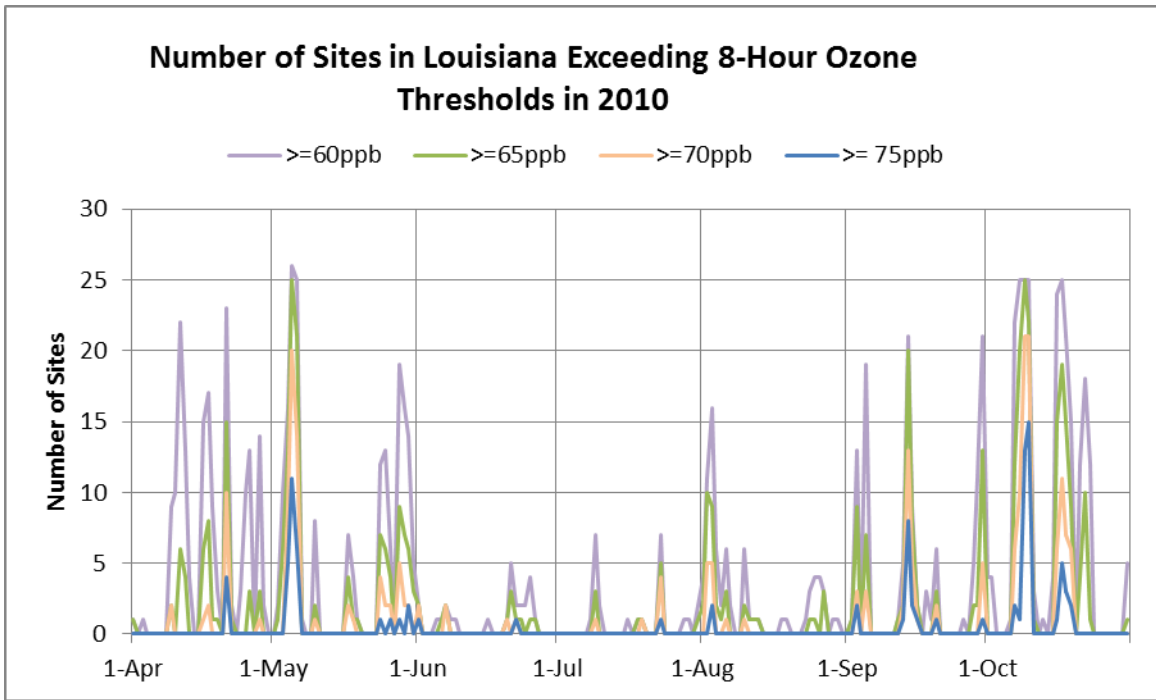
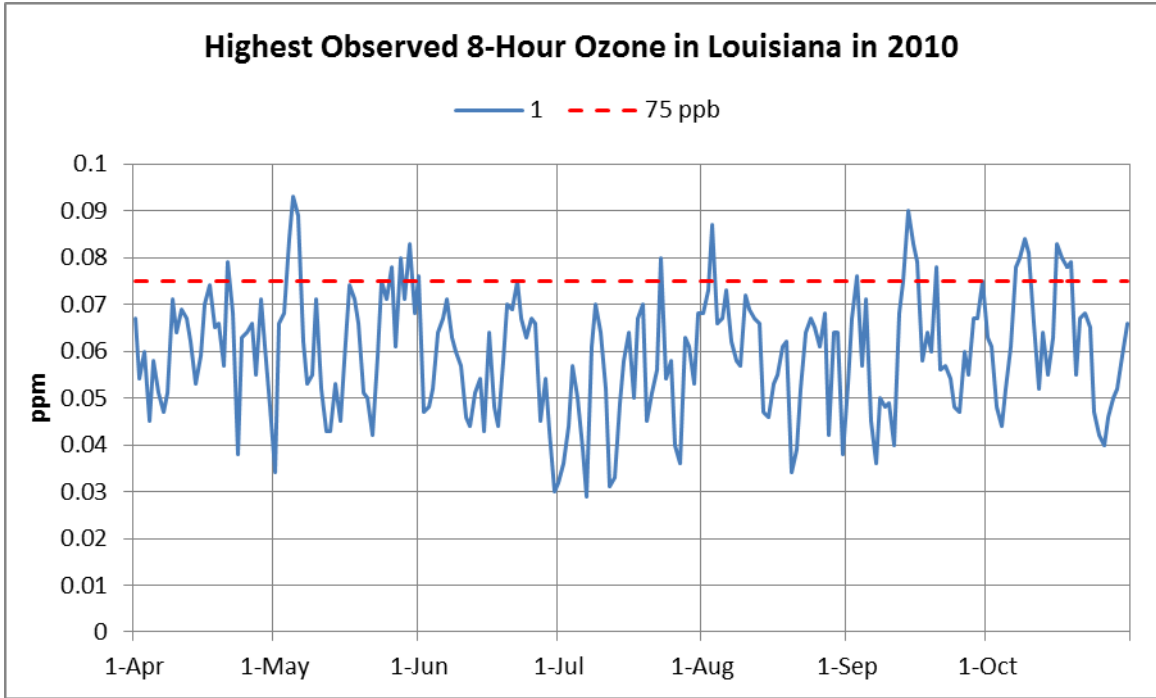


Figure 2-8. Time series of the highest observed 8-hour ozone (top) and number of ozone sites above selected thresholds (bottom) in Louisiana in 2010.

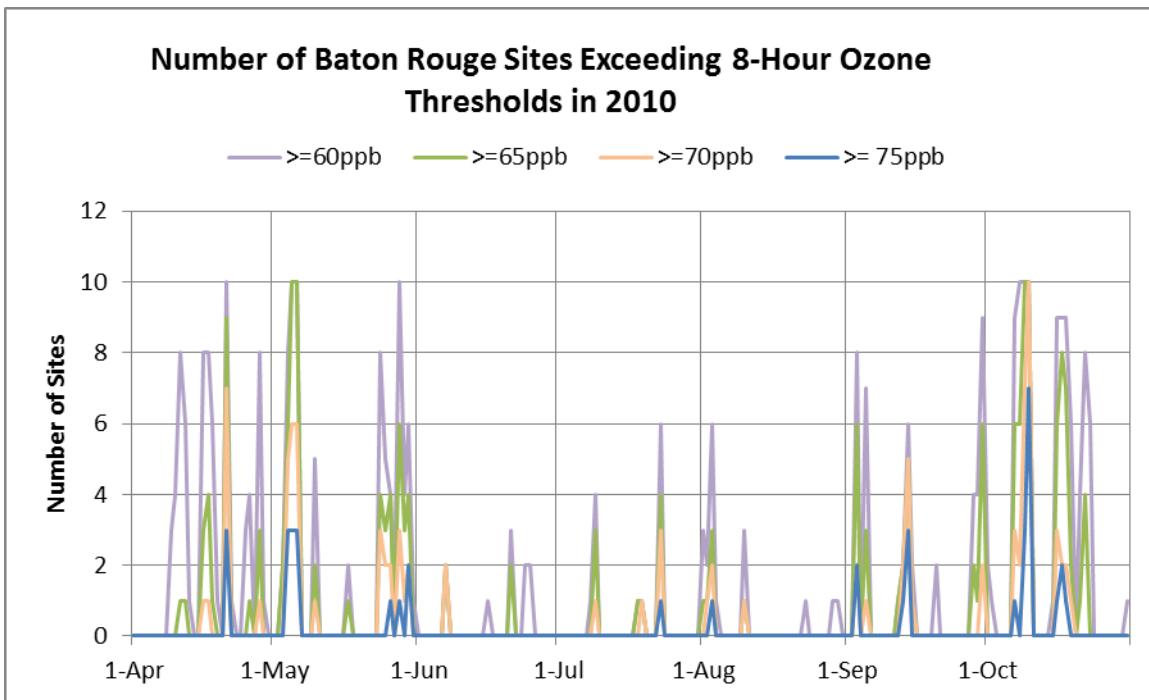
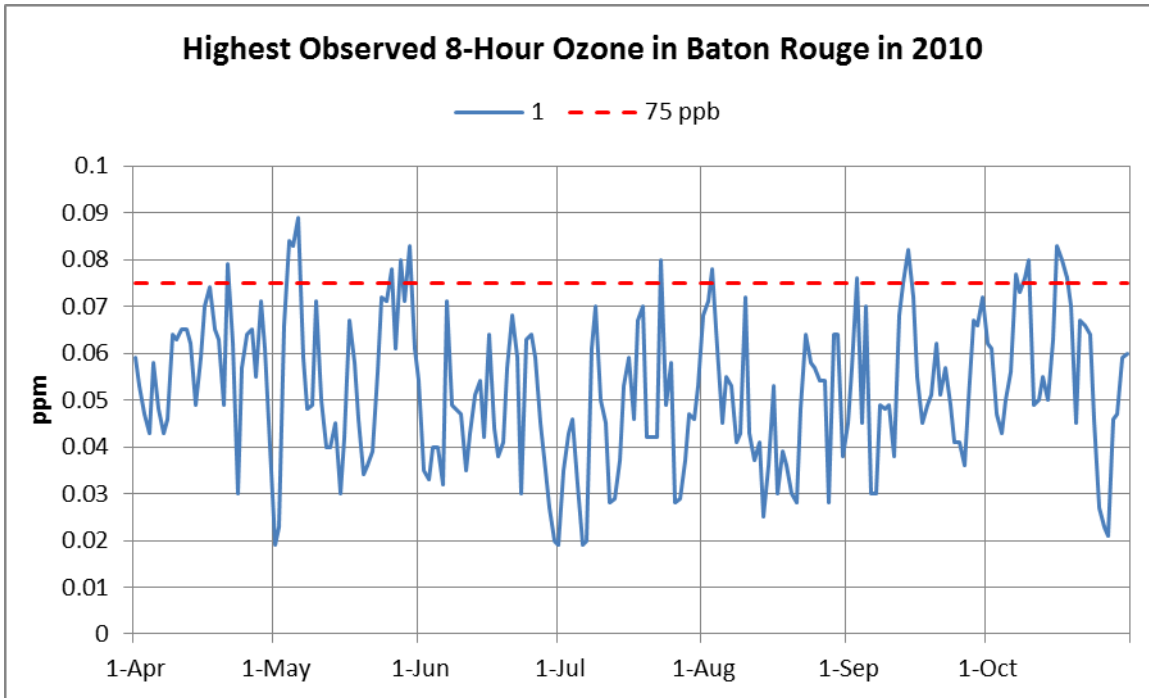


Figure 2-9. Time series of the highest observed 8-hour ozone (top) and number of ozone sites above selected thresholds (bottom) in Baton Rouge in 2010.

Table 2-5. 2010 ozone observation statistics.

Ozone threshold (ppb)	All Louisiana monitors		Baton Rouge monitors	
	Number of days	Number of site-days	Number of days	Number of site-days
≥ 75 ppb	27	88	18	39
≥ 70 ppb	44	217	35	95
≥ 65 ppb	77	427	49	184
≥ 60 ppb	107	791	72	329

Table 2-6. Total number of 75 ppb exceedances in 2010 by region.

Region	Number of days	Number of site-days
Baton Rouge	18	39
New Orleans	8 (8) ¹	15 (21) ¹
Shreveport	11	14
Lake Charles	5	9

¹when including 1 additional site not available in 2008

economy as much as it hurt other Gulf States because the idled fishermen were hired to help clean up the oil spill and because Louisiana's beaches are not typically a tourist destination.

Nevertheless, especially during the first few months of the oil spill, emissions patterns in the Gulf were significantly altered from normal oil and gas production activities, commercial marine shipping, and fishing operations, not to mention fire-related and evaporative emissions from the ocean surface. As a precaution, we have elected to disregard the spring of 2010 to avoid potential impacts from the oil spill. Ozone monitoring statistics for the August-October, 2010 period are summarized in Tables 2-7 and 2-8. Modeling late 2010 would include the widespread ozone event on October 10, when 15 of the 26 ozone monitors across the state exceeded 75 ppb. However, this would reduce the number of 75 ppb exceedances in all regions; Lake Charles would only have 4 days and 6 exceedances over 75 ppb if the modeling period was confined to August through October. Except for Baton Rouge, the total number of exceedance site-days in late 2010 is consistent with the total in 2009 in other regions of the State, and certainly higher than in 2008.

Table 2-7. August-October 2010 ozone observation statistics.

Ozone threshold (ppb)	All Louisiana monitors		Baton Rouge monitors	
	Number of days	Number of site-days	Number of days	Number of site-days
≥ 75 ppb	16	57	10	22
≥ 70 ppb	20	129	17	47
≥ 65 ppb	38	247	23	93
≥ 60 ppb	53	412	33	158

Table 2-8. Total number of 75 ppb exceedances in August-October 2010 by region.

Region	Number of days	Number of site-days
Baton Rouge	10	22
New Orleans	6	12 (15) ¹
Shreveport	8	11
Lake Charles	4	6

¹when including 1 additional site not available in 2008

2.5 Final Consideration and Selection

Table 2-9 summarizes the number of 75 ppb exceedances for each potential modeling period, broken down for the entire State and for each region. We ruled out 2008 because of the low number of exceedances, particularly in New Orleans, Shreveport, and Lake Charles, and the unusually active tropical season. We believe 2009 would have been adequate, but it had the fewest number of exceedance days in Baton Rouge and across the state. Sites like Westlake and Monroe only exceeded 60 ppb on 5 days during the entire season. If 60 ppb is the lowest observed 8-hour ozone in which dates can be used for design value scaling, then these sites would barely apply the minimum allowed.

Table 2-9. Summary of the number of 75 ppb exceedances during four potential modeling periods, by region (extracted from Tables 1 through 8).

Region	2008	2009	2010	2010 (Aug-Oct)
Louisiana	43	68	88	57
Baton Rouge	26	35	39	22
New Orleans	1	10	15	12
Shreveport	3	6	14	11
Lake Charles	2	11	9	6

Table 2-10 displays the total number of days in which each site in Baton Rouge exceeded 60, 65, 70, and 75 ppb for five potential modeling periods (adding a combination of June-August 2009 and August-October 2010). These data are useful to compare how many days above each concentration threshold are available in each period for the design value scaling approach as outlined in the EPA's current ozone modeling guidance.

The full 2010 ozone season had the most number of exceedance days, sites, and site-days in most regions, and was the ideal period to model, but complications from the Gulf oil spill could be an issue especially in the first few months following the oil rig explosion. If only the last three months of the 2010 ozone season were modeled, some sites like Pride and French Settlement, where the 4th highest 8-hour daily maximum ozone in 2010 was in exceedance (76 ppb), would also be close to the minimum number of days available for design value scaling (French Settlement had only 8 days above 60 ppb in the August to October, 2010 period).

Ultimately we selected September-October 2010 as the primary modeling period for the ozone modeling attainment demonstration. Only two Louisiana exceedances occurred in August

during the first few days of the month, and the remainder of August was characterized by low state-wide peak 8-hour ozone ranging between 30-60 ppb. This decision also included a special consideration for Shreveport, which had the highest number of exceedance days during the fall of 2010.

Table 2-10. Summary of number of days during five potential modeling periods when daily 8-hour ozone exceeded 60, 65, 70, and 75 ppb at each monitoring site in the Baton Rouge nonattainment area.

Site	Threshold	2008	2009	2010	Aug - Oct, 2010	Jun -Aug, 2009 + Aug-Oct, 2010
Baton Rouge/Capitol	75 ppb	0	4	5	2	6
	70 ppb	1	7	10	4	11
	65 ppb	8	10	19	9	19
	60 ppb	22	15	34	16	29
Baker	75 ppb	2	2	5	2	4
	70 ppb	6	5	7	3	7
	65 ppb	13	7	16	9	15
	60 ppb	26	14	30	14	24
Bayou Plaquemine	75 ppb	7	2	3	2	4
	70 ppb	15	4	10	6	9
	65 ppb	27	11	23	12	19
	60 ppb	42	16	42	22	30
Baton Rouge/LSU	75 ppb	1	11	7	3	14
	70 ppb	9	13	14	4	16
	65 ppb	20	15	26	11	25
	60 ppb	33	25	42	21	42
Carville	75 ppb	3	4	2	1	5
	70 ppb	11	5	10	7	12
	65 ppb	25	14	24	12	22
	60 ppb	30	28	38	19	37
Dutchtown	75 ppb	2	3	6	6	9
	70 ppb	11	4	13	9	13
	65 ppb	19	10	19	13	23
	60 ppb	31	19	34	17	31
French Settlement	75 ppb	4	4	4	2	5
	70 ppb	12	6	6	3	8
	65 ppb	24	14	12	4	13
	60 ppb	43	20	22	8	22
Grosse Tete	75 ppb	3	1	3	2	3
	70 ppb	4	4	14	6	10
	65 ppb	8	9	23	12	20
	60 ppb	26	14	41	17	29
Port Allen	75 ppb	1	1	1	1	2
	70 ppb	5	4	5	3	7
	65 ppb	14	7	14	8	15
	60 ppb	21	12	24	14	25
Pride	75 ppb	3	3	3	1	4
	70 ppb	11	6	6	2	7
	65 ppb	23	13	8	3	11
	60 ppb	36	16	22	10	20

3.0 METEOROLOGICAL MODELING EVALUATION

The WRF model, version 3.3.1, was run by Alpine Geophysics from August through October 2010 to cover the LDEQ 36, 12, and 4 km photochemical modeling domains. WRF output was used to prepare meteorological inputs for the CAMx photochemical model. Since CAMx model performance depends on the accuracy of meteorology, predicted wind, temperature, and precipitation patterns on the 4 km grid were evaluated against available measurement data across Louisiana. Emphasis was placed on the 16 dates when 8-hour ozone exceeded 75 ppb from at least one ozone monitor in the State – August 3; September 3, 13-16, 20, and 30; and October 7-10 and 16-19. This section details the WRF model performance over the State of Louisiana and serves as a supplementary evaluation report to the original documentation developed by Alpine (2012).

Meteorological data sites were grouped into two regions – northern Louisiana, which includes Shreveport, and southern Louisiana, which includes Baton Rouge, New Orleans, and Lake Charles. This breakout allows us to separately analyze WRF performance for a coastal-influenced zone, and an inland zone. Figure 3-1 shows the locations of all monitoring stations used in this analysis.

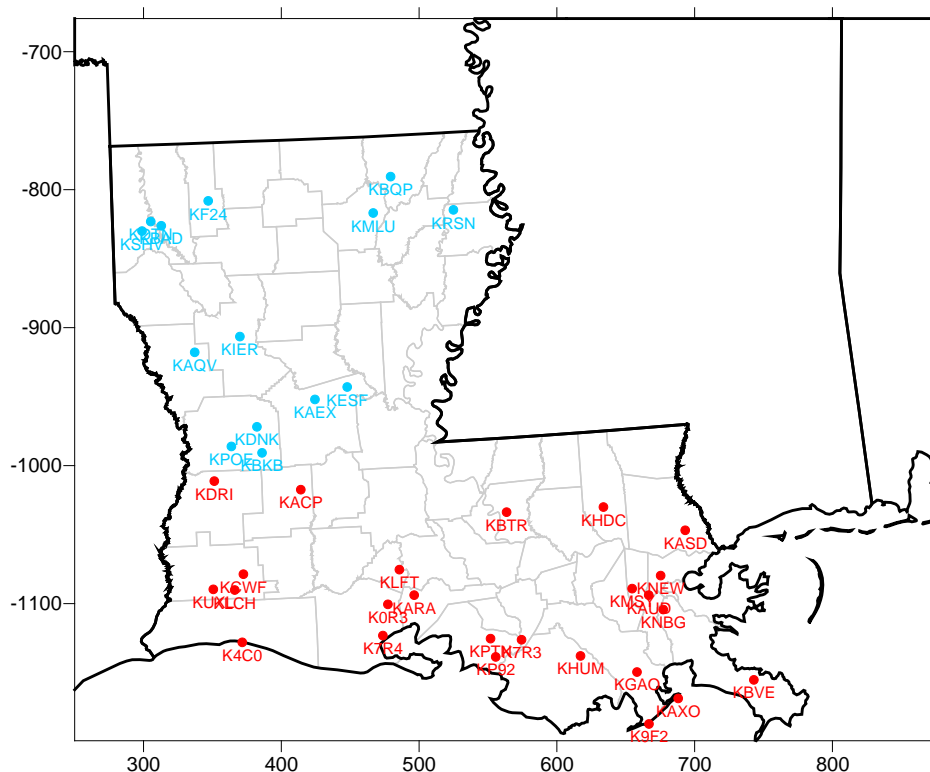


Figure 3-1. Meteorology stations in Louisiana with the north and south sites colored in blue and red, respectively.

3.1 Wind speed

Figure 3-2 compares hourly time series of predicted and observed wind speed from August to October, 2010 averaged over all sites in northern Louisiana. Blue lines represent the WRF-predicted wind speeds; black lines show the observed. Vertical lines representing midnight CST for each date are plotted to differential the days. Figure 3-3 shows the hourly time series of wind speed bias in northern Louisiana.

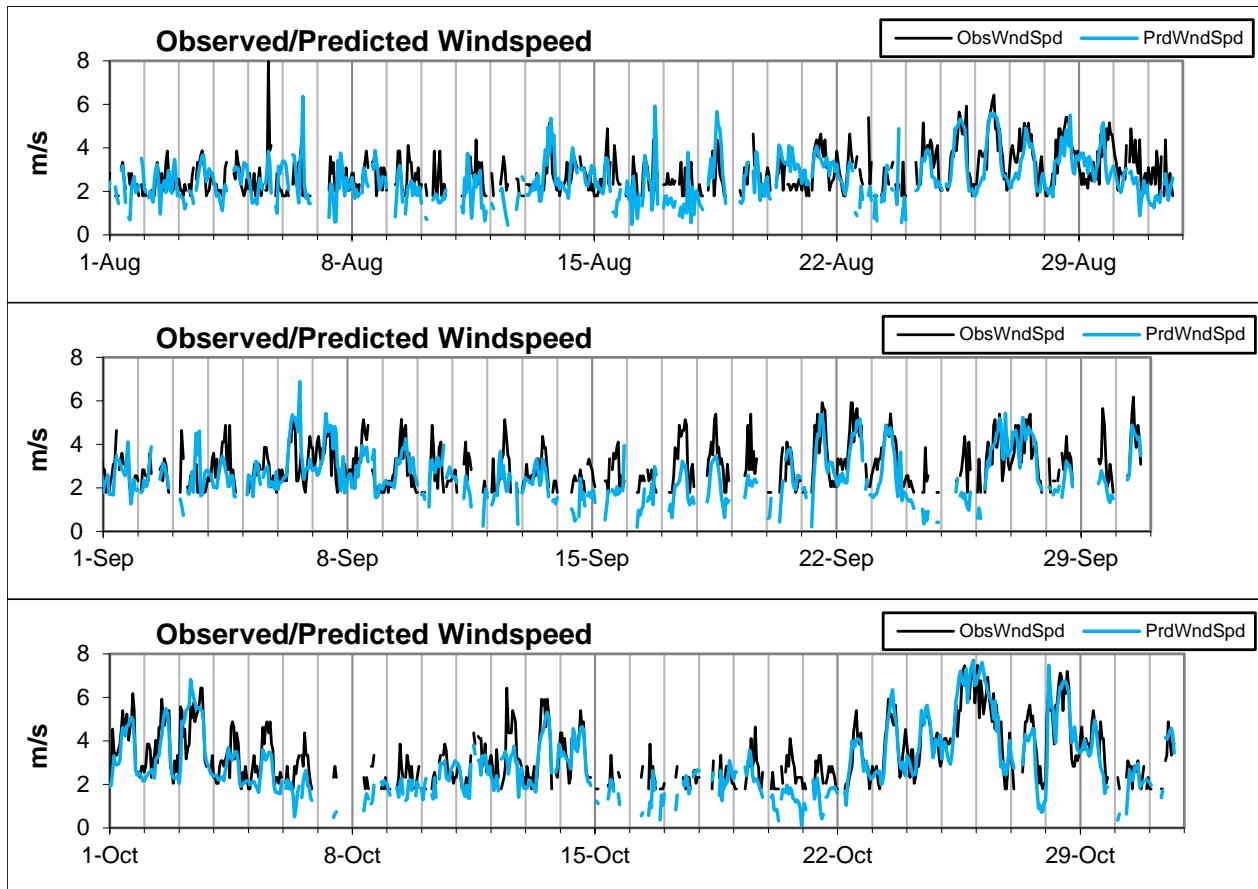


Figure 3-2. Hourly predicted (blue) and observed (black) wind speed averaged over all sites in northern Louisiana for August (top), September (middle) and October (bottom).

WRF tended to under predict winds in northern Louisiana, especially from mid-September to mid-October, when the bulk of the high ozone dates occurred. The under predicted wind speeds could result in more stagnation and higher ozone concentrations in CAMx.

Similar sets of time series are shown in Figures 3-4 and 3-5, respectively, for southern Louisiana. WRF is shown in red; the observed is in black. The bias was within ± 2 m/s for most hours, but

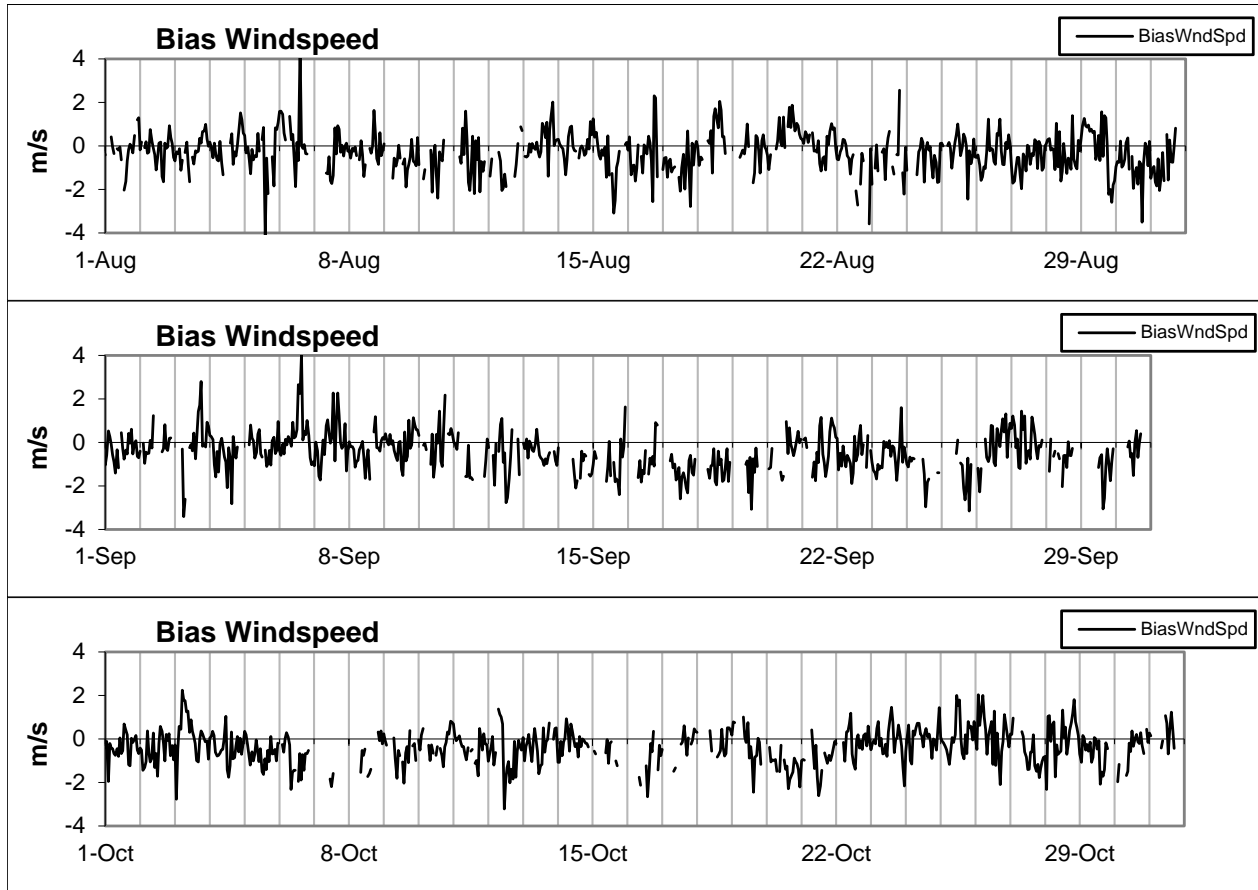


Figure 3-3. Hourly wind speed bias over all sites in northern Louisiana for August (top), September (middle) and October (bottom).

there tended to be an under prediction of wind speeds during most hours on the episode dates in October. Agreement tended to be slightly better than in northern Louisiana.

Figure 3-6 contains four scatter plots comparing hourly predicted and observed wind speeds, but the pairings were limited to the dates when 8-hour ozone exceeded 75 ppb anywhere in the state. Northern Louisiana pairings are shown on the top and southern Louisiana are shown on the bottom. Hours with episode dates in September are shown on the left, hours with episodes dates in October are shown on the right. August was excluded because it is only used for model spin-up. Red circles represent daytime hours (8 AM – 6 PM CST) and blue represents nighttime hours (7 PM to 7 AM). Ideally, all of the pairings should line up on the solid black diagonal line, but any pairings between the two black dashed lines, which represent wind speeds within ± 2 m/s of the observed, are considered to perform well. Statistics are also included to show the regression line and the fraction of hours when the bias is between ± 0.5 , 1, and 2 m/s.

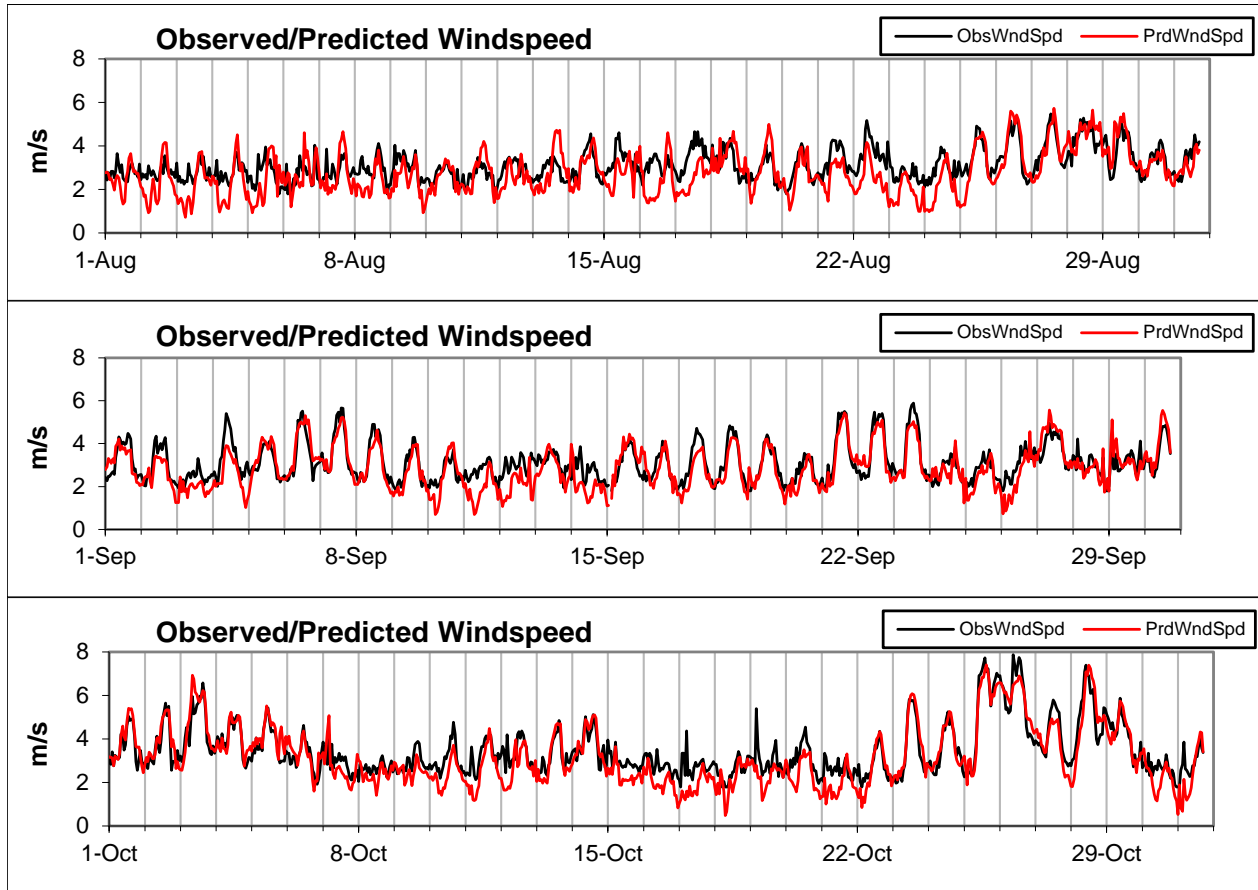


Figure 3-4. Time series of hourly predicted (red) and observed (black) wind speeds averaged over all sites in southern Louisiana for August (top), September (middle) and October (bottom).

WRF predicted wind speeds within 2 m/s of the observed during most hours of the episode dates in both northern and southern Louisiana. The hours that exceeded the ± 2 m/s bias were all under predicted. WRF performed the best in September in southern Louisiana, when 99% and 89% of the episode hours were within 2 and 1 m/s of the observed, respectively. In October, the daytime wind speeds, which were generally faster than at night, were mostly under predicted throughout Louisiana.

Figure 3-7 shows “soccer goal” plots displaying daily wind speed performance statistics. The plots are ordered similarly to Figure 3-6. Statistics for all dates of the month are plotted, but the high ozone dates are highlighted in red. The “goals” (outlined in blue) represent benchmarks for exceptionally good performance; daily wind speed bias no greater than ± 0.5 m/s and wind speed root mean squared error (RMSE) no greater than 2 m/s.

In northern Louisiana, all dates in both September and October met the daily RMSE performance benchmark while the daily bias benchmark was met on about 60% of all dates

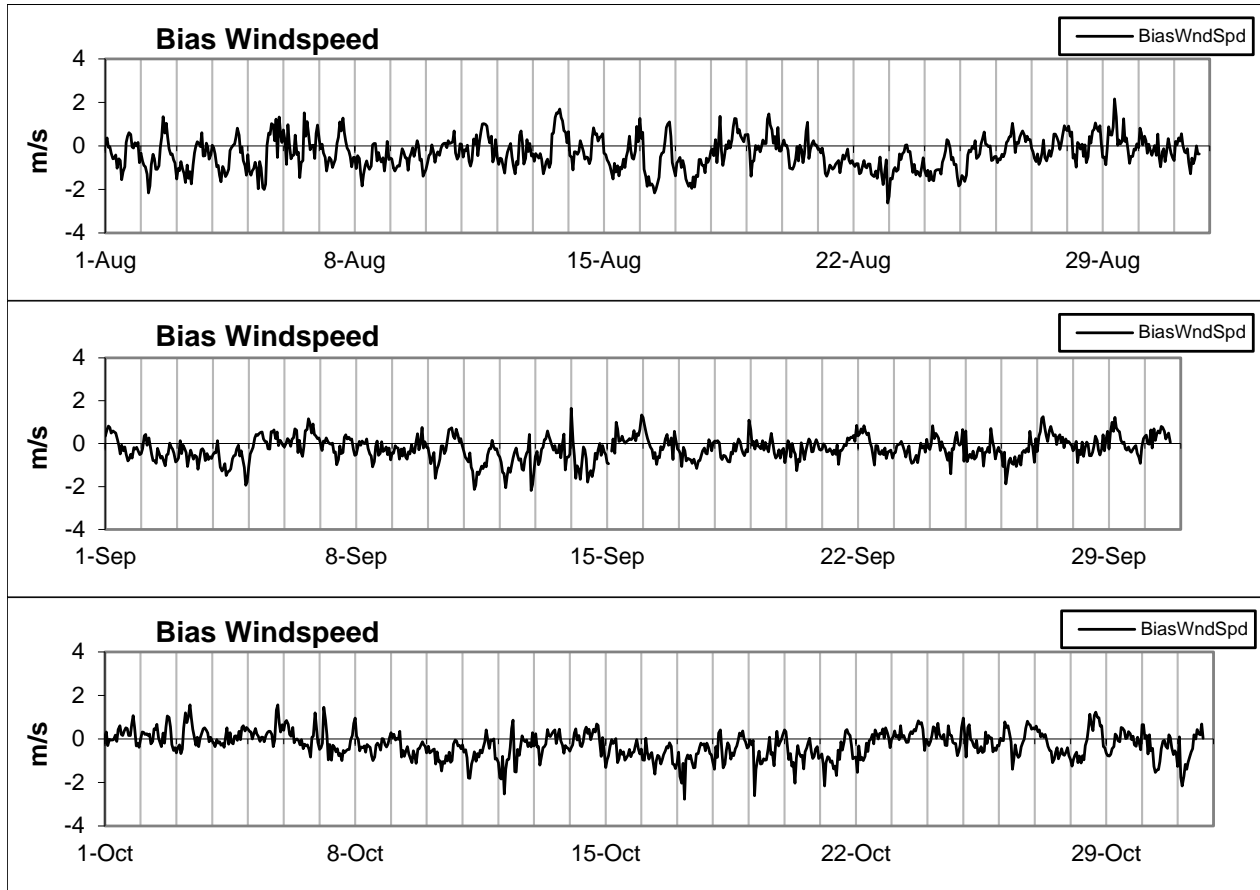


Figure 3-5. Time series of hourly wind speed bias over all sites in southern Louisiana for August (top), September (middle) and October (bottom).

during the 2 month period. Among the episode dates, all had a negative wind speed bias with 7 of the 15 dates in the 2 month period inside the soccer goal line. However, most dates were within -1 m/s bias, which is also quite good.

In southern Louisiana, the daily wind speed bias statistics were better, especially in September when over 70% of all dates and episode dates met the performance goals. In October, the high ozone dates all had negative biases, with half of these within the bias benchmark and all within -1 m/s bias.

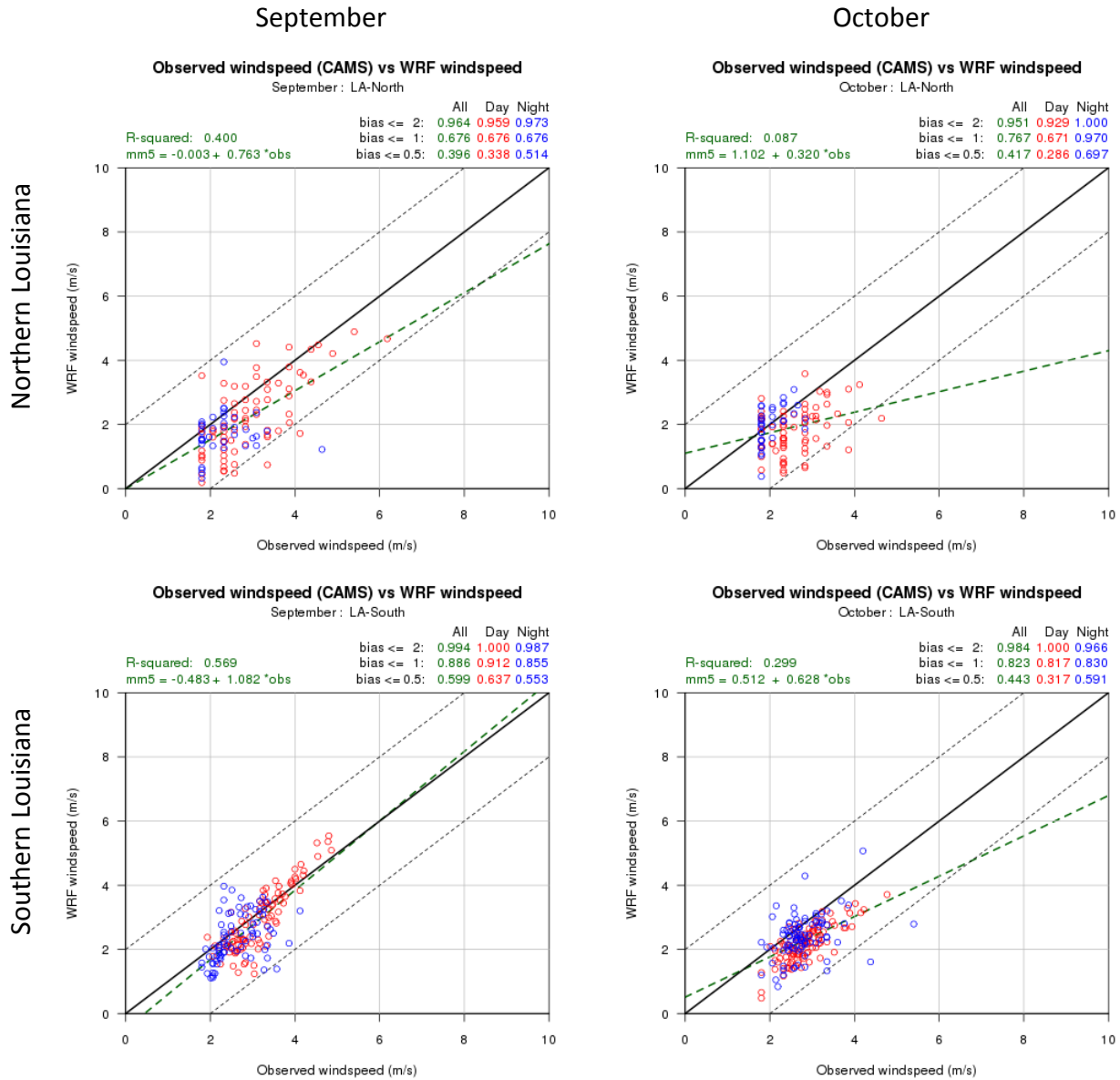


Figure 3-6. Scatter plots of hourly predicted and observed wind speeds on high ozone dates during September (left) and October (right) for northern Louisiana (top) and southern Louisiana (bottom). Red circles represent daytime hours (8 AM – 6 PM CST), blue represents nighttime hours (7 PM to 7 AM). The solid black diagonal line is the 1:1 perfect correlation line; the two black dashed lines represent the ±2 m/s bias envelope. Statistics show the regression line and the fraction of hours when the bias is between ±0.5, 1, and 2 m/s.

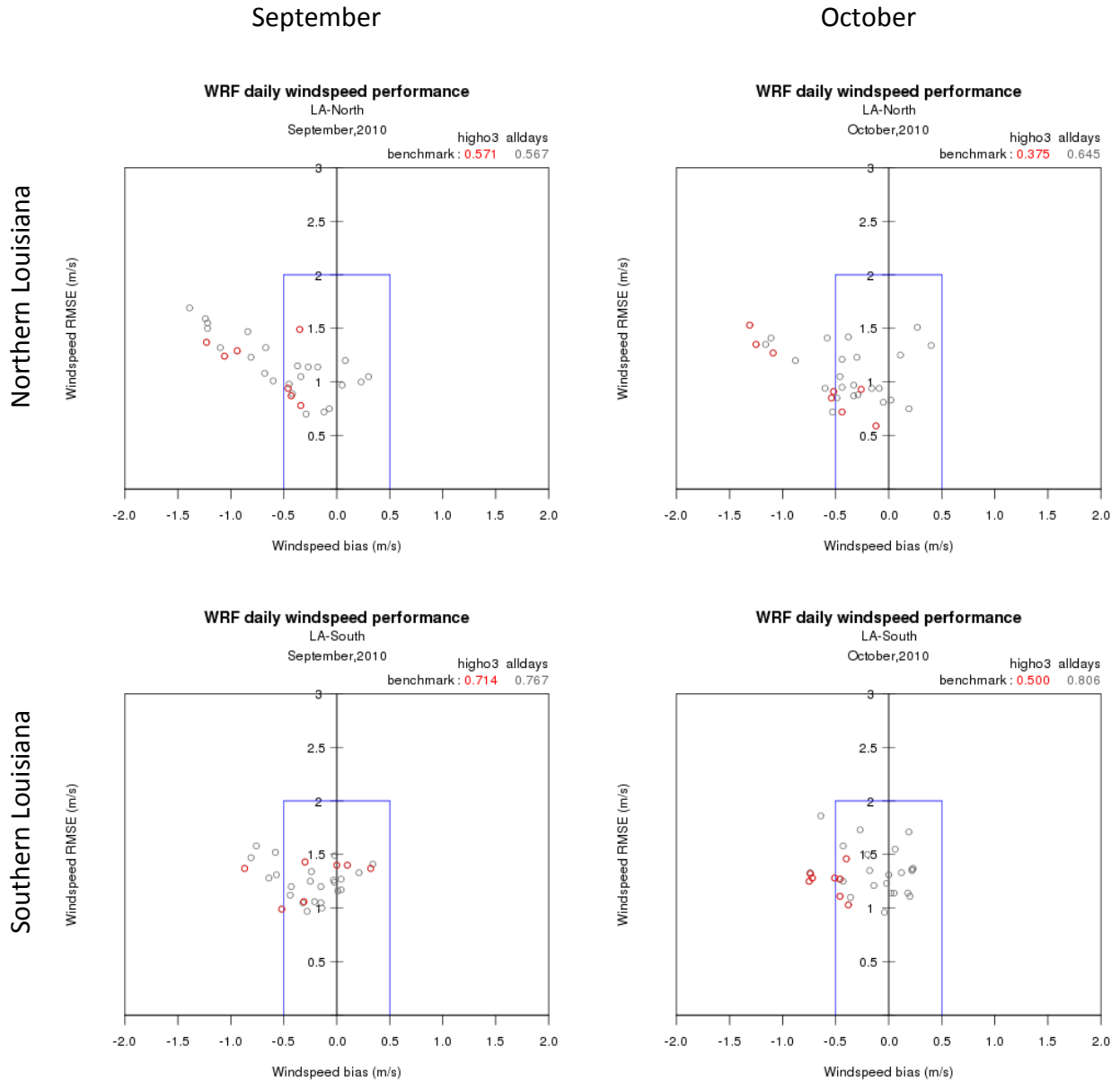


Figure 3-7. Soccer goal plot of daily wind speed statistics. Red circles highlight the high ozone dates.

3.2 Wind Direction

Figures 3-8 and 3-9 show hourly time series of predicted and observed wind direction averaged among all the meteorology stations in northern and southern Louisiana, respectively. The scatter plots shown in Figure 3-10 limit the hourly predicted and observed wind direction pairings to the high ozone dates, with red circles representing daytime hours and blue representing nighttime hours. The two dotted diagonal lines highlight daily-averaged bias within 30 degrees of the observed.

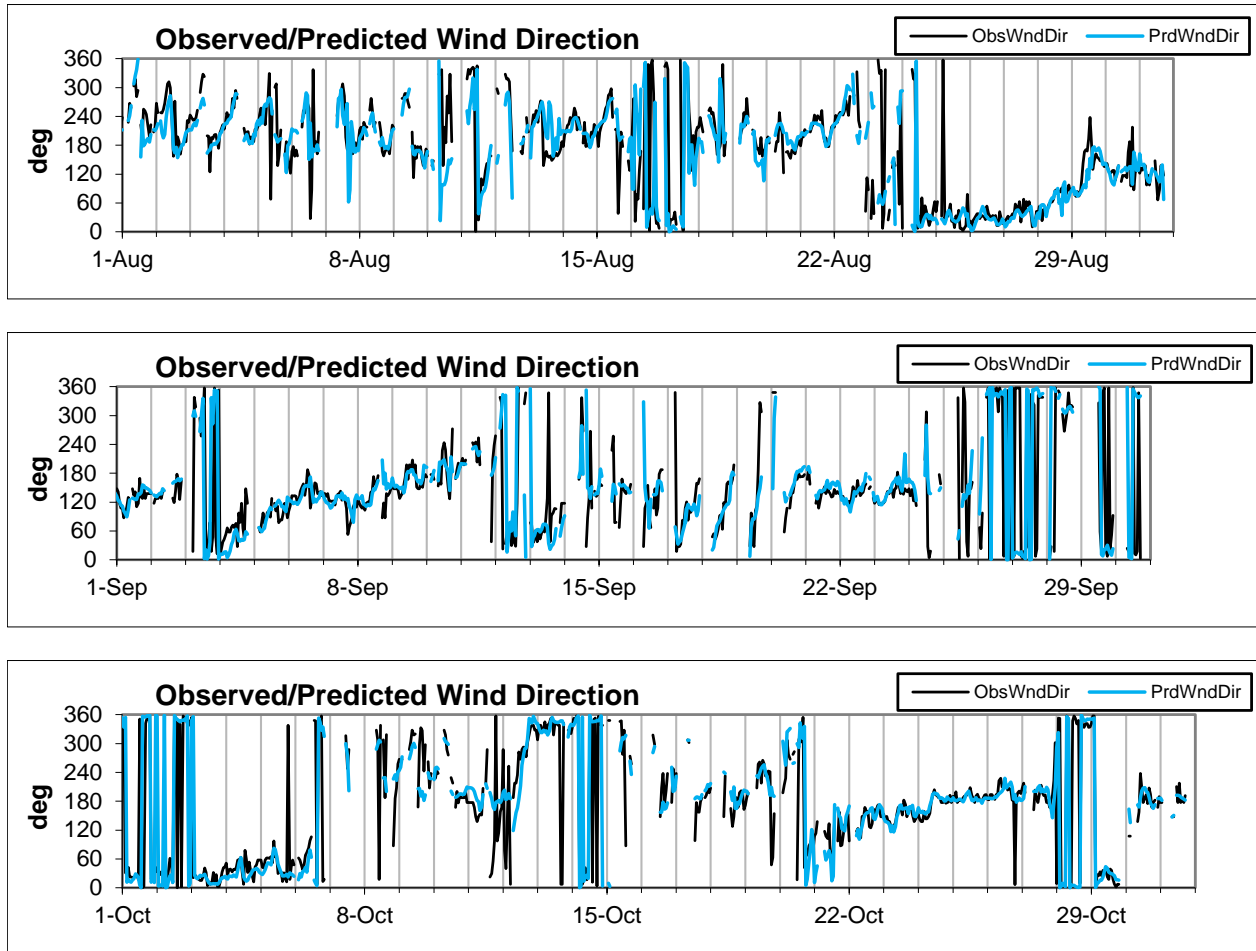


Figure 3-8. Hourly predicted (blue) and observed (black) wind direction averaged over all sites in northern Louisiana for August (top), September (middle) and October (bottom).

In northern Louisiana, the hourly wind direction bias was within ± 30 degrees for about 60% of all hours on the episode dates. September wind direction performance was somewhat scattered, likely due to the very light wind speeds predicted, which can result in more variability

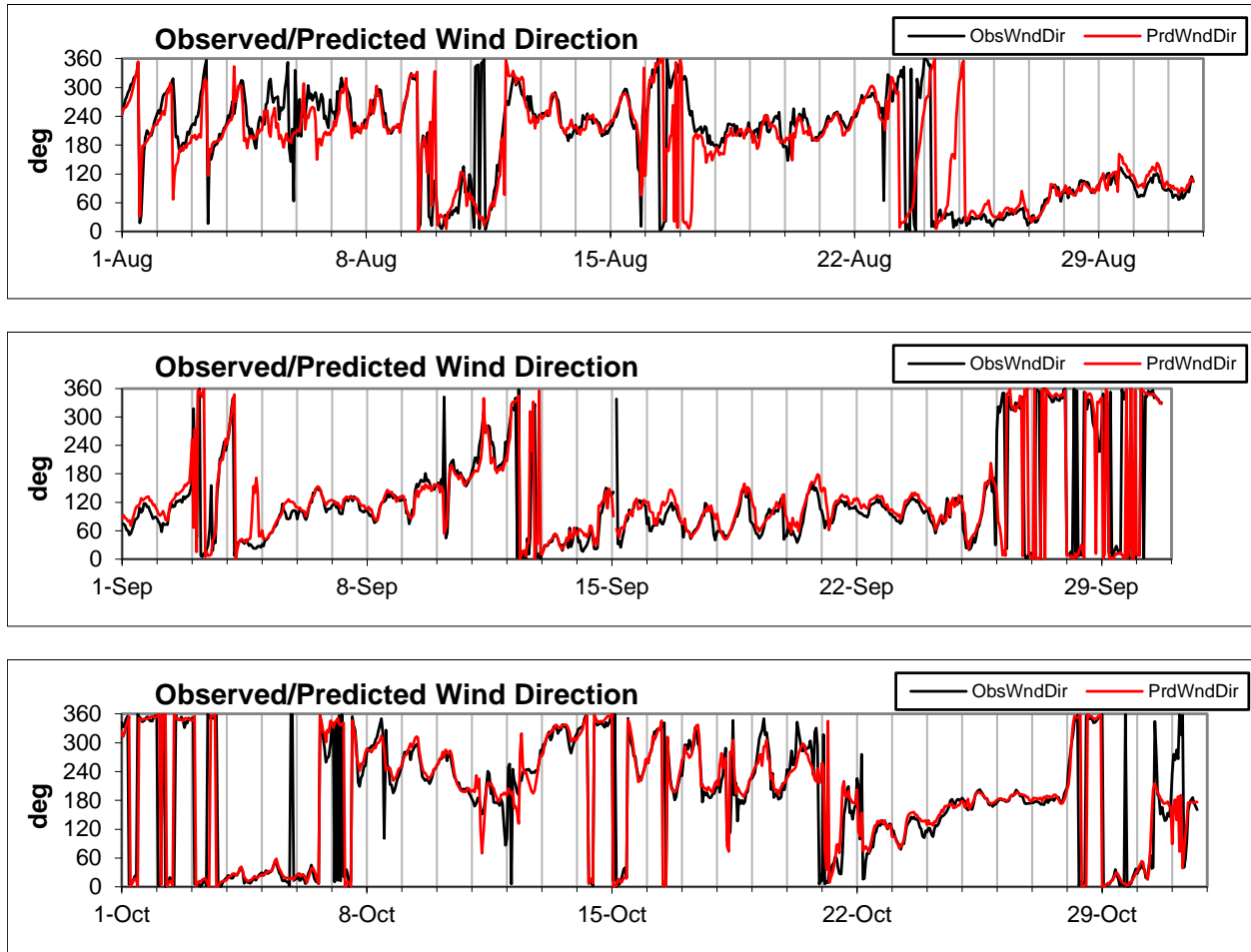


Figure 3-9. Hourly predicted (red) and observed (black) wind direction averaged over all sites in southern Louisiana for August (top), September (middle) and October (bottom).

in direction. October had numerous hours in which WRF predicted southwest winds when the observed were west to northwesterly.

WRF performed better in southern Louisiana than northern Louisiana. Over 85% of all hours on the episode dates had a bias within ± 30 degrees in southern Louisiana. The best performance took place in September during the daylight hours, when 90% of the hours had a bias between ± 30 degrees. WRF correctly predicted that the wind direction during most high ozone dates would be between north and southeast direction (going clockwise) in September, and between the southwest and north in October.

Soccer goal plots comparing daily wind direction error with wind speed RMSE are shown in Figure 3-11. The benchmark for exceptional performance is for RMSE below 2 m/s and wind direction error less than 30 degrees. All dates in the month are shown; high ozone dates are highlighted in red. In all four plots, the fraction of dates meeting the performance goals were

September

October

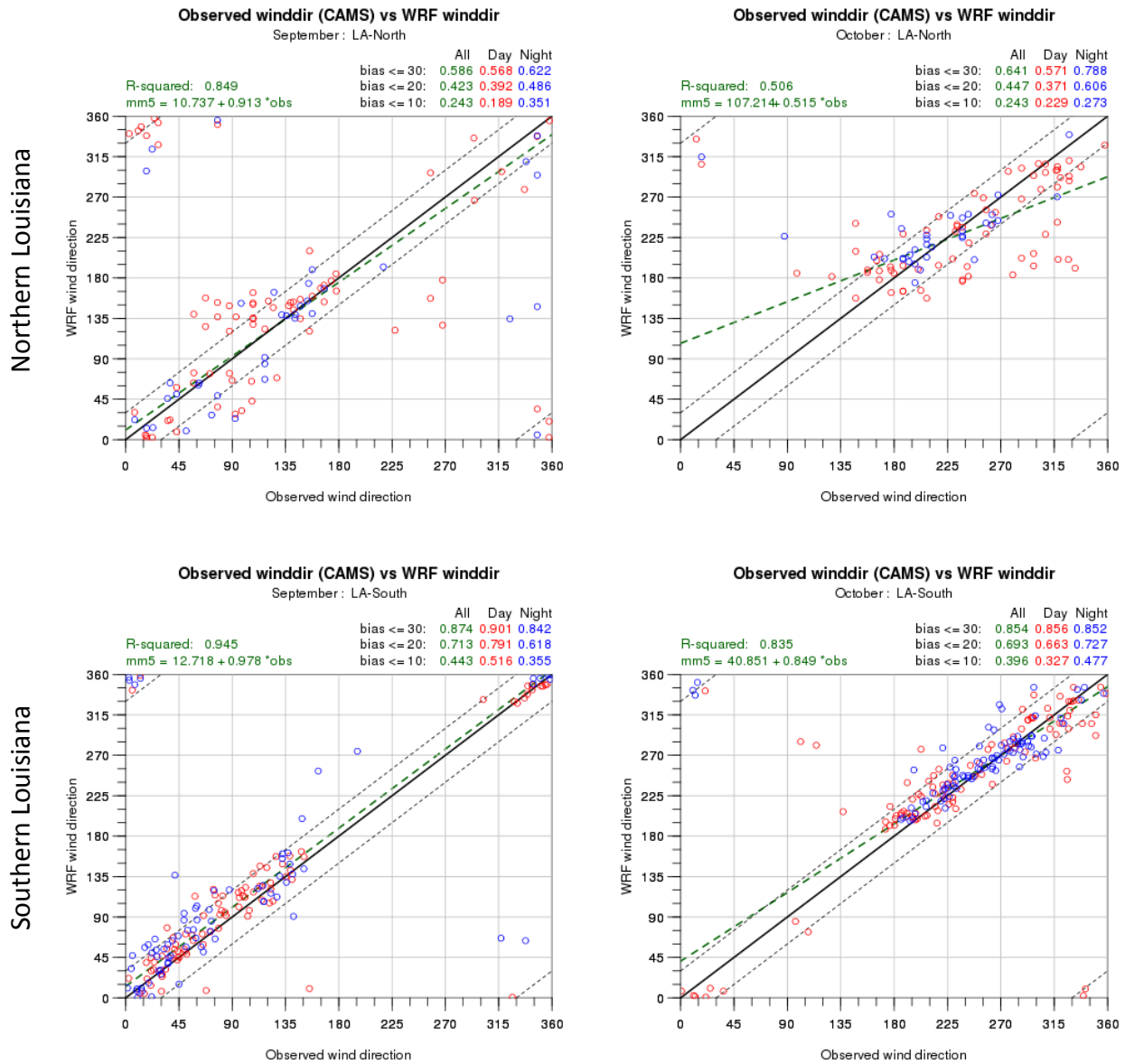


Figure 3-10. Scatter plots of hourly predicted and observed wind direction on high ozone dates during September (left) and October (right) for northern Louisiana (top) and southern Louisiana (bottom). Red circles represent daytime hours (8 AM – 6 PM CST), blue represents nighttime hours (7 PM to 7 AM). The solid black diagonal line is the 1:1 perfect correlation line; the two black dashed lines represent the ±30 degree bias envelope. Statistics show the regression line and the fraction of hours when the bias is between ±10, 20, and 30 degrees.

September

October

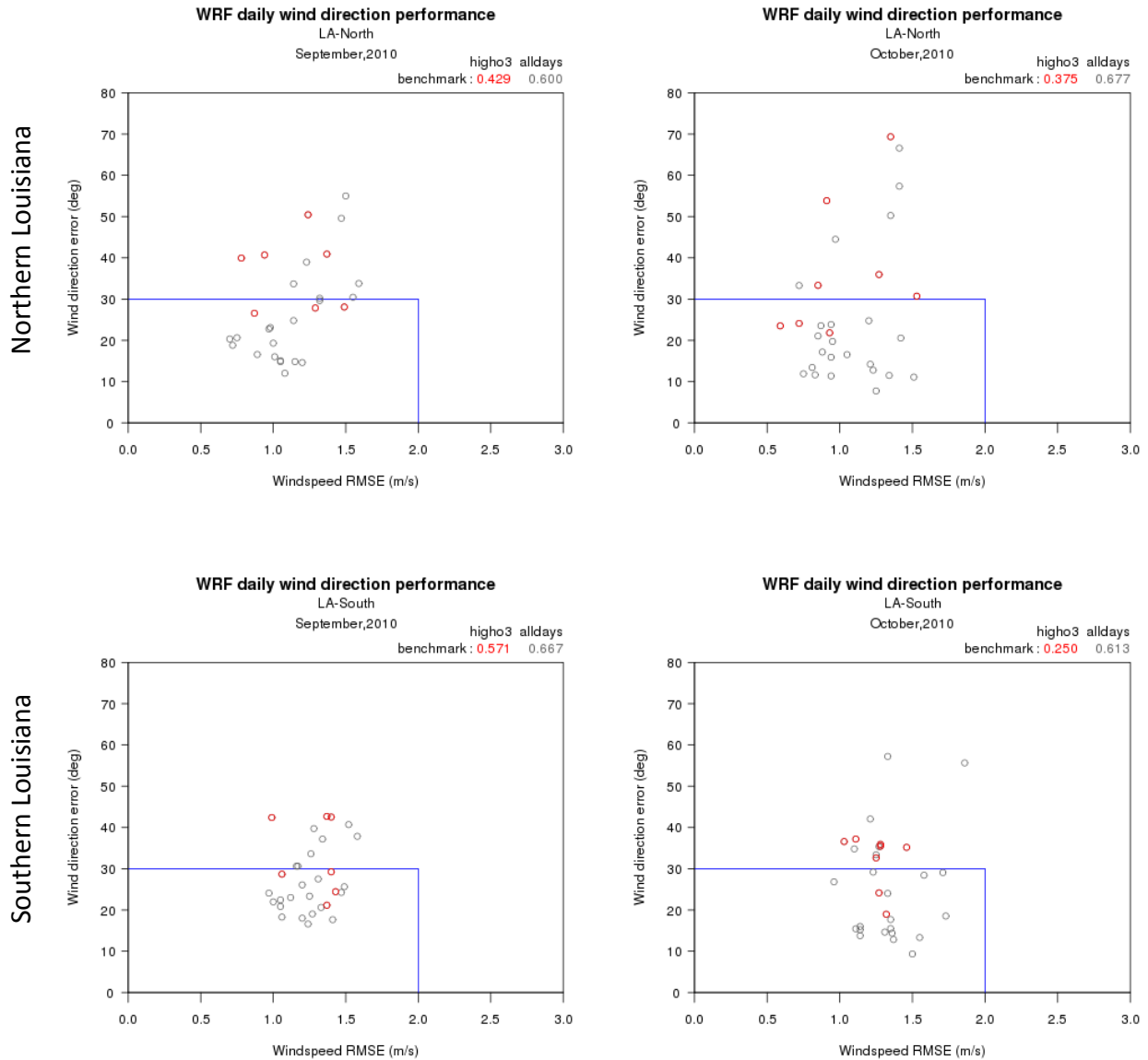


Figure 3-11. Soccer goal plots of daily wind direction statistics. Red circles highlight the high ozone dates.

lower when considering only high ozone dates than when using all dates in the month. On high ozone dates, stagnant air and low wind speeds are common, which may have resulted in more light and variable wind conditions on these dates, making it more difficult to achieve a directional error of less than 30 degrees. September in southern Louisiana had the highest fraction of high ozone dates inside the goal (57%); October in southern Louisiana had the

lowest fraction (25%). Overall, wind direction performance in this application is better than most WRF applications we have analyzed in other areas of the US.

3.3 Temperature

Figures 3-12 and 3-13 display hourly time series of predicted and observed temperatures from August to October, 2010 averaged over all sites in northern and southern Louisiana, respectively. The scatterplots in Figure 3-14 show hourly predicted and observed pairings on the high ozone dates, separated for daytime and nighttime hours. Points within the two dotted lines represent predicted temperatures within 2 K of the observed. Soccer goal plots in Figure 3-15 display daily temperature bias and error statistics, where the performance benchmarks are defined for a bias within ± 0.5 K and an error of less than 2 K. High ozone dates are highlighted in red.

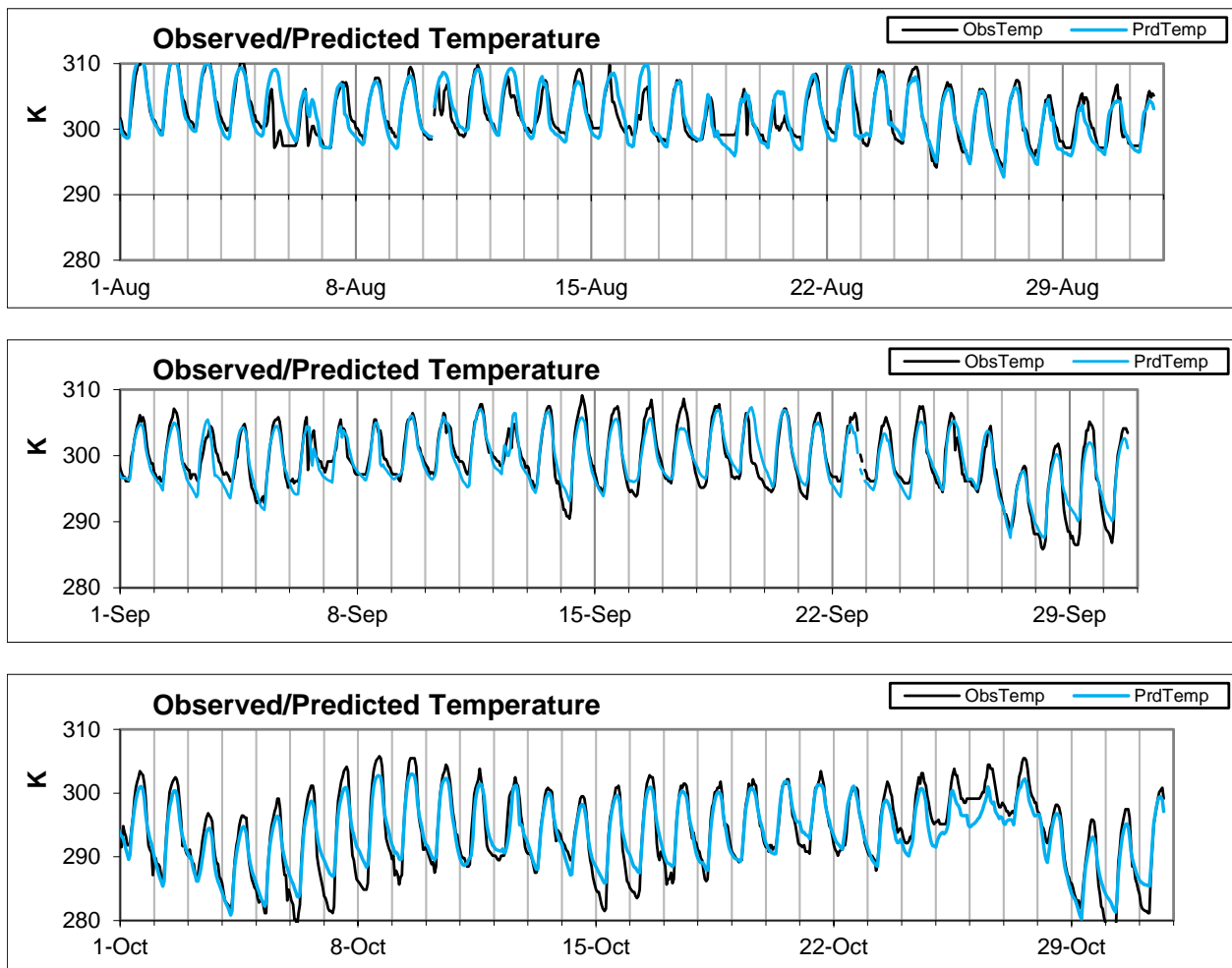


Figure 3-12. Hourly predicted (blue) and observed (black) temperature averaged over all sites in northern Louisiana for August (top), September (middle) and October (bottom).

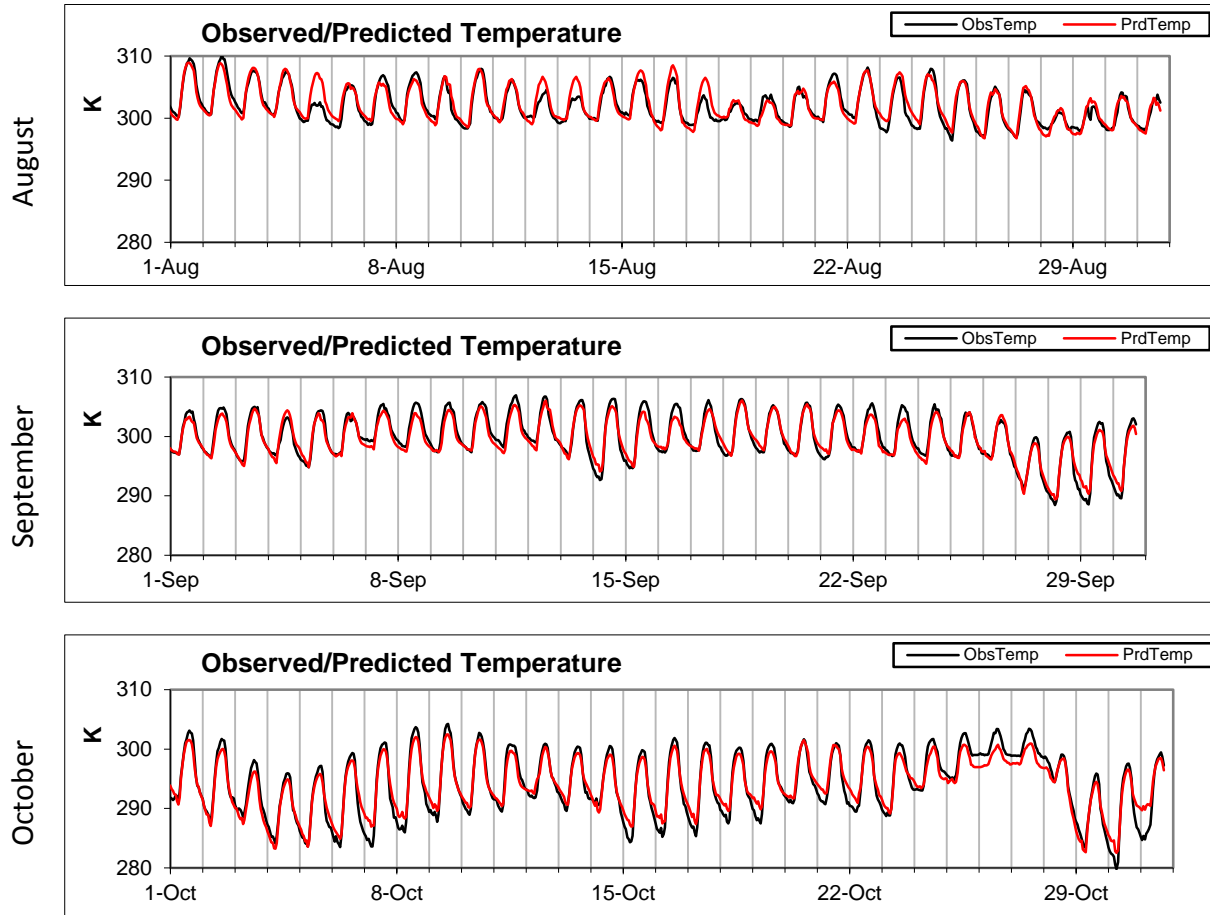


Figure 3-13. Hourly predicted (red) and observed (black) temperature averaged over all sites in southern Louisiana for August (top), September (middle) and October (bottom).

In both areas of Louisiana, WRF simulated larger diurnal variations in temperature in October than in August in accordance with observations. However, the predicted diurnal range in October was not as great as the observed as daytime highs were under predicted and nighttime lows were over predicted, as can be seen in both the time series and scatter plots. September daytime peaks also tended to be under predicted. WRF correctly predicted strong drops in temperature on September 27 and October 28, and smaller diurnal ranges on October 25-27, but those temperatures were under predicted.

WRF performed better in southern Louisiana, where over 90% of the predicted temperatures during the daytime hours on high ozone dates were within 2 K of the observed. In northern Louisiana, around 70 % of the hours on the episode dates were within 2 K of the observed.

Daily temperature statistics revealed somewhat scattered performance in both months in northern Louisiana. Southern Louisiana temperatures fared much better, especially in September when the daily temperature error never exceeded 2 K and the daily bias on the high

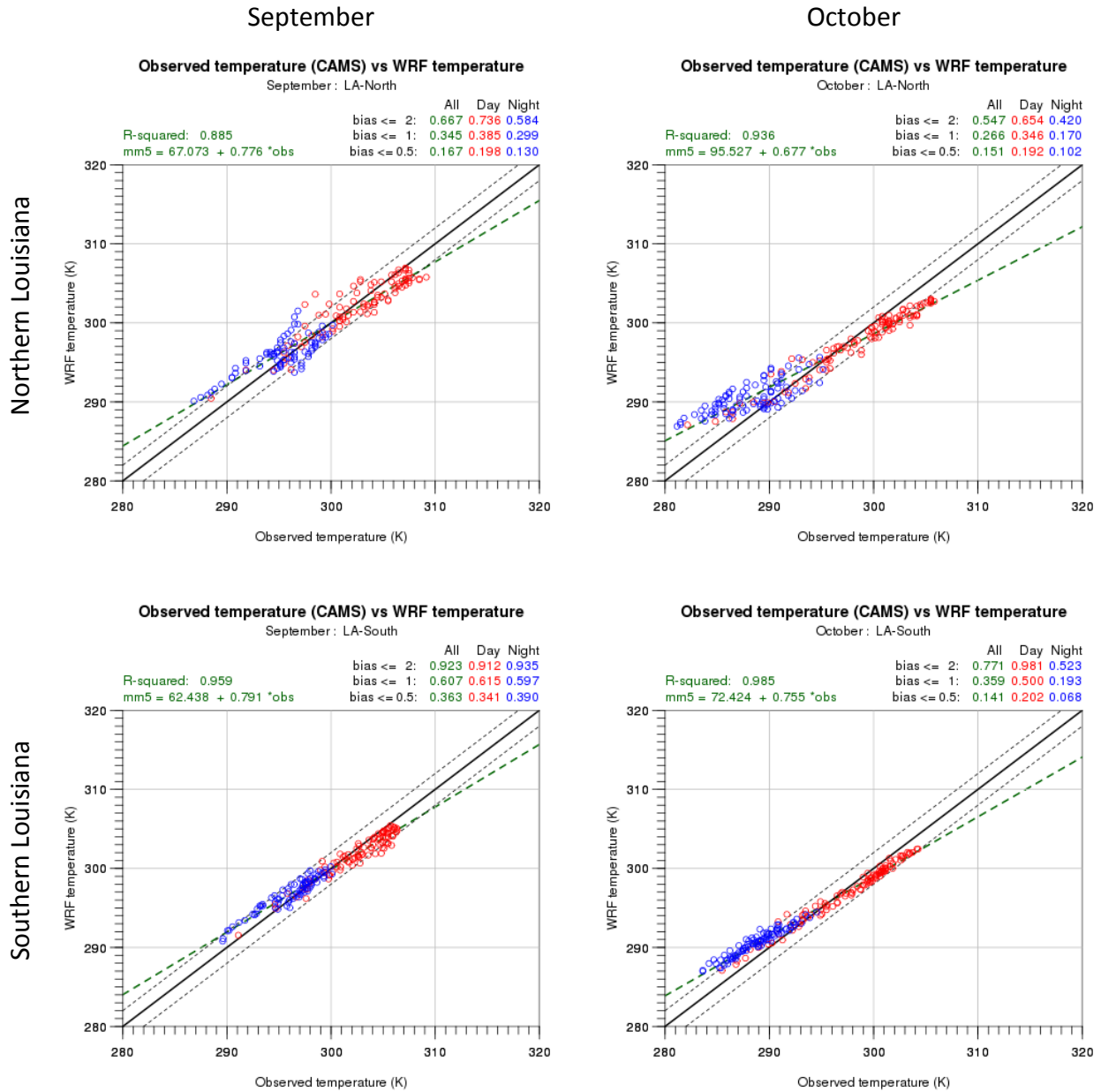


Figure 3-14. Scatter plots of hourly predicted and observed temperature on high ozone dates during September (left) and October (right) for northern Louisiana (top) and southern Louisiana (bottom). Red circles represent daytime hours (8 AM – 6 PM CST), blue represents nighttime hours (7 PM to 7 AM). The solid black diagonal line is the 1:1 perfect correlation line; the two black dashed lines represent the ±2 K bias envelope. Statistics show the regression line and the fraction of hours when the bias is between ±.5, 1, and 2 K.

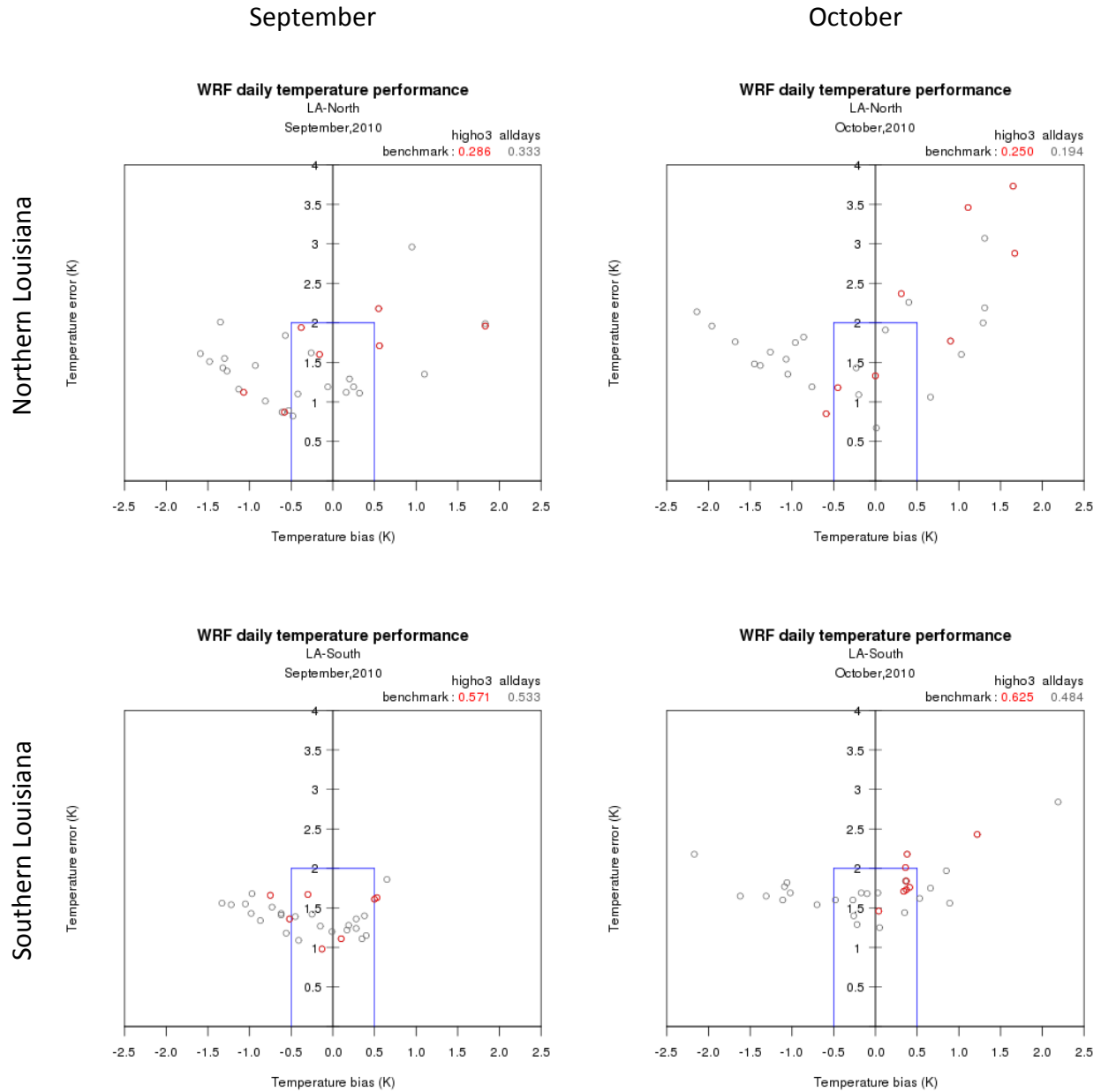


Figure 3-15. Soccer goal plots of daily temperature bias and error. Red circles highlight the high ozone dates.

ozone dates were inside or very close to the ± 0.5 K benchmark. October daily temperature statistics met the performance goals on 5 of the 8 high ozone dates. The daily biases on these 8 dates were all positive. Overall, this temperature performance is on par with our experience using WRF in other areas of the US.

3.4 Precipitation

Predicted 24-hour precipitation totals were compared to precipitation analysis fields from the Advanced Hydrologic Prediction Service (AHPS), which were downloaded from http://water.weather.gov/precip/p_download_new/2010/ and reformatted to match the LDEQ 4 km modeling domain. All totals were for the 24-hour period ending at 12 UTC (6 AM CST).

Ozone production rates are greater on sunny and warm days so little or no precipitation would be expected on the high ozone dates. For the most part, little cloudiness and precipitation was predicted over Louisiana on high observed ozone days. Instead of showing multiple precipitation plots on the high ozone dates when WRF correctly predicted dry conditions across Louisiana, we focused on two high ozone dates when there was precipitation – September 13 and 16. Figure 3-16 shows spatial plots of the observed and predicted 24-hour precipitation totals for two consecutive dates to include all hours of September 13. Figure 3-17 is similar, but for September 16.

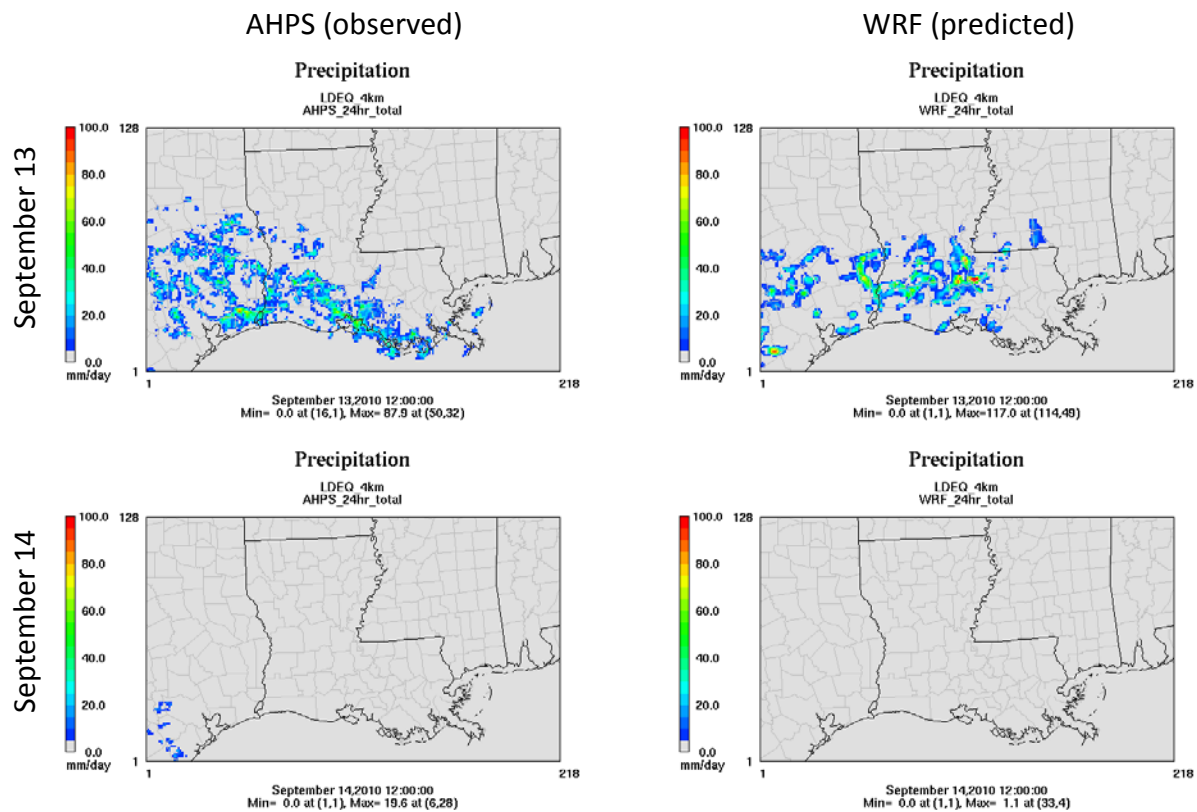


Figure 3-16. Observed (left) and predicted (right) 24-hour precipitation ending at 6 AM CST on September 13 (top) and 14 (bottom).

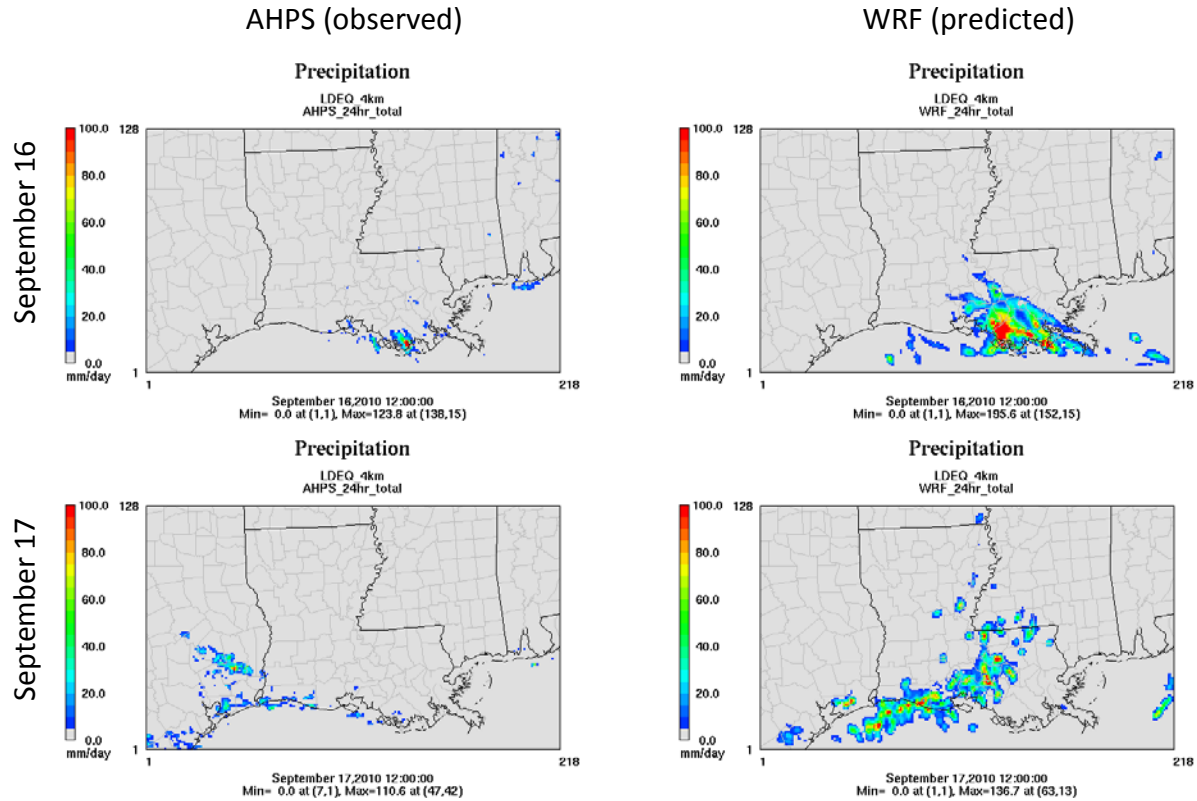


Figure 3-17. Observed (left) and predicted (right) 24-hour precipitation ending at 6 AM CST on September 16 (top) and 17 (bottom).

On September 13, WRF correctly predicted convective activity over southern Louisiana during the 24 hours ending at 6 AM on September 13, and dry conditions during the next 24 hours, which included all of the daytime hours of the high ozone date.

September 16 was one of the dates when WRF did not predict precipitation well over southern Louisiana. Precipitation in southeast Louisiana was over predicted during both the 24-hour periods ending at 6 AM on September 16 and 17. Fortunately, Shreveport was the only ozone monitor in Louisiana that observed 8-hour ozone greater than 75 ppb on September 16; WRF maintained dry conditions over northern Louisiana, as were observed.

Figure 3-18 compares the observed and predicted 24-hour precipitation fields on three other dates in which WRF corresponded well with the observed pattern.

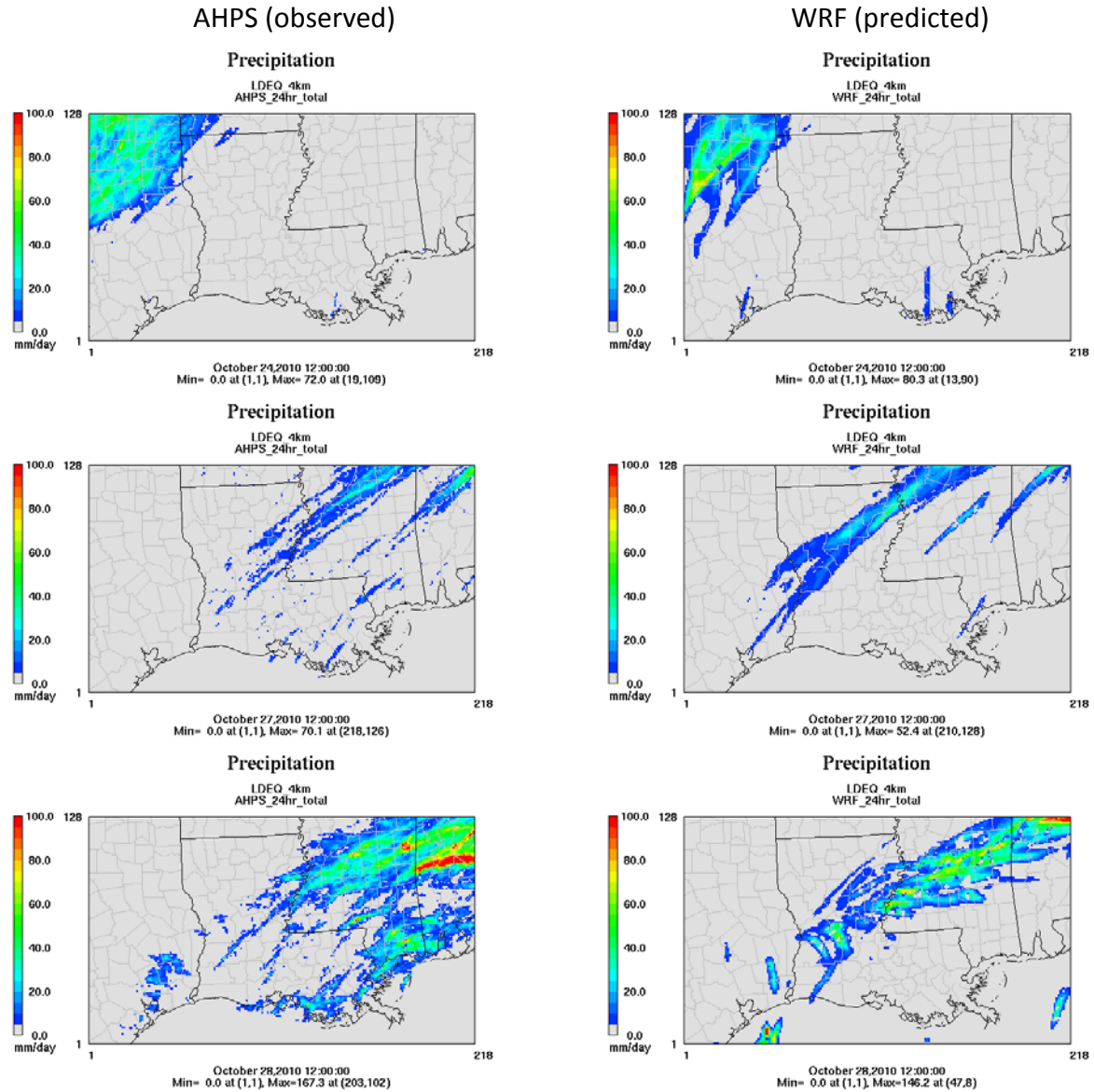


Figure 3-18. Daily observed (left) and predicted (right) precipitation on selected episode dates (October 24, 27, and 28).

3.5 Summary

A model performance evaluation was performed on the 4 km WRF meteorology, which was used to develop meteorology inputs for CAMx. Performance for wind speed, wind direction, and temperature was examined by computing hourly and daily statistics from all meteorology stations in northern and southern Louisiana. WRF performance in southern Louisiana in September was very good for all three variables. In October, the daytime wind speed and temperatures in southern Louisiana were both slightly under predicted. The former could lead to more stagnation and higher ozone, which may be compensated by slower ozone production rates due to the cooler predicted temperatures. Performance was consistently better in southern Louisiana than northern Louisiana, where daytime wind speeds and temperatures were also under estimated.

Overall, performance for wind speed and direction were markedly better than usually achieved in other WRF applications across the country. Temperature performance was on par with other applications. Precipitation performance on high ozone days was quite good, and did not exhibit the usually high degree of over prediction so often identified in past applications.

4.0 PHOTOCHEMICAL MODEL INPUTS

Inputs for the CAMx photochemical model were prepared for the Louisiana September-October 2010 modeling period. Inputs include emissions, meteorology, landuse, albedo-haze-ozone, photolysis rates, and initial/boundary conditions. This section describes details on the creation of all input files except the emissions, which are documented separately in Section 5.

4.1 Meteorology

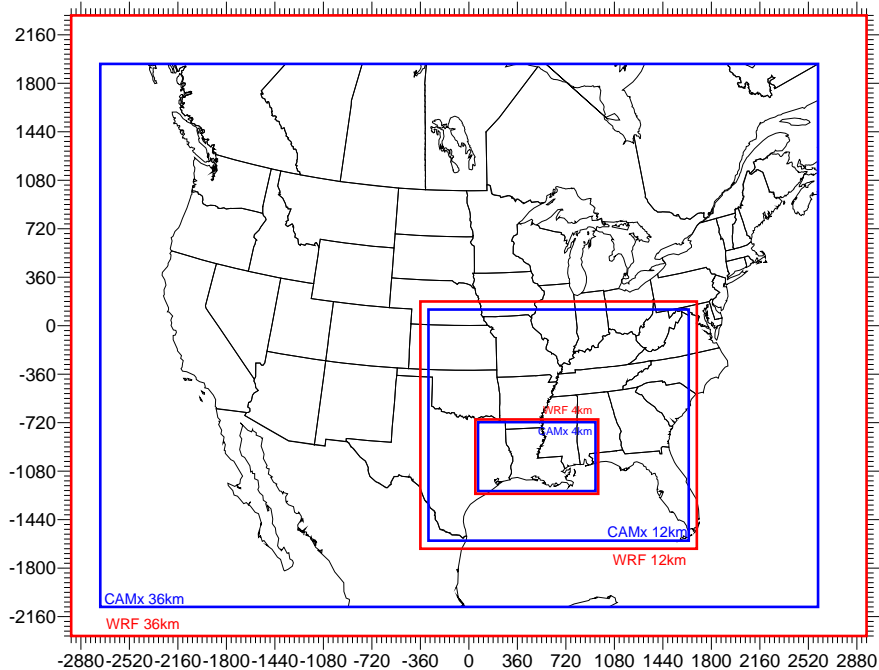
WRF version 3.3.1 was run from August through October 2010 to cover the LDEQ 36, 12, and 4 km photochemical modeling domains (Alpine, 2012). The WRF output was then used to generate CAMx meteorological input files using the WRFCAMx version 3.3 converter. The CAMx and WRF domains are shown in Figure 4-1, where the CAMx domain was at least 5 grid cells inside any of the WRF boundaries. The Lambert Conformal Projection (LCP) in WRF was the same as CAMx, where the projection center was at 40°N/97°W with true latitudes of 33°N and 45°N.

Six binary CAMx meteorological files are generated by WRFCAMx for each simulation date, which include the following hourly-varying three-dimensional fields:

- Height (m)/pressure (mb)
- Wind (as separate east-west and north-south components, m/s)
- Temperature (K)
- Vertical diffusivity (m^2/s)
- Humidity (ppm)
- Cloud and rain water (g/m^3)

A 26-category landuse file is also output, but is not used because it is derived from WRF's dominant landuse category in each grid cell. A better alternative is to create landuse files based on high-resolution land cover datasets, processed with Geographic Information System (GIS) software, from which to develop the fraction of each land cover category in each grid cell. Details on the GIS-based landuse files are provided below.

WRFCAMx was configured to time-shift the meteorology from its native Coordinated Universal Time (UTC) to Central Standard Time (CST) and extract 27 vertical layers of meteorological data up to 11 km, near the top of the troposphere, using the layer structure shown in Table 4-1. A layer averaging scheme that combined multiple WRF layers into single CAMx layers was applied to layers above 3 km to focus on the photochemical simulation in the lower to mid troposphere and to reduce computational time.



Louisiana WRF/CAMx Modeling Domains

- CAMx
 - 36 km: 148 x 112 (-2736, -2088) to (2592, 1944)
 - 12 km: 161 x 143 (-300, -1596) to (1632, 120)*
 - 04 km: 218 x 128 (68, -1228) to (940, -716)*
- WRF
 - 36 km: 165 x 129 dot points (-2952, -2304) to (2952, 2304)
 - 12 km: 172 x 154 dot points (-360, -1656) to (1692, 180)
 - 04 km: 229 x 139 dot points (48, -1248) to (960, -696)

* includes buffer cells

Figure 4-1. Map of CAMx and WRF modeling domains.

WRF/CAMx was set to diagnose sub-grid clouds in the 36 km and 12 km domains, but not in the 4 km domain, where grid-scale convection was explicitly treated by WRF’s resolved cloud microphysics algorithm.

WRF/CAMx includes several methods for computing the vertical turbulent exchange coefficients (or “diffusivities”, K_v). Since WRF was configured with the Mellor-Yamada-Janjic (MYJ) turbulent kinetic energy (TKE) boundary layer scheme, the MYJ TKE option was selected to compute the vertical diffusivities from the TKE fields output by WRF. The minimum K_v was set to $0.1 \text{ m}^2/\text{s}$.

An additional program (KVPATCH) is often applied to the vertical diffusivity files to enhance mixing in specific environments. Two patches within the program were applied. The first enhances the minimum K_v floor in urban areas according to the profile methodology of O’Brien (1970). This maintains low-level urban mixing in the stable nighttime hours with the lowest 200 m to account for urban heating and turbulence induced by the urban canopy. The second patch

Table 4-1. CAMx and WRF vertical layer structures.

WRF Meteorological Model				CAMx Air Quality Model		
Layer Index	Sigma	Height (m)	Depth (m)	Layer Index	Height (m)	Depth (m)
43	0.000	18872	736			
42	0.010	18135	970			
41	0.025	17165	1110			
40	0.045	16055	959			
39	0.065	15096	1045			
38	0.090	14050	918			
37	0.115	13132	975			
36	0.145	12157	869			
35	0.175	11288	909	27	11288	2678
34	0.210	10379	931			
33	0.250	9449	839			
32	0.290	8610	765	26	8610	2044
31	0.330	7845	704			
30	0.370	7140	574			
29	0.405	6566	540	25	6566	1050
28	0.440	6026	510			
27	0.475	5516	484	24	5516	879
26	0.510	5033	396			
25	0.540	4637	380	23	4637	745
24	0.570	4258	365			
23	0.600	3893	352	22	3893	691
22	0.630	3541	339			
21	0.660	3202	328	21	3202	328
20	0.690	2874	317	20	2874	317
19	0.720	2556	307	19	2556	307
18	0.750	2249	249	18	2249	249
17	0.775	2000	243	17	2000	243
16	0.800	1757	237	16	1757	237
15	0.825	1520	232	15	1520	232
14	0.850	1288	136	14	1288	136
13	0.865	1152	135	13	1152	135
12	0.880	1017	133	12	1017	133
11	0.895	884	131	11	884	131
10	0.910	753	86	10	753	86
9	0.920	667	86	9	667	86
8	0.930	581	85	8	581	85
7	0.940	496	84	7	496	84
6	0.950	412	84	6	412	84
5	0.960	328	83	5	328	83
4	0.970	245	82	4	245	82
3	0.980	163	82	3	163	82
2	0.990	81	49	2	81	49
1	0.996	32	32	1	32	32

enhances vertical diffusivities through the depth of convective clouds capping the daytime boundary layer, which is often suppressed within models such as WRF.

4.2 Landuse

Landuse within CAMx is specified through a binary input file (SURFACE) that contains a time-invariant two-dimensional gridded field of landuse distribution. For the Zhang dry deposition scheme, the fractional distributions of 26 landuse categories and two-dimensional fields of leaf area index (LAI) are specified for each grid cell. These are used to define surface resistances for dry deposition calculations and to set default surface roughness lengths. These landuse categories are described in Table 4-2 for the Zhang dry deposition scheme.

The landuse/landcover (LULC) data were extracted from the North America Land Cover (NALC) database for the year 2000 (Latifovic, et al. 2002). NALC was developed jointly by the Natural Resources Canada - Canada Centre for Remote Sensing, and the USGS EROS Data Center as part of the larger Global Land Cover 2000 project implemented by the Global Vegetation Monitoring Unit, Joint Research Center (JRC) of the European Commission. The North American database was compiled using satellite data during the 2000 growing season at a spatial resolution of 1-km. The data are available as GIS raster datasets for each continent, in a geodetic coordinate system and can be obtained from the project website at http://edc2.usgs.gov/glcc/nadoc2_0.php. The NALC land use classification scheme includes 29 separate categories as presented in Table 4-3. The landuse classes available in the source GIS database were cross referenced to those required for the Zhang dry deposition schemes used by CAMx. Table 4-4 shows the cross references used for the Zhang scheme.

Gridded LAI data are an optional input for use with the Zhang dry deposition scheme in CAMx. We derived gridded LAI inputs from the Model of Emissions of Gases and Aerosols from Nature (MEGAN) biogenic emissions model. The data are provided as un-projected global 30 arc second (~1-km horizontal resolution) GIS raster datasets. LAI is defined as the ratio of total upper leaf surface area divided by the surface area of the land on which the vegetation grows. The LAI data available with the MEGAN databases represent average values over each raster, in units of m^2/m^2 and are available as monthly averaged datasets for calendar year 2001. The LAI data can be obtained as ArcGIS raster GRID files from <http://acd.ucar.edu/~guenther/MEGAN/MEGAN.htm>.

A suite of GIS and Perl-based processors were used to prepare landcover and LAI input datasets for CAMx. Arc Macro Language (AML) scripts were used to process the raster-based and vector-based GIS data and export text datasets for subsequent processing with Perl scripts and FORTRAN programs. User-defined options are used to specify various parameters including the definition of output modeling domains, map projection parameters, and the input LULC and MEGAN LAI databases. The CAMx landuse file was prepared for the LDEQ 36/12/4km grids. Figure 4-2 shows a spatial map displaying the dominant land cover category for each grid cell in the 4 km domain.

Table 4-2. CAMx landuse categories for the Zhang dry deposition scheme.

Category Number	Land Cover Category
1	Water
2	Ice
3	Inland Lake
4	Evergreen Needleleaf Trees
5	Evergreen Broadleaf Trees
6	Deciduous Needleleaf Trees
7	Deciduous Broadleaf Trees
8	Tropical Broadleaf Trees
9	Drought Deciduous Trees
10	Evergreen Broadleaf Shrubs
11	Deciduous Shrubs
12	Thorn Shrubs
13	Short Grass and Forbs
14	Long Grass
15	Crops
16	Rice
17	Sugar
18	Maize
19	Cotton
20	Irrigated Crops
21	Urban
22	Tundra
23	Swamp
24	Desert
25	Mixed Wood Forests
26	Transitional Forest

Table 4-3. NALC LULC classification.

Code	Description
1	Tropical or Sub-tropical Broadleaved Evergreen Forest - Closed Canopy
2	Tropical or Sub-tropical Broadleaved Deciduous Forest - Closed Canopy
3	Temperate or Sub-polar Broadleaved Deciduous Forest - Closed Canopy
4	Temperate or Sub-polar Needleleaved Evergreen Forest - Closed Canopy
5	Temperate or Sub-polar Needleleaved Evergreen Forest - Open Canopy
6	Temperate or Sub-polar Needleleaved Mixed Forest - Closed Canopy
7	Temperate or Sub-polar Mixed Broadleaved or Needleleaved Forest - Closed Canopy
8	Temperate or Sub-polar Mixed Broadleaved or Needleleaved Forest - Open Canopy
9	Temperate or Subpolar Broadleaved Evergreen Shrubland - Closed Canopy
10	Temperate or Subpolar Broadleaved Deciduous Shrubland - Open Canopy
11	Temperate or Subpolar Needleleaved Evergreen Shrubland - Open Canopy
12	Temperate or Sub-polar Mixed Broadleaved and Needleleaved Dwarf-Shrubland - Open Canopy
13	Temperate or Subpolar Grassland
14	Temperate or Subpolar Grassland with a Sparse Tree Layer
15	Temperate or Subpolar Grassland with a Sparse Shrub Layer
16	Polar Grassland with a Sparse Shrub Layer
17	Polar Grassland with a Dwarf-Sparse Shrub Layer
18	Cropland
19	Cropland and Shrubland/woodland
20	Subpolar Needleleaved Evergreen Forest Open Canopy - lichen understory
21	Unconsolidated Material Sparse Vegetation (old burnt or other disturbance)
22	Urban and Built-up
23	Consolidated Rock Sparse Vegetation
24	Water bodies
25	Burnt area (resent burnt area)
26	Snow and Ice
27	Wetlands
28	Herbaceous Wetlands
29	Tropical or Sub-tropical Broadleaved Evergreen Forest - Open Canopy

Table 4-4. LULC mapping between the 29 NALC categories and the 26 CAMx categories.

GRID-CODE	CAMx-CODE	Description
1	8	Tropical or Sub-tropical Broadleaved Evergreen Forest - Closed Canopy
2	8	Tropical or Sub-tropical Broadleaved Deciduous Forest - Closed Canopy
3	7	Temperate or Sub-polar Broadleaved Deciduous Forest - Closed Canopy
4	4	Temperate or Sub-polar Needleleaved Evergreen Forest - Closed Canopy
5	4	Temperate or Sub-polar Needleleaved Evergreen Forest - Open Canopy
6	25	Temperate or Sub-polar Needleleaved Mixed Forest - Closed Canopy
7	25	Temperate or Sub-polar Mixed Broadleaved or Needleleaved Forest - Closed Canopy
8	25	Temperate or Sub-polar Mixed Broadleaved or Needleleaved Forest - Open Canopy
9	10	Temperate or Subpolar Broadleaved Evergreen Shrubland - Closed Canopy
10	11	Temperate or Subpolar Broadleaved Deciduous Shrubland - Open Canopy
11	10	Temperate or Subpolar Needleleaved Evergreen Shrubland - Open Canopy
12	10	Temperate or Sub-polar Mixed Broadleaved and Needleleaved Dwarf-Shrubland - Open Canopy
13	14	Temperate or Subpolar Grassland
14	14	Temperate or Subpolar Grassland with a Sparse Tree Layer
15	13	Temperate or Subpolar Grassland with a Sparse Shrub Layer
16	22	Polar Grassland with a Sparse Shrub Layer
17	22	Polar Grassland with a Dwarf-Sparse Shrub Layer
18	15	Cropland
19	15	Cropland and Shrubland/woodland
20	4	Subpolar Needleleaved Evergreen Forest Open Canopy - lichen understory
21	13	Unconsolidated Material Sparse Vegetation (old burnt or other disturbance)
22	21	Urban and Built-up
23	24	Consolidated Rock Sparse Vegetation
24	1	Water bodies
25	24	Burnt area (resent burnt area)
26	2	Snow and Ice
27	23	Wetlands
28	23	Herbaceous Wetlands
29	10	Tropical or Sub-tropical Broadleaved Evergreen Forest - Open Canopy

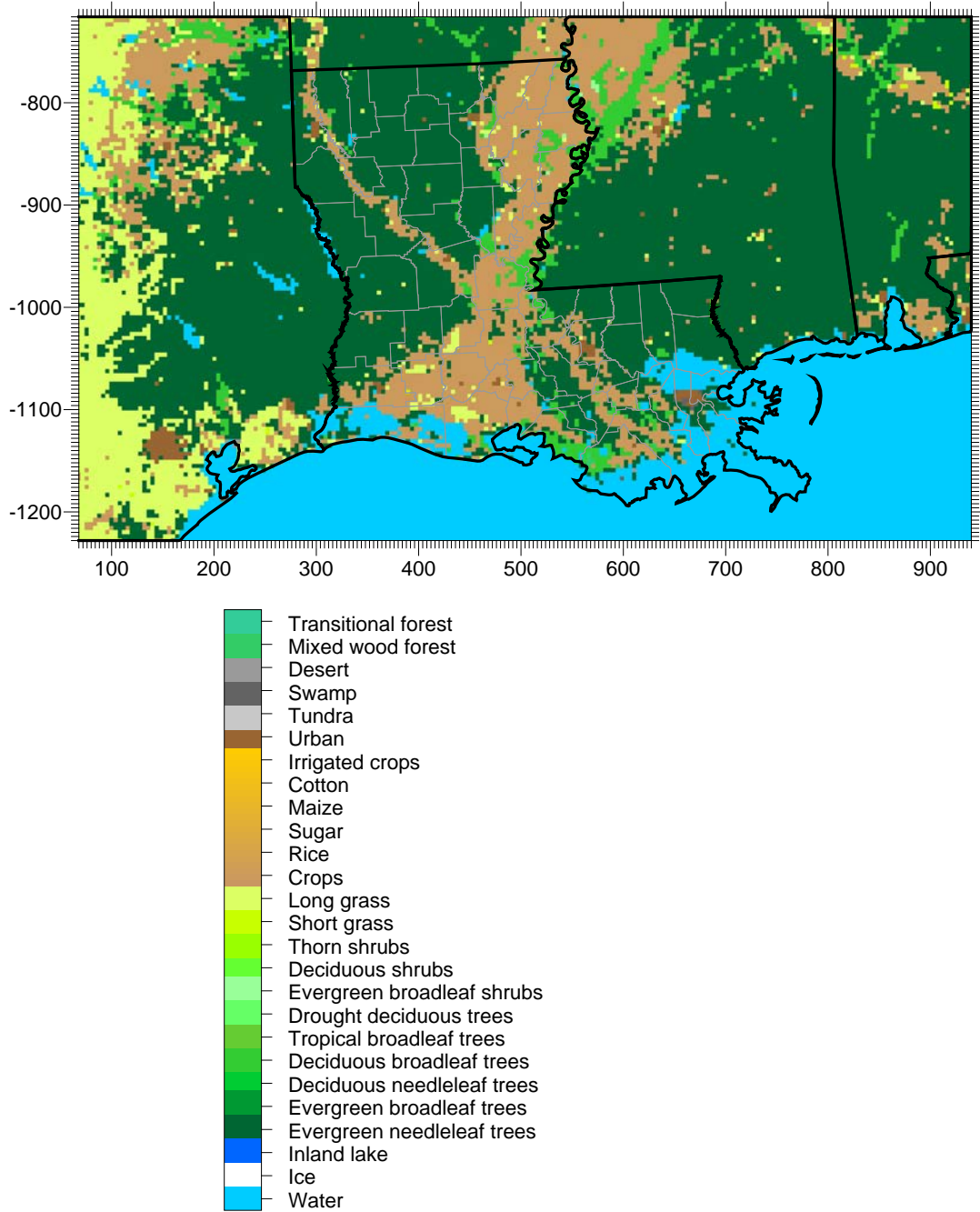


Figure 4-2. Dominant landuse type in each grid cell of the 4 km CAMx domain.

4.3 Albedo-Haze-Ozone

The CAMx preprocessor, AHOMAP version 4, was used to create a CAMx text input file containing gridded surface albedo, total atmospheric column haze opacity, and total atmospheric ozone column data. The program reads in CAMx landuse files for all domains to be modeled and daily Ozone Monitoring Instrument (OMI) data in 1 degree resolution, which can be downloaded for each episode date from <http://ozoneaq.gsfc.nasa.gov/OMIOzone.md>. All daily ozone column datasets for each month of the episode were run together to yield one albedo-haze-ozone file per month. For haze opacity, a default uniform field was specified representing a typical continental aerosol loading. Optional fields such as snow cover, surface roughness, and drought stress were not added.

4.4 Clear-Sky Photolysis Rates

Version 4.8 of the TUV radiative transfer model, developed by the National Center for Atmospheric Research (NCAR), reads the ranges of albedo, haze opacity and ozone column and creates a lookup table of clear-sky photolysis rates for a range of heights above the ground and solar zenith angles. The TUV program was run for each month in the modeling period to develop rates for the specific photolysis reactions defined by the Carbon Bond version 6 (CB6) and Carbon Bond 2005 (CB05) chemical mechanism. The photolysis rates are internally adjusted within CAMx for hourly cloud conditions within each grid column.

4.5 Initial and Boundary Conditions

Initial conditions are used to represent an initial three-dimensional concentration distribution throughout the master grid from which the simulation starts. Boundary conditions are used to represent concentration patterns outside of the outer CAMx modeling domain that are subsequently transported into the grid system. Data for initial and boundary conditions were derived from the output of the global Model for Ozone and Related chemical Tracers, version 4 (MOZART-4). MOZART outputs are available from <http://www.acd.ucar.edu/wrf-chem/mozart.shtml> and were downloaded for the 2010 episode.

MOZART was run with 1.9 by 2.5 degree horizontal resolution and 56 vertical layers, and output data in 6-hour intervals. By comparison, MOZART data used for the 2006 Baton Rouge ozone simulation had 2.8 by 2.8 degree resolution with 28 vertical layers.

Native MOZART-4 output data in netCDF format were first converted to IOAPI format using the NCF2IOAPI program. Then, the MOZART2CAMx program horizontally and vertically interpolated the data onto the CAMx domain and remapped the chemical species to CB6 and CB05 speciation. Daily boundary condition files were generated for each date to be simulated by CAMx with the assumption that each MOZART 6-hourly time period was representative of the next six hours in CAMx. Boundary conditions were then time shifted from UTC to CST; initial conditions, based on MOZART fields at 6 AM UTC (midnight CST) on August 17, did not need to be time shifted.

5.0 DEVELOPMENT OF 2010 BASE YEAR EMISSIONS

Emission estimates were prepared for the September-October 2010 Base Year modeling period. Details on the creation of certain emission input files for the CAMx photochemical model are described in this section, specifically including Louisiana and Gulf of Mexico anthropogenic sources, and biogenic and fire sources throughout the North American modeling domain. Alpine Geophysics developed anthropogenic emission estimates for the remainder of the North American modeling domain.

5.1 Introduction

A key component of an ozone modeling study is the underlying emissions inventory. Spatially, temporally and chemically resolved estimates of volatile organic compounds (VOC), nitrogen oxides (NO_x), and carbon monoxide (CO) from sources such as industries, electric generating units (EGUs), on-road motor vehicles, and vegetation are critical inputs to an air quality model. This section documents the development of certain components of the 2010 Base Year emission inventories, and the preparation of CAMx-ready emission inputs for the 4, 12, and 36 km modeling domains (Figure 4-1).

Emphasis was placed on developing emissions estimates within the State of Louisiana (LA). EPS3 was used to convert the LA emission inventory into the hourly, chemically speciated, and gridded formats needed by CAMx. Other emission modeling tools were used to estimate emissions from specific categories; MEGAN and BEIS for biogenics, MOVES/CONCEPT for on-road, NMIM for non-road sources, and FINN for wildfires, and agricultural/prescribed burning.

EPS3 requires emission inventory files and support data (cross-reference files, spatial surrogates, temporal and speciation profiles) as input. Area and point source emissions in Louisiana were prepared by ERG, working closely with the LDEQ. Day- and hour-specific 2010 NO_x emissions for sources throughout the modeling domain that are subject to continuous emissions monitoring (CEM) under the Title V Acid Rain Program (ARP) were extracted from the EPA's database and were reconciled against, and supplemented with, data provided by LDEQ. Gulf-wide offshore emissions were developed by ERG from the BOEM 2008 Gulf-wide Emission Inventory Study. Biogenic and fire emissions were estimated for all three modeling grids for each hour of each day of the September and October 2010 modeling period.

5.2 Emissions in Louisiana

EPS3 was set up to process criteria pollutant emissions into the CAMx configuration using the Carbon Bond version 6 (CB6) chemical mechanism. Emissions for the following model species were generated:

Nitrogen oxides:	NO, NO ₂ , HONO
Volatile organic compounds:	ACET, ALD2, ALDX, BENZ, ETH, ETHA, ETHY, ETOH, FORM, IOLE, ISOP, KET, MEOH, OLE, PAR, PROP, TERP, TOL, XYL
Carbon monoxide:	CO

Speciation to CB6 compounds was performed by applying standard source-specific profiles derived from the EPA SPECIATE 4.3 database. These profiles were assigned to each of the source categories contained in the raw emissions inventory files using default EPA cross-references. Because of its backward-compatibility, CB6 speciation can be subsequently reverted back to CB05 by combining certain CB6-specific VOCs to the generic alkane “PAR” as follows:

BENZ → 1 PAR (+ 5 “non-reactive” moles in compounds that are ignored);
 PROP → 1.5 PAR (+ 1.5 “non-reactive”)
 ACET → 3 PAR
 ETHY → 1 PAR
 KET → 1 PAR,

where emissions for the five CB6 species listed above are set to zero after the conversion.

Temporal allocation for most source categories was performed by applying default EPA seasonal, monthly, day-of-week, and hourly profiles and cross-references for the inventory components.

Gridding surrogates were developed for the 4 km modeling domain using the EPA Spatial Allocator tool that is available from <http://www.cmascenter.org/index.cfm>. Typical surrogate types were created including: population, various road types and other transportation networks, agriculture, residential, commercial and industrial land, retail, and water bodies. The EPA Spatial Allocator tool creates surrogates formatted for the SMOKE emissions model, which were reformatted to the EPS3 requirements. The surrogate list used for spatial allocation of LA emissions is listed in Table 5-1.

EPS3 generated model-ready hourly point, area, non-road mobile, and on-road mobile emissions of CB6 compounds on the 36/12/4 km grid system. Annual and ozone season emission estimates were used to develop a representative weekday, Saturday and Sunday. Day specific estimates were developed for on-road mobile, acid rain point, and fire sources. The remainder of this sub-section details the emissions processing by source category.

1.1.1 Point Sources

The 2010 point source emissions were based upon a point source inventory provided by LDEQ (2012a). In consultation with LDEQ staff, the modeling team partitioned the inventory into two groups: those electricity generating units that are subject to the EPA’s Clean Air Markets Division (CAMD) Acid Rain Program (ARP), and all other point sources.

As required by law, units subject to ARP must submit their hourly nitrogen oxide (NOx) and sulfur oxide (SOx) emissions data to the EPA. Because these data were reported on an hourly basis, these data are considered to provide a more accurate representation of the temporal distribution of emissions compared to annual emission estimates. In order to avoid double-counting, all ARP units and their associated emissions were removed from LDEQ’s point source

Table 5-1. Spatial surrogate codes developed for Louisiana emissions processing.

SURROGATE	SURROGATE CODE	SURROGATE	SURROGATE CODE
Population	100	Commercial, Industrial and Institutional	520
Housing	110	Golf Courses, Institutional, Industrial and Commercial	525
Urban Population	120	Single Family Residential	527
Rural Population	130	Residential - High Density	530
Housing Change	137	Residential + Commercial + Industrial + Institutional + Government	535
Housing Change and Population	140	Retail Trade	540
Residential Heating - Natural Gas	150	Personal Repair	545
Residential Heating - Wood	160	Retail Trade plus Personal Repair	550
0.5 Residential Heating - Wood plus 0.5 Low Intensity Residential	165	Professional/Technical plus General Government	555
Residential Heating - Distillate Oil	170	Hospital	560
Residential Heating - Coal	180	Medical Office/Clinic	565
Residential Heating - LP Gas	190	Heavy and High Tech Industrial	570
Urban Primary Road Miles	200	Light and High Tech Industrial	575
Rural Primary Road Miles	210	Food, Drug, Chemical Industrial	580
Urban Secondary Road Miles	220	Metals and Minerals Industrial	585
Rural Secondary Road Miles	230	Heavy Industrial	590
Total Road Miles	240	Light Industrial	595
Urban Primary plus Rural Primary	250	Industrial plus Institutional plus Hospitals	596
0.75 I Roadway Miles plus 0.25 Population	255	Gas Stations	600
Total Railroad Miles	260	Refineries and Tank Farms	650
Class 1 Railroad Miles	270	Refineries , Tank Farms, and Gas Stations	675
Class 2 and 3 Railroad Miles	280	Airport Points	710
Low Intensity Residential	300	Airport Areas	700
Total Agriculture	310	Military Airports	720
Orchards/Vineyards	312	Navigable Waterway Miles	807
Forest Land	320	Marine Ports	800
Strip Mines/Quarries	330	Navigable Waterway Activity	810
Land	340	Golf Courses	850
Water	350	Mines	860
Rural Land Area	400	Wastewater Treatment Facilities	870
Commercial Land	500	Drycleaners	880
Industrial Land	505	Commercial Timber	890
Commercial plus Industrial	510	Gulf of Mexico non-platform	990
Commercial plus Institutional Land	515		

database. However, only ARP units were removed at any given facility; any non-ARP units were left in the database unchanged.

The 2010 hourly emissions data for all units subject to ARP were downloaded from U.S. EPA's Air Markets Program Data website (EPA, 2012). Because only NO_x and SO_x emissions data were reported to ARP, VOC and CO ratios were used to estimate hourly VOC and CO emissions. Annual unit-specific VOC-to-NO_x ratios were calculated using data from LDEQ's point source database and then applied to the hourly NO_x emissions for ARP units to estimate hourly VOC emissions; a similar CO-to-NO_x ratio was developed to estimate hourly CO emissions for ARP units.

Emissions from the LDEQ point source database for all other non-ARP point sources were incorporated into the inventory without any adjustments. However, some basic quality assurance checks were performed on the point source data, including review of the largest emitters, review of important sectors such as electricity generation and refineries, and visual review of plotted stack coordinate data to ensure that all coordinates were located within the State of Louisiana. The 2010 ARP hourly emissions data was compared with the annual emission estimates contained in the LDEQ point source inventory database. In general, the summation of the 2010 hourly emissions data for the units subject to ARP equaled the annual estimates. However, in a few instances the summation of the 2010 hourly emissions data slightly exceeded the annual estimates. In these cases, it was assumed that the hourly emissions reported to EPA were correct.

Non-ARP point sources report annual emissions as tons per year (TPY). These sources were temporally allocated to month, day of week, and hours, according to source category code using default EPA profiles and cross-reference files. All point source emissions were speciated to CB6 compounds using default EPA profiles and cross-reference files. All acid rain point sources were treated as elevated sources. The non-ARP points were processed as elevated sources when stack information indicated a sufficient plume rise to warrant elevated treatment. All point source emissions were located in the CAMx grid system according to their reported coordinates.

5.2.1 Area Sources

Area sources comprise stationary sources that are not identified as individual points and are distributed over a large spatial extent (i.e. parish). Annual parish-level area source emissions inventory data were provided by the LDEQ (2012b). The inventory data were taken from the 2009 attainment demonstration for nitrogen oxides (NO_x), carbon monoxide (CO), and volatile organic compounds (VOC). Because of the proximity of the year for which data were obtained, it was decided that 2009 area source estimates would be used for 2010 without any projection. All data were checked for completeness (e.g., combustion categories had NO_x, CO, and VOC emissions; solvent evaporation categories had VOC; all parishes had solvent evaporation and fuel combustion categories; etc.).

The VOC emissions were speciated to CB6 compounds. All sources were temporally allocated to month of year, day of week and hour of day using the EPA defaults by source category. The emissions were spatially allocated to the CAMx grid system by mapping source category code to a spatial surrogate code using the default EPA cross-reference file.

5.2.2 On-Road Mobile Sources

On-road mobile emissions are pollutants emitted from highway motor vehicles during both driving operation and while parked. However, emissions from the refueling of motor vehicles at service stations (Stage 2 Refueling) are included under area sources. Two models were used to develop the on-road mobile inventory for the full state of Louisiana:

- MOTO Vehicle Emission Simulator (MOVES);
- CONSolidated Community Emissions Processor Tool, Motor Vehicle (CONCEPT MV).

5.2.2.1 MOVES

This EPA regulatory model was run in the mode referred to as Emission Rate Calculation Type for individual Louisiana parishes using the County Scale/Domain with local data inputs provided by the LDEQ. Under this particular MOVES configuration, the model outputs emission factor tables in units of grams/mile or grams/vehicle/hour, depending on emission process (e.g. start or running). MOVES was run under a wide range of conditions to produce lookup tables so that relatively few MOVES runs produced emission factors applicable to many hours and grid cells. The model and database version used for this work were MOVES2010a and movesdb20100830, respectively.

The important MOVES inputs for emission factor calculations include temperature, humidity, fuels, inspection and maintenance (I/M) programs, vehicle fleet age distribution, and the ratio of vehicle-miles traveled (VMT) to vehicle population. The full range of meteorological conditions input to MOVES was determined by an analysis of WRF meteorological data using ENVIRON's MET2MOVES tool. LDEQ provided the other MOVES input data, including:

- Age Distribution, Fuels and I/M programs, by parish
- Annual average day VMT by road type and parish
- Vehicle population by parish for four source types:
 1. Motorcycle
 2. Passenger Car
 3. Passenger Truck
 4. Light Commercial Truck

After analysis of the MOVES input data, three distinct groups of parishes were selected due to their unique combinations of age distribution, fuel properties, and I/M programs. Table 5-2 shows the assignment of parish to the three representative parishes.

Table 5-2. Representative Louisiana parish groups for MOVES model runs.

East Baton Rouge Parish	Jefferson Parish	St. Tammany Parish			
<i>I/M and RVP controls</i>	<i>RVP controls only</i>	<i>Neither I/M nor RVP controls</i>			
Ascension	Beauregard	Acadia	De Soto	Natchitoches	Tangipahoa
East Baton Rouge	Calcasieu	Allen	East Carroll	Ouachita	Tensas
Iberville	Grant	Assumption	East Feliciana	Plaquemines	Terrebonne
Livingston	Jefferson	Avoyelles	Evangeline	Rapides	Union
West Baton Rouge	Lafayette	Bienville	Franklin	Red River	Vermilion
	Lafourche	Bossier	Iberia	Richland	Vernon
	Orleans	Caddo	Jackson	Sabine	Washington
	Pointe Coupee	Caldwell	Jefferson Davis	St. Helena	Webster
	St. Bernard	Cameron	La Salle	St. John the Baptist	West Carroll
	St. Charles	Catahoula	Lincoln	St. Landry	West Feliciana
	St. James	Claiborne	Madison	St. Martin	Winn
	St. Mary	Concordia	Morehouse	St. Tammany	

LDEQ specified fuel formulations and I/M properties by parish. For September 1-15, the Reid Vapor Pressure (RVP) of gasoline used was 7.8 psi in the 17 parishes represented by East Baton Rouge and Jefferson, with 9.0 psi in the remaining 47 parishes represented by St. Tammany in Table 5-2. For September 16 through Oct 31, LDEQ specified 11.5 psi RVP in all parishes. MOVES defaults were used for all other non-RVP gasoline parameters and for diesel fuel.

LDEQ specified using 2005 I/M programs in the 5-parish nonattainment area represented by East Baton Rouge in Table 5-2. The I/M program parameters shown below in MOBILE6-format were converted to MOVES-equivalent test standard identifications according to Table 3.10.4 of the technical guidance (EPA, 2010). Also per guidance (Appendix A-3 in EPA, 2010), the MOBILE6 vehicle classes were mapped to MOVES source types through the use of the MOVES I/M compliance factor percent.

* 2005 I/M and ATP for Baton Rouge Non-attainment Area

```

* I/M program On Board Diagnostics (exhaust)
*
I/M PROGRAM      : 1 2002 2050 1 TRC OBD I/M
I/M MODEL YEARS : 1 1996 2050
I/M VEHICLES    : 1 22222 21111111 1
I/M STRINGENCY  : 1 20.0
I/M EFFECTIVENESS : 0.75 0.75 0.75
I/M COMPLIANCE  : 1 96.0
I/M WAIVER RATES : 1 0.0 0.0
I/M GRACE PERIOD : 1 2
    
```

```

*
* Baton Rouge I/M programs (evaporative)
*
I/M PROGRAM      : 2 2000 2001 1 TRC GC
I/M MODEL YEARS : 2 1980 2001
    
```

```

I/M VEHICLES      : 2 22222 21111111 1
I/M COMPLIANCE   : 2 96.0
*
I/M PROGRAM      : 3 2002 2006 1 TRC GC
I/M MODEL YEARS  : 3 1980 2006
I/M VEHICLES     : 3 11111 21111111 1
I/M COMPLIANCE   : 3 96.0
*
I/M PROGRAM      : 4 2002 2050 1 TRC EVAP OBD & GC
I/M MODEL YEARS  : 4 1996 2050
I/M VEHICLES     : 4 22222 11111111 1
I/M STRINGENCY   : 4 20.0
I/M COMPLIANCE   : 4 96.0
I/M GRACE PERIOD : 1 2
*
I/M PROGRAM      : 5 2007 2050 1 TRC EVAP OBD & GC
I/M MODEL YEARS  : 5 2007 2050
I/M VEHICLES     : 5 11111 21111111 1
I/M STRINGENCY   : 5 20.0
I/M COMPLIANCE   : 5 96.0
I/M GRACE PERIOD : 1

```

The parish-level age distributions provided by LDEQ were averaged for each representative parish using a weighted average of vehicle populations in constituent parishes. In the data provided by LDEQ, just four of the 13 source types had unique age distributions by parish: motorcycle, passenger car, passenger truck, and light commercial truck. The other nine source types each had a single age distribution identical to the rest of the state.

Lastly, the input ratio of VMT to population is important in MOVES because it directly affects the magnitude of evaporative hydrocarbon emission factors from parked vehicles. LDOTD provided annual average day VMT by parish, which needed to be further broken out to vehicle type. The disaggregation was performed using Louisiana's temporal profiles (discussed later). Population provided by LDEQ covered only four source types of 13. For the nine source types not included in the LDEQ dataset, we used MOVES2010a default annual mileage accumulation rates (miles/vehicle/year) and the disaggregated VMT dataset (VMT/year) to estimate the population for the nine source types. LDEQ provided 2011 data for both VMT and Population, which was used directly for the 2010 base year without adjustment.

After preparing all MOVES inputs, ENVIRON's RUNSPEC generator tool was run to automatically create the input files to run MOVES for all conditions in the episode and domain. Once MOVES runs had completed, a post-processing tool was used to reformat the emission factors for input to CONCEPT MV.

5.2.2.2 CONCEPT MV

The CONCEPT MV tool completely replaces EPS3 for the on-road mobile sector; the tool outputs air quality model-ready emissions files that are gridded, hourly, and speciated using the Carbon Bond version 6 (CB6) chemical mechanism. CONCEPT MV combines emission factors from MOVES2010a with VMT, vehicle population, and speed activity from transportation planning sources.

Louisiana on-road emissions were processed at the parish-level (as opposed to link level) with VMT input at the level of detail of parish and road type. Each episode day was processed one day at a time using hourly, gridded meteorological data (61 episode days).

Activity input to CONCEPT MV includes both VMT and vehicle population. CONCEPT MV gridded each activity type to the modeling domain using spatial surrogates according to road type or specific emissions type as shown in Table 5-3. The spatial surrogate assignments were based on EPA's cross-reference included in the SMOKE model.

Table 5-3. Spatial surrogates used in CONCEPT MV processing.

Surrogate	Surrogate Code	Applicability in CONCEPT
Urban Population	120	Grids all VMT from road type U19
Rural Population	130	Grids all VMT from road type R09
Urban Primary Roads	200	Grids all VMT from road types U11, U12, U14, U16
Rural Primary Roads	210	Grids all VMT from road types R01, R02, R06
Urban Secondary Roads	220	Grids all VMT from road type U17
Rural Secondary Roads	230	Grids all VMT from road types R07, R08
Urban and Rural Primary Roads	250	Grids Combination Long-haul Truck population for calculation of extended idling emissions only.
0.75 Total Roadway Miles + 0.25 Population	255	Grids all population for calculation of parked vehicle emissions (except from extended idling).

CONCEPT MV estimates hourly VMT from an annual average day by applying a series of temporal profiles for month of year, day of week, and hour of day. The monthly temporal profiles were provided by LDEQ and are shown by road type in Figure 5-1. These monthly temporal profiles tend to show higher VMT in summer months.

Figure 5-2 shows the day of week temporal profiles from Louisiana's previous SIP modeling, which we used again in the current work. The day of week profiles show generally lower VMT on Saturday and Sunday (exception for urban local roads, U19) and the profiles feature a single weekday day type with no variation Monday through Friday.

The hourly temporal profile patterns differ according to weekday or weekend. Figure 5-3 shows each relative distribution of daily VMT to hours. The hourly profiles came from two sources. Weekday hourly profiles were prepared by LDEQ in the previous SIP. A weekend hourly profile was provided by LDOTD, applicable to all road types. The weekday profile has more pronounced VMT peaks during commuter periods in the morning and afternoon rush hours.

A fourth and final type of temporal profile CONCEPT uses are hourly fleet mix temporal profiles. The weekday fleet mix was derived from the previous Louisiana SIP, and the weekend fleet mix was a daily average of weekday and specified as the same mix at all hours.

All of the VMT was temporally allocated from average day total to hour specific by vehicle class and allocated to the grid. Population was directly allocated to the grid.

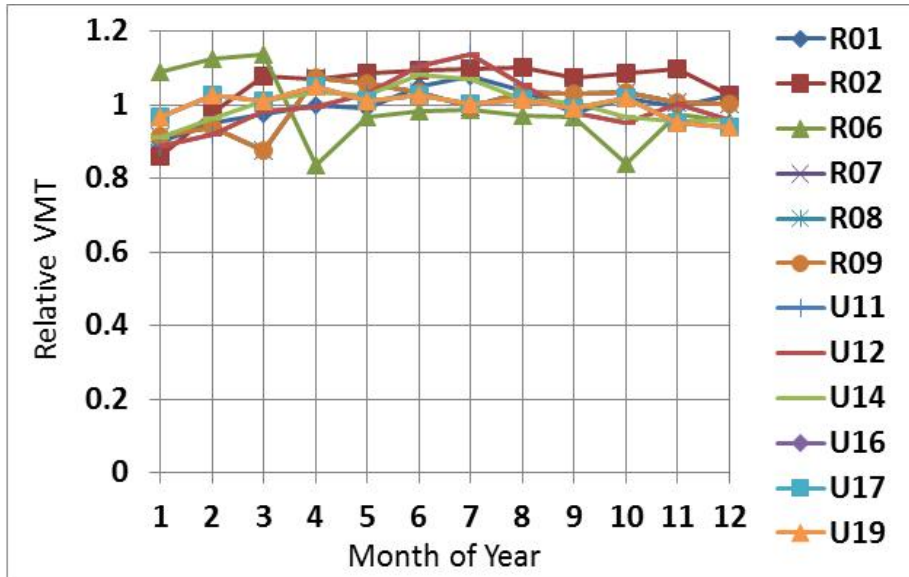


Figure 5-1. Monthly temporal profiles by roadway type.

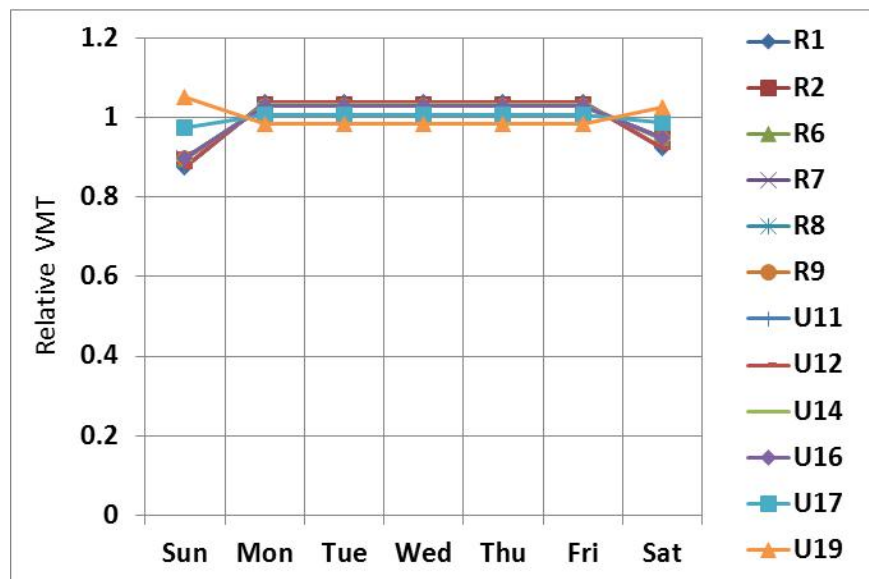


Figure 5-2. Day of week temporal profiles by roadway type.

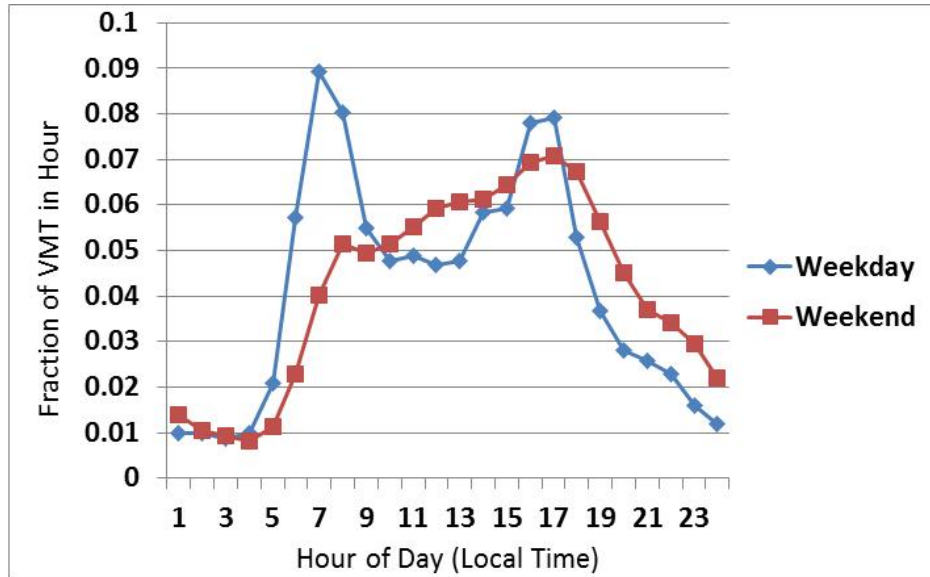


Figure 5-3. Hourly temporal profiles for all roadways on weekdays and weekends.

Daily average vehicle speeds by road type were provided by the DOTD. Provided speeds shown in Table 5-4 were 90% of the design speed for their conformity plan.

Table 5-4. Louisiana average vehicle speeds.

Road Type	Average Speed (mph)
Rural Interstate	63.0
Rural Principal Arterial	58.5
Rural Minor Arterial	49.5
Rural Major Collector	45.0
Rural Minor Collector	36.0
Rural Local	27.0
Urban Interstate	58.5
Urban Other Expressway	58.5
Urban Principal Arterial	49.5
Urban Minor Arterial	45.0
Urban Collector	36.0
Urban Local	27.0

In summary, CONCEPT MV temporally allocated average day VMT to hourly by vehicle type using temporal profiles. The model then gridded the VMT using spatial surrogates according to roadway type and vehicle population using a combination of spatial surrogate. CONCEPT MV looked up the MOVES emission factors closest to the road type speed and grid cell temperature and humidity and interpolated the emission factor. After this interpolation, CONCEPT MV multiplied emission factors in grams/mile with the hourly gridded VMT and emission factors in grams/vehicle/hour with the gridded vehicle populations to calculate the full inventory. Figures 5-4 and 5-5 show a snapshot of the modeling episode at 8-9 AM on September 1, 2010. Figure 5-4 shows the species nitrous oxide (NO) and Figure 5-5 shows alkane (“PAR”) emissions in units of moles/hour.

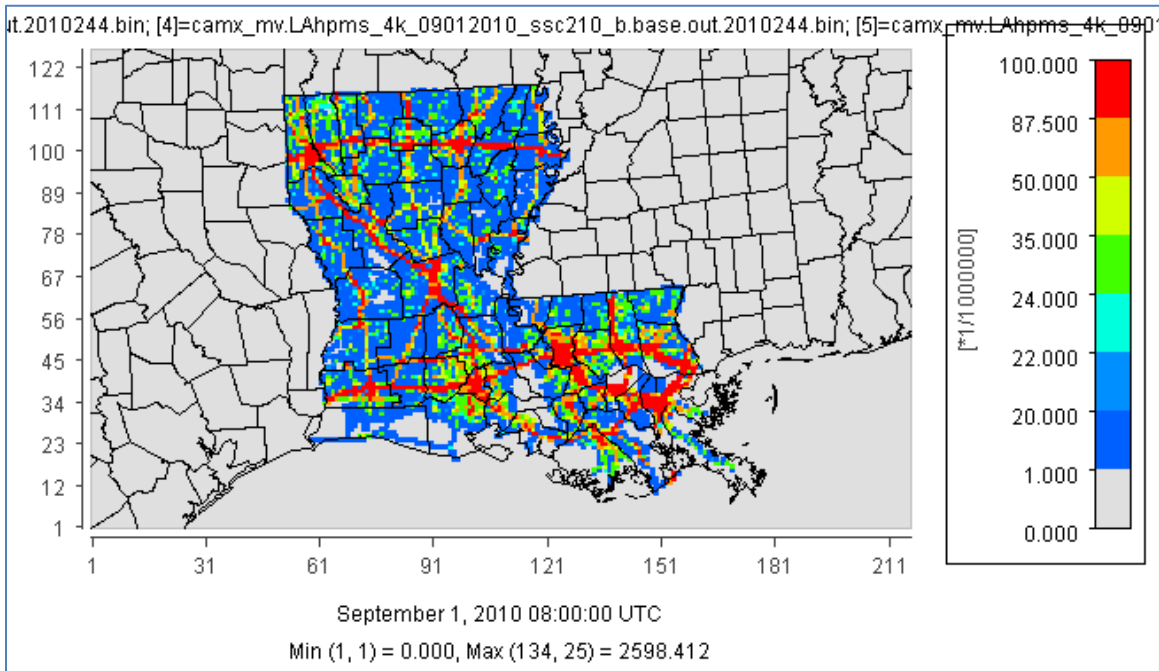


Figure 5-4. Louisiana on-road NO emissions (mol/h) during 8-9 AM LST September 1, 2010.

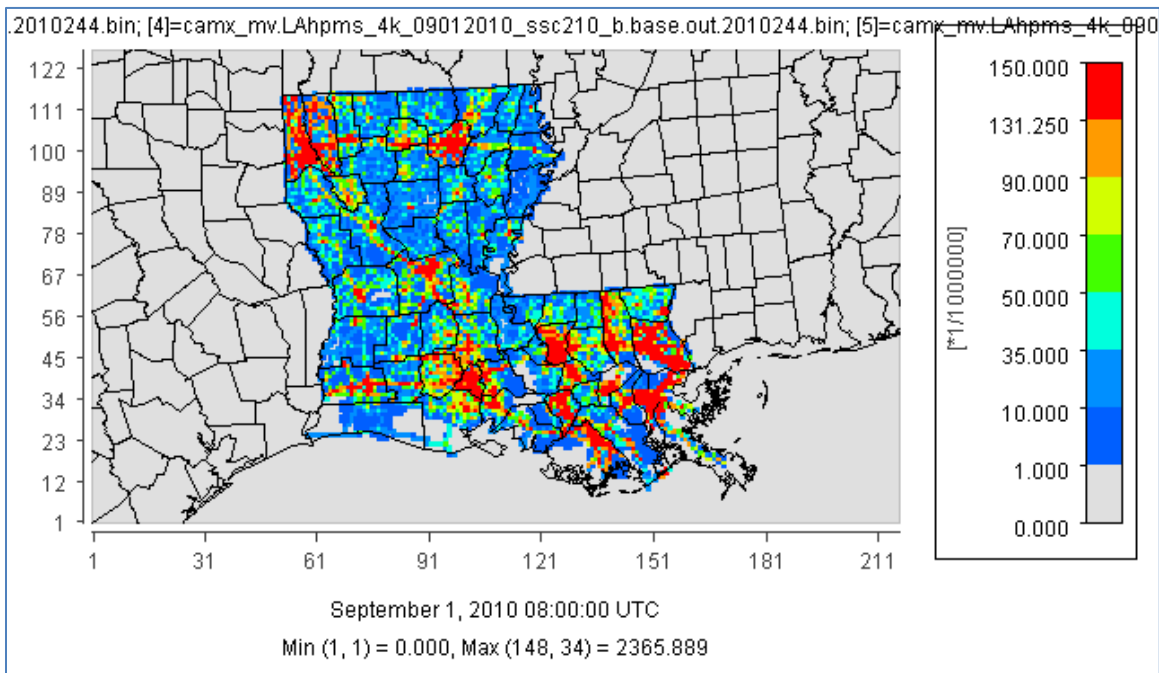


Figure 5-5. Louisiana on-road alkane (PAR) emissions (mol/h) during 8-9 AM LST September 1, 2010.

5.2.3 Off-Road Sources

The EPA's NMIM was used to generate Louisiana statewide parish-level off-road equipment emissions estimates for September and October 2010. NMIM is a tool for estimating on-road and non-road emissions by county for the entire US to support updates to the EPA National Emissions Inventory (NEI). For this modeling effort NMIM version NMIM20090504 was run with county database NCD20090531 and NONROAD2008a. Emissions were estimated from off-road equipment in the following categories:

- Agricultural equipment, such as tractors, combines, and balers;
- Airport ground support, such as terminal tractors and supply vehicles;
- Construction equipment, such as graders and back hoes;
- Industrial and commercial equipment, such as fork lifts and sweepers;
- Residential and commercial lawn and garden equipment, such as leaf blowers;
- Logging equipment, such as shredders and large chain saws;
- Recreational equipment, such as off-road motorbikes and ATVs; and
- Recreational marine vessels, such as power boats.

Local data were used for gasoline fuel parameters with guidance from LDEQ and to be consistent with the on-road mobile inventory. All non-gasoline equipment used default parameters. Gasoline sources used non-default gasoline fuel RVP values. For September 1 through September 15, inclusive, the set of parishes listed in Table 5-5 had an RVP of 7.8 psi. Outside these parishes gasoline was assigned an RVP of 9 psi. After September 15 all parishes used 11.5 psi RVP gasoline.

Table 5-5. Parishes assigned 7.8 RVP for episode days September 1- 15, 2010.

Parish	
Ascension	Livingston
Beauregard	Orleans
Calcasieu	Pointe Coupee
East Baton Rouge	St. Bernard
Grant	St. Charles
Iberville	St. James
Jefferson	St. Mary
Lafayette	West Baton Rouge
Lafourche	

In order to support the different gas RVP values NMIM was run with:

1. Non-gasoline equipment run for September and October (default fuel parameters)
2. Gasoline-only equipment run for September and October with 11.5 psi, all parishes
3. Gasoline-only equipment run for September with 7.8 psi to represent Table 5 parishes

4. Gasoline-only equipment run for September with 9 psi, to represent parishes outside the Table 5-5 list.

Run types 3 and 4 representing September 1-15 were averaged with run 2 representing September 16-31 to determine average September day emissions.

For quality assurance, the Louisiana (compiled) inventory was compared with a simple state-wide Louisiana NMIM/NONROAD run for September and October. The expectation was that non-gasoline emissions would match exactly for both September and October. Gasoline emissions would be similar between runs, with differences in magnitude attributable to RVP. Differences were primarily in evaporative total organic gasses (TOG).

Using EPS3, the off-road emissions were speciated to CB6 compounds, temporally allocated to day of week and hour of day, and spatially allocated using EPA default source category cross-reference files.

NONROAD and NMIM do not include emission estimates for railroad locomotives, aircraft, and marine vessels (excluding maintenance equipment). Louisiana emissions for locomotives and aircraft were extracted from the EPA 2008 NEI (version 2) and processed as area sources. The development of emissions from commercial marine vessels is described next.

5.2.4 Commercial Marine Vessels: Shipping Channels and Ports

Emissions from commercial marine vessels servicing the ports along the Mississippi River and the Port of Lake Charles were processed separately from other area sources.

ENVIRON (2010) updated the commercial marine shipping emissions inventory for the State of Louisiana for the year 2006. This emissions inventory was further modified for the 2010 Base Year. The inventory is based on the latest estimates from the EPA for “Category 3” ocean-going vessels. The EPA estimates are provided by port and by transit mode in a spatially precise and accurate link-based format that is suitable for emissions processing. These data were reformatted for input to the EPS3 PRESHP module. PRESHP is a link-based module specifically designed to handle shipping lane emissions. Five Louisiana ports were processed:

- Baton Rouge
- Lake Charles
- New Orleans
- Port of Plaquemines
- Port of South Louisiana

These data include the following transit modes:

- Hoteling (at port, auxiliary engines only, no propulsion engines used)
- Maneuvering (at or near port)

- Reduced Speed Zone (RSZ; navigating away from a port towards the open ocean, often through a river system)
- Cruise Mode (CM; the vessel is away from constrained waterways and traveling at cruise speed)

The hoteling and maneuvering emissions were modeled as points located at the port center. The RSZ emissions were modeled as line emission sources, which are defined as multiple straight line segments with known endpoint coordinates. The CM emissions were not used for the current project to avoid double counting emissions with the existing ocean traffic emissions inventory developed from the BOEM database (see Gulf Sources below).

EPA shipping emissions were estimated as total annual emissions for 2002. Previous LDEQ emissions were prepared for 2006 (ENVIRON, 2010). To obtain 2010 emissions, the 2006 emissions were scaled based on growth and control factors. Growth factors were based on the annual total commodity tonnage summary from the US Army Corp of Engineers (USACE) Waterborne Commerce Statistics, principal ports database (<http://www.ndc.iwr.usace.army.mil/data/datappor.htm>). Table 5-6 provides a summary of commodities processed using the total tonnage for the 5 Louisiana ports. The growth factor from 2006 to 2010 was estimated as 1.0035.

Table 5-6. Principal Ports Commodity Tonnage by year.

Year	Louisiana Combined Principal Ports Commodity Tonnage	Growth Factor
2002	468,612,466	1.0000
2003	453,217,009	0.9671
2004	468,528,396	0.9998
2005	438,011,524	0.9347
2006	473,034,017	1.0094
2007	482,759,763	1.0302
2008	466,330,458	0.9951
2009	435,745,874	0.9299
2010	474,661,368	1.0129
2010/2006	-	1.0035

EPA estimated NO_x control factors for the year 2020 for different engine/ship types. These values were interpolated from 2006 values to estimate a 2010 control factor for NO_x as 0.9781.

The growth and control factors were applied to adjust the 2006 emissions to estimated 2010 emissions. The emissions were projected to the 4 km modeling grid shown in Figure 4-1. Ocean going vessels typically emit from stacks that are between 40–60 m in height. This corresponds to the second vertical layer in the CAMx model, which spans from 32 m to 81 m. For this application plume heights for all transit modes were set to 56 m, ensuring that emissions were injected into the second model layer. No temporal variation was assigned, i.e.

the emissions were assumed to be constant in time. Figure 5-6 is an example of the spatial distribution of 24 hr average NO_x emissions.

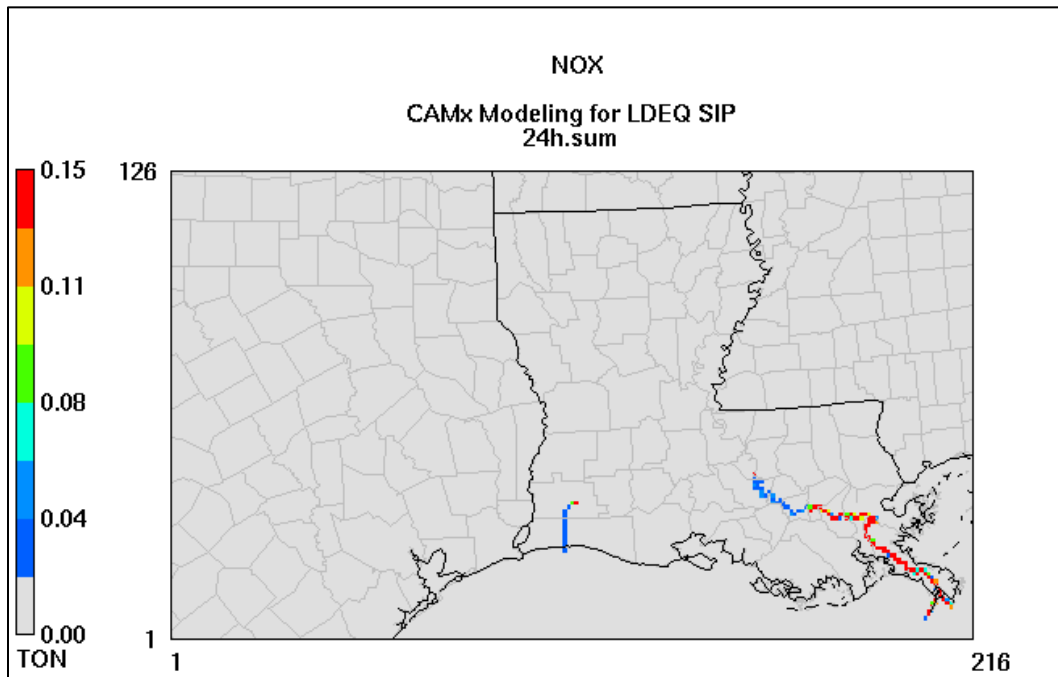


Figure 5-6. 24-hour commercial marine shipping NO_x emissions at Louisiana deep draft ports and along RSV shipping lanes.

5.2.5 Port Fourchon

According to LDEQ, emission estimates may have been historically underestimated for Port Fourchon, which is a harbor located on the Gulf coast in southeastern Louisiana that specifically supports offshore oil and gas development activities. Emission estimates were updated based on a report by Starcrest Consulting Group, LLC and Louisiana State University (2010). Figure 5-7 is an image of the emissions summary (Table 2.1) from that report. The off-shore source estimates from this table were not included as they are already represented in the Gulf platform and non-platform inventories from the BOEM data (discussed below).

The Port Fourchon emission estimates were spatially allocated to two grid cells that the port spans. The coordinates of the port were acquired from Wikipedia and plotted in GIS overlaying a street map and imagery layer with the 4 km grid. Based on a visual inspection of the plot (Figure 5-8) the Port Fourchon emission estimates were distributed equally between two grid cells.

Source Category	NO _x	VOC	CO
Marine Vessels	10.0	0.36	1.15
Cargo Handling Equipment	0.30	0.03	0.07
Heavy-Duty Vehicles	0.14	0.01	0.03
Aircraft	0.22		0.63
Off-Shore Non-Platform Sources	12.1	2.3	2.8
Off-Shore Platform Sources	7.6	4.3	9.1
Total	30.4	7.0	13.8

Figure 5-7. Table 2.1 from the Port Fourchon Ozone Day Port-Related Emissions Inventory Study (Starcrest and LSU, 2010).

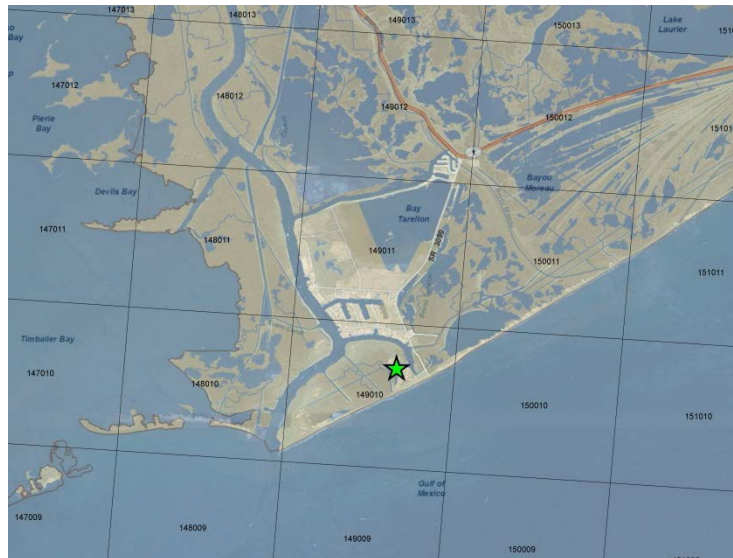


Figure 5-8. Port Fourchon with 4 km grid overlay.

5.2.6 Haynesville Shale

The Haynesville Shale is a rock formation that lies at depths of 10,000 to 13,000 feet below the surface and straddles the border between Northeast Texas and Northwest Louisiana near Shreveport. This formation is estimated to contain very large recoverable reserves of natural gas, and during the first two years since the drilling of the first highly productive wells in 2007-2008, it was the focus of aggressive exploration and leasing activity.

In 2009, Northeast Texas Air Care (NETAC; www.netac.org), a local stakeholder group comprised of representatives of local government, business and industry, the general public, and environmental interest groups, undertook a study to investigate how development in the Haynesville Shale may impact future ozone air quality in Northeast Texas. Well production data, the historical record of activity in the nearby Barnett Shale, and other available literature were used to project future activity in the Haynesville Shale. Annual natural gas production for the years 2009-2020 was estimated for three scenarios corresponding to aggressive, moderate, and limited development of the Haynesville Shale (Grant et al., 2009).

The 2009 study generated model-ready emission inventories of Haynesville Shale sources for the year 2012. These emissions data included low, moderate, and high scenarios for each of three general sources categories (exploration, production, and “midstream” processing), resulting in a total of nine separate inventories. Specific 2012 model-ready inventories for the exploration category (drill rigs and other non-road sources) and the production category (wells) were incorporated into the 2010 Louisiana emissions inventory. Based on a review of the actual 2010 reported well counts, the limited development (low) scenario for 2012 production sources most accurately reflected 2010, while the number of drill rigs in 2010 was comparable to the aggressive (high) scenario for 2012 exploration sources. The midstream sources (e.g., permitted compressor stations and gas processing plants) were assumed to be included in the Louisiana 2010 point source permitting inventory and no adjustment was made to reflect any different emissions in 2010 from these specific Haynesville sources.

Spatial allocation of the Haynesville Shale emissions was based on Louisiana Department of Natural Resources, Haynesville Shale wells data in GIS shape files. These were obtained from http://sonris-www.dnr.state.la.us/gis/agsweb/arcgisserver/arcgisoutput/extData/shp/Haynesville_wells.zip. Active well location data for 2010 were used as weight factors in developing the spatial surrogates.

5.3 Gulf Sources

There are a number of emission sources located in the Gulf of Mexico (GoM). Emissions from the GoM were obtained from the Year 2008 Gulfwide Emission Inventory Study (BOEM, 2010). Emissions were obtained for both platform sources and non-platform sources.

The platform source emissions included a wide number of emission sources, including: amine units, boilers/heaters/burners, diesel and gasoline engines, drilling rigs, combustion flares, fugitives, glycol dehydrators, flashing losses, mud degassing, natural gas engines and turbines, pneumatic pumps, pressure/level controllers, storage tanks, and cold vents.

The non-platform sources consisted of oil and gas production-related and non-production related sources. The production-related sources included drilling rigs, pipelaying operations, support helicopters, support vessels, and survey vessels. The non-production-related sources included: biogenic and geogenic emissions, commercial fishing vessels, commercial marine vessels, the Louisiana Offshore Oil Port (LOOP), military vessels, and vessel lightering.

The 2008 platform source emissions were projected to 2010 using lease-specific projection factors based upon 2008 and 2010 total oil and gas production quantities converted to a BTU-basis (BOEM, 2012). If lease-specific production quantities were unavailable for either 2008 or 2010, then a GoM average projection factor of 0.901, based upon GoM-wide production, was used to project 2008 emissions to 2010.

The 2008 non-platform source emissions associated with production were projected to 2010 using a GoM average projection factor of 0.901 based upon GoM-wide production quantities for 2008 and 2010. It was assumed that the 2008 non-platform source emissions not associated with production were representative of 2010, so the 2008 emissions were carried forward to 2010 without any projection.

5.4 Anthropogenic Emissions Outside of Louisiana

Anthropogenic emission estimates for states outside of Louisiana, as well as for Canada, Mexico, and commercial marine shipping outside the Gulf of Mexico, were developed by Alpine Geophysics. Alpine developed a 2008 inventory on the Regional Planning Organization (RPO) continental US (CONUS) domain for several concurrent regional modeling programs, and provided these data for use in this project. The inventory was based on the most complete and consistent inventory available at the time modeling commenced; namely, version 2 of the 2008 National Emission Inventory (2008 NEIv2, publicly released on the NEI website on April 10, 2012). A draft Technical Support Document (TSD) for the 2008 NEIv2 has been developed by EPA and is available at http://www.epa.gov/ttn/chief/net/2008neiv2/2008_neiv2_tsd_draft.pdf.

The EPA maintains and updates the NEI every three years, which consists of a comprehensive and detailed estimate of air emissions of both criteria and hazardous air pollutants from all air emissions sources in the US by county as well as for Canada and Mexico. The NEI is based primarily upon emission estimates and emission model inputs provided by State, Local, and Tribal air agencies for sources in their jurisdictions, and supplemented by data developed by the EPA. The 2008 NEIv2 contained the most recent updates to the point, nonpoint (other area), non-road, and on-road motor vehicle emissions categories. All source categories except county-level on-road and commercial marine shipping outside the Gulf of Mexico were processed.

On-Road Mobile sources were separately developed using the MOVES2010a model in “inventory mode”, run for each US county outside of Louisiana, using a representative weekday/weekend day activity per month. Marine shipping emissions outside of the Gulf of Mexico were developed for 2008 using an inventory derived from the EPA 2005v4.1 modeling platform (<ftp.epa.gov/EmisInventory/2005v4.1>, April 2011).

The 2008 inventories were processed by Alpine using the EPA Sparse Matrix Operator Kernel Emissions (SMOKE, v3.1) processor using the ancillary data for spatial, temporal, and speciation distribution supplied with the emissions input files. SMOKE was used to generate gridded,

speciated, temporally allocated emissions for the 36, 12, and 4 km modeling domains. The 2008 data were used for the 2010 base year modeling without year-to-year adjustment.

5.5 Biogenic Emissions

Biogenic sources are important contributors to air emissions in North America and must be combined with anthropogenic emissions for photochemical model simulations. The Model of Emissions of Gases and Aerosols from Nature (MEGAN) version 2.10 (ENVIRON, 2012) was initially used to develop the biogenic emissions inventory. Subsequently, BEIS was run by Alpine Geophysics as an alternative source of biogenic emissions, which was successful in reducing over predicted isoprene emissions that were shown in CAMx simulations to contribute to ozone over predictions throughout the domain. The biogenic emissions from MEGAN and BEIS are gridded, hourly files formatted for input to the CAMx model using the CB6 chemical mechanism.

5.5.1 MEGAN Processing

MEGAN estimates net emissions of gases and aerosols from terrestrial ecosystems to the atmosphere (Sakulyanontvittaya, 2008; Guenther et al., 2006). Emission calculations are driven by land cover, weather, and atmospheric chemical composition. MEGAN has global land cover data with a base resolution of approximately 1 km². The latest version of MEGAN includes an explicit canopy environment, updated emission algorithms, and a soil NO_x emission model that accounts for fertilizer application and precipitation. Land cover and emission factor inputs were updated with: 1) Leaf Area Index (LAI) based on improved 2008 satellite data products with 8-day temporal resolution, 2) improved Plant Functional Type fractional (PFTf) coverage data based on 30-meter 2008 LANDSAT TM data; and 3) emission factors based on recent emission measurements and improved U.S. species composition data.

The LAI dataset provided with MEGAN contains a set of 46 eight-day 1-km spatial resolution LAIv files for North America which were developed from 2008 NASA MODIS LAI product version 5 (ENVIRON, 2012). The dataset has been reviewed using ARCGIS and eco-region average, minimum, and maximum values were examined for quality assurance. The default LAI data in ESRI 1-km GRID format were interpolated using a zonal average method and reformatted to text format for the modeling grid.

The PFTf dataset provided with MEGAN contains a set of 9 PFTf data files with 56-m or 1-km resolution for the contiguous US, which were developed from 2008 National Land Cover Dataset (NLCD) with 30-meter resolution and 2008 Cropland Data Layer (CLD) with 56-meter resolution (ENVIRON, 2012). MEGAN includes a total of 17 PFTs but 8 types (e.g., tropical and boreal PFTs) do not occur within the CAMx modeling domain. The 9 PFTf files that do occur are for needle leaf evergreen tree, needle leaf deciduous tree, broadleaf evergreen tree, broadleaf deciduous tree, broadleaf deciduous shrub, cold grass, warm grass, other crops, and corn categories. Each file was reviewed in ARCGIS and ecoregion average and minimum and maximum values were examined for quality assurance. The dataset was processed in the same manner as LAI.

MEGAN calculates emissions for 20 categories of biogenic compounds. Some are individual compounds while others represent groups of compounds that are then allocated to individual compounds using built-in speciation profiles. Geo-gridded emission factor maps were calculated based on plant species composition and plant species specific emission factors for 10 biogenic compounds; isoprene, methyl butenol, nitric oxide (NO), and 7 monoterpenes. PFT-average emission factors are combined with the geo-gridded PFTs for an additional 10 categories. The emission factor map data was processed using a zonal average method and reformatted from ESRI GRID format to text format for the modeling domain.

MEGAN requires meteorological data near the surface, such as temperature, solar radiation, and wind speed to drive emission algorithms. For this project, we processed the WRF data using MCIP version 4 for August - November, 2010. This provides all parameters needed for the emission estimates.

Photosynthetically Active Radiation (PAR) is an important driving variable for MEGAN. MEGAN provides two options for PAR input data; solar radiation from a meteorological model (in MCIP output format) or PAR data from satellite observation. MCIP data are usually available and have no problems with missing data, but are subject to uncertainties in simulated cloud cover (a parameter for which PAR is very sensitive). MEGAN internally estimates PAR from MCIP solar radiation data by assuming 45% of the solar radiation is in the 400-700 nm spectral region. Usually satellite data provide a better approximation of PAR but are subject to missing data periods. The development of 2010 biogenic emission for this project used the predicted solar radiation from WRF/MCIP because satellite PAR data were not available for this period.

MEGAN estimates emissions for 150 chemical species, which were converted into CB6 model compounds for CAMx modeling. Biogenic emissions were processed for each hour of each day on all three of the 36/12/4 km modeling grids. The time zone of the data was set to CST. The inventories were visually checked for quality assurance.

5.5.2 BEIS Processing

Alternative biogenic emissions were processed using BEIS3.14 contained in the SMOKE3.1 emissions processing system (<http://www.cmascenter.org/>). Reference emission files for BEIS3.14 rely on the BELD3 (Biogenic Emissions Landuse Database, version 3) available at <http://www.epa.gov/ttn/chief/emch/biogenic/>. This North American database contains fractional area information on 230 individual forest, grass, and crop types at 1-km horizontal resolution. Tools for spatial allocation of BELD3 data into common user defined grids are also available at this website. As part of the reference emission preprocessing, BEIS3.14 contains season-specific and vegetation-specific information for emissions of 33 individual VOC species (including isoprene and 14 monoterpenes), biogenic/agricultural NO, and LAI (Leaf Area Index) information needed in the canopy light dependence calculations of isoprene, methanol and methyl-butenol.

The BELD3 files were used to develop the required input data for the 36, 12 and 4 kilometer grids. The project specific gridded hourly meteorological data generated by WRF for 2010 were used to produce hourly, temperature adjusted biogenic emissions.

5.6 Wildland, Agricultural, and Prescribed Fires

Fire emissions were based on the FINN version 1 dataset, which were downloaded from <http://bai.acd.ucar.edu/Data/fire/>. The global dataset contained daily emissions for each satellite pixel, which represented an area of approximately 1 km². Emission species included NO, NO₂, PM_{2.5}, CO, and non-methane organic compounds (NMOC) speciated into MOZART-4 species for six fire types – tropical, temperate, and boreal forests, cropland, shrublands, and grasslands. The data were windowed to the 36/12/4 km modeling grids and mapped to CAMx CB6 speciation. Fire points within 5 km of one another were assumed to be part of the same fire and assigned properties of a larger fire.

The daily fire emissions were then processed from August to October, 2010 using an updated version of EPS3 (version 3.20). EPS3 incorporated the WRAP methodology to temporally and vertically (by altitude) allocate the fire emissions. Temporally, the same diurnal profile was applied to all fires such that emissions were highest in the early afternoon and lowest at night. Vertically, a fraction of each hour's emissions was assigned to the lowest layer; the rest was distributed into multiple point sources directly above with one point assigned to each CAMx layer between the plume bottom and plume top, weighted by the thickness of each layer. The fraction in layer 1 and the plume bottom and top were all dependent on the hour of the day and size of the fire. All emissions were output into a point source file and flagged with no additional plume rise.

Figure 5-9 shows monthly total NO_x emissions for September and October, 2010. Near Louisiana, fire emissions were highest in eastern Arkansas, especially in September and October due to crop burning.

5.7 Summary of 2010 Louisiana Emissions

Parish level emissions for 2010 are reported in Table 5-6. As biogenic and fire emissions are not reported at the county level they are not included in this comparison. Figures 5-10 through 5-12 show examples of the spatial distribution of total model-ready 2010 weekday low-level (gridded – not including point sources) emission of NO_x, CO, and VOC over the 4 km modeling domain.

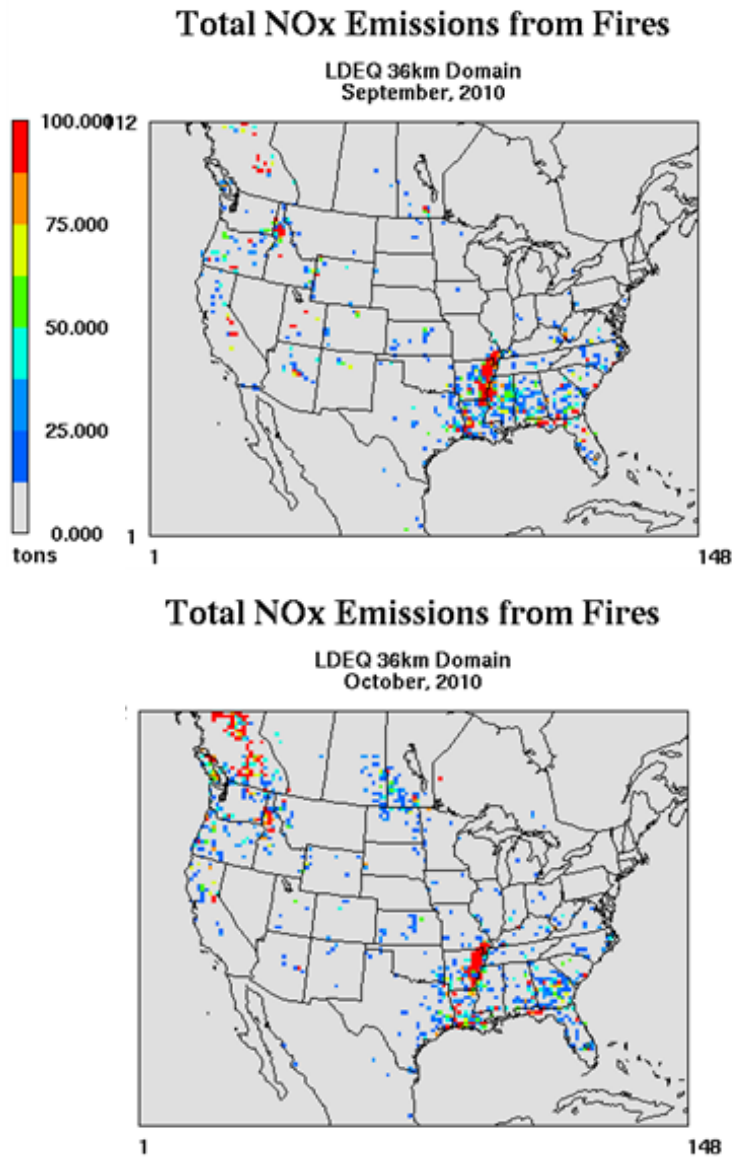


Figure 5-9. FINN-based fire NOx emissions for September and October 2010.

Table 5-7. Summary of 2010 Louisiana emissions (tons/day) for typical September weekday.

Parish	NOx				CO				VOC	TOG	TOG	VOC
	Area	Off-road	On-road	Points	Area	Off-road	On-road	Points	Area	Off-road	On-road	Points
Acadia	1.08	1.56	5.35	8.08	2.12	6.28	35.04	3.16	4.26	0.96	4.51	1.33
Allen	0.31	0.83	2.16	1.65	1.33	1.77	13.04	2.95	1.70	0.18	1.68	0.19
Ascension	3.01	1.63	5.48	20.01	15.75	9.99	36.98	10.75	22.05	0.83	4.74	8.44
Assumption	0.87	0.44	2.85	3.33	13.32	2.12	25.98	2.52	2.15	0.31	5.42	1.42
Avoyelles	0.82	1.47	2.96	0.38	8.95	4.75	19.21	0.17	3.30	0.60	2.69	0.07
Beauregard	0.51	1.49	3.42	7.51	1.42	6.31	21.55	6.50	2.40	1.41	2.56	2.88
Bienville	2.52	0.66	3.11	5.58	2.40	1.97	16.11	2.92	1.75	0.26	1.54	1.51
Bossier	4.25	2.90	7.94	1.87	10.42	12.99	56.67	1.38	4.07	1.68	7.36	1.41
Caddo	11.68	6.69	15.03	4.06	10.43	53.59	105.24	2.39	14.91	4.86	13.23	3.19
Calcasieu	4.67	5.14	11.11	56.06	10.86	31.62	78.18	39.58	31.45	5.56	8.27	19.07
Caldwell	0.07	0.72	1.58	0.15	0.44	1.44	9.54	0.01	0.93	0.20	1.33	0.01
Cameron	0.31	0.56	1.01	4.01	1.77	8.00	6.01	2.03	1.25	2.97	0.73	2.13
Catahoula	0.22	0.85	1.51	0.00	2.29	2.71	8.46	0.00	1.03	0.42	1.00	0.00
Claiborne	0.25	0.32	2.23	0.70	0.76	3.20	11.97	1.01	1.68	0.76	1.49	0.22
Concordia	0.08	1.04	1.99	0.00	0.39	4.62	11.92	0.00	1.66	1.08	1.41	0.00
De Soto	24.65	1.25	4.87	19.24	16.67	4.94	26.35	8.58	7.88	0.95	2.43	7.44
E Baton Rouge	5.73	5.42	15.95	30.25	5.34	51.87	112.75	30.82	32.99	4.13	15.38	17.85
East Carroll	0.18	1.20	1.28	0.33	2.22	1.89	6.73	0.08	0.62	0.30	0.61	0.04
East Feliciana	0.15	0.31	1.53	0.79	0.60	2.42	9.14	0.25	0.91	0.64	1.28	1.31
Evangeline	0.54	0.88	2.76	2.81	3.41	4.03	16.63	9.32	5.81	0.87	2.12	0.52
Franklin	0.20	1.03	1.46	0.28	0.60	2.84	9.95	0.15	1.24	0.32	1.51	0.04
Grant	0.26	0.93	2.42	0.54	1.04	3.07	13.14	2.43	1.22	0.79	1.42	0.39
Iberia	2.63	1.82	2.19	4.63	21.39	12.16	15.57	4.49	6.34	1.30	1.92	1.96
Iberville	2.30	1.38	2.08	21.80	17.82	4.22	11.92	14.65	18.10	0.55	1.41	6.53
Jackson	0.65	0.26	1.68	4.81	1.08	1.92	9.64	4.66	1.16	0.24	1.27	2.04
Jefferson	7.51	8.25	12.53	37.62	6.19	67.48	104.01	4.14	27.99	7.20	15.47	1.93
Jeff Davis	0.38	1.70	3.72	2.48	3.63	5.51	21.46	0.62	4.30	0.89	2.13	0.24
Lafayette	3.23	3.84	9.70	5.85	7.79	36.66	72.92	0.48	9.70	4.39	8.52	0.35
Lafourche	12.65	1.52	4.70	5.22	15.01	11.09	34.99	4.47	8.79	2.03	4.02	2.40
La Salle	0.21	0.47	1.91	0.42	0.42	2.53	10.49	0.11	1.18	0.40	1.20	0.04
Lincoln	0.83	1.20	4.86	4.10	2.38	6.28	29.37	1.47	3.07	0.47	2.88	0.87
Livingston	0.95	1.05	6.08	0.18	10.51	7.81	41.26	0.79	4.59	1.38	5.75	0.76
Madison	0.14	2.05	3.31	0.20	1.70	3.01	17.10	0.06	1.16	0.43	1.11	0.12
Morehouse	0.65	1.75	2.88	1.95	4.09	3.51	17.96	0.30	1.73	0.40	2.42	0.06
Natchitoches	1.28	1.19	5.97	6.53	3.46	4.42	32.50	3.81	4.62	0.63	3.09	3.39
Orleans	4.67	4.74	10.57	14.35	3.83	48.30	77.37	5.32	10.50	6.63	8.02	1.10
Ouachita	3.53	3.08	9.10	11.66	9.72	20.79	64.76	9.13	13.97	3.10	8.12	7.27
Plaquemines	0.83	1.34	1.06	36.05	1.36	16.04	8.02	10.27	3.39	4.62	1.36	6.01
Pointe Coup	1.25	1.60	1.88	44.98	21.39	4.50	11.10	105.06	2.71	0.54	1.19	2.09

Parish	NOx				CO				VOC	TOG	TOG	VOC
	Area	Off-road	On-road	Points	Area	Off-road	On-road	Points	Area	Off-road	On-road	Points
Rapides	1.75	2.96	11.46	14.99	7.46	15.91	73.36	9.27	9.26	1.93	8.08	1.60
Red River	13.22	0.65	1.70	0.56	8.61	2.57	11.30	0.42	2.52	0.72	1.83	0.34
Richland	0.50	1.44	3.42	2.00	6.49	2.56	17.59	0.94	1.89	0.27	1.56	0.31
Sabine	0.42	1.38	2.82	0.53	1.08	4.77	16.01	1.28	2.17	1.21	1.97	0.49
St. Bernard	0.73	0.79	0.73	11.19	0.61	9.50	6.87	4.92	0.94	2.47	1.14	3.47
St. Charles	2.11	1.58	3.51	37.62	2.31	8.42	23.71	22.56	14.96	1.32	2.48	12.74
St. Helena	0.11	0.12	0.90	1.11	0.52	0.72	5.82	0.33	1.49	0.08	0.87	0.25
St. James	0.90	0.88	1.44	14.91	1.17	2.72	8.72	6.52	6.20	0.30	0.98	3.92
St. J Baptist	1.07	1.05	3.64	14.28	2.88	5.89	23.98	5.17	5.57	1.15	2.63	4.51
St. Landry	1.21	2.64	6.64	3.81	8.65	8.79	42.24	1.51	5.45	1.27	5.16	2.11
St. Martin	1.49	0.80	3.71	2.72	14.84	6.72	24.62	1.80	4.48	1.79	3.02	1.34
St. Mary	2.46	1.73	2.60	21.26	13.83	10.33	18.63	19.40	9.56	1.35	2.14	3.66
St. Tammany	1.82	3.85	13.27	0.07	15.81	36.33	98.25	0.00	9.64	7.12	13.49	0.05
Tangipahoa	1.37	1.68	9.41	0.02	5.79	14.14	61.21	0.19	5.95	2.55	6.91	0.34
Tensas	0.18	1.03	1.25	0.00	3.65	2.15	6.07	0.00	1.37	0.41	0.52	0.00
Terrebonne	1.92	2.30	5.00	2.89	3.55	25.98	39.91	3.70	4.41	5.13	6.06	1.82
Union	0.73	0.43	2.57	0.55	3.26	3.87	14.15	0.32	2.50	0.47	1.78	0.45
Vermilion	1.31	1.47	3.25	9.40	11.64	11.63	21.92	3.52	3.85	2.57	3.15	1.46
Vernon	0.19	1.21	3.91	0.14	1.13	4.74	24.50	0.08	1.90	0.94	3.27	0.12
Washington	0.82	0.45	1.98	11.11	2.88	3.20	14.24	21.17	3.47	0.30	2.28	4.78
Webster	1.69	0.85	4.02	3.16	2.69	4.35	24.89	2.67	4.40	0.47	2.74	1.79
W Baton Rouge	1.26	0.84	2.23	3.21	6.26	7.61	12.59	6.36	4.08	1.06	1.22	1.68
West Carroll	0.37	0.55	0.87	2.38	7.21	1.42	5.46	0.23	1.18	0.14	0.78	0.06
West Feliciana	0.32	0.29	0.95	1.34	1.16	1.51	5.47	1.29	0.87	0.24	0.69	0.33
Winn	0.41	0.27	2.81	0.88	0.75	1.91	14.53	3.60	2.42	0.20	1.32	2.25
Total	144.39	105.79	276.31	530.61	378.48	676.38	1847.05	414.08	379.09	100.75	228.67	156.51

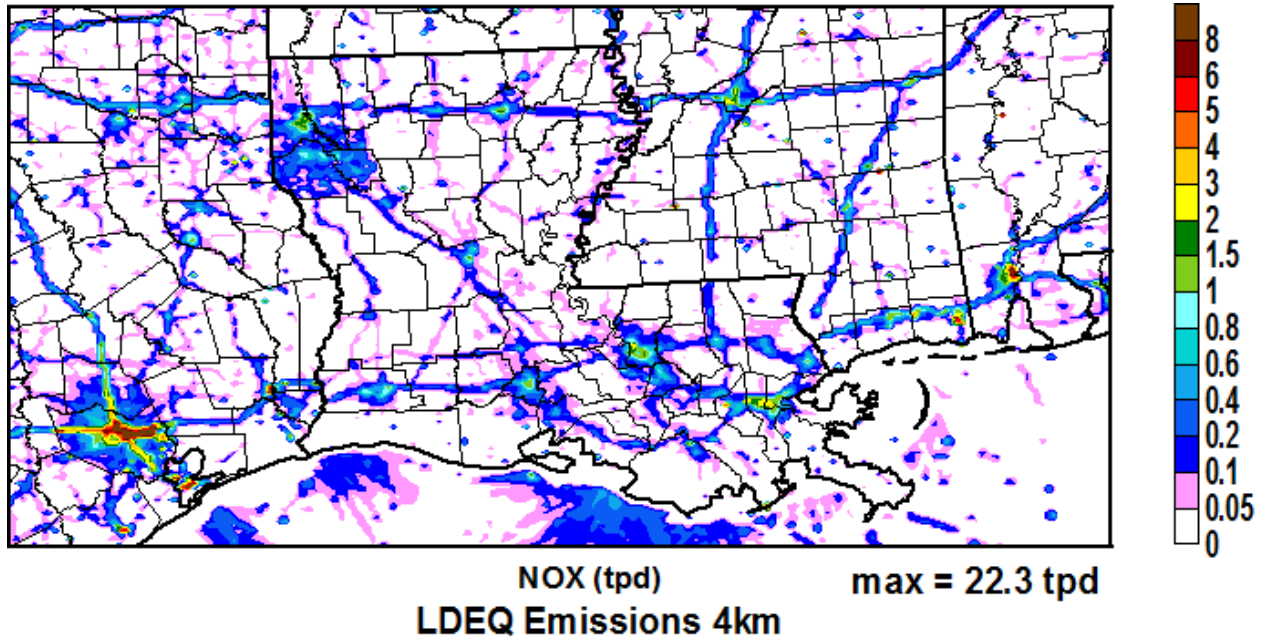


Figure 5-10. Spatial distribution of total (anthropogenic and biogenic) weekday surface NOx emissions (tons/day) in 2010.

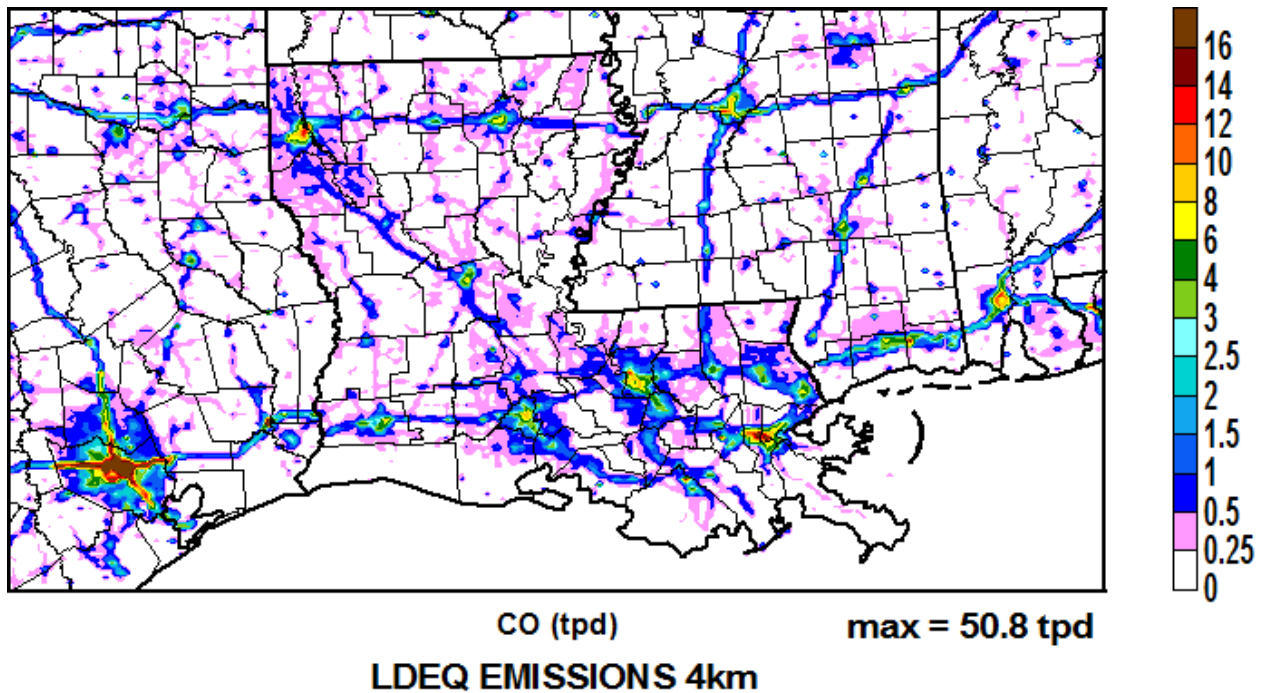


Figure 5-11. Spatial distribution of total weekday surface CO emissions (tons/day) in 2010.

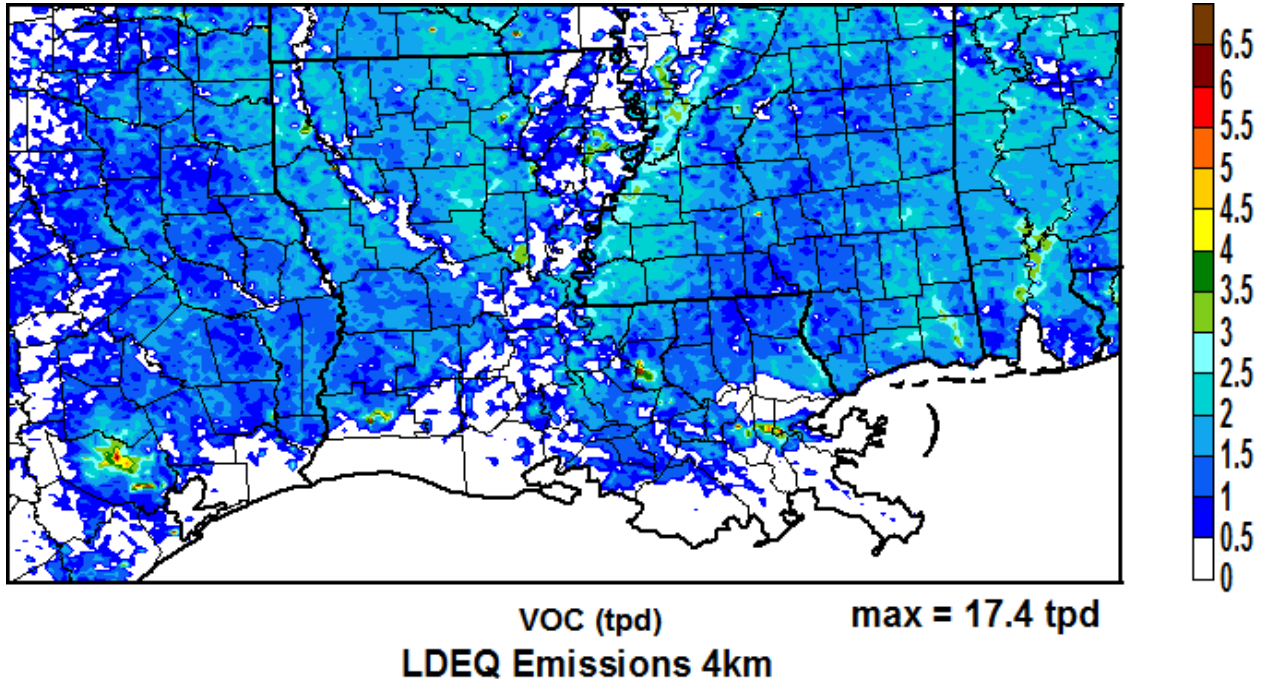


Figure 5-12. Spatial distribution of total (anthropogenic and biogenic) weekday surface VOC emissions (tons/day) in 2010.

6.0 BASE YEAR MODEL PERFORMANCE EVALUATION

The Comprehensive Air quality Model with extensions (CAMx) was used to simulate ozone levels throughout Louisiana during the period of September 1 to October 31, 2010. The methodology described in this section comprised the base year component of the wider modeling program designed to provide the technical underpinnings of the attainment demonstration for the 2008 8-hour ozone NAAQS. The base year modeling was conducted according to the approach described in the Modeling Protocol (ENVIRON and ERG, 2012) and follows the photochemical modeling guidance established by the EPA (2007).

All ozone simulations were run on the nested grid domains shown in Figures 4-1 using CAMx v5.4 (ENVIRON, 2011). Predictions of ozone were compared to measurements recorded at monitoring sites throughout Louisiana (Figure 2-1), while predictions of NO_x and VOC precursors were evaluated against monitoring measurements in the Baton Rouge area (Figure 5-1). A multitude of CAMx diagnostic runs were conducted and evaluated in an effort to improve model performance and to characterize ozone sensitivity to changes in various model inputs.

6.1 Overview and Context

A model performance evaluation (MPE) is the process of testing a model's ability to accurately estimate observed atmospheric properties over a range of spatial, temporal, and geophysical conditions. In general terms, the process to establish reliable photochemical modeling consists of the following cycle:

- Exercise the modeling system for the base year, attempting to replicate the time and space behavior of observed ozone concentrations as well as concentrations of precursor and product species;
- Identify sources of error and/or compensating biases, through evaluation of pre-processor models (e.g., WRF, EPS3), air quality model inputs, mass budgets and conservation, process analysis, etc.;
- Through a documented process of diagnostic and sensitivity investigation, pinpoint and correct the performance problems via model refinement, additional data collection and/or analysis, or theoretical considerations;
- Re-run the model for the base year and re-evaluate performance until adequate, justifiable performance is achieved, or time and/or resources are expended, or the episode is declared unsuited for further use based on documented performance problems.

To the extent possible, these steps were undertaken by the modeling team, culminating in a modeling application exhibiting sufficiently minimal bias and error that it can be used reliably to perform the 8-hour ozone attainment demonstration. The modeling team selected the final model configuration for the CAMx base year simulation based on the following factors:

- Model performance obtained using the initial model configuration and input data;

- Model performance impacts from diagnostic sensitivity tests;
- The modeling team's knowledge and experience with model options and their associated performance attributes;
- Experience performing sensitivity tests and model performance evaluation for a multitude of other local and regional applications;
- Comments from EPA and other participants.

The objective in identifying the optimum model configuration is to obtain the best performance for the right reasons consistent with sound science and EPA guidance. Sometimes, decisions must be made that trade off better/poorer model performance for one pollutant against another. These factors were considered and potential issues discussed among the LDEQ modeling team, EPA and others.

6.1.1 Evaluation Datasets

A variety of chemical concentration measurements were available for the MPE phase of the project. Available air quality monitoring data were extracted from the following network databases:

Air Quality System (AQS): Hourly ozone and NO_x concentration measurements were extracted for sites shown in Figure 4-1. Typical surface measurements include ground-level (i.e., 2 to 10 m) ozone, NO₂, NO_x and CO.

Photochemical Assessment Monitoring Sites (PAMS): Four PAMS sites operated in Baton Rouge in 2010. These PAMS sites are co-located with the Capitol, LSU, Pride and Bayou Plaquemine AQS sites (Figure 5-1). PAMS sites collect ground-level ozone, NO_x, hydrocarbons, and other parameters. Multi-hour concentrations for 55 individual hydrocarbons are determined from canister samples.

Clean Air Status and Trends Network (CASTNET): these sites monitor rural ground-level gas and PM pollutant concentrations. Hourly ozone concentrations from CASTNET sites in the south-central US were used to evaluate model performance at the regional scale.

6.1.2 Model Configuration

The initial CAMx base year simulation ("Run 1") used the meteorological, emissions, and ancillary input datasets described in Sections 4 and 5. The model simulated the evolution of ozone and precursor concentrations over the entirety of September and October 2010. A spinup period between August 15-31 was run to ensure a chemically balanced simulation and to remove the effects of initial conditions at coarse resolution.

CAMx provides some run-time options that need to be set for each specific simulation. Most options and capabilities are defined or provided to the model through the various input files. The CAMx configuration for the initial base year simulation is listed below (see ENVIRON [2011] for specific details):

- Time zone: Central Standard Time (CST)
- I/O frequency: 1 hour
- Map projection: Lambert conformal (see Section 4.1)
- Nesting: 2-way fully interactive 36/12/4-km computational grids (Figure 4-1)
- Chemistry mechanism: CB6 gas-phase only (without PM)
- Chemistry solver: Euler-Backwards Iterative (EBI)
- Advection solver: Piecewise Parabolic Method (PPM)
- Plume-in-Grid sub-model: Off
- Probing Tools: Off
- Asymmetric Convective Model: On
- Photolysis Adjustments for Clouds: in-line TUV
- Photolysis Adjustment for Aerosols: input AHOMAP
- Dry deposition: Zhang03
- Wet deposition: On

6.2 Initial CAMx Run

Figure 6-1 presents spatial plots of maximum daily 8-hour (MDA8) ozone over the 4-km nested grid on days when ozone exceeded the 2008 ozone NAAQS at any location in Louisiana. Simulated ozone was over predicted substantially on a vast majority of these days. Relative to observed MDA8 concentrations in Baton Rouge, over predictions in excess of 15-20 ppb covered large portions of the area, especially in mid-September. In particular, the highest simulated ozone occurred on September 14, reaching 190 ppb to the northeast of Baton Rouge and exceeding certain measurements by up to 30 ppb. The 190 ppb simulated peak occurred near a large prescribed fire complex according to the FINN fire inventory and State fire reports, but nearby monitoring indicated ozone reaching less than 60 ppb.

Statistical model performance was calculated for 1-hour ozone for four areas of the state that exceed (Baton Rouge) or nearly exceed (Shreveport, New Orleans, Lake Charles) the 2008 ozone NAAQS. Daily average normalized bias and gross error were calculated for all prediction-observation pairs at all sites when observed ozone exceeded 40 ppb following EPA's modeling guidance (EPA, 2007). This guidance de-emphasizes the use of statistical "goals" for 8-hour ozone as a means of defining acceptable model performance, and instead stresses performing corroborative and confirmatory analysis to assure that the model is working correctly. Older 1-hour ozone modeling guidance (EPA, 1991) established performance goals for certain statistical parameters, including mean normalized bias ($< \pm 15\%$) and mean normalized gross error ($< 35\%$), respectively. While now considered obsolete, these 1-hour statistical metrics nevertheless provide established benchmarks that modern photochemical models should be expected to achieve.

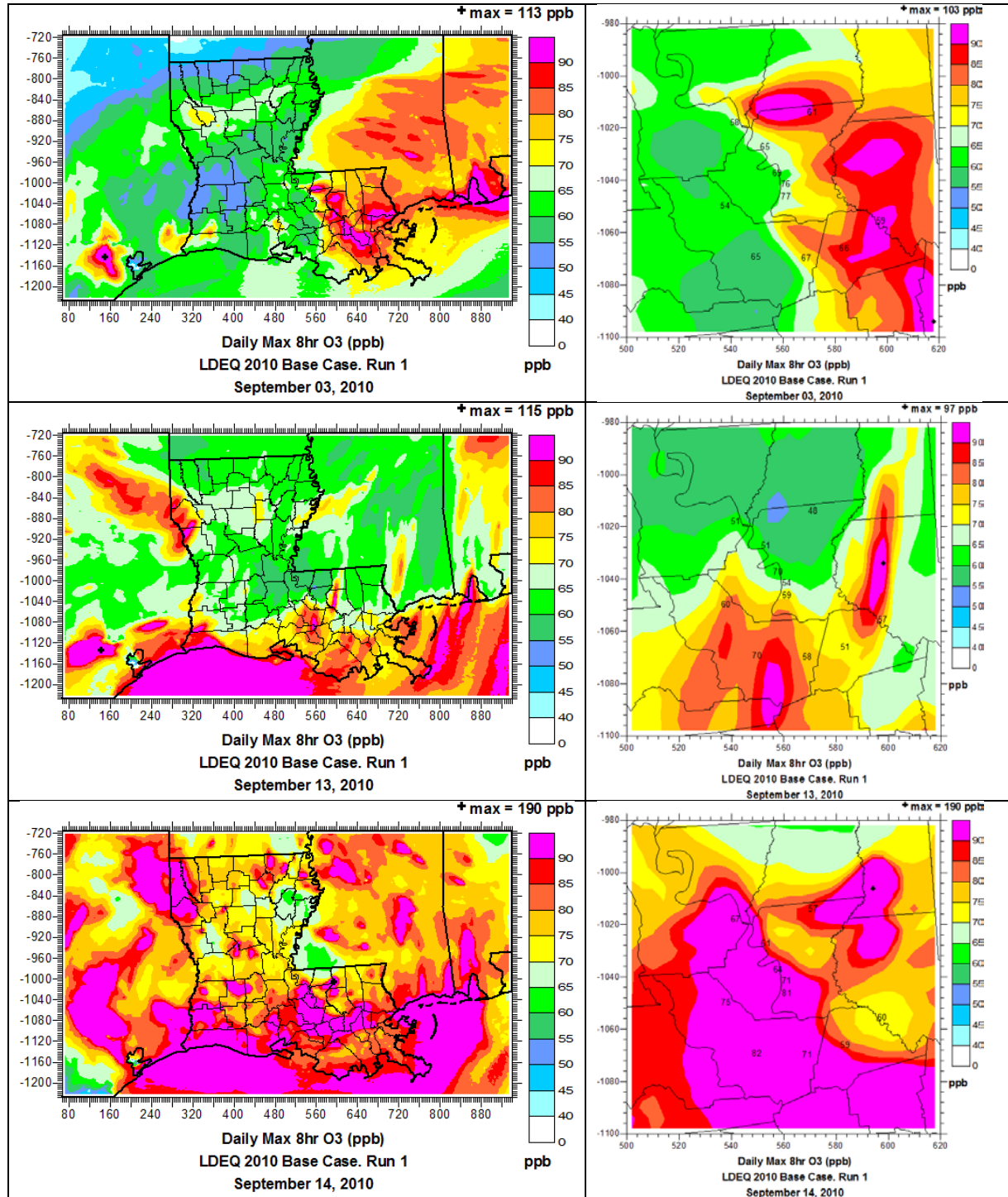


Figure 6-1. Spatial distribution of predicted MDA8 ozone (ppb) from the initial base year run on days exceeding the 2008 ozone NAAQS in Louisiana. Plots are shown for the entire 4 km modeling grid (left) and for south-central Louisiana focusing on Baton Rouge, with observed MDA8 ozone overlaid at monitor locations (right).

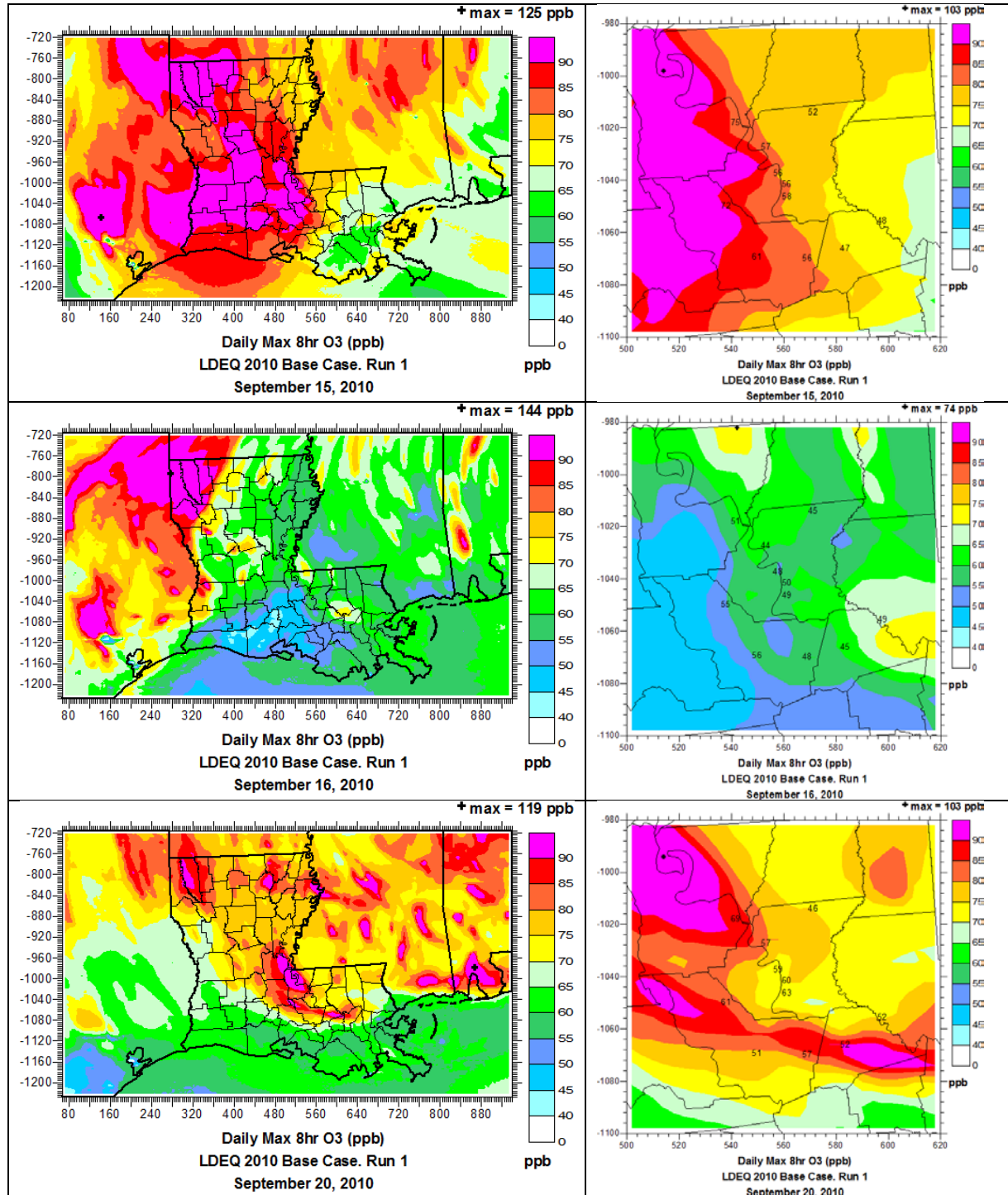


Figure 6-1 (continued).

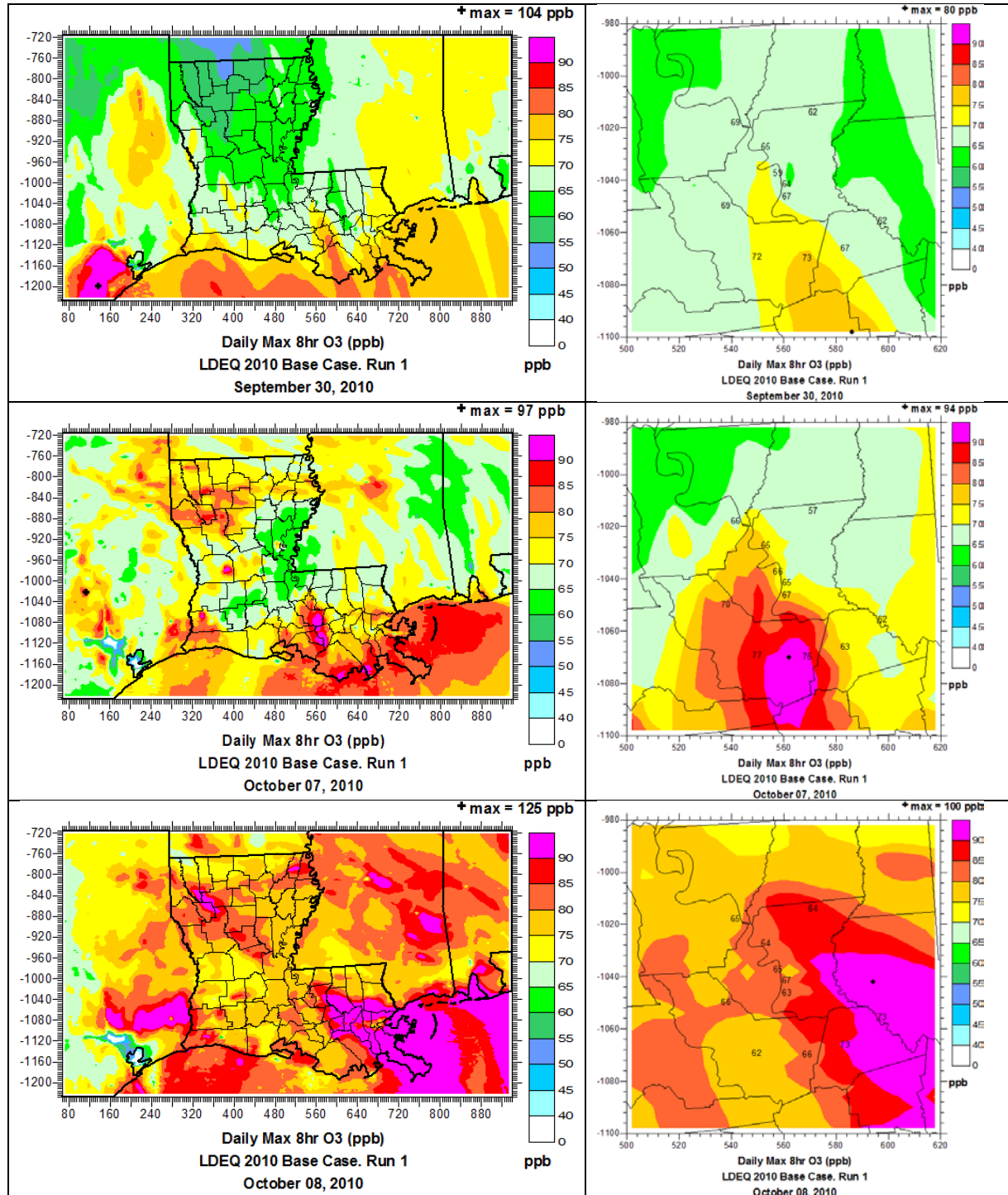


Figure 6-1 (continued).

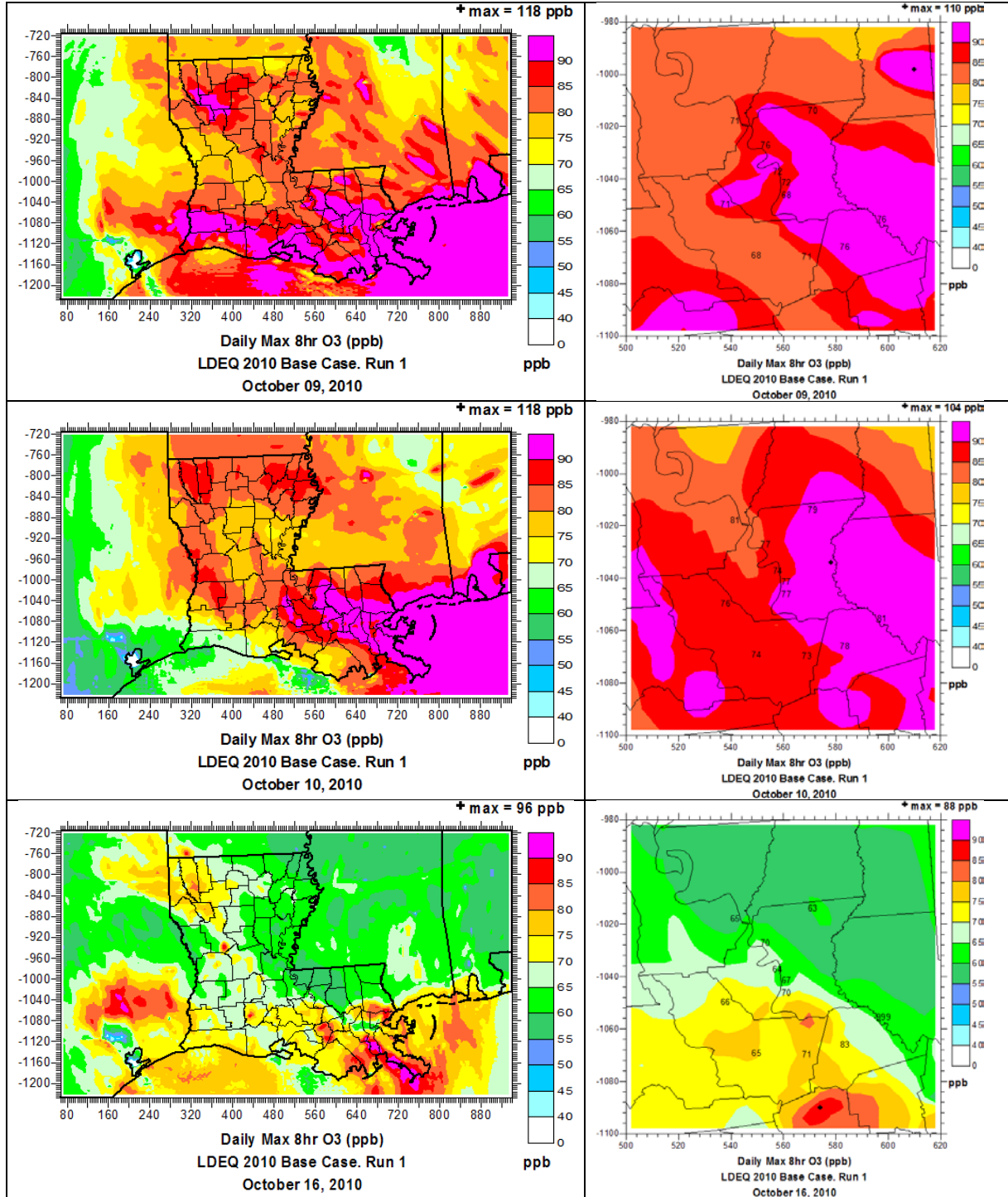


Figure 6-1 (continued).

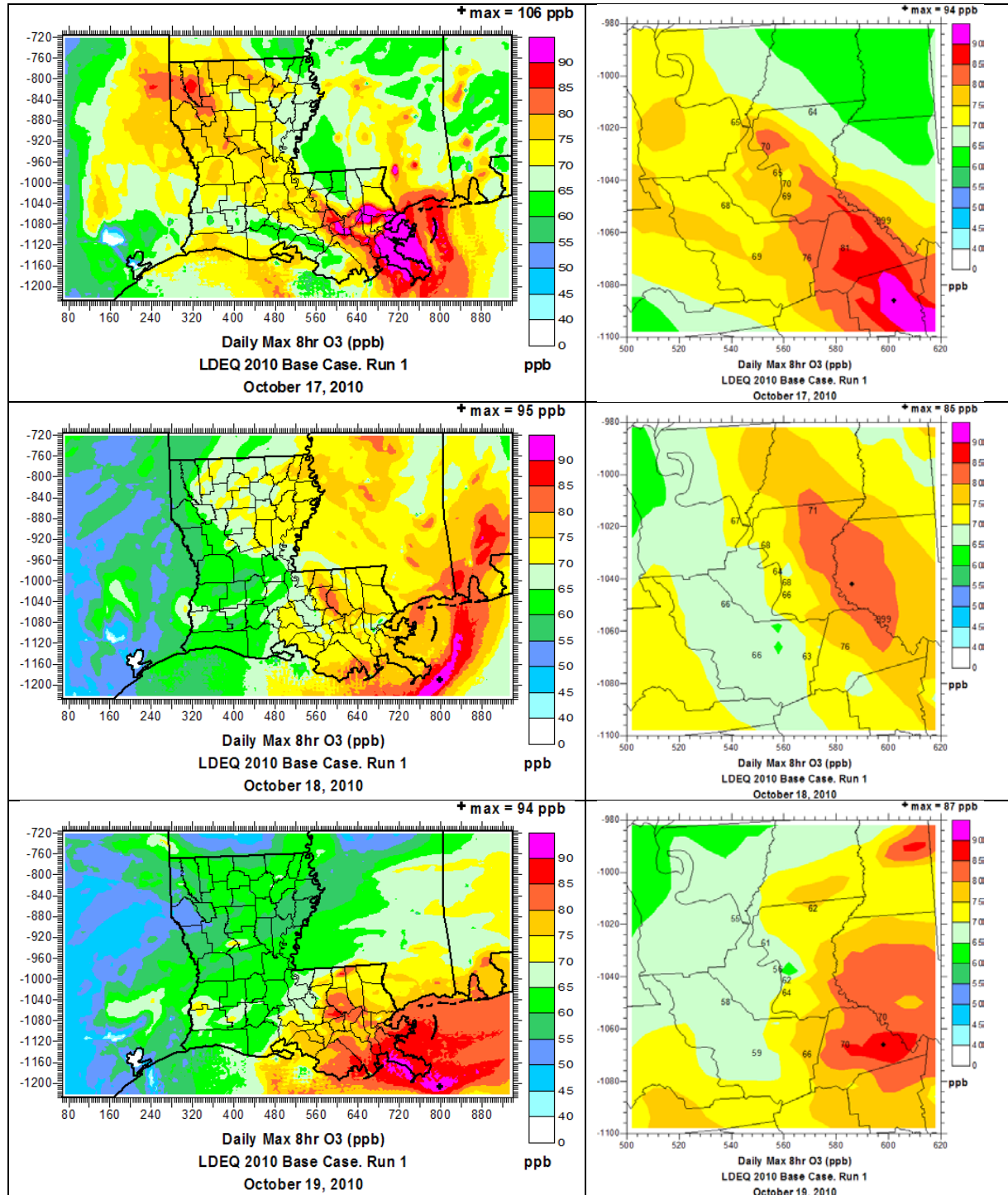


Figure 6-1 (concluded).

Time series of daily statistics for Baton Rouge are shown in Figure 6-2; the old 1-hour goals for normalized bias and gross error are also shown for reference. Performance in September was clearly worse than in October. The pattern for over prediction bias in September was consistently 30-50% and not particularly related to observed levels, whereas over prediction patterns in October tended to be associated with high ozone episodes.

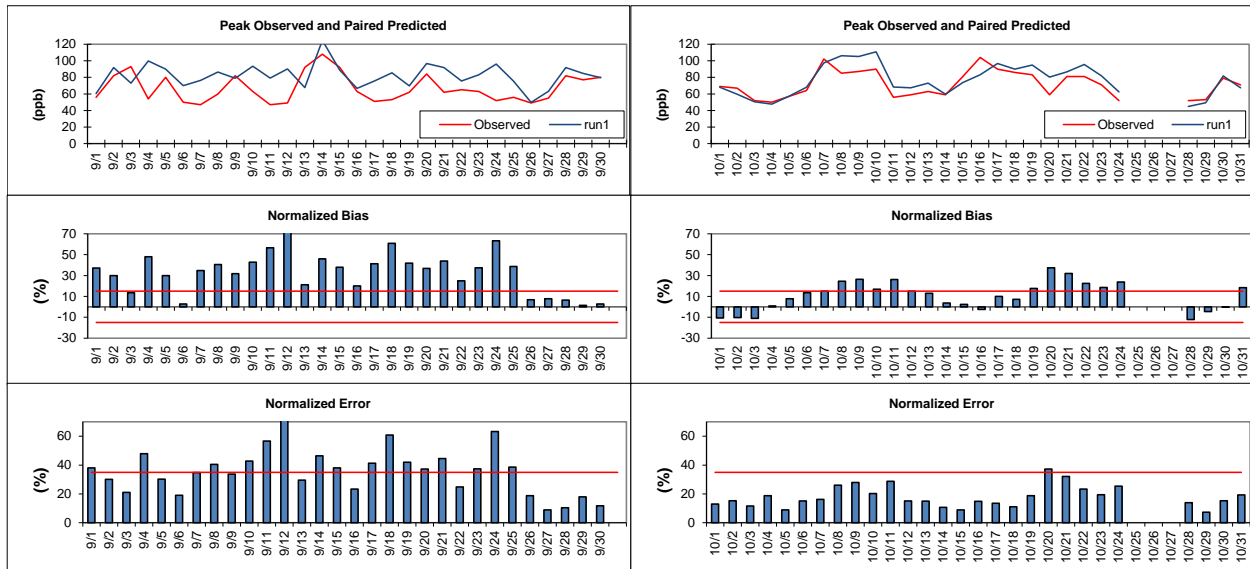


Figure 6-2. Daily statistical performance for the initial base year run at all Baton Rouge monitoring sites and for all hours when observed ozone was greater than 40 ppb, for September (left) and October (right), 2010. Top row: maximum daily peak 1-hour observed ozone (red) and paired simulated peak at the same site (blue). Middle row: daily mean normalized bias (bars) with $\pm 15\%$ bias highlighted (red lines). Bottom row: daily mean normalized gross error (bars) with 35% error highlighted (red lines).

Figure 6-3 presents the same data shown for the daily bias and error statistics in Figure 6-2, but in terms of a two-dimensional error space, with bias on the horizontal axis and gross error on the vertical axis. The 1-hour benchmarks have been plotted to represent a “goal” within which the bulk of paired daily bias and gross error points should fall to indicate a well-performing model. We have plotted the error points in different colors; those in red signify the ozone exceedance days in Louisiana as shown in Figure 6-1. Each figure notes the fraction of days within the goal. In Baton Rouge, the September over prediction bias is clearly evident for most days, regardless of observed ozone level. Performance in October was better but also exhibited an over prediction tendency.

Similar plots are shown for New Orleans, Shreveport, and Lake Charles in Figures 6-4 through 6-6, respectively. Large over predictions are evident in all cases, although Shreveport performance in September was not as extreme as in the southern cities.

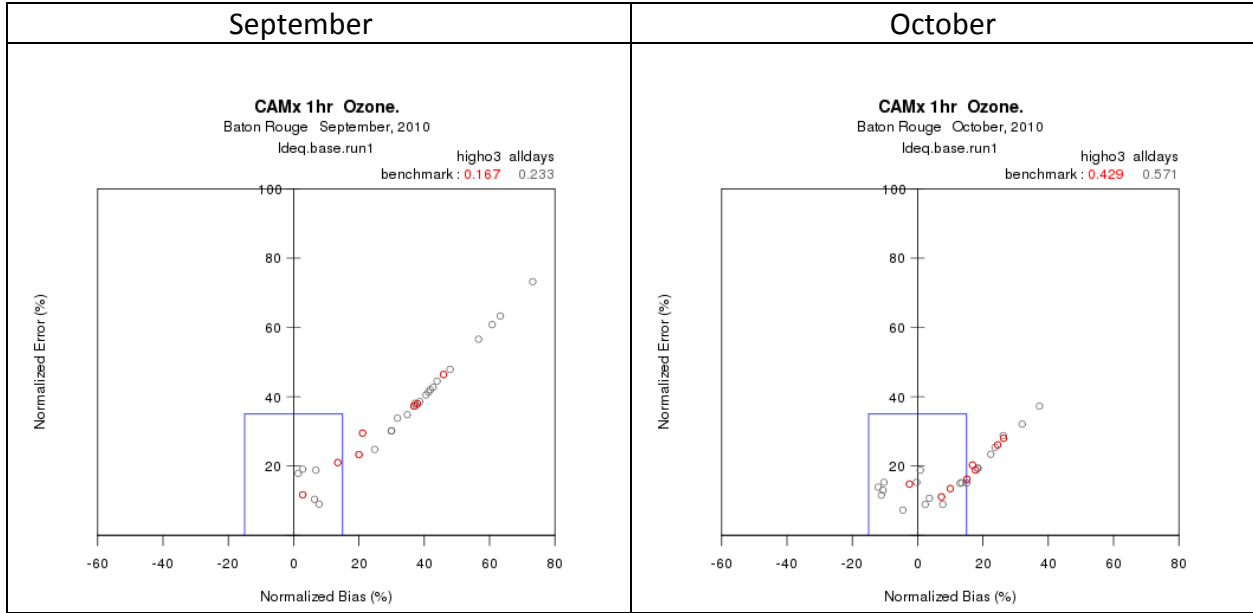


Figure 6-3. “Goal” plots of daily normalized bias and error from the initial base year run in Baton Rouge for September (left) and October (right). The blue goal denotes statistics within the 1-hour performance benchmarks. Red points are the high ozone days shown in Figure 6-1.

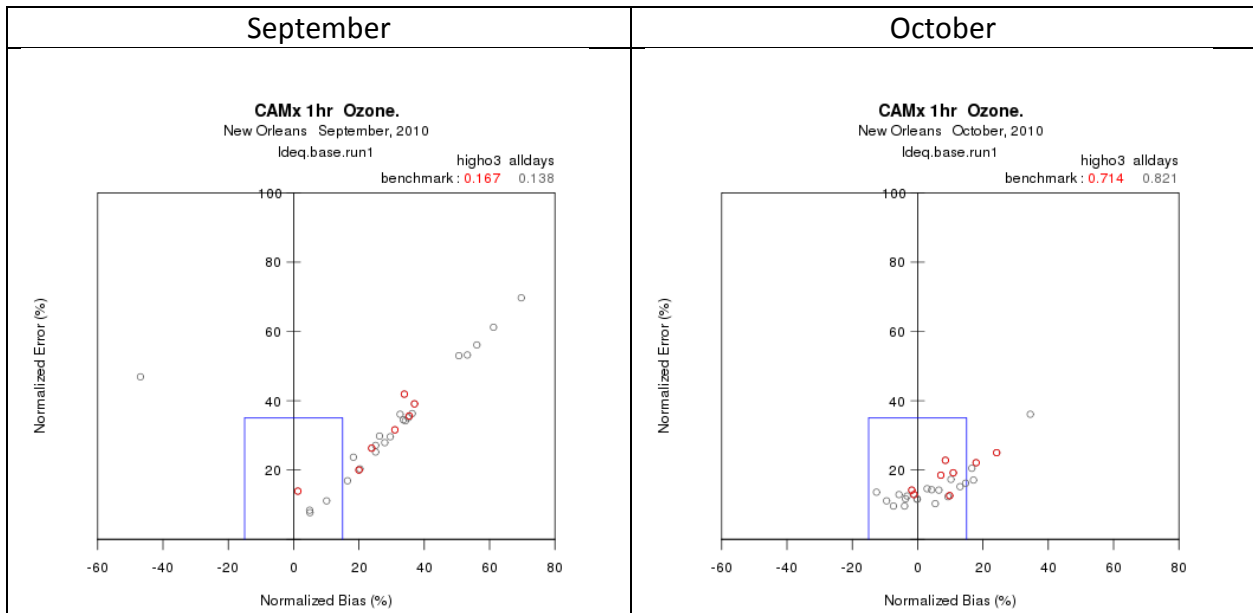


Figure 6-4. “Goal” plots of daily normalized bias and error from the initial base year run in New Orleans for September (left) and October (right). The blue goal denotes statistics within the 1-hour performance benchmarks. Red points are the high ozone days.

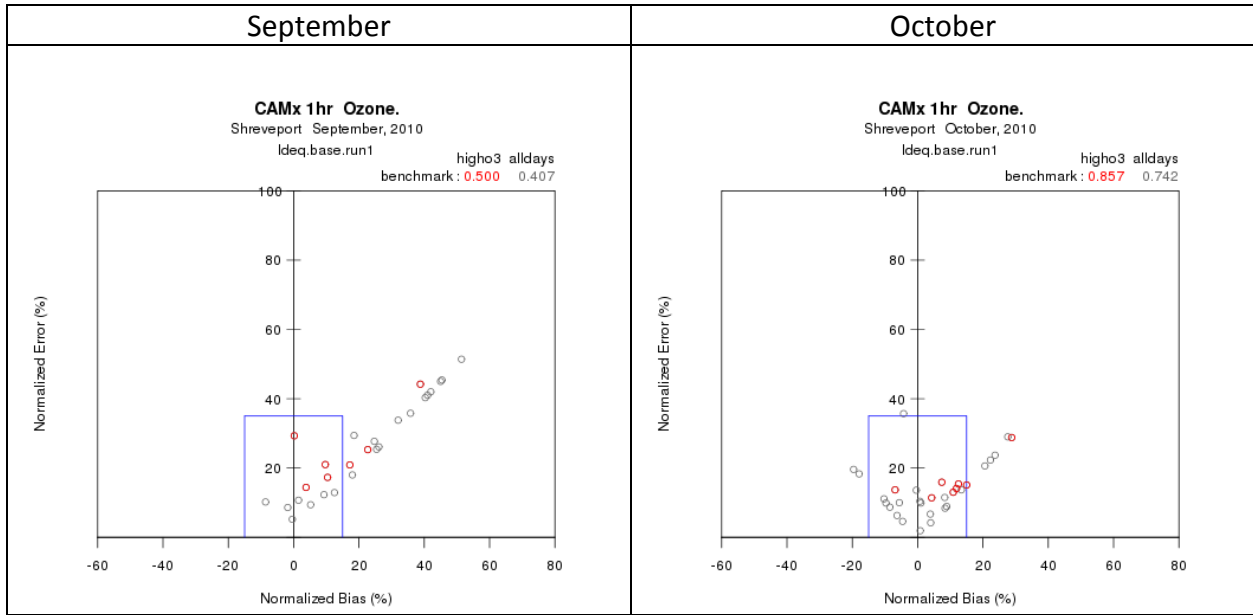


Figure 6-5. “Goal” plots of daily normalized bias and error from the initial base year run in Shreveport for September (left) and October (right). The blue goal denotes statistics within the 1-hour performance benchmarks. Red points are the high ozone days.

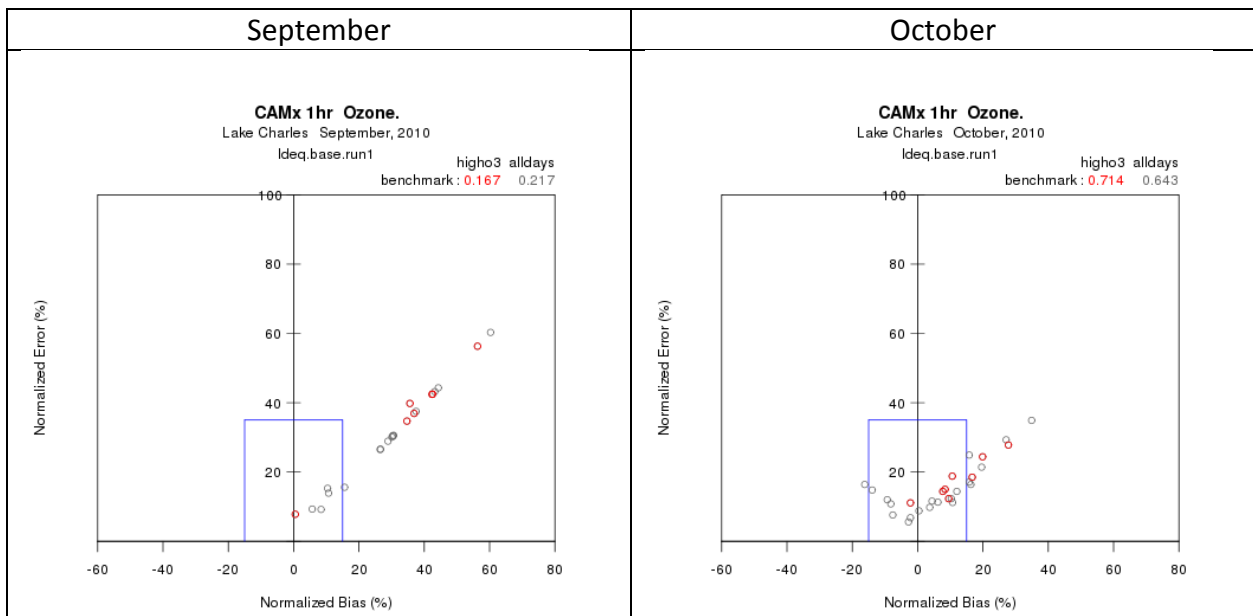


Figure 6-6. “Goal” plots of daily normalized bias and error from the initial base year run in Lake Charles for September (left) and October (right). The blue goal denotes statistics within the 1-hour performance benchmarks. Red points are the high ozone days.

Time series of simulated and observed hourly ozone and NO_x at the urban LSU monitor throughout September and October are shown in Figures 6-7 and 6-8, respectively. Among all Baton Rouge sites, the LSU monitor recorded the highest ozone of the modeling period. In September, daily ozone over predictions occurred for most hours, although they were more extreme during the daytime. Performance was much better in October, when only a few of the highest ozone days exhibited similarly large over predictions. Hourly NO_x concentrations were simulated well at LSU, especially during the daytime. The only exceptions were for occasional peak nighttime values when the model under predicted NO_x by factors of up to 2 or 3. The under prediction of nighttime NO_x is not likely related to improper characterization of nighttime emissions, but rather to an inability to resolve local emission at 4 km grid scale (i.e., over-dilution to grid volume) and meteorological influences such as excessive nocturnal vertical mixing.

Similar time series for ozone and NO_x are shown at the Dutchtown monitor in Figures 6-9 and 6-10; this site represents a high NO_x emissions site as it is located very near the I-10 freeway south of Baton Rouge. Similar large daytime ozone over prediction patterns occurred at this site in September, and perhaps better performance occurred in October at Dutchtown than at LSU. Predicted and observed NO_x agreed rather well, with generally higher NO_x and much more diurnal variability (as expected). It is possible that higher levels of fresh NO_x emissions predicted at Dutchtown may have controlled ozone over predictions to some extent through chemical scavenging.

A final set of time series is shown for the rural Pride site in Figures 6-11 and 6-12, which is located northwest of Baton Rouge. From the standpoint of daily peak hourly ozone, over predictions were not as extreme as at LSU, but the entire time series exhibited over predictions for very nearly every hour of both months. In particular, nighttime ozone was far too high, taking on the characteristics typical of rural background ozone with small diurnal amplitude that is not influenced by scavenging from local NO_x. However, the observations clearly show nightly ozone scavenging to zero each night. Indeed, NO_x observations were surprisingly high for a rural site, and likely indicated a local source that contributed to nightly ozone reductions around the monitor. NO_x tended to be under predicted, but even during the few nights with over predictions, simulated ozone was not greatly affected.

The consistent dichotomy in ozone performance between September and October across all regions of Louisiana suggests a fundamental and systematic difference in the characterization of the photochemical environment. The two most obvious inputs that define this environment are meteorology and emissions, and their impacts may not be mutually independent. For example, temperature is very influential for various important emissions categories (e.g., biogenic and on-road sources), while wind patterns affect the source mix contributing to high ozone levels. Figures 6-13 and 6-14 reiterate the wind direction and temperature patterns, respectively, that were prevalent in southern Louisiana during September and October of 2010. Note that September was warm with winds from the east, while October was much cooler with winds from the west. At least meteorologically, these two months were indeed very different.

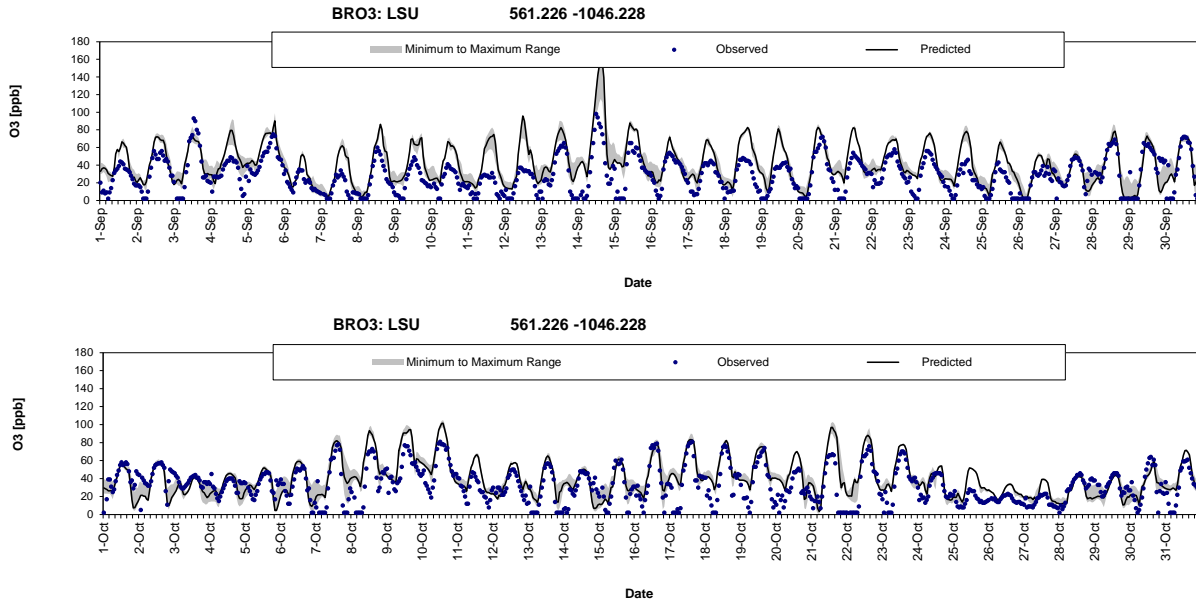


Figure 6-7. Hourly time series of observed (blue dots) and predicted (solid line) ozone at the LSU monitoring site during September (top) and October (bottom). Grey shading indicates the range of predicted ozone among the nine grid cells surrounding the monitor.

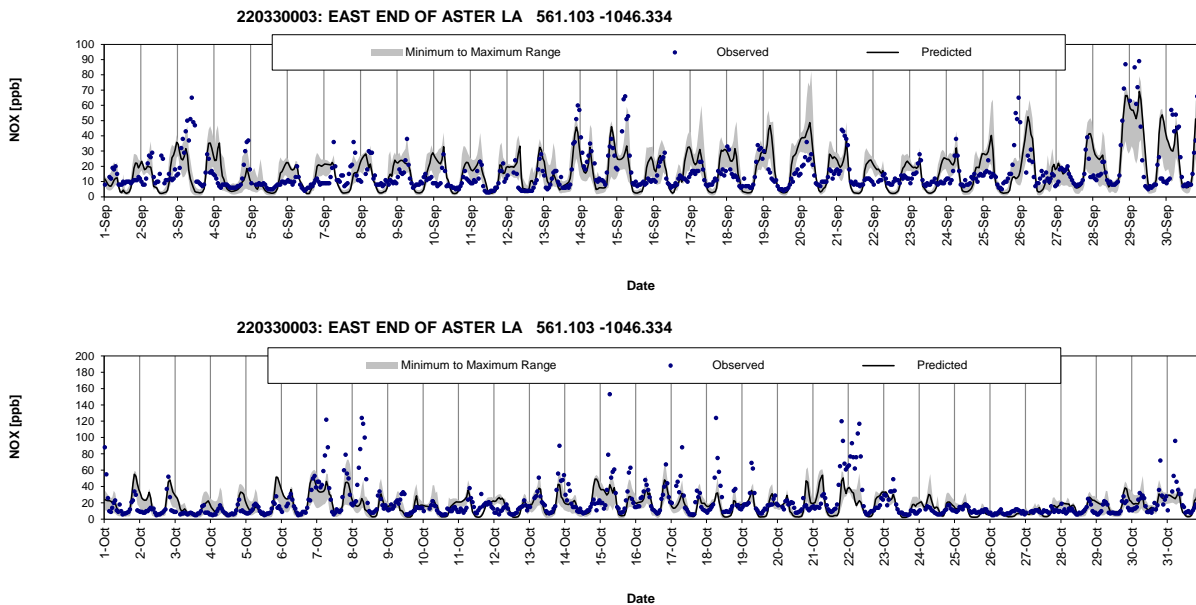


Figure 6-8. Hourly time series of observed (blue dots) and predicted (solid line) NOx at the LSU monitoring site during September (top) and October (bottom). Grey shading indicates the range of predicted NOx among the nine grid cells surrounding the monitor.

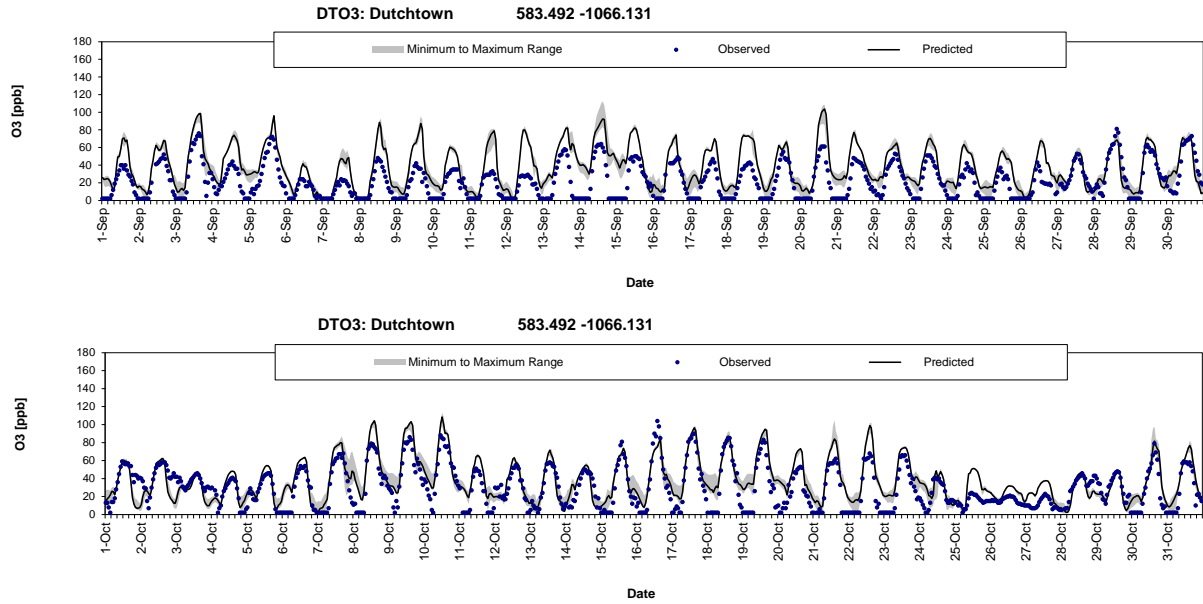


Figure 6-9. Hourly time series of observed (blue dots) and predicted (solid line) ozone at the Dutchtown monitoring site during September (top) and October (bottom). Grey shading indicates the range of predicted ozone among the nine grid cells surrounding the monitor.

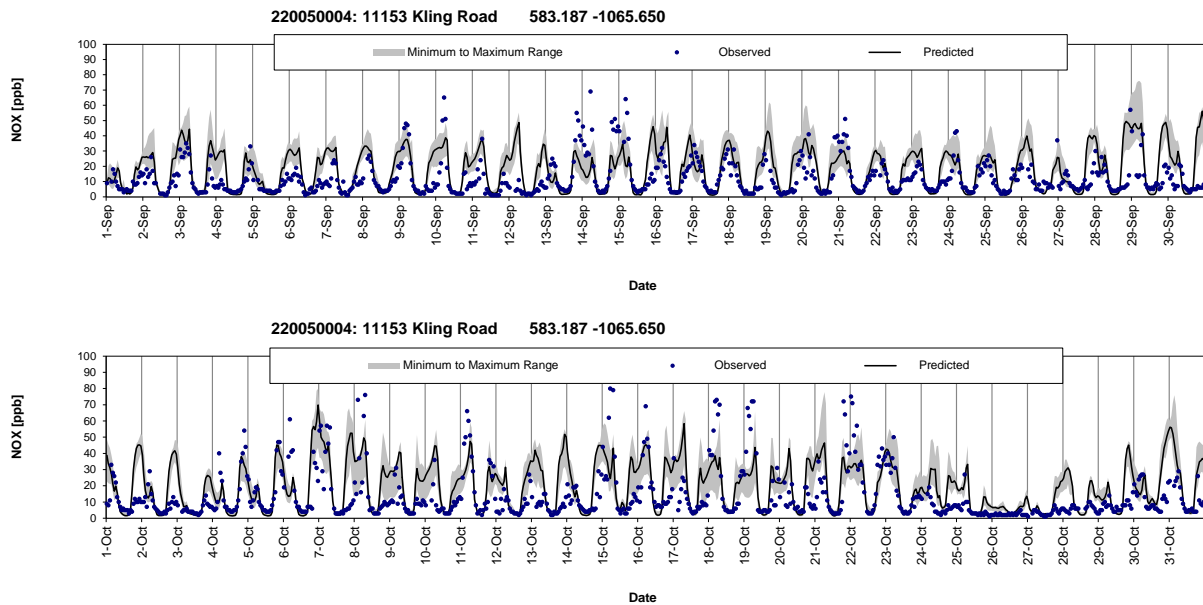


Figure 6-10. Hourly time series of observed (blue dots) and predicted (solid line) NOx at the Dutchtown monitoring site during September (top) and October (bottom). Grey shading indicates the range of predicted NOx among the nine grid cells surrounding the monitor.

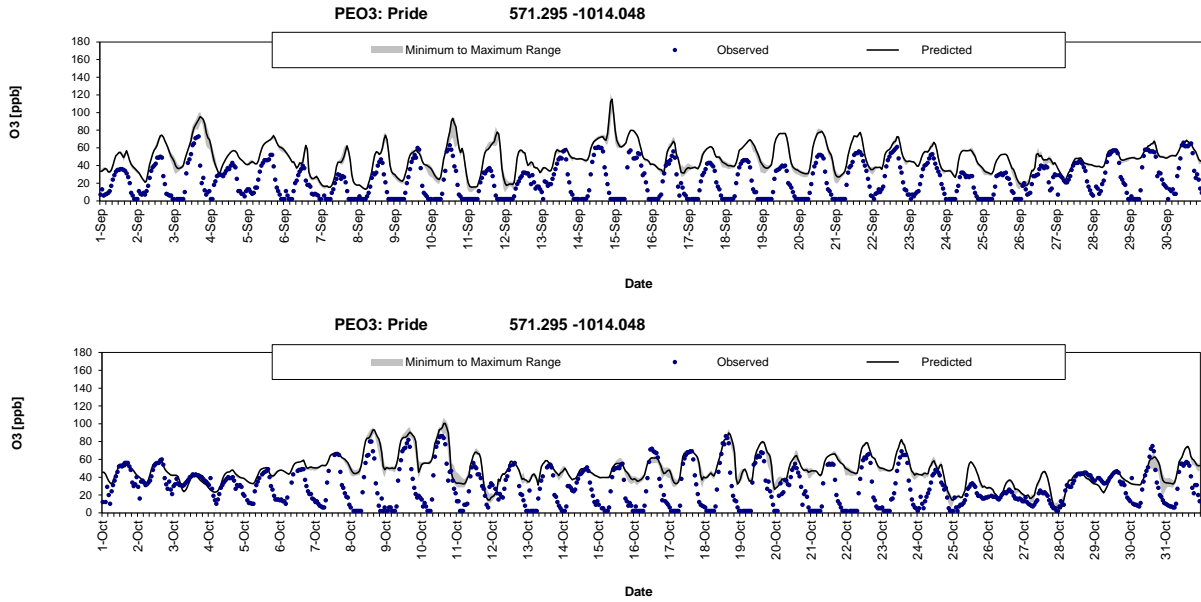


Figure 6-11. Hourly time series of observed (blue dots) and predicted (solid line) ozone at the Pride monitoring site during September (top) and October (bottom). Grey shading indicates the range of predicted ozone among the nine grid cells surrounding the monitor.

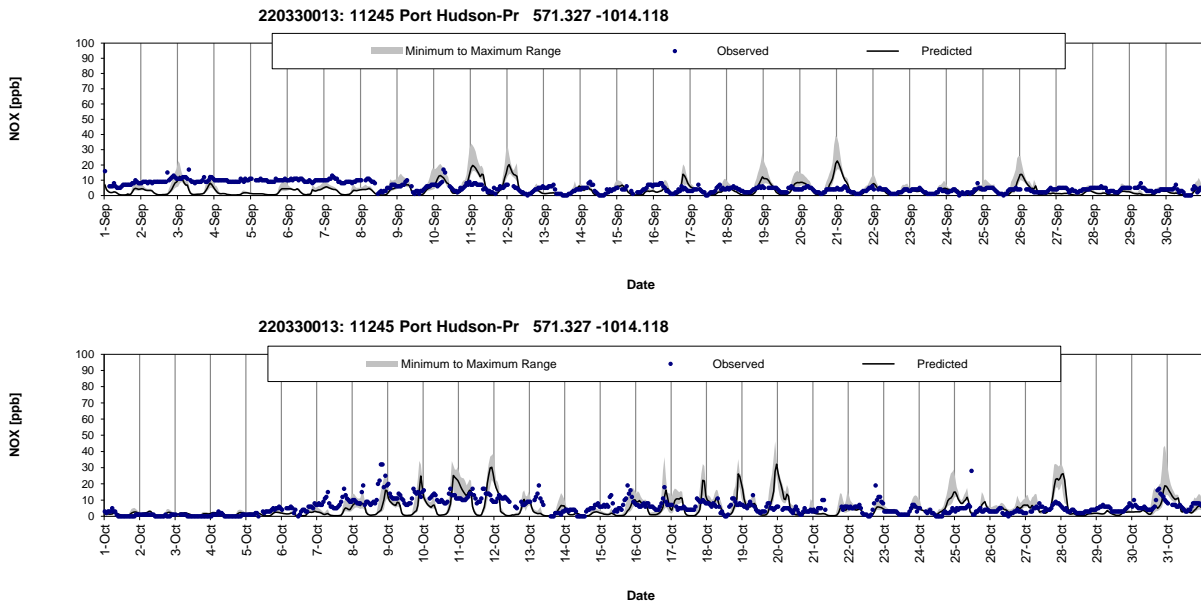


Figure 6-12. Hourly time series of observed (blue dots) and predicted (solid line) NOx at the Pride monitoring site during September (top) and October (bottom). Grey shading indicates the range of predicted NOx among the nine grid cells surrounding the monitor.

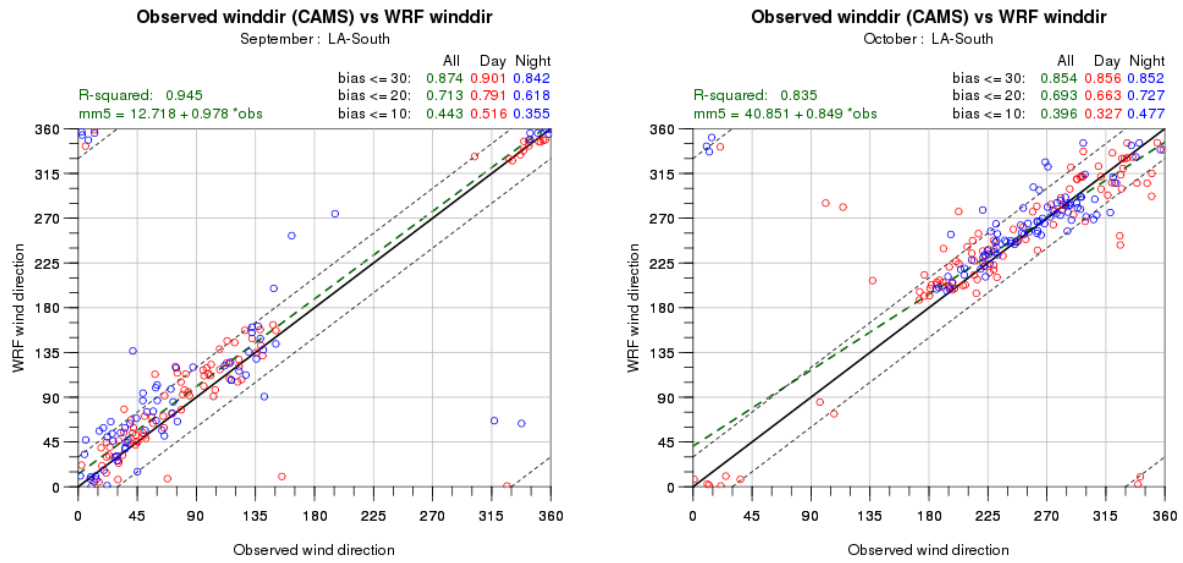


Figure 6-13. WRF performance for wind direction against observations in southern Louisiana in September (left) and October (right). Figure is duplicated from Figure 3-10.

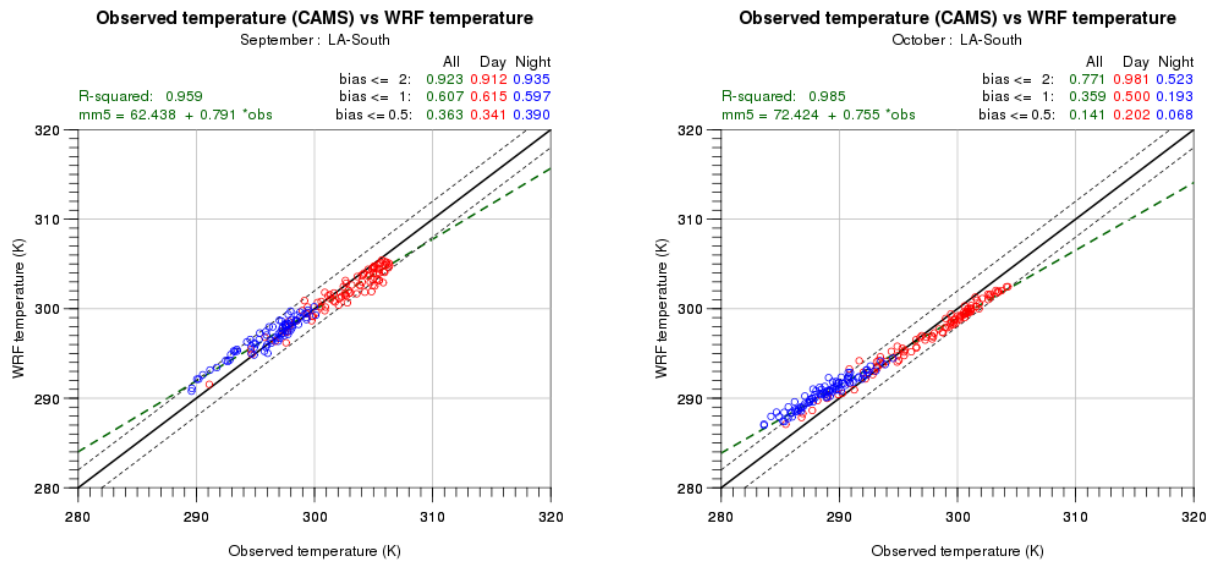


Figure 6-14. WRF performance for temperature against observations in southern Louisiana in September (left) and October (right). Figure is duplicated from Figure 3-14.

6.3 Diagnostic Sensitivity Testing (Phase 1)

A series of diagnostic sensitivity tests were conducted for the month of September to identify and potentially rectify the ubiquitous ozone over predictions evident from the initial base year run. Table 6-1 summarizes each of the Phase 1 sensitivity tests, including their purpose and their results.

Table 6-1. Phase 1 diagnostic sensitivity tests performed on the CAMx 2010 base year simulation.

Run ID	Purpose	Results
2	Remove all wildfire emissions to isolate their impact	Large local ozone reductions in fire plumes; Minor regional ozone reductions; Negligible impact on statistical performance
3	Remove Kv “patching” to quantify its impact	Negligible impact on daytime NO _x and ozone; Increased nighttime NO _x , lower nighttime ozone; Better nighttime ozone performance
5	Remove wildfire NO _x emissions to verify it as the driver for locally high ozone	Nearly identical results to Run 2; Confirms NO _x -sensitive rural conditions
6	Calculate Kv from WRF/YSU technique to test sensitivity to Kv approach	Minor mixed impacts on MDA8 patterns; Mostly higher ozone
7	Replace CB6 chemistry with Carbon Bond 2005 (CB05) to test sensitivity to choice of mechanism	Large widespread reductions in MDA8 ozone; Improved statistical performance
8	Scale MOVES on-road emissions in 4 km domain to emulate MOBILE6; derived from 2008 EPA NEI for LA parishes (30% NO _x reduction, 34% VOC increase)	Minor impacts to statistical performance; Minor mixed impacts on MDA8 patterns; Confirms VOC-sensitive urban conditions; LDEQ elected to stay with MOVES
9	Scale wildfire NO _x down by 80%, add emissions of PAN and HNO ₃ to represent aged NO _y	Moderate local ozone reductions in fire plumes; Minor regional ozone reductions; Negligible impact on statistical performance

We also analyzed other issues beyond additional CAMx simulations, including:

- *Does the gasoline RVP switch in late September impact on-road emissions?* We evaluated daily total on-road emissions for each day throughout September and October. No obvious RVP signal was seen, and the largest day-to-day variation was caused by temperature fluctuations.
- *Were any emissions double-counted during processing into model-ready inputs?* Further quality assurance checks revealed no double-counting.
- *Are biogenic isoprene emissions too high?* Other concurrent regional modeling efforts have observed that MEGAN isoprene estimates in the eastern US are much higher than other models, such as EPA’s Biogenic Emission Inventory System (BEIS), thereby contributing to ozone over predictions. September isoprene emissions in the 4 km grid were about two times higher than in October. A review of 8-day satellite vegetative fields exhibited only slight reductions from September to October. There were negligible changes in sunlight. A sudden shift to cooler temperatures on September 25 tracked well with the downward shift

in isoprene and ozone bias. Therefore, excessive biogenic emissions were considered a possible cause for the September over predictions.

- *Is the depth of daytime vertical diffusion too shallow in September?* We compared modeled mixing depths against 6 PM Shreveport rawinsonde temperature profiles. Relatively large day-to-day variations in mixing depth occurred in both the observations and the model, but the model tended to grossly track observed variability with no consistent high or low bias. Therefore, results were inconclusive. However, since this was a single point comparison per day, we could not extend results to entire State.

An intermediate simulation (Run 10) was performed over the entire September-October modeling period by combining several of the most significant changes listed in Table 6-1. Specifically, the run included:

- CB05 chemical mechanism: emissions for a certain few VOC compounds specific to CB6 were aggregated into CB05 compounds and the TUV preprocessor was run to calculate photolysis rates specific to CB05;
- No nocturnal Kv “patch”: enhanced urban vertical mixing at night was removed, but the daytime patch was retained to maximize vertical diffusion;
- Revised wildfire NO_y emissions per Run 9, following the approach of Alvarado et al. (2010): Reduced NO_x by 80% to align NO_x:CO ratios, and added new emissions of PAN (94% of final NO_x) and HNO₃ (50% of final NO_x) to align NO_x:NO_y ratios and to emulate rapid oxidation of NO_x during plume rise and prior to release into the grid.

Figure 6-15 presents spatial plots of MDA8 ozone from Run 10 on September 14, along with the difference in MDA8 from Run 1. This particular day was chosen because it possessed the highest observed ozone of the period in Baton Rouge and exhibited the largest over predictions in Run 1. Dramatic reductions of MDA8 ozone by 10-20+ ppb are evident throughout the domain, but concentrations in Baton Rouge continued to be over predicted by 10-20 ppb on this day. The peak MDA8 continued to be predicted in the fire plume northwest of Baton Rouge, but that peak was reduced by 44 ppb (from 190 ppb).

Figures 6-16 through 6-19 show September and October bias and gross error goal plots for Baton Rouge, New Orleans, Shreveport, and Lake Charles, respectively. Daily bias and gross error were reduced substantially in all four regions and on all days of September, and October daily performance met performance goals on nearly every day. However, the majority of exceedance days in September continued to exhibit high ozone bias in all regions except Shreveport.

6.4 Evaluation of Ozone Precursors

Despite rather good October performance achieved in Run 10, the continued large over prediction tendencies in most areas of Louisiana during September indicated that a fundamental systematic problem remained that influenced September more than October. This further gave rise to concerns as to whether good October performance was achieved for

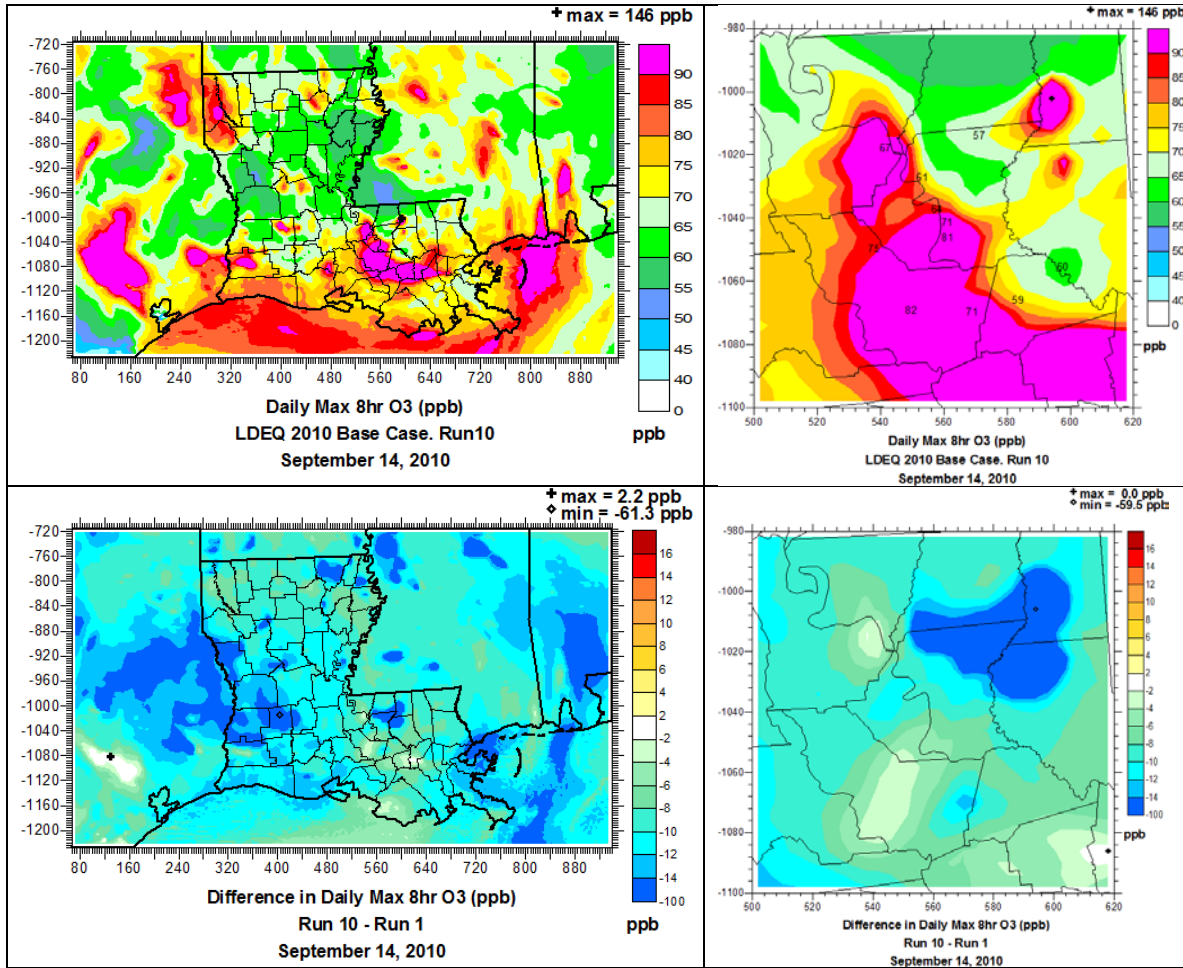


Figure 6-15. Top row: Spatial distribution of predicted MDA8 ozone (ppb) from Run 10 on September 14. Plots are shown for the entire 4 km modeling grid (left) and for south-central Louisiana focusing on Baton Rouge, with observed MDA8 ozone overlaid at monitor locations (right). Bottom row: Spatial distribution of differences (Run 10 – Run 1) in MDA8 on the 4 km modeling grid (left) and over south-central Louisiana (right).

the correct reason(s).

We hypothesized that higher NO_x estimated by MOVES could be driving the over predictions. However, results from the MOBILE6 emulation test (Run 8) resulted in minor impacts on simulated urban ozone, despite 30% reductions in NO_x. Such insensitivity to NO_x is common in NO_x-rich urban areas where on-road emissions dominate. But the question remained: should Baton Rouge be more NO_x-sensitive?

Analyses comparing simulated and observed NO_x, VOC, and VOC:NO_x ratios were undertaken to evaluate the emissions inventory for Baton Rouge and to better understand the chemical conditions leading to high ozone in the region. Four PAMS sites are located in Baton Rouge, co-

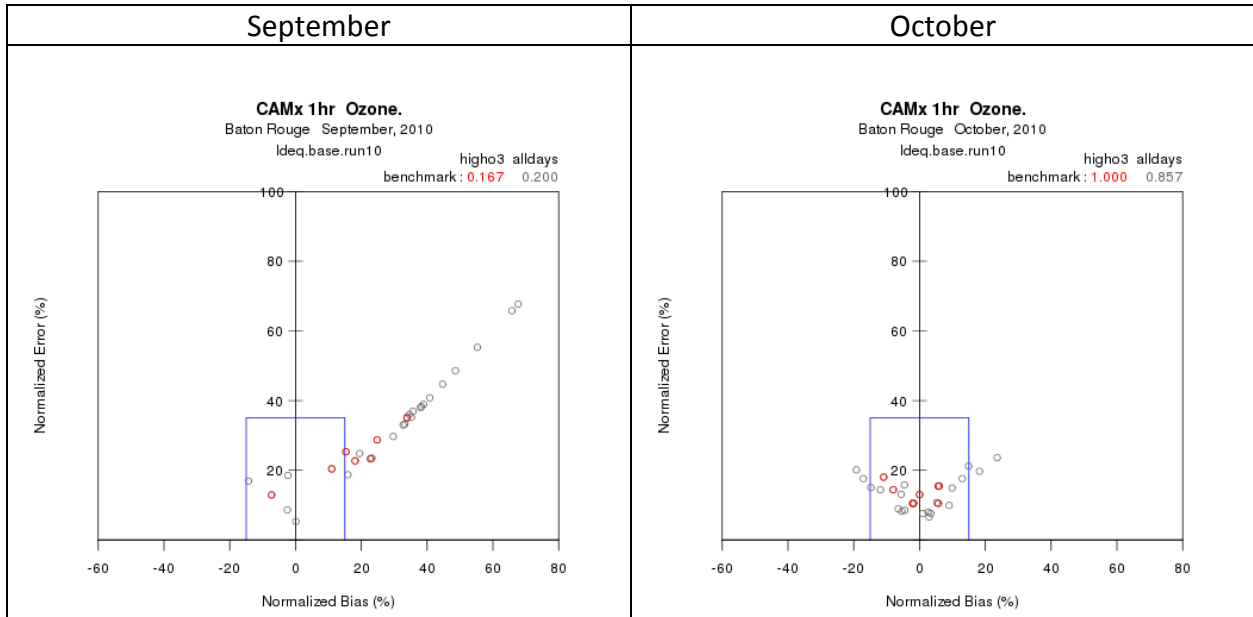


Figure 6-16. “Goal” plots of daily normalized bias and error from Run 10 in Baton Rouge for September (left) and October (right). The blue goal denotes statistics within the 1-hour performance benchmarks. Red points are the high ozone days shown in Figure 6-1.

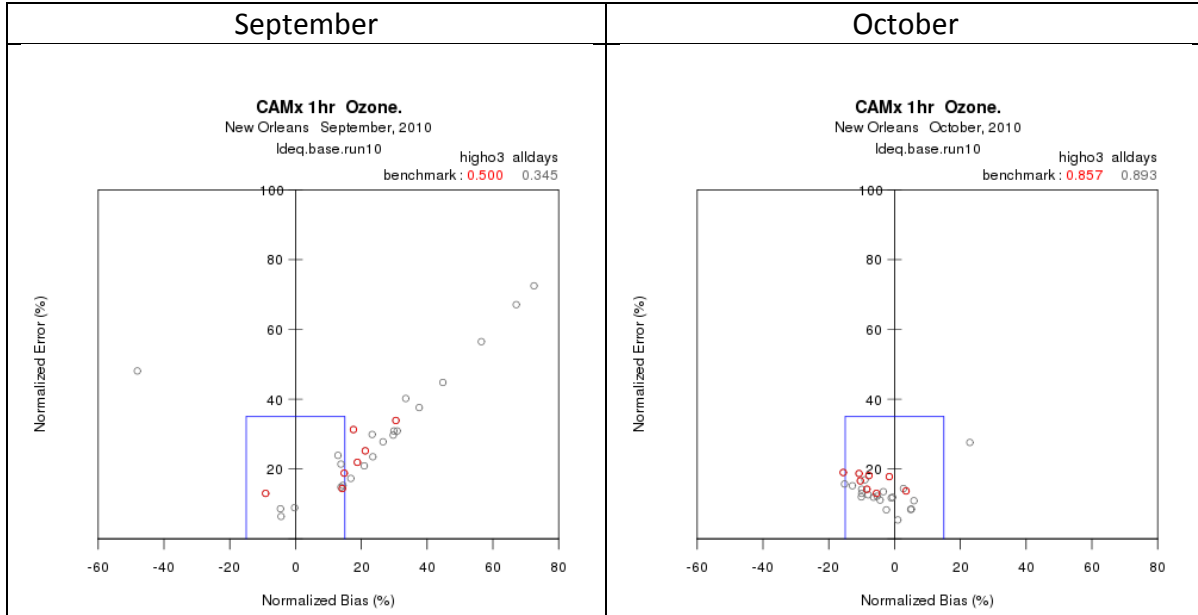


Figure 6-17. “Goal” plots of daily normalized bias and error from Run 10 in New Orleans for September (left) and October (right). The blue goal denotes statistics within the 1-hour performance benchmarks. Red points are the high ozone days shown in Figure 6-1.

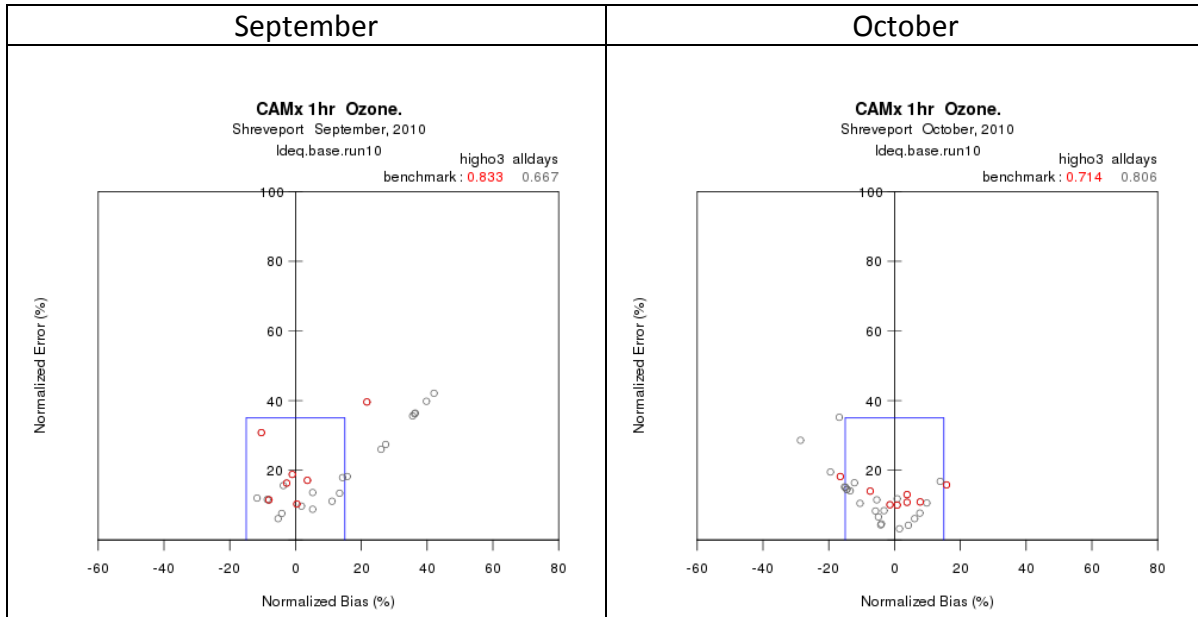


Figure 6-18. “Goal” plots of daily normalized bias and error from Run 10 in Shreveport for September (left) and October (right). The blue goal denotes statistics within the 1-hour performance benchmarks. Red points are the high ozone days shown in Figure 6-1.

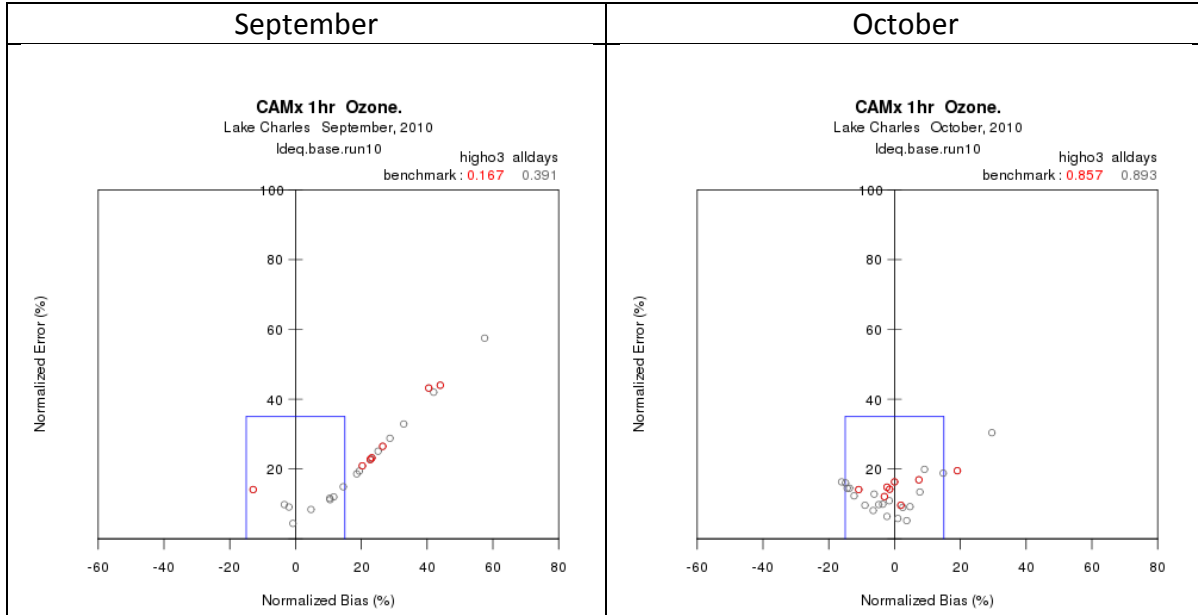


Figure 6-19. “Goal” plots of daily normalized bias and error from Run 10 in Lake Charles for September (left) and October (right). The blue goal denotes statistics within the 1-hour performance benchmarks. Red points are the high ozone days shown in Figure 6-1.

General precursor comparisons at all four PAMS sites are summarized in Table 6-2, expressed as 6-9 AM averages over September and October. At the urban sites (Capitol and Dutchtown), both NO_x and VOC tend to be over predicted, but VOC:NO_x ratios are adequately predicted and indicate NO_x-rich, VOC-limited conditions. Precursor over predictions may be associated with inadequate morning ventilation in the growing mixed layer, and/or too much emission allocated to the 6-9 AM period. At the rural sites (Pride and Bayou Plaquemine), NO_x is well-predicted, but VOC is over predicted and that leads to higher simulated VOC:NO_x ratios than observed, particularly at Pride (NO_x-sensitive conditions).

Table 6-2. September and October averages of 6-9 AM observed and simulated NO_x, VOC, and VOC:NO_x ratio at four PAMS sites in Baton Rouge. VOC:NO_x ratios are colored according to VOC-limited (blue), NO_x-limited (red), and transition (purple) conditions.

	Capitol		Dutchtown		Pride		B. Plaquemine	
	Sep	Oct	Sep	Oct	Sep	Oct	Sep	Oct
Obs NO _x (ppb)	21	36	14	23	6	7	13	14
Prd NO _x (ppb)	29	37	21	26	3	4	16	12
Obs VOC (ppbC)	104	214	59	72	24	30	70	72
Prd VOC (ppbC)	188	184	150	172	66	66	104	88
Obs VOC:NO _x	5	6	4	3	4	5	5	5
Prd VOC:NO _x	6	5	7	7	23	15	6	8

Figure 6-21 shows absolute comparisons of 6-9 AM CB05 VOC concentrations at all four sites as an example of a poor performing high ozone day (September 14); relative distributions are shown in Figure 6-22. Figure 6-21 also includes annotations indicating 6-9 AM NO_x comparisons and VOC:NO_x ratios on that day. All sites exhibit over predictions of VOC, especially isoprene at rural sites. At all sites except Pride, simulated NO_x is close to measurements, and this leads to VOC:NO_x ratios that are too high into the transitioning from VOC-sensitive to NO_x-sensitive. At Pride, the excessive isoprene is driving VOC:NO_x ratios far too high. Whereas NO_x should be inhibiting ozone formation at these sites, both NO_x and VOC are likely contributing to ozone formation and that could explain ozone over predictions on this day.

Plotting these distributions as relative contributions to total VOC indicates the extent to which emissions are speciated correctly (Figure 6-22). On September 14, the relative distributions of CB05 species are well-replicated except for the consistent under prediction of ethane. Ethane is not well characterized in emission inventories, and its presence at measured values shown in Figure 6-21 suggest regional contributions from natural gas sources (production, distribution, processing). While this suggests a missing component in the emission inventory, ethane reacts very slowly and thus has little impact on local ozone generation.

Figures 6-23 and 6-24 show the absolute and relative VOC concentrations as an example of a good performing high ozone day (October 23), but are otherwise identical to the plots for September 14. Again VOCs tend to be over predicted but so is NO_x at all sites except Pride, leading to excellent agreement in VOC:NO_x ratios at three of the four sites. Note the

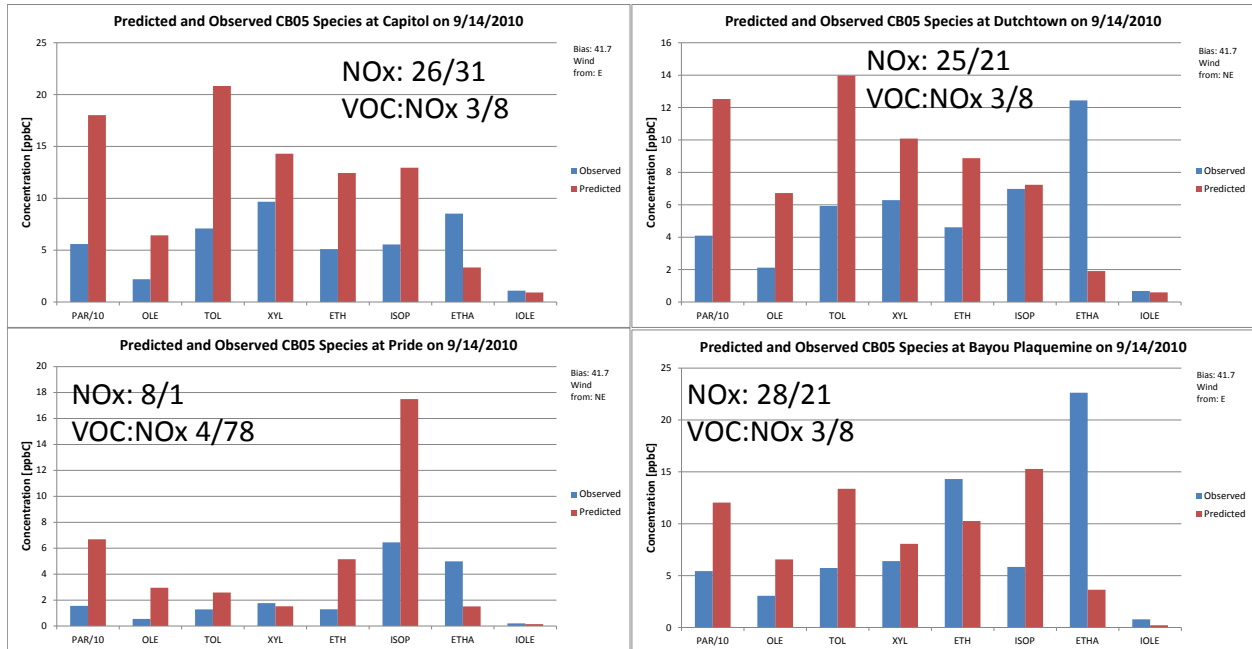


Figure 6-21. Comparison of 6-9 AM observed (blue) and simulated (red) CB05 VOCs at four PAMS sites in Baton Rouge on September 14, 2010. Plots are annotated with 6-9 AM observed/predicted NOx and VOC:NOx ratio.

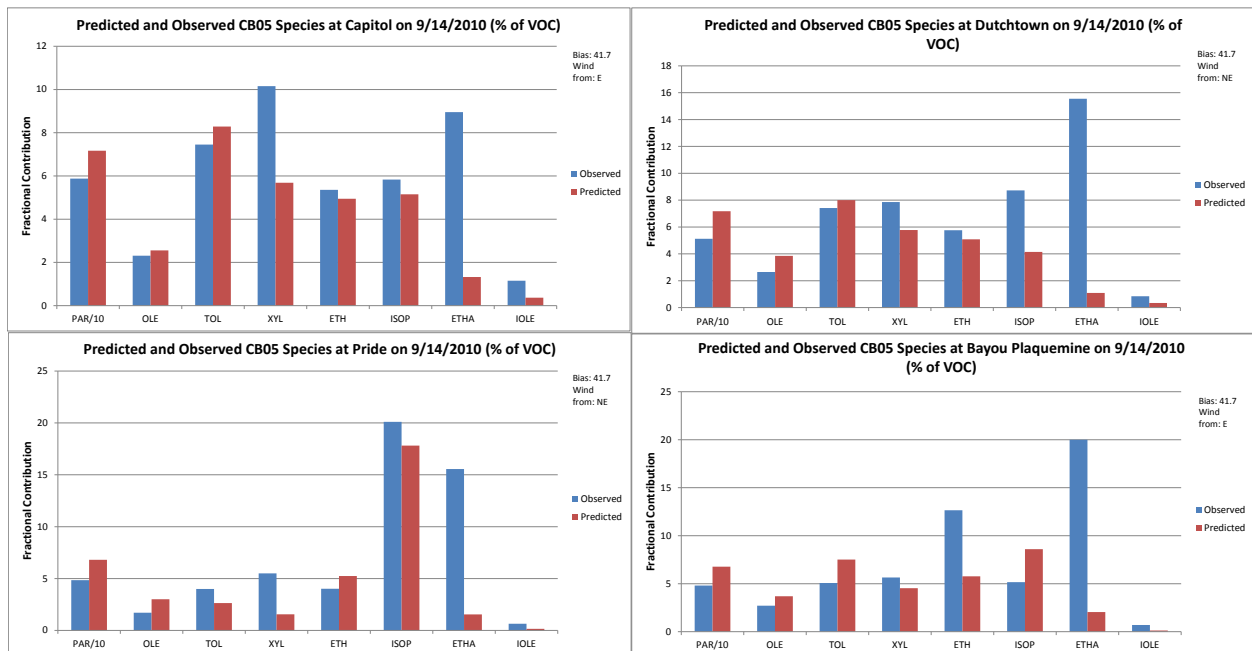


Figure 6-22. Comparison of 6-9 AM observed (blue) and simulated (red) relative contributions of CB05 VOCs to total VOC at four PAMS sites in Baton Rouge on September 14, 2010.

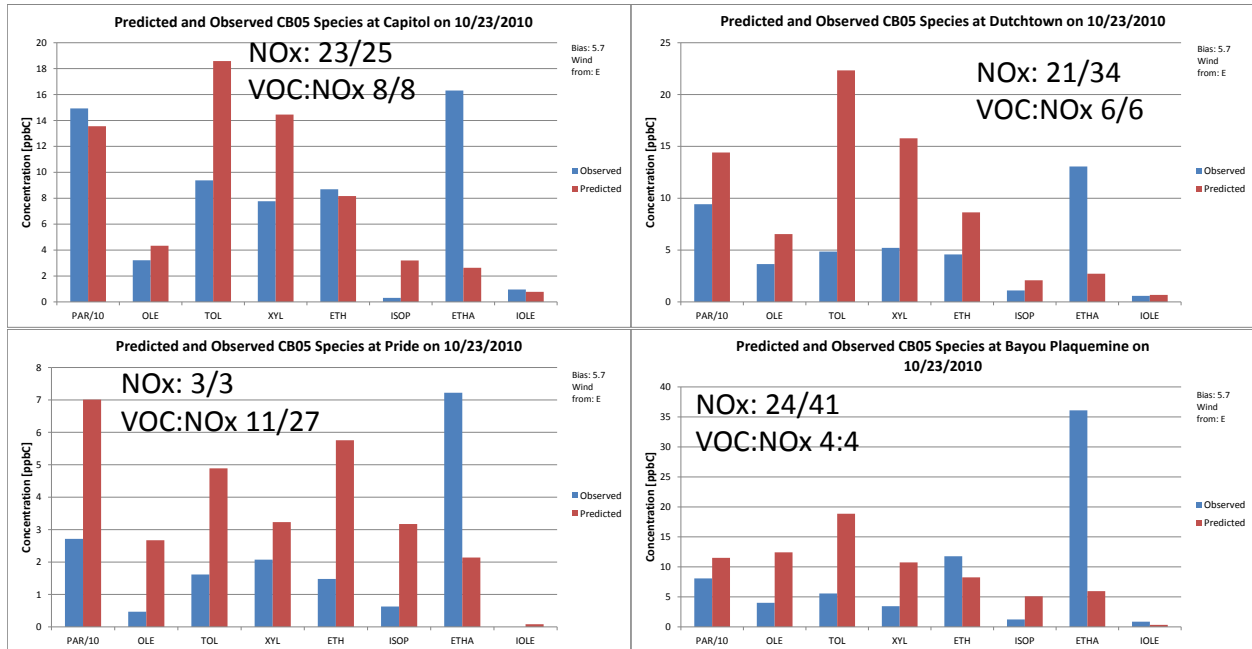


Figure 6-23. Comparison of 6-9 AM observed (blue) and simulated (red) CB05 VOCs at four PAMS sites in Baton Rouge on October 23, 2010. Plots are annotated with 6-9 AM observed/predicted NOx and VOC:NOx ratio.

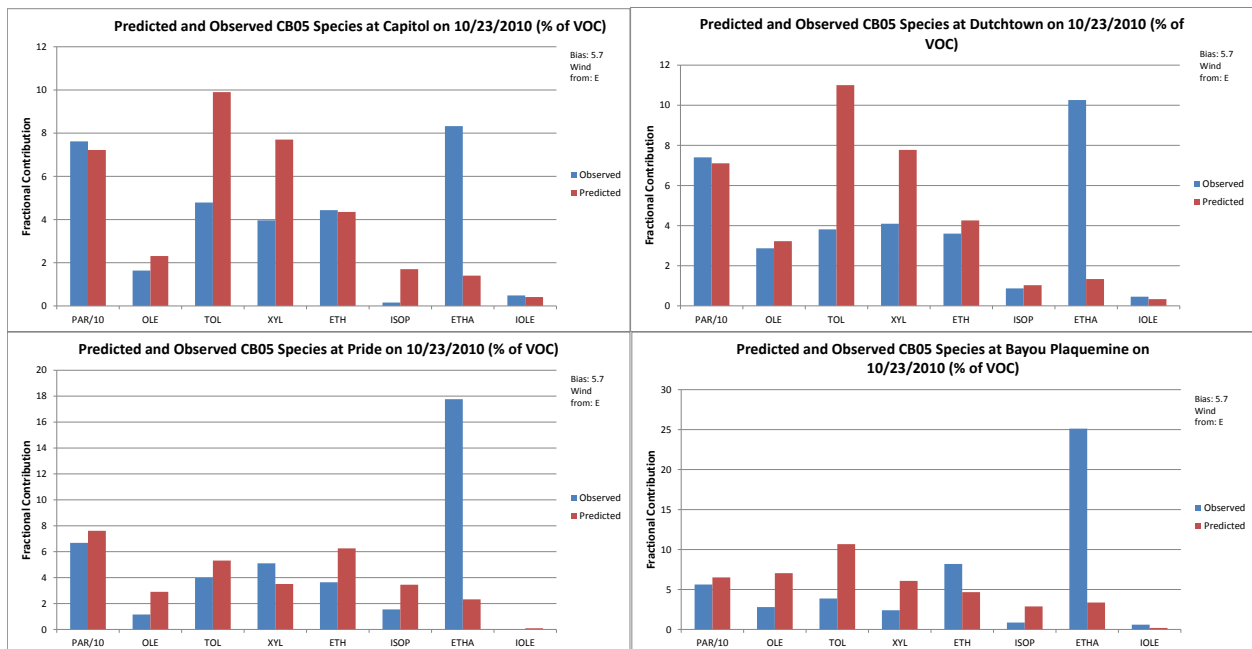


Figure 6-24. Comparison of 6-9 AM observed (blue) and simulated (red) relative contributions of CB05 VOCs to total VOC at four PAMS sites in Baton Rouge on October 23, 2010.

dramatically lower isoprene contributions at all sites. The relative plots show good agreement in the VOC distributions, except the urban sites exhibit larger proportions of aromatics (toluene and xylene), which suggest contributions from gasoline sources. Again, the ethane contribution is dominant at all four sites.

In summary, VOC:NOx ratios were replicated well at 3 of the 4 Baton Rouge PAMS sites over the entire modeling period. Both NOx and VOC tended to be equivalently too high. Generally, primary precursor emissions should be under predicted in grid models because of instantaneous dilution into large grid volumes. Over predictions in both NOx and VOC may be caused by too little vertical mixing during the morning hours, or an incorrect proportion of emissions allocated to that period of the day.

Based on VOC:NOx ratios, morning NOx and VOC emissions appear to be in the correct proportion. Furthermore, speciated (CB05) VOC emissions are correctly proportioned relative to total VOC except for isoprene and ethane. Simulated VOC:NOx ratios were too high on September days when ozone was grossly over predicted, and over estimates of isoprene were found to be a significant contributor to this. VOC:NOx ratios were in excellent agreement on good performing October days, when isoprene was much lower. Ethane appears to be largely missing in the emissions inventory, but this should be a negligible contributor to local ozone formation. PAMS measurements also showed occasionally large spikes in two additional compounds: light alkanes (PAR), which are usually associated with fugitive or evaporative sources; and ethylene, which is a highly reactive VOC released from petrochemical facilities.

With respect to the issue of higher NOx generated by MOVES, these analyses do not support the hypothesis that the on-road NOx inventory is driving ozone over predictions. The simple MOBILE6 test that reduced NOx and increased VOC should have raised VOC:NOx ratios, thereby misaligning from observed conditions and pushing the urban photochemical environment toward a more NOx-sensitive regime.

6.5 Additional Sensitivity Testing (Phase 2)

Based on new information gleaned from the precursor assessment described above, an additional series of diagnostic sensitivity tests were conducted for the high ozone period of September 10-25. Table 6-3 summarizes each of the Phase 2 sensitivity tests, including their purpose and their results. All tests were performed based on the Run 10 configuration.

A biogenic reduction test (Run 11) investigated the ozone impact from a 50% isoprene emission reduction. The choice of this factor was based on analyses of predicted and measured midday isoprene concentrations at PAMS sites during the September-October modeling period. Figure 6-25 shows an example at the Capitol site, where isoprene measurements were over predicted by an average factor of 2.5 throughout the period. Subsequent comparisons between MEGAN-derived isoprene emissions over the entire 4-km grid and estimates from the EPA's BEIS model also show differences by similar factors for August and September, and much smaller differences in October (Figure 6-26).

Table 6-3. Phase 2 diagnostic sensitivity tests performed on the CAMx 2010 base year simulation.

Run ID	Purpose	Results
11	Reduce biogenic isoprene by 50% according to PAMS measurements	Large widespread reductions in MDA8 ozone; Improved statistical performance
12	Increase haze turbidity by a factor of 5 to investigate impact to photolysis rates from heavy fire-derived aerosol burdens	Negligible impacts to statistical performance; Negligible impacts on MDA8 patterns;
13	Calculate Kv from ACM2 technique to test sensitivity to increased mixing (no changes to mixing depth)	Minor mixed impacts to statistical performance; Minor mixed impacts on MDA8 patterns
15	Replace Zhang03 dry deposition with Wesely89 to test sensitivity to choice of algorithm; gridded landuse derived from WRF	Large widespread reductions in MDA8 ozone; Improved statistical performance
16	Scale mixing depth upward by 25%, consistent with remaining average September over prediction bias, to test sensitivity to deeper mixing (no changes to Kv methodology)	Mixed impacts to statistical performance; Moderate mixed impacts on MDA8 patterns

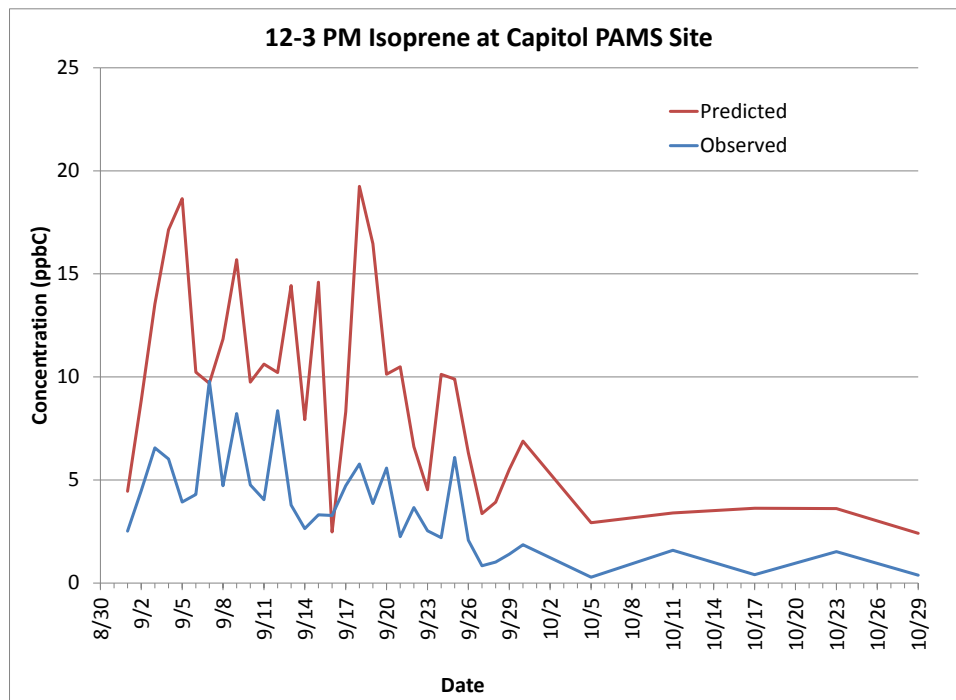


Figure 6-25. Midday (12-3 PM) observed and predicted (Run 10) isoprene concentrations at the Capitol PAMS site on sampling days throughout September and October 2010.

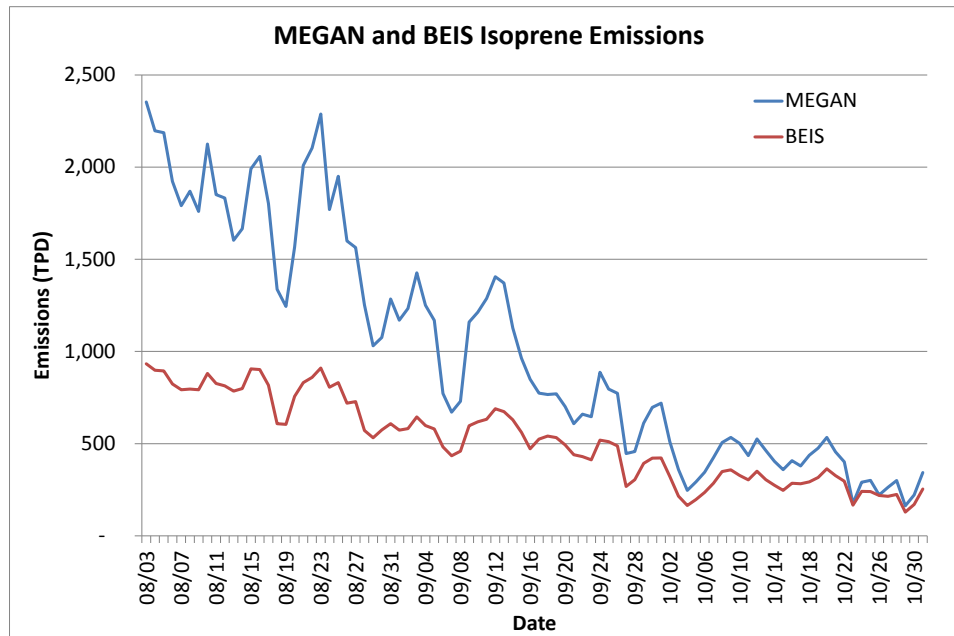


Figure 6-26. Daily total isoprene emissions across the entire 4 km modeling grid estimated by MEGAN and BEIS for each day of August through October 2010.

Figure 6-27 presents spatial plots of MDA8 ozone from Run 11 on September 14, along with the difference in MDA8 from Run 10. Results show much lower ozone in NO_x-heavy, VOC-sensitive areas (i.e., urban). Widespread ozone reductions of 5-10 ppb were common throughout southern and northwestern where NO_x emissions were highest. This strengthens evidence that over estimated biogenic emissions drive ozone over predictions, especially in September.

Two additional vertical mixing tests were conducted: the first employed an alternative K_v calculation methodology (ACM2) that consistently leads to much higher mixing rates than any other option available in the WRF-CAMx pre-processor (Run 13); the second increased the depth of mixing by 25% (Run 16). The first test was designed to test if insufficient mixing rates within the same mixing depth were leading to ozone over predictions. Minor positive and negative ozone changes occurred (< ±5 ppb), scattered throughout the domain. The second test attempted to apply an ad-hoc increase to daily mixing volumes by a factor consistent with the September over prediction bias, thereby reducing the bias toward zero. Larger mixed signals were generated in this test, but impacts to statistical performance were not significant. These two tests show that ozone patterns did not respond linearly to modified vertical mixing rates or depths. Together with the original Phase 1 test using mixing rates calculated using the YSU option (Run 6), it is clear that the September over predictions were not driven by uncertainties in boundary layer mixing.

An alternative dry deposition algorithm, referred to as WESELY89, was employed in Run 15 to test sensitivity to pollutant removal to the surface. The WESELY89 option is the original scheme in CAMx, and it requires a different landuse classification scheme based on 11 types (as

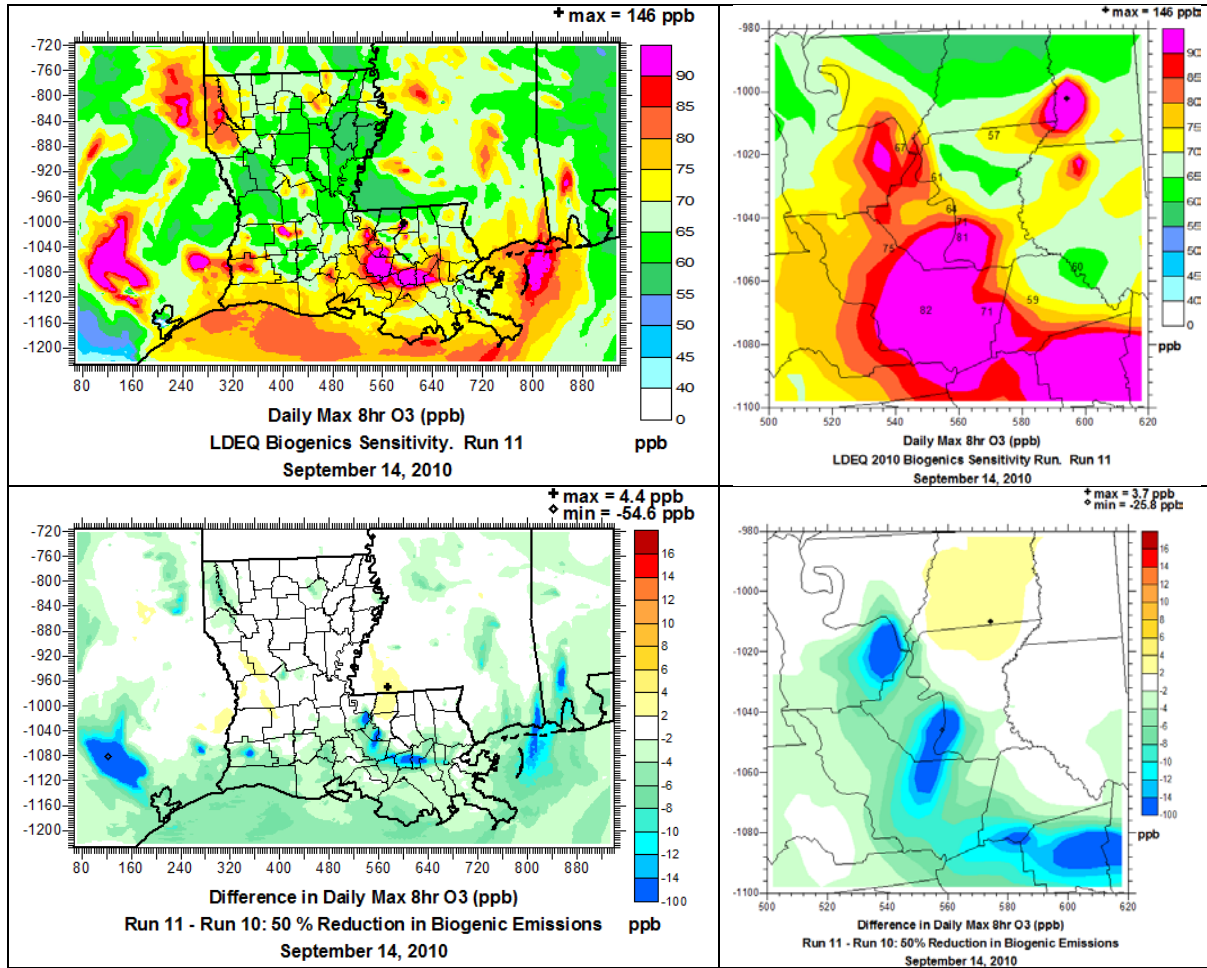


Figure 6-27. Top row: Spatial distribution of predicted MDA8 ozone (ppb) from Run 11 on September 14. Plots are shown for the entire 4 km modeling grid (left) and for south-central Louisiana focusing on Baton Rouge, with observed MDA8 ozone overlaid at monitor locations (right). Bottom row: Spatial distribution of differences (Run 11 – Run 10) in MDA8 on the 4 km modeling grid (left) and over south-central Louisiana (right).

opposed to 26 types in ZHANG03). Alternative gridded landuse input fields were derived from WRF output, which reports the dominant landuse type in each grid cell using a 26-category USGS classification scheme. The WRF landuse types were mapped to the 11 WESELY89 types using the WRFCAMx pre-processor. Run 15 included the 50% biogenic isoprene reduction from Run 11 to carry on that important modification. Relative to Run 11, the alternative deposition option resulted in additional large reductions in MDA8 ozone throughout the September 10-25 test period and significant improvements in statistical model performance in the Baton Rouge area. Figure 6-28 presents spatial plots of MDA8 ozone from Run 15 on September 14, along with the difference in MDA8 from Run 11 (the 50% biogenic test) to isolate the deposition signal. Reductions of MDA8 consistently reached 5-15+ ppb over much of the 4 km modeling

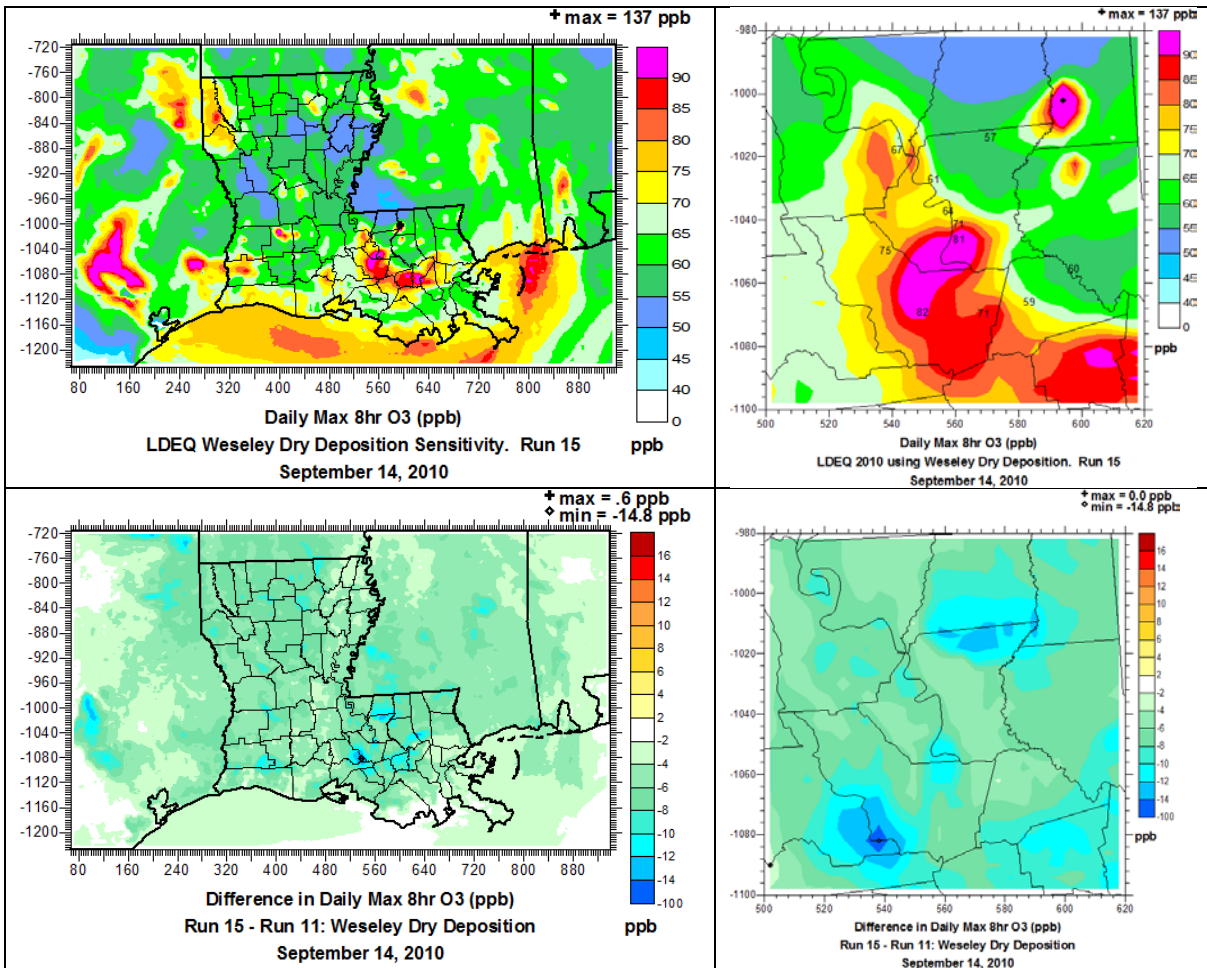


Figure 6-28. Top row: Spatial distribution of predicted MDA8 ozone (ppb) from Run 15 on September 14. Plots are shown for the entire 4 km modeling grid (left) and for south-central Louisiana focusing on Baton Rouge, with observed MDA8 ozone overlaid at monitor locations (right). Bottom row: Spatial distribution of differences (Run 15 – Run 11) in MDA8 on the 4 km modeling grid (left) and over south-central Louisiana (right).

grid. Average model bias for 1-hour ozone in Baton Rouge during September exceedance days was reduced to 6% in Run 15, compared to 13% in Run 11 (reduced biogenics), 23% in Run 10 (Phase 1 interim simulation), and 32% in Run 1.

6.6 Final Base Year CAMx Run

The final CAMx base year simulation (“Run 17”) incorporated certain modifications from the sensitivity tests that collectively led to improved model performance for ozone. Otherwise, the simulation used identical inputs as in Run 1, and was performed for the entirety of September and October 2010 (including the August 15-31 spinup period). The CAMx configuration for the final base year simulation is listed below (red highlighted items note modifications from Run 1):

- Time zone: Central Standard Time (CST)
- I/O frequency: 1 hour
- Map projection: Lambert conformal (see Section 4.1)
- Nesting: 2-way fully interactive 36/12/4-km computational grids (Figure 4-1)
- **Chemistry mechanism: CB05 gas-phase only (without PM)**
- Chemistry solver: Euler-Backwards Iterative (EBI)
- Advection solver: Piecewise Parabolic Method (PPM)
- Plume-in-Grid sub-model: Off
- Probing Tools: Off
- Asymmetric Convective Model: On
- Photolysis Adjustments for Clouds: in-line TUV
- Photolysis Adjustment for Aerosols: input AHOMAP
- **Dry deposition: Wesely89**
- Wet deposition: On
- **Biogenic emissions: EPA BEIS**
- **Wildfires: Reduced NO_x, addition of aged NO_y**
- **Kv Patch: No nighttime urban patch**

Figure 6-29 presents spatial plots of MDA8 ozone over the 4-km nested grid on days when ozone exceeded the 2008 ozone NAAQS at any location in Louisiana (compare to Figure 6-1). Simulated ozone over predictions were reduced substantially on all of these days. The highest simulated ozone continued to occur on September 14, reaching 137 ppb in a very isolated area to the northeast of Baton Rouge, but the peak value of 57 ppb at Pride was well simulated. Closer to Baton Rouge, predicted ozone exceeded 90 ppb to the south of the city whereas peak observations reached 82 ppb at Bayou Plaquemine.

Another series of high ozone days occurred in the Baton Rouge area on October 8-10, with peak predictions reaching 82 to 89 ppb. However, these maxima occurred in areas well east of any monitoring sites so their magnitude cannot be verified. The model shows much lower ozone in the areas of the Baton Rouge monitors on these days, with concentrations in the 60-80 ppb range, which agrees rather well with measurements.

Time series of daily statistics for Baton Rouge are shown in Figure 6-30 (compare to Figure 6-2). Performance in September continued to be worse than in October, but the large errors prevalent in the initial base year run were dramatically reduced to the benchmarks for a well-performing model, particularly on high ozone days. Figure 6-31 presents the same data as Figure 6-30 but as goal plots; Figures 6-32 through 6-34 show results for New Orleans, Shreveport, and Lake Charles (compare to Figures 6-3 through 6-6). In all areas, performance on September high ozone days improved to within the statistical benchmarks. Performance in October shifted toward a slight under prediction tendency in most areas.

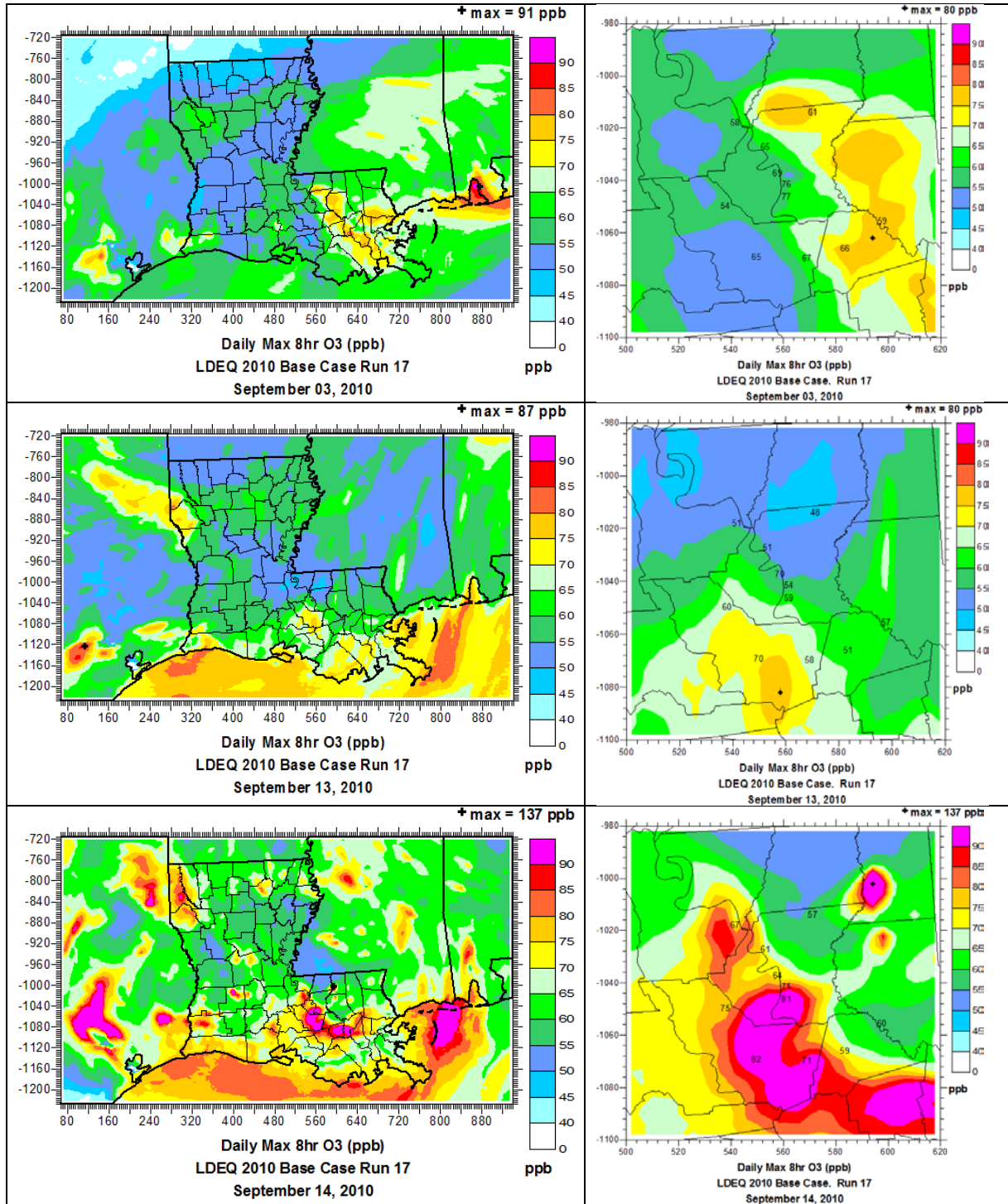


Figure 6-29. Spatial distribution of predicted MDA8 ozone (ppb) from the final base year run on days exceeding the 2008 ozone NAAQS in Louisiana. Plots are shown for the entire 4 km modeling grid (left) and for south-central Louisiana focusing on Baton Rouge, with observed MDA8 ozone overlaid at monitor locations (right).

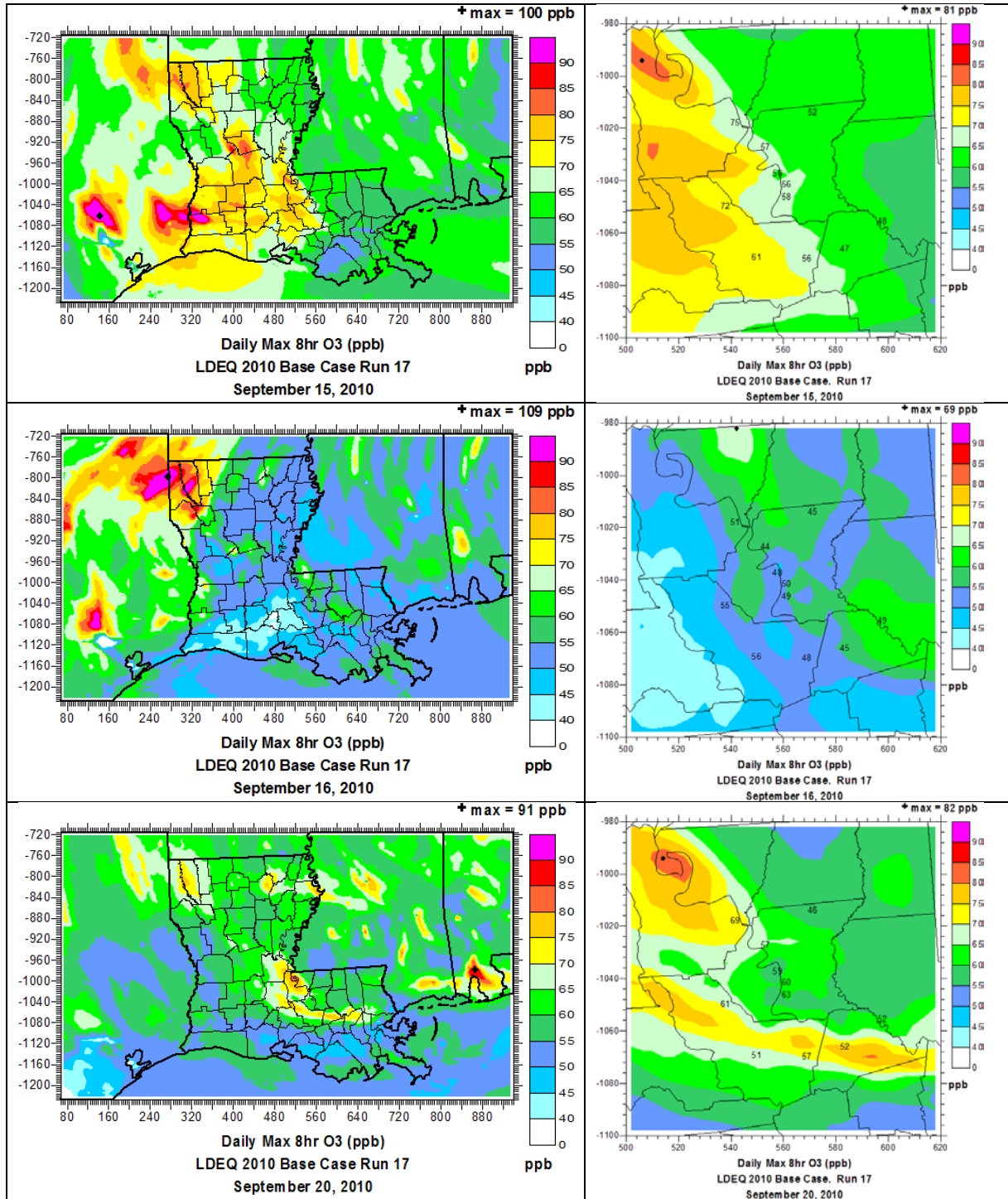


Figure 6-29 (continued).

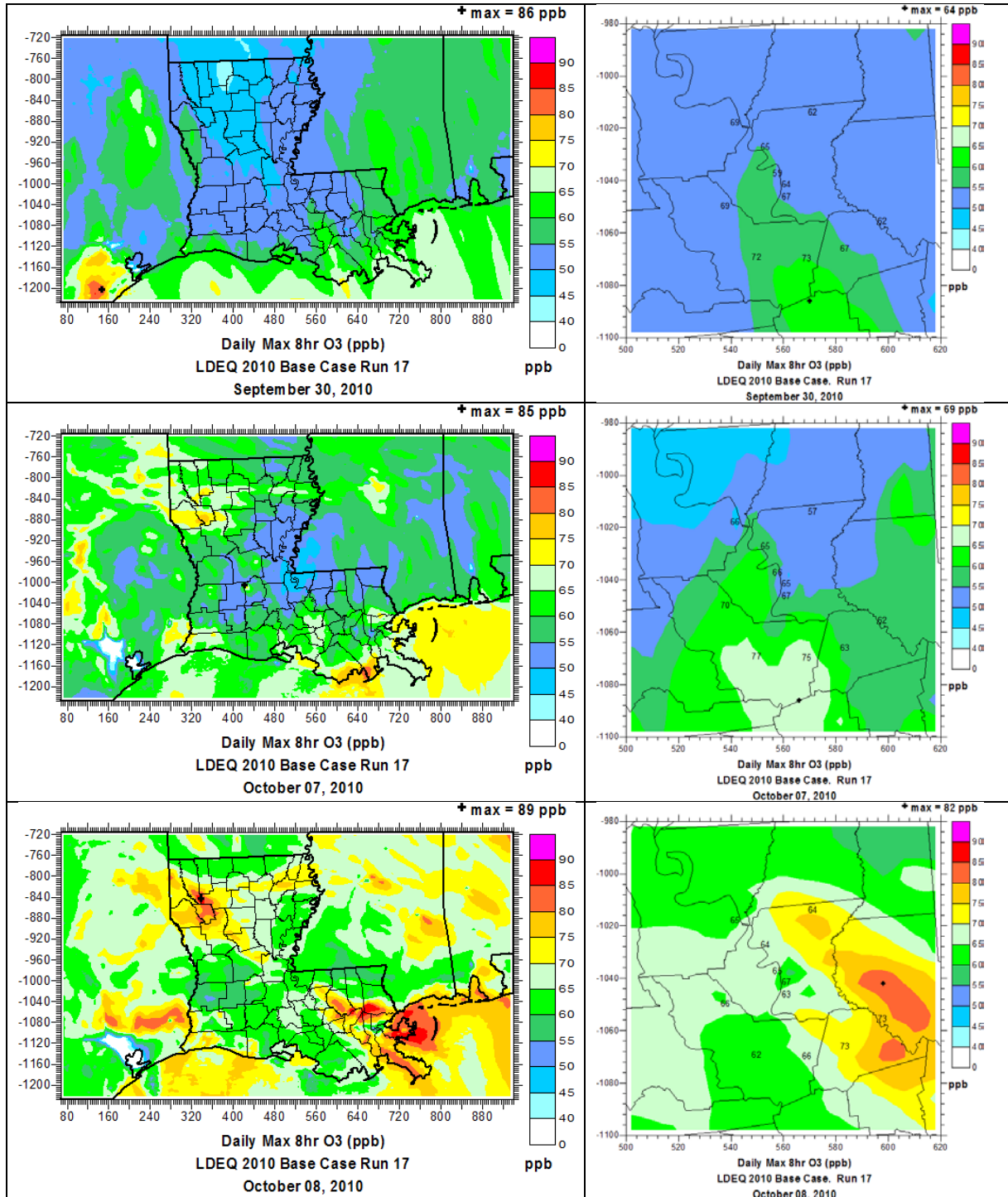


Figure 6-29 (continued).

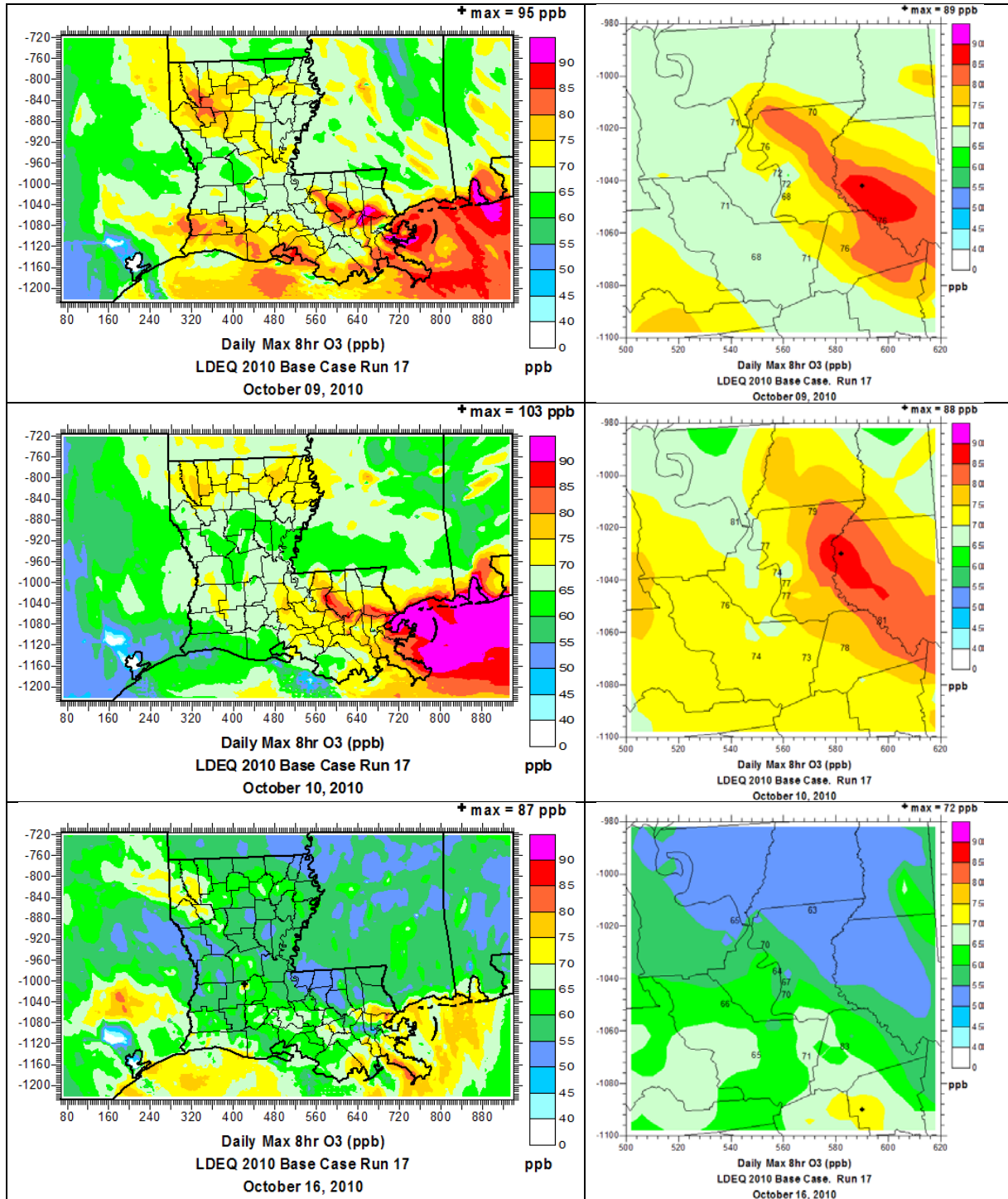


Figure 6-29 (continued).

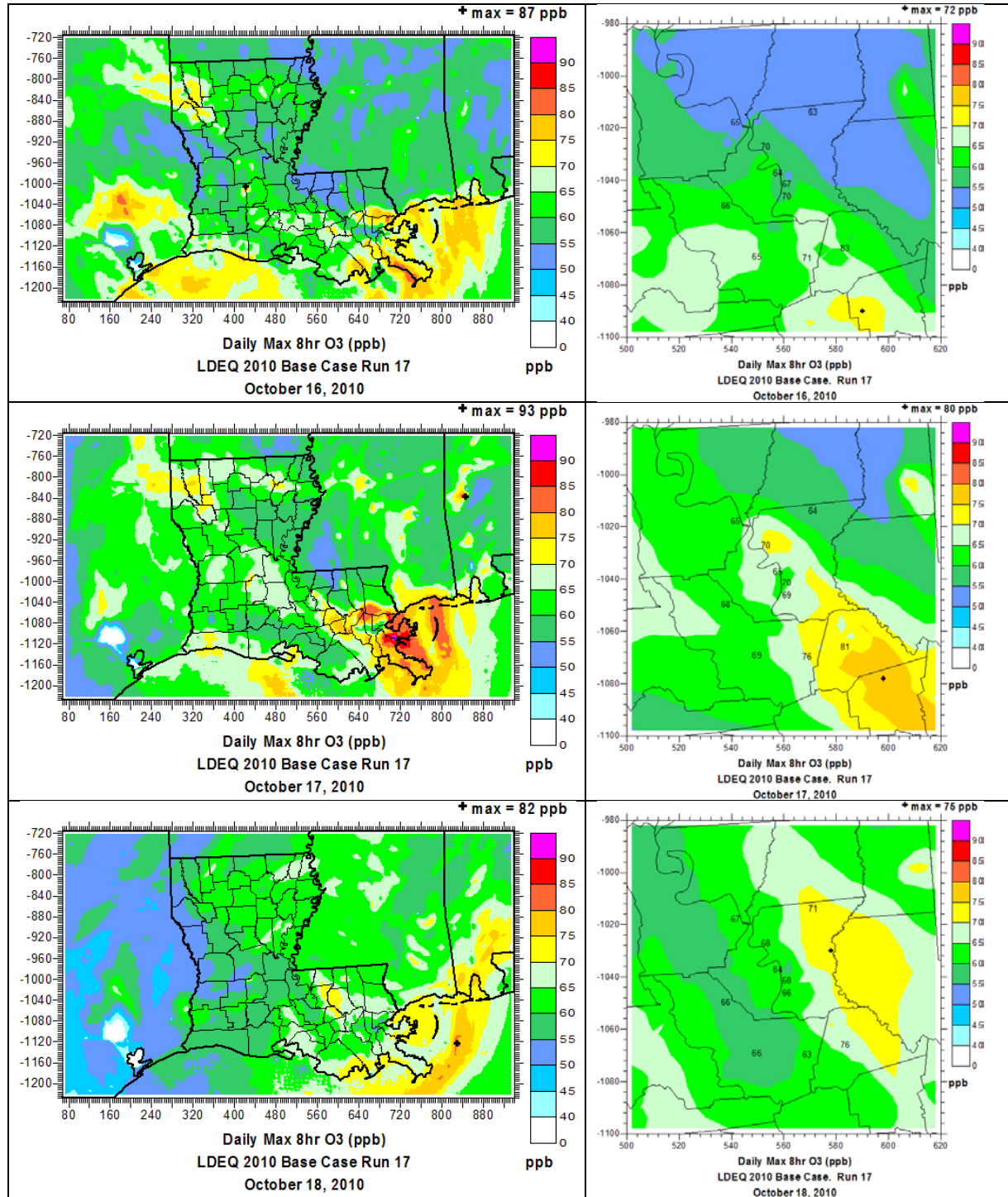


Figure 6-29 (concluded).

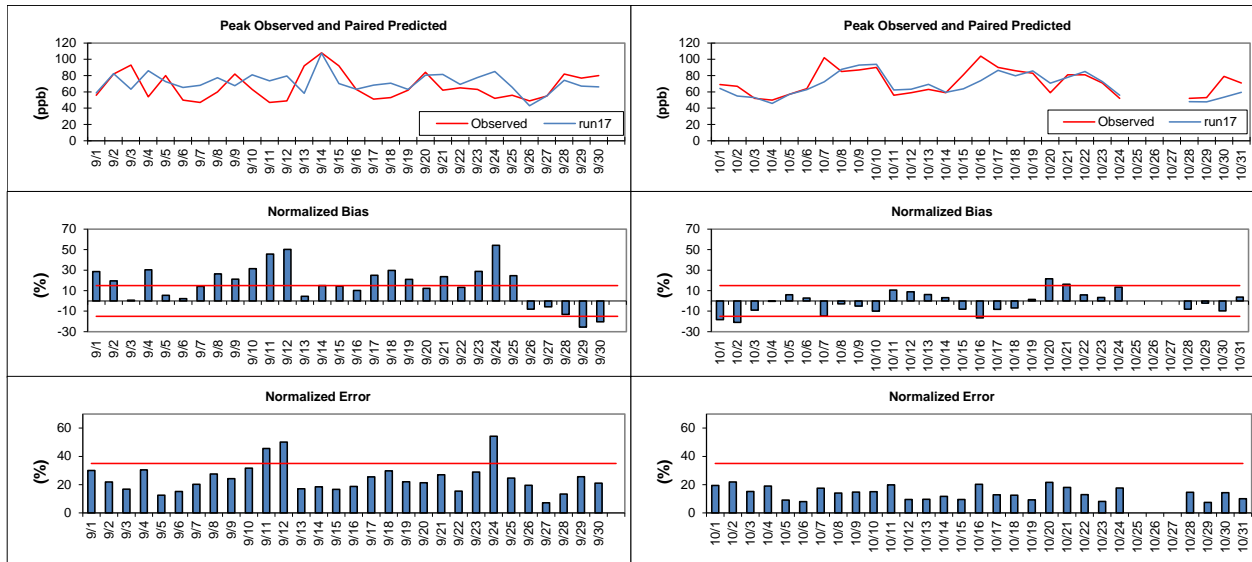


Figure 6-30. Daily statistical performance for the final base year run at all Baton Rouge monitoring sites and for all hours when observed ozone was greater than 40 ppb, for September (left) and October (right), 2010. Top row: maximum daily peak 1-hour observed ozone (red) and paired simulated peak at the same site (blue). Middle row: daily mean normalized bias (bars) with $\pm 15\%$ bias highlighted (red lines). Bottom row: daily mean normalized gross error (bars) with 35% error highlighted (red lines).

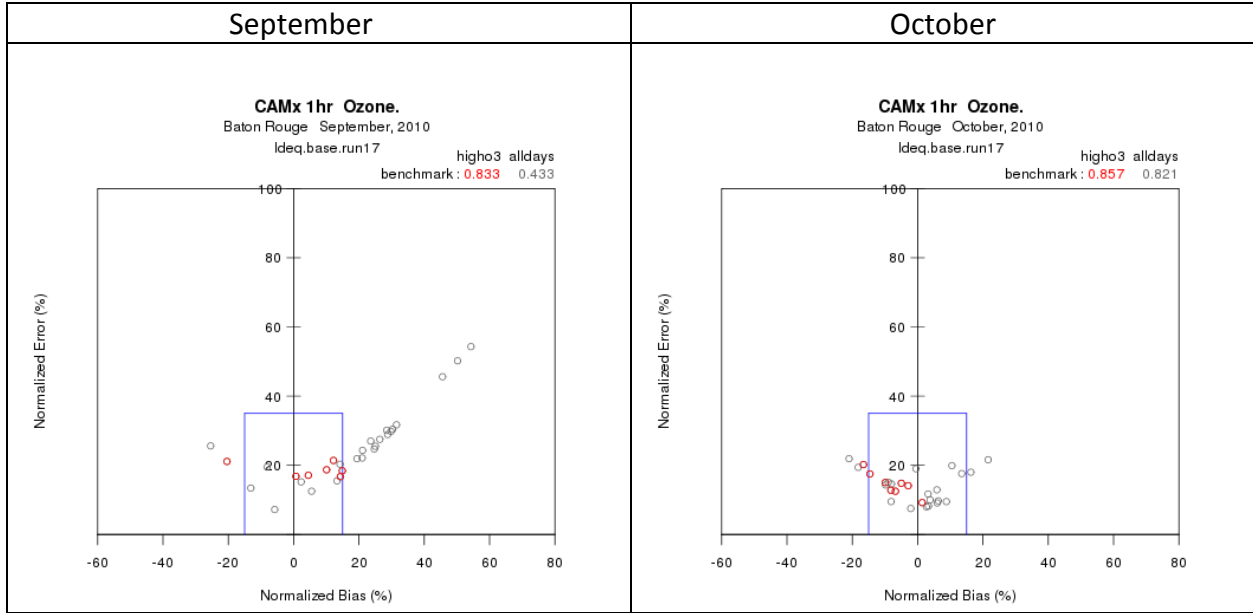


Figure 6-31. “Goal” plots of daily normalized bias and error from the final base year run in Baton Rouge for September (left) and October (right). The blue goal denotes statistics within the 1-hour performance benchmarks. Red points are the high ozone days shown in Figure 6-1.

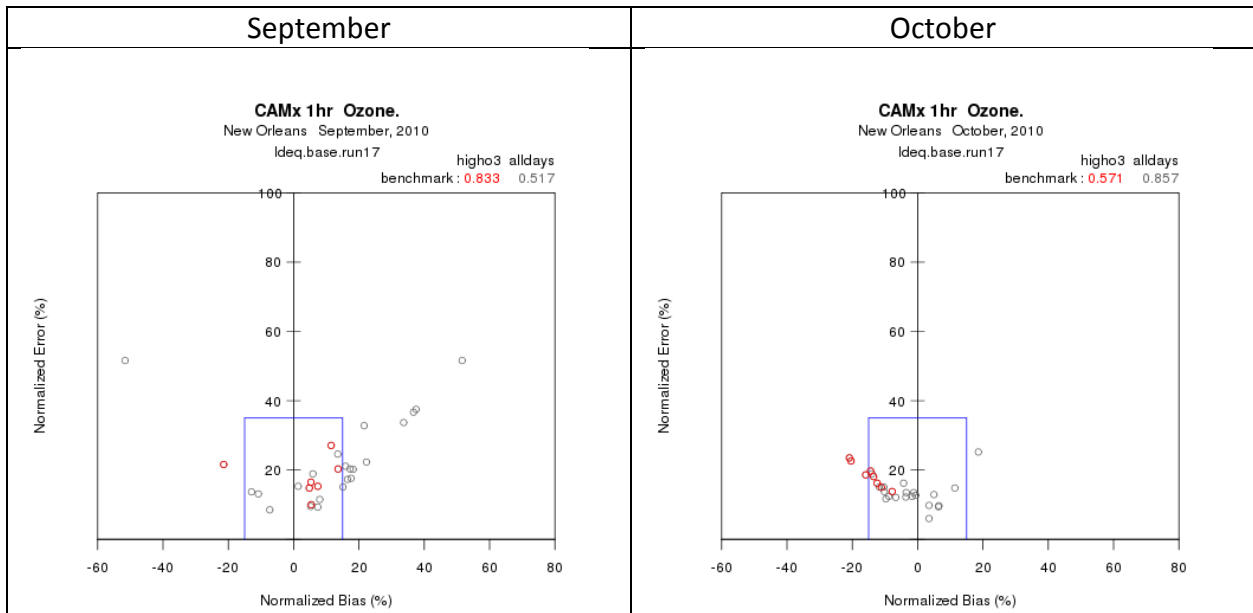


Figure 6-32. “Goal” plots of daily normalized bias and error from the final base year run in New Orleans for September (left) and October (right). The blue goal denotes statistics within the 1-hour performance benchmarks. Red points are the high ozone days.

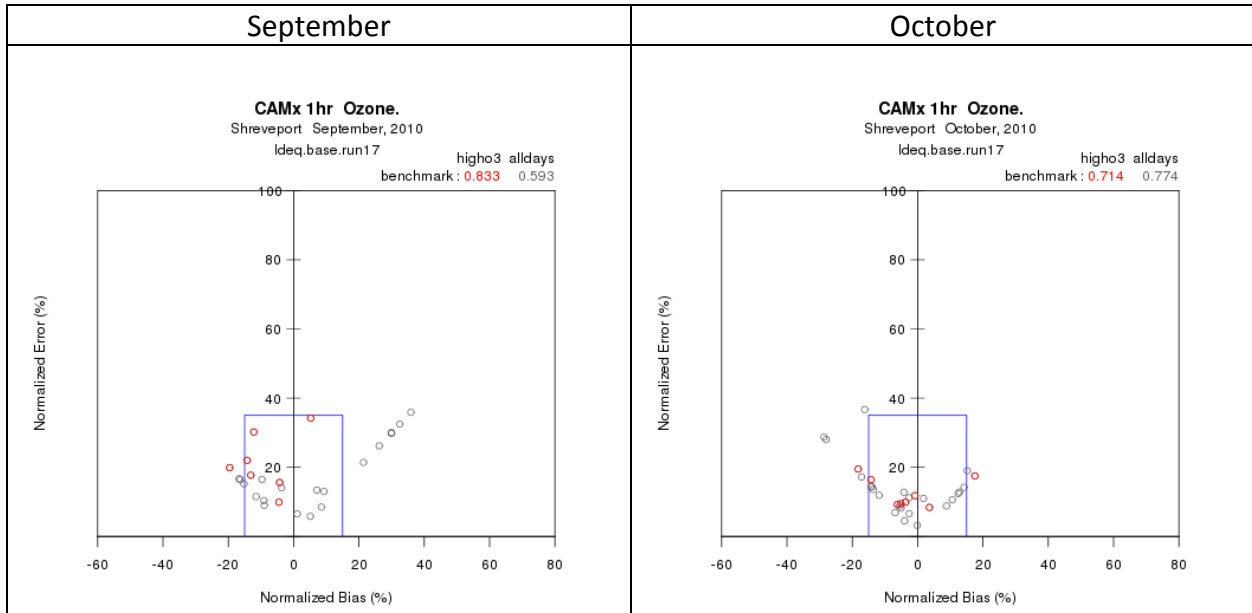


Figure 6-33. “Goal” plots of daily normalized bias and error from the final base year run in Shreveport for September (left) and October (right). The blue goal denotes statistics within the 1-hour performance benchmarks. Red points are the high ozone days.

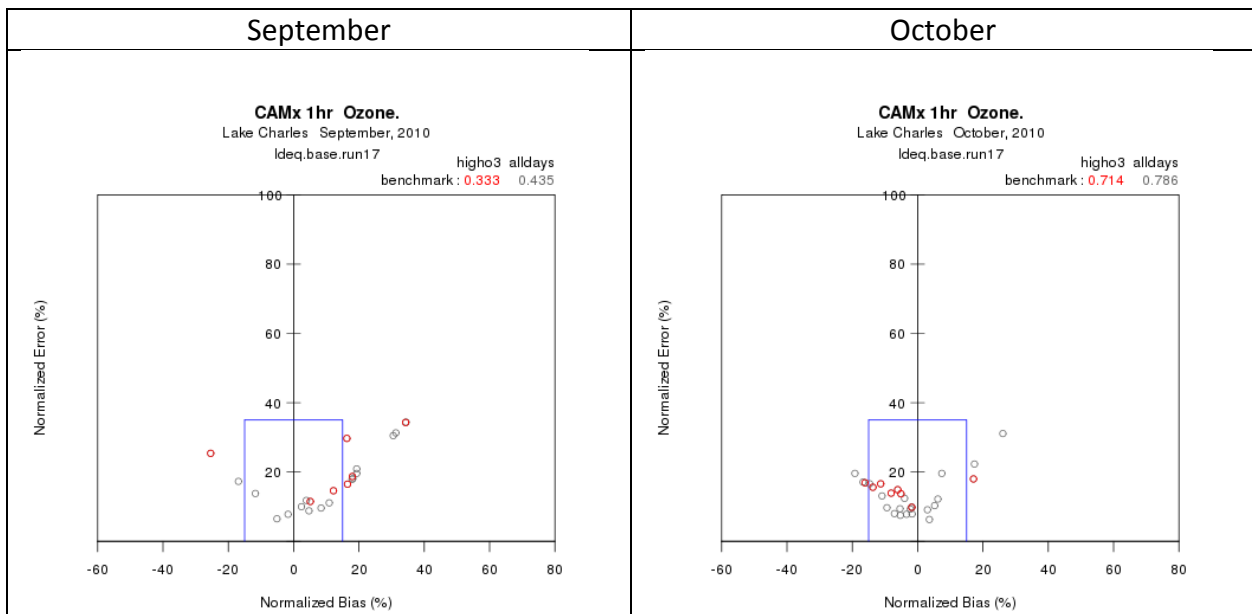


Figure 6-34. “Goal” plots of daily normalized bias and error from the final base year run in Lake Charles for September (left) and October (right). The blue goal denotes statistics within the 1-hour performance benchmarks. Red points are the high ozone days.

Time series of simulated and observed hourly ozone at the urban LSU monitor throughout September and October are shown in Figure 6-35 (compare to Figure 6-7). Performance in both September and October was quite good on an hourly basis, and the model properly captured the large intra-diurnal ranges of ozone. Similar time series for ozone are shown at the Dutchtown and Pride monitors in Figures 6-36 and 6-37 (compare to Figures 6-9 and 6-11). Again, performance was dramatically improved at both sites. However, nighttime ozone continued to be too high at Pride, taking on the characteristics typical of rural background ozone with small diurnal amplitude that is not influenced by scavenging from local NO_x. Ozone observations suggest that a local NO_x source contributed to nightly ozone reductions around the monitor that was not resolved by the model.

6.6.1 Regional Ozone Performance

September ozone over predictions in Louisiana may be related to various inaccuracies in local emission estimates to a certain extent (e.g., prescribed fire activity), but over predictions of regional (background) ozone entering Louisiana may contribute as well. We analyzed ozone performance in neighboring states to address this issue. Specifically, we identified CASTNET and AQS sites that are situated in rural areas to the east, north, and west of Louisiana (Figure 6-38) and calculated ozone performance statistics to gauge whether the model is adequately characterizing the amount of background surface ozone that should be entering Louisiana according to general wind patterns.

Figures 6-39 through 6-41 present daily normalized bias and gross error for 1-hour ozone on each day of September and October, in the form of bar chart time series, for the western, northern, and eastern groups of monitoring sites shown in Figure 6-38. In the west, a high bias prevailed in September but bias was much better and balanced in October, very similar to the bias patterns in Louisiana. The highest bias days were not associated with the highest ozone days in Louisiana. Good performance for gross error was achieved in both months. In the north, good performance was achieved for bias in both months, with a tendency for slight under prediction. All days except three were well within the $\pm 15\%$ benchmark. Very good performance for gross error was achieved, with typical values well below 20%. In the east, good performance was also achieved on most days of both months, with a more balanced positive and negative variability. Only six days exceeded the $\pm 15\%$ bias benchmark. Very good performance for gross error was achieved with values similar to the northern sites.

Note that the similarities between performance for the western regional sites and sites within Louisiana may be related to two factors: (1) the western sites were contained within the Louisiana 4 km grid, whereas the northern and eastern sites were all in the 12 km grid, suggesting a grid-specific sensitivity for the ozone simulation; and (2) western sites located along the Texas-Louisiana border may have received outflow from Louisiana on many of these days, which would lead to similar performance as seen in Lake Charles and Shreveport. Overall, the model simulated ozone patterns rather well in the region surrounding Louisiana during the entire modeling period. There was no indication that ozone formation and subsequent transport from neighboring states is improperly characterized.

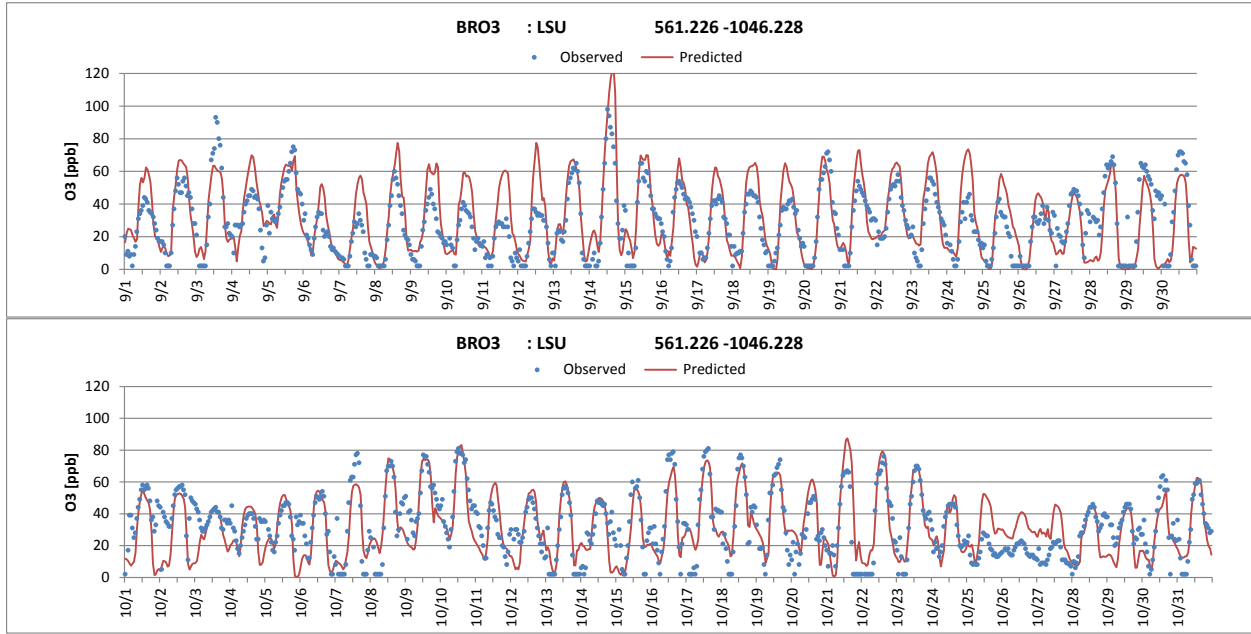


Figure 6-35. Hourly time series of observed (blue dots) and predicted (solid red line) ozone from the final base year run at the LSU monitoring site during September (top) and October (bottom).

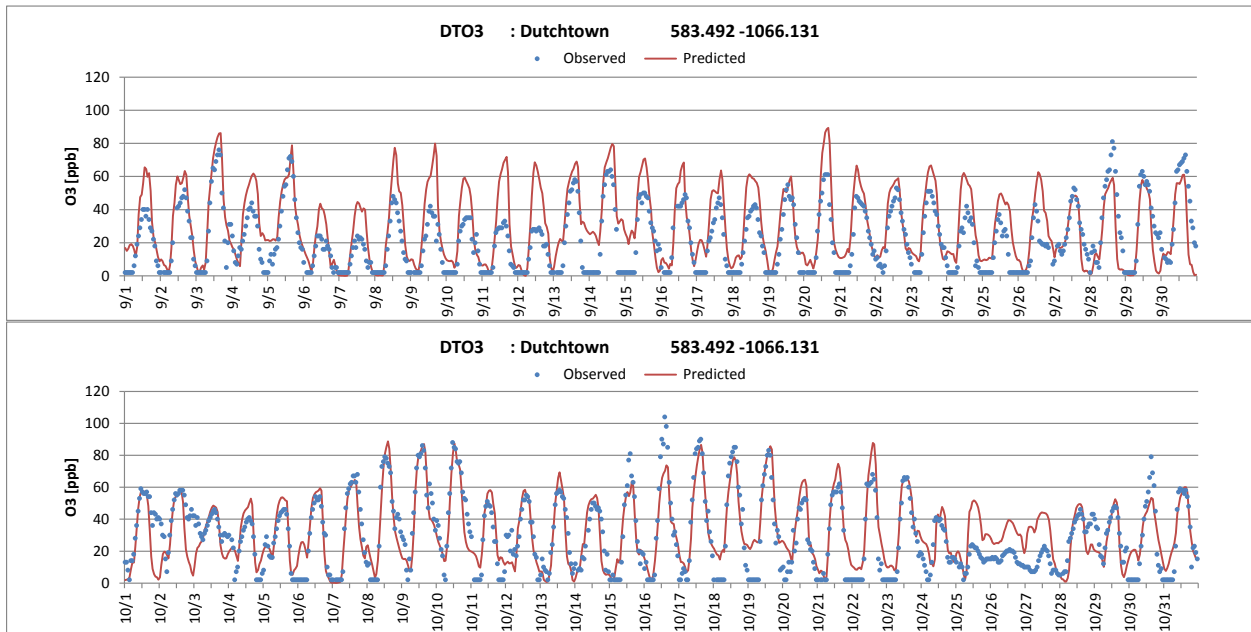


Figure 6-36. Hourly time series of observed (blue dots) and predicted (solid red line) ozone from the final base year run at the Dutchtown monitoring site during September (top) and October (bottom).

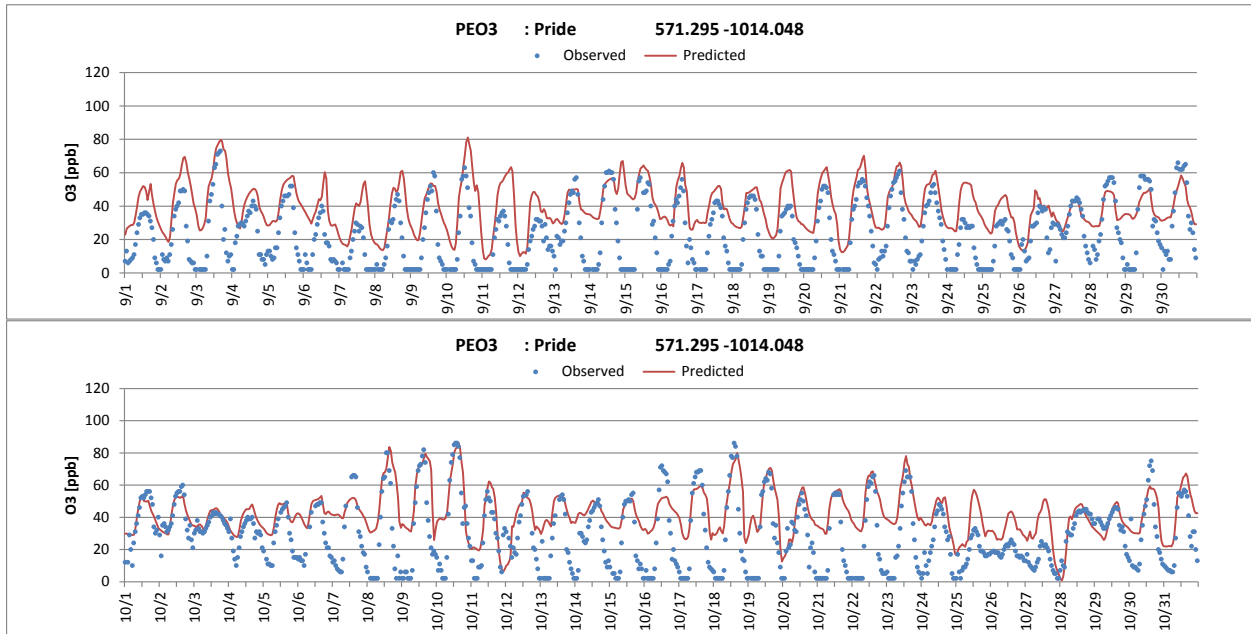


Figure 6-37. Hourly time series of observed (blue dots) and predicted (solid red line) ozone from the final base year run at the Pride monitoring site during September (top) and October (bottom).

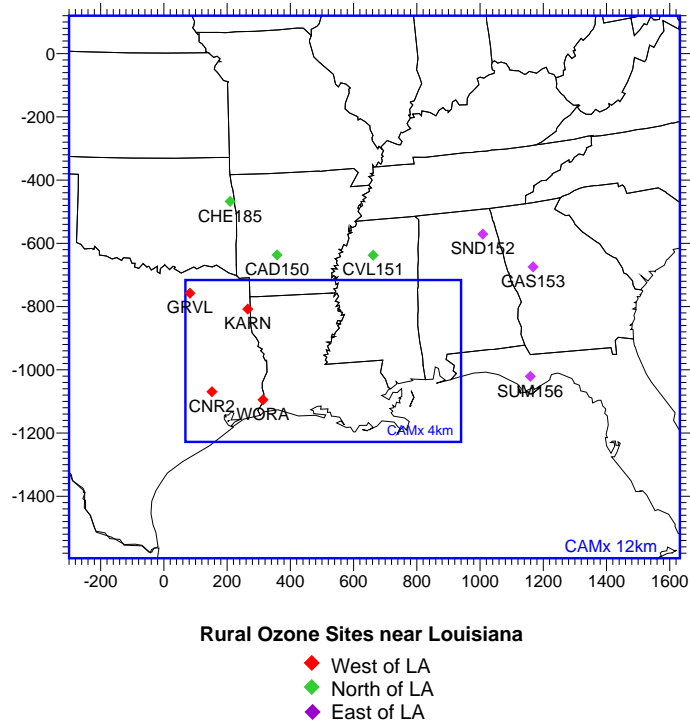


Figure 6-38. Locations of regional monitoring sites in areas surrounding Louisiana, relative to the CAMx modeling grid system.

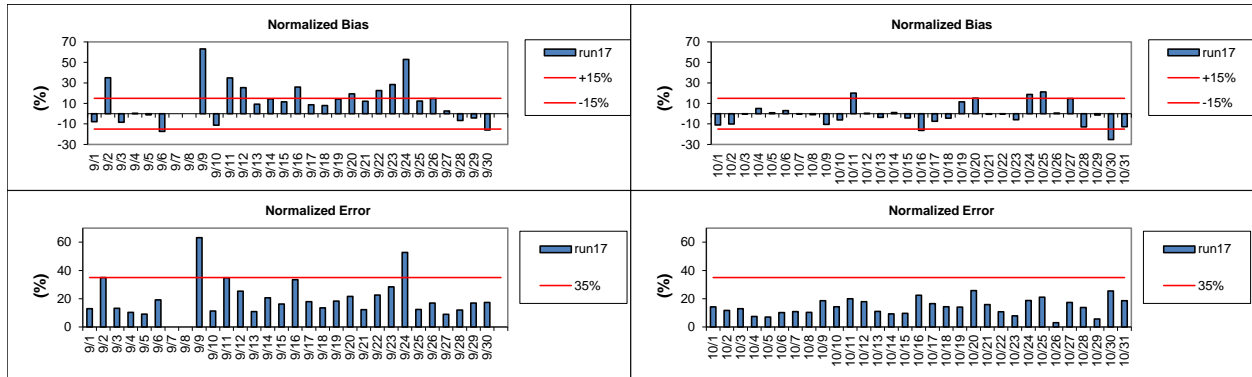


Figure 6-39. Daily statistical performance for the final base year run at all western regional monitoring sites and for all hours when observed ozone was greater than 40 ppb, for September (left) and October (right), 2010. Top row: daily mean normalized bias (bars) with $\pm 15\%$ bias highlighted (red lines). Bottom row: daily mean normalized gross error (bars) with 35% error highlighted (red lines).

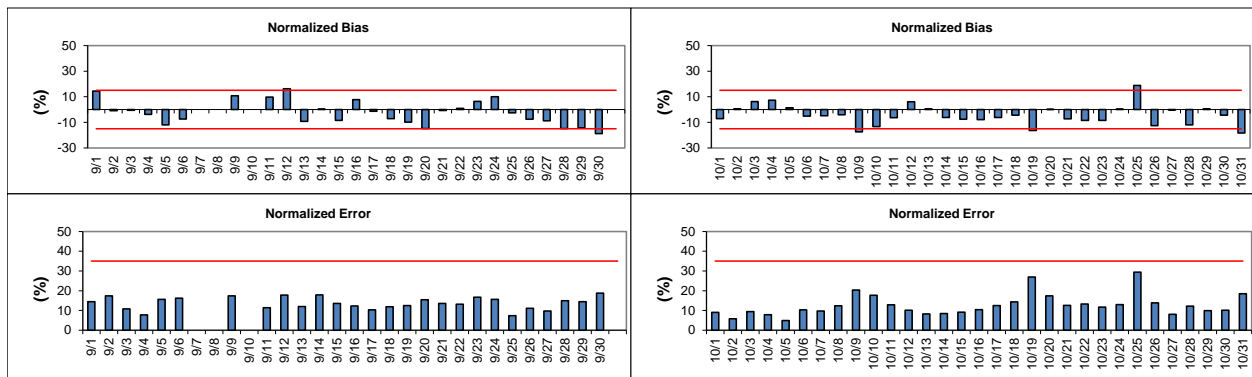


Figure 6-40. As in Figure 6-42, but at all northern regional monitoring sites.

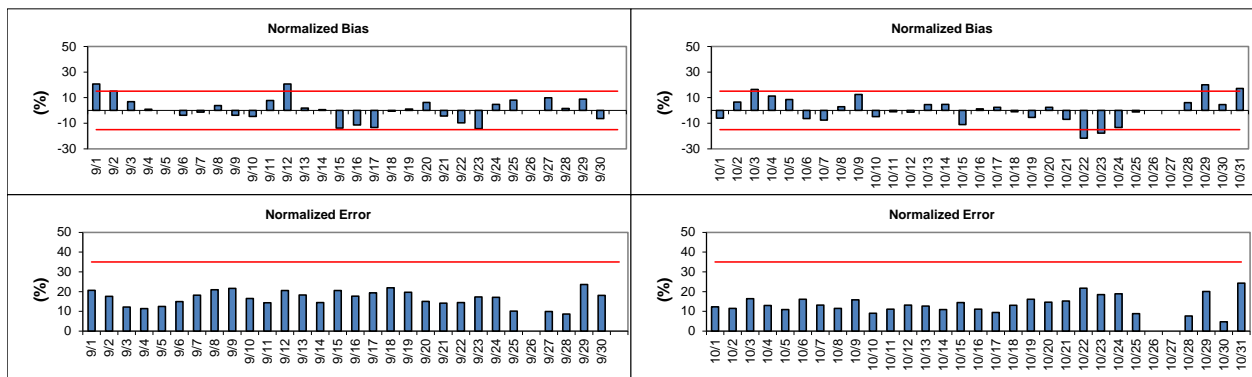


Figure 6-41. As in Figure 6-42, but at all eastern regional monitoring sites.

7.0 2017 FUTURE YEAR OZONE PROJECTION

7.1 Development of Future Year Emissions

Anthropogenic emission estimates for the September-October 2010 modeling period were projected to the 2017 future year. Details on the preparation of certain emission sectors are described in this section, specifically including Louisiana and Gulf of Mexico anthropogenic sources. Alpine Geophysics developed anthropogenic emission estimates for the remainder of the North American modeling domain. Day- and hour-specific BEIS biogenic and FINN fire emissions from the 2010 base year, as well as base year emissions estimates for Canada and Mexico, were used without modification for the 2017 future year.

As with the 2010 base year, emphasis was placed on developing 2017 emissions estimates within the State of Louisiana (LA) using EPS3 to convert the LA emission inventory into the hourly, chemically speciated, and gridded formats needed by CAMx. In some cases emissions were projected from 2010 to 2017 based on growth and control factors. In other cases emission modeling tools were used to estimate 2017 emissions for specific categories; MOVES/CONCEPT for on-road and NMIM for non-road sources. Area and point source emissions in Louisiana were prepared by ERG, working closely with the LDEQ. Gulf-wide offshore emissions were developed by ERG from the BOEM 2008 Gulf-wide Emission Inventory Study and by reviewing estimated oil and gas production rates for future years.

7.1.1 Emissions in Louisiana

The 2017 emissions were processed similarly to the approach used to develop the 2010 base year. EPS3 was set up to process criteria pollutant emissions into the CAMx configuration. EPS3 generated model-ready hourly point, area, non-road mobile, and on-road mobile emissions of CB6 compounds on the 36/12/4 km grid system. Certain CB6 VOCs were subsequently reverted back to CB05 speciation to be consistent with the decision to run the 2010 base year with CB05. Annual and ozone season emission estimates for most sectors were used to develop a representative weekday, Saturday and Sunday. Day specific estimates were developed for the on-road mobile sector. The remainder of this sub-section details the emissions processing by source category.

7.1.1.1 Point Sources

The 2017 point source emissions are based on the 2010 point source inventory provided by LDEQ (2012a). For the purposes of this project, it was decided that all point sources not part of the Acid Rain Program (ARP) or future interstate cap-and-trade programs were to be held constant at their 2010 estimates.

The hourly, day-specific 2010 ARP point source inventory was first converted to annual (“typical”) emission estimates for each point source by summing their emissions over the entire year. These annual estimates were then adjusted to reflect relevant control programs. Two types of emission limits were applied to the ARP units; those developed under the Clean Air Interstate Rule (CAIR), and any current Plant-wide Applicability Limits (PAL). LDEQ provided the

Table 7-1. Louisiana 2015 CAIR Program annual NOx allocations.

Facility Name Unit Designation	Unit ID (ORIS)	Amount tons/year	Facility Name Unit Designation	Unit ID (ORIS)	Amount tons/year
Rodemacher - Unit 1	006190	233	Morgan City Electrical Gen Facility	001449	12
Rodemacher - Unit 2		2056	Houma - 15	001439	9
Rodemacher - Unit 3		2584	Houma - 16		8
RS Nelson - 6	001393	2780	D G Hunter - 3	006558	4
RS Nelson - 3		72	D G Hunter - 4		9
RS Nelson - 4		361	Hargis-Hebert Electric Gen - U-1	056283	20
Big Cajun 2 - 2B3	006055	2923	Hargis-Hebert Electric Gen - U-2		29
Big Cajun 2 - 2B1		2883	Natchitoches	001450	0
Big Cajun 2 - 2B2		3138	T J Labbe Electric - U-1	056108	12
Dolet Hills	000051	3487	T J Labbe Electric - U-2		10
Entergy Little Gypsy - 1	001402	118	Acadia Power Station - CT-1	055173	42
Entergy Little Gypsy - 2		209	Acadia Power Station - CT-2		62
Entergy Little Gypsy - 3		351	Acadia Power Station - CT-3		40
Monroe	001448	0	Acadia Power Station - CT-4		42
Entergy Ninemile Point - 1	001403	17	Bayou Cove Peaking Power - CTG-1	055433	3
Entergy Ninemile Point - 2		0	Bayou Cove Peaking Power - CTG-2		3
Entergy Ninemile Point - 3		43	Bayou Cove Peaking Power - CTG-3		3
Entergy Ninemile Point - 4		622	Bayou Cove Peaking Power - CTG-4		3
Entergy Ninemile Point - 5		467	Big Cajun 1 - CTG2	001464	12
Perryville Power Sta - 1-1	055620	110	Big Cajun 1 - CTG1		16
Perryville Power Sta - 1-2		203	Big Cajun 1 - 1B1		17
Perryville Power Sta - 2-1		82	Calcasieu Power, LLC - GTG2	055165	65
Sterlington - 10	001404	0	Calcasieu Power, LLC - GTG1		35
Sterlington - 7AB		2	Carville Energy Center - COG01	055404	132
Sterlington - 7C		3	Carville Energy Center - COG02		150
Entergy Waterford - 1	008056	152	Evangeline Power (Coughlin) - 7-2	001396	71
Entergy Waterford - 2		95	Evangeline Power (Coughlin) - 7-1		81
Entergy A B Paterson - 3	001407	0	Evangeline Power (Coughlin) - 6-1		52
Entergy A B Paterson - 4		0	Exxon Mobil Louisiana 1 - 1A	001391	140
Entergy Michoud - 1	001409	0	Exxon Mobil Louisiana 1 - 2A		150
Entergy Michoud - 2		163	Exxon Mobil Louisiana 1 - 3A		148
Entergy Michoud - 3		537	Exxon Mobil Louisiana 1 - 4A		908
Entergy Louisiana 2 - 10	001392	0	Exxon Mobil Louisiana 1 - 5A		284
Entergy Louisiana 2 - 11		0	Plaquemine Cogen Facility - 500	055419	93
Entergy Louisiana 2 - 12		0	Plaquemine Cogen Facility - 600		103
Entergy Willow Glen - 1	001394	10	Plaquemine Cogen Facility - 700		91
Entergy Willow Glen - 2		32	Plaquemine Cogen Facility - 800		96
Entergy Willow Glen - 3		0	Quachita Power, LLC - CTGEN1	055467	29
Entergy Willow Glen - 4		52	Quachita Power, LLC - CTGEN2		24

Facility Name Unit Designation	Unit ID (ORIS)	Amount tons/year	Facility Name Unit Designation	Unit ID (ORIS)	Amount tons/year
Entergy Willow Glen - 5		0	Quachita Power, LLC - CTGEN3		28
Teche Power Station - 2	001400	9	R S Cogen - RS-5	055117	375
Teche Power Station - 3		254	R S Cogen - RS-6		368
Arsenal Hill Power Plant	001416	28	Taft Cogeneration Facility - CT-2	055089	181
Lieberman Power Plant - 4	001417	22	Taft Cogeneration Facility - CT-1		171
Lieberman Power Plant - 3		18	Taft Cogeneration Facility - CT-3		179
Doc Bonin - 1	001443	4	NISCO - Unit 1A	050030	460
Doc Bonin - 2		26	NISCO - Unit 2A		660
Doc Bonin - 3		17			

2015 CAIR allocations for all such sources in the State of Louisiana (Table 7-1). The 2010 annual estimates were adjusted to the 2015 CAIR values. In addition, the Big Cajun 2 unit was adjusted to account for its Plant-wide Applicability Limit from a recent consent decree (LDEQ, 2013b). The Big Cajun 2 facility emissions, based on PAL, were estimated at 8950 TPY NO_x, 35590 TPY CO, and 287 TPY VOC.

New facilities and expansion projects at existing facilities (e.g., adding new units, expanding capacity, etc.) were included in the 2017 emission inventory. LDEQ (2013a) provided information and estimated emissions for seven new and six expansion projects expected to be on-line by 2017.

The sources were temporally allocated to month, day of week, and hours, according to source category code using default EPA profiles and cross-reference files. All point source emissions were speciated to CB6 compounds using default EPA profiles and cross-reference files. All ARP point sources were treated as elevated sources. The non-ARP points were processed as elevated sources when stack information indicated a sufficient plume rise to warrant elevated treatment. All point source emissions were located in the CAMx grid system according to their reported coordinates.

7.1.1.2 Area Sources

The 2010 base year area source emissions inventory was projected to 2017 using a variety of projection factors based upon the projections of various surrogates, including: population, employment, vehicle miles travelled (VMT), and oil and gas production.

The population-based projection factor is based upon parish-level population estimates for 2010 and 2011 obtained from the US Census Bureau at the parish level (US Census, 2012). The annual population change (increase or decrease) was then applied for a 7-year period to develop the 2017 population based projection factor. Vehicle miles travelled (VMT) projection factors were based upon ENVIRON's development of 2017 on-road emissions and associated VMT activity. A state-wide VMT projection factor of 1.039 was estimated and applied to every parish.

Employment projections were obtained from the Louisiana Workforce Commission (LWC, 2013). The employment projections for 2020, based on a 2010 base year, were detailed by NAICS code and Regional Labor Market Area (RLMA); the specific RLMAs are defined below in Table 7-2. Employment projection factors were developed by linearly interpolating these data to 2017.

Table 7-2. Louisiana Regional Labor Market Areas (RLMAs)

Regional Labor Market Area	Parishes
RLMA 1 - (New Orleans)	Jefferson, Orleans, Plaquemines, St. Bernard, St. Charles, St. James, St. John the Baptist, St. Tammany
RLMA 2 - (Baton Rouge)	Ascension, East Baton Rouge, East Feliciana, Iberville, Livingston, Pointe Coupee, St. Helena, Tangipahoa, Washington, West Baton Rouge, West Feliciana
RLMA 3 - (Houma)	Assumption, Lafourche, Terrebonne
RLMA 4 - (Lafayette)	Acadia, Evangeline, Iberia, Lafayette, St. Landry, St. Martin, St. Mary, Vermilion
RLMA 5 - (Lake Charles)	Allen, Beauregard, Calcasieu, Cameron, Jefferson Davis
RLMA 6 - (Alexandria)	Avoyelles, Catahoula, Concordia, Grant, LaSalle, Rapides, Vernon, Winn
RLMA 7 - (Shreveport)	Bienville, Bossier, Caddo, Claiborne, Desoto, Lincoln, Natchitoches, Red River, Sabine, Webster
RLMA 8 - (Monroe)	Caldwell, East Carroll, Franklin, Jackson, Madison, Morehouse, Ouachita, Richland, Tensas, Union, West Carroll

Oil and gas production projections were obtained from the *2013 Annual Energy Outlook (AEO)* published by the Energy Information Administration (EIA, 2012). The 2010 oil and gas production statistics and 2017 oil and gas production projections for the Onshore (Gulf Coast) and Offshore (Gulf – Shallow and Deep) regions were converted to a BTU basis for purposes of developing the projection factor; the resulting area source oil and gas projection factor was 1.594.

7.1.1.3 On-Road Mobile Sources

Emissions from on-road vehicles are expected to fall significantly by 2017. Louisiana statewide total on-road emissions of TOG, CO, and NO_x are estimated to be 33%, 30%, and 43% lower, respectively, than in 2010. The reductions are due to fleet turnover as new vehicles meet the latest emission standards and older higher-emitting vehicles retire. Fleet turnover more strongly impacts vehicle emissions than the projected increase in both vehicle populations and vehicle-miles traveled (VMT). The effects of the latest emission standards on vehicle emission rates are incorporated into EPA's Motor Vehicle Emission Simulator (MOVES) model. LDEQ provided ENVIRON with estimates of 2017 VMT by functional class and parish. An overall VMT growth of 4% was estimated for all parishes and road types.

Similarly to the approach for the 2010 base year, MOVES version 2010a (with database "movesdb20100830") was run in the mode referred to as "County Domain/Scale in Emission Rate Calculation" for three representative parishes. Each parish-level MOVES run used local input data provided by the LDEQ, including fuel properties, age distribution, and inspection and maintenance programs. MOVES estimated the 2017 emission factors for each pollutant and emission process by source type (vehicle class), fuel type, and representative parish, over a wide range of vehicle speeds and ambient temperature and humidity. The emission factors

were formatted into a lookup table and then subsequently input to the emissions processor CONCEPT MV, a tool that replaces EPS3 for the on-road mobile sector.

First, CONCEPT calculated the emissions inventory by multiplying VMT and population with the appropriate MOVES emission factor for each grid cell and episode hour. The 2010 gridded temperature and humidity data were used in the emission factor lookup tables. A state-wide VMT projection factor of 1.039 was estimated and applied to every parish. CONCEPT then further processed the hourly gridded emissions into chemical species and output the emissions files formatted for CAMx. On-road statewide TOG, CO, and NO_x emissions for 2017 totaled 153, 1,287, and 158 TPD, respectively.

7.1.1.4 Off-Road Sources

Emissions from off-road vehicles are expected to decrease by 2017. Similar to 2010, the EPA's NMIM was used to generate 2017 Louisiana statewide parish-level off-road equipment emissions estimates for the months of September and October. NMIM is a tool for estimating on-road and non-road emissions by county for the entire US to support NEI updates. For this modeling effort NMIM version NMIM20090504 was run with county database NCD20090531 and NONROAD2008a.

The 2017 NMIM emission estimates were processed using EPS3. The off-road emissions were speciated to CB6 compounds, temporally allocated to day of week and hour of day, and spatially allocated using EPA default source category cross-reference files. Louisiana statewide total 2017 non-road emissions for a September weekday for TOG, CO, and NO_x are 36%, 18%, and 37% lower than in 2010, respectively.

NONROAD and NMIM do not include emission estimates for railroad locomotives, aircraft, and marine vessels (excluding maintenance equipment). The 2010 Louisiana emissions for locomotives and aircraft were projected to 2020 using the EPA's Modeling Clearinghouse 2008-based Modeling Platform. Louisiana statewide total of VOC, CO and NO_x for these sources are projected to decrease by 23%, 1%, and 23% respectively.

Emissions from commercial marine vessels servicing the ports along the Mississippi River and the Port of Lake Charles were processed separately from other area sources. The 2010 base year emissions from commercial marine shipping channels and ports were held constant for the 2017 modeling.

7.1.1.5 Port Fourchon

The 2010 Port Fourchon emission estimates were projected to 2017 based on projections for Gulf oil and gas sources. Port Fourchon activity is directly linked to gulf development and production activity so it is reasonable to expect a similar future year pattern. Since the port emissions did not distinguish between fuel types, the base and future year gulf-wide non-platform estimates were used to develop pollutant-specific projection factors (see below for more information). The overall Gulf non-platform projections from 2010 to 2017 were 97% NO_x, 96% CO, and 97% VOC.

7.1.1.6 Haynesville Shale

As stated in Section 5.2.6, a 2009 NETAC study was referenced to estimate 2010 emissions due to Haynesville Shale exploration and production (Grant et al., 2009). A more recent analysis of the Haynesville Shale (Grant et al., 2013) was used to develop projection factors to adjust the 2010 base year exploration and production sources to 2017 estimates. This recent analysis was used for the 2017 projection primarily because it more accurately reflects slower development activity in this area than previously projected. However, the updates provided by Grant et al. (2013) do not extend back to 2010 and so were unavailable for use in developing the original base year inventory. The 2011 and 2017 “median” scenarios from Grant et al. (2013) for both production (well/area sources) and exploration (drills/non-road sources) were used to develop projection factors, which were then applied to the respective 2010 emission estimates. As with the 2010 inventory, the reported Haynesville Shale midstream emissions (e.g., compressors and processing plants) were not included in this projection and were assumed to be incorporated in the point source permitting database. Note that these sources were held constant at their 2010 values (Section 7.1.1.1).

Though there is variation on a source by source basis, the Haynesville Shale projections to 2017 from well production and exploration show an overall decrease in NO_x, CO, and VOC of 81%, 80%, and 62% respectively. The production source estimates increase by 13% to 120% depending on the specific source type. However, exploration source estimates decrease by more than 80%. Exploration sources constitute a higher fraction of emissions than production sources, and so the overall reduction in emission is driven by exploration sources.

Spatial allocation of the 2017 Haynesville Shale emission estimates was the same as the 2010 base year. No additional information on future well locations was available for the Haynesville Shale area.

7.1.2 Gulf Sources

The 2010 base year offshore emissions inventory was projected to 2017 using projection factors based on oil and gas production projections from the *2013 Annual Energy Outlook (AEO)* (EIA, 2012). The 2010 oil and gas production statistics and 2017 oil and gas production projections for the Offshore (Gulf – Shallow and Deep) region were converted to a BTU basis for purposes of developing the projection factors. Three different projection factors were developed: oil only (1.050), natural gas only (0.830), and oil and natural gas combined (1.003). All three factors were applied to platform sources depending upon whether a particular emission source could be assigned specifically to oil or natural gas production. For most non-platform source categories, the combined oil and natural gas projection was applied because the category was not specifically assigned to oil or natural gas production. For four non-platform source categories (i.e., biogenic and geogenic emissions, commercial marine vessels, fishing vessels, and military vessels), the projected 2017 emissions were assumed to be identical to the 2010 base year emissions.

7.1.3 Future Emissions Outside of Louisiana

Anthropogenic emission estimates for states outside of LA, as well as for commercial marine shipping outside the Gulf of Mexico, were developed by Alpine Geophysics. County-level future year estimates for all source categories (including the on-road sector and commercial marine shipping outside of the Gulf of Mexico) were taken from the EPA 2020 modeling inventory used in the EPA's 2012 PM NAAQs modeling analyses. The 2020 inventory is based on projections applied to the 2008 NEIv2 database. This inventory version was obtained from the EPA FTP site (ftp.epa.gov/EmisInventory/2007v5/2020re_v5_07c_inputs.tar) on January 24, 2013.

Documentation on the contents of the inventory can be obtained at ftp.epa.gov/EmisInventory/2007v5/README_pm_naaqs_2007ee_2007re_2020re.txt. Emissions from Canada and Mexico were held constant at their respective base year estimates.

The 2020 inventories were processed using SMOKE3.1 using the ancillary data for spatial, temporal, and speciation distribution supplied with the emissions input files. Alpine generated gridded, speciated, temporally allocated emissions for the 36, 12, and 4 km modeling domains. The 2020 data were used for the 2017 future year modeling without year-to-year adjustment.

7.1.4 2017 Emissions Summary

Parish-level 2017 anthropogenic emissions are reported in Table 7-3. As biogenic and fire emissions are not reported at the county level they are not included in this comparison. Table 7-4 presents the percentage change in emission estimates from 2010 to 2017.

Point source emissions contribute 46% of all anthropogenic NO_x in the 2010 base year inventory. We see a reduction in point source NO_x of 8% by 2017. Points contribute a larger percentage (54%) of total anthropogenic NO_x in 2017 because both on-road and off-road mobile sources have a much larger NO_x reductions throughout the State (43% and 37% respectively).

A few parish-level anomalies in Table 7-4 include: 1) a few very large decreases in off-road emissions due to the reduction in Haynesville Shale drilling; 2) some very large percentage increases in point source emissions attributed to new sources; and 3) large reductions in point source NO_x are due to the CAIR allocations.

Figures 7-1 through 7-3 show examples of the spatial distribution of 2017 total model-ready low-level (gridded – not including elevated point sources) emission of NO_x, CO, and VOC over the 4 km modeling domain.

Table 7-3. Summary of 2017 Louisiana emissions (tons/day) for typical September weekday.

Parish	NOx				CO				VOC	TOG	TOG	VOC
	Area	Off-road	On-road	Points	Area	Off-road	On-road	Points	Area	Off-road	On-road	Points
Acadia	1.15	1.08	3.09	8.10	2.20	5.32	24.22	2.89	4.45	0.66	3.05	1.27
Allen	0.37	0.55	1.23	1.65	1.37	1.50	8.82	2.95	1.86	0.13	1.13	0.19
Ascension	3.24	1.24	3.25	19.76	17.43	8.05	27.43	10.73	24.59	0.53	3.34	8.43
Assumption	0.89	0.31	2.05	3.33	13.27	1.73	19.22	2.52	2.15	0.19	3.86	1.42
Avoyelles	0.85	1.03	1.74	0.38	8.94	3.91	13.22	0.17	3.37	0.39	1.82	0.07
Beauregard	0.63	1.01	1.90	7.51	1.62	5.69	14.84	6.50	2.65	1.01	1.69	2.88
Bienville	0.58	0.76	1.66	5.58	1.22	1.81	10.74	2.92	1.50	0.25	0.98	1.51
Bossier	1.74	2.30	4.61	1.87	9.89	11.35	39.21	1.38	4.06	1.25	4.94	1.41
Caddo	5.25	5.71	8.61	3.68	6.55	47.06	72.29	2.18	15.30	3.66	8.73	3.15
Calcasieu	5.84	4.81	6.25	59.42	12.08	28.12	56.05	48.72	36.48	3.95	5.64	20.41
Caldwell	0.07	0.48	0.91	0.15	0.42	1.24	6.51	0.01	0.89	0.14	0.90	0.01
Cameron	0.33	0.79	0.55	22.05	1.77	6.88	4.09	21.81	1.29	1.83	0.49	2.70
Catahoula	0.23	0.60	0.84	0.00	2.28	2.22	5.69	0.00	1.05	0.27	0.67	0.00
Claiborne	0.24	0.23	1.23	0.70	0.70	2.90	8.02	1.01	1.69	0.55	0.98	0.22
Concordia	0.09	0.73	1.12	0.00	0.40	3.98	8.02	0.00	1.76	0.73	0.94	0.00
De Soto	0.87	5.03	2.62	16.13	2.24	6.49	17.73	8.69	4.49	1.50	1.57	7.44
E Baton Rouge	6.08	4.55	8.93	28.75	5.65	44.48	76.76	31.16	34.37	2.85	9.38	17.83
East Carroll	0.18	0.88	0.68	0.33	2.21	1.45	4.40	0.08	0.61	0.20	0.38	0.04
East Feliciana	0.16	0.21	0.88	0.79	0.58	2.20	6.28	0.25	0.92	0.47	0.87	1.31
Evangeline	0.56	0.62	1.57	3.05	3.41	3.48	11.31	8.89	6.11	0.61	1.42	0.46
Franklin	0.20	0.71	0.85	0.28	0.61	2.33	6.90	0.15	1.31	0.21	1.04	0.04
Grant	0.28	0.64	1.31	0.54	1.03	2.75	9.10	2.43	1.28	0.55	0.95	0.39
Iberia	2.73	1.26	1.25	4.63	21.49	10.11	10.41	4.49	6.55	0.83	1.27	1.96
Iberville	2.39	1.26	1.19	21.31	17.76	3.15	8.73	14.49	18.65	0.33	0.99	6.56
Jackson	0.68	0.12	0.95	4.81	1.12	1.56	6.55	4.66	1.17	0.18	0.85	2.04
Jefferson	7.90	11.79	7.73	7.79	6.51	58.66	76.77	4.91	28.40	4.96	10.73	2.17
Jefferson Davis	0.40	1.17	2.03	2.48	3.66	4.87	14.50	0.62	4.51	0.63	1.39	0.24
Lafayette	3.44	2.52	5.61	4.00	7.97	32.22	52.64	0.51	10.30	3.09	5.86	0.31
Lafourche	12.91	1.10	2.70	5.22	15.25	8.96	24.94	4.47	9.52	1.21	2.75	2.40
La Salle	0.23	0.30	1.06	0.42	0.45	2.13	7.05	0.11	1.47	0.26	0.81	0.04
Lincoln	0.82	0.77	2.64	4.10	2.40	5.39	19.83	1.47	3.13	0.34	1.85	0.87
Livingston	1.04	0.65	3.73	0.18	11.83	6.59	31.20	0.79	5.00	0.92	4.16	0.76
Madison	0.14	1.45	1.71	0.20	1.70	2.49	11.40	0.06	1.18	0.27	0.66	0.12
Morehouse	0.67	1.23	1.65	1.95	4.06	2.79	12.19	0.30	1.72	0.26	1.61	0.06
Natchitoches	1.25	0.77	3.24	6.53	3.41	3.48	21.93	3.81	4.67	0.39	2.00	3.39
Orleans	5.09	8.59	5.81	2.98	4.17	41.97	54.54	3.49	12.73	4.59	5.25	0.69
Ouachita	3.70	2.05	5.27	12.12	10.16	17.87	44.51	9.12	14.84	2.15	5.43	7.21
Plaquemines	0.88	16.81	0.70	20.42	1.44	14.06	5.77	8.95	3.63	3.31	0.98	5.42
Pointe Coup	1.26	1.12	1.03	29.39	21.37	3.79	7.76	102.61	2.72	0.35	0.80	2.10

Parish	NOx				CO				VOC	TOG	TOG	VOC
	Area	Off-road	On-road	Points	Area	Off-road	On-road	Points	Area	Off-road	On-road	Points
Rapides	1.93	2.02	6.39	16.44	7.82	13.81	49.93	9.31	9.84	1.33	5.33	1.86
Red River	0.35	2.72	1.04	0.56	0.76	3.49	7.94	0.42	0.64	0.96	1.27	0.34
Richland	0.51	1.00	1.82	2.00	6.53	2.09	11.84	0.94	2.03	0.17	1.00	0.31
Sabine	0.42	0.95	1.59	0.53	1.12	3.91	10.81	1.28	2.25	0.74	1.32	0.49
St. Bernard	0.80	1.32	0.49	10.52	0.69	7.52	5.20	4.87	1.18	1.48	0.82	3.45
St. Charles	2.21	2.21	1.96	27.21	2.40	6.74	17.03	22.52	15.48	0.80	1.69	12.65
St. Helena	0.11	0.06	0.51	1.11	0.47	0.60	4.01	0.33	1.51	0.06	0.58	0.25
St. James	0.94	0.88	0.80	14.62	1.16	2.12	6.22	6.50	6.30	0.19	0.66	3.91
St. J Baptist	1.12	8.92	2.04	6.56	2.92	5.39	16.56	4.97	5.65	0.96	1.74	4.71
St. Landry	1.27	1.83	3.78	3.81	8.72	7.49	29.07	1.51	5.60	0.87	3.45	2.11
St. Martin	1.56	0.57	2.14	2.72	15.19	5.91	17.05	1.80	4.70	1.21	2.05	1.34
St. Mary	2.58	1.25	1.48	17.99	13.92	8.32	13.30	19.42	10.01	0.81	1.46	3.67
St. Tammany	1.95	2.54	7.87	0.07	17.26	32.31	68.65	0.00	10.15	4.88	9.11	0.05
Tangipahoa	1.47	1.12	5.29	0.02	6.26	12.59	42.16	0.19	6.30	1.80	4.58	0.34
Tensas	0.18	0.73	0.65	0.00	3.61	1.69	3.94	0.00	1.38	0.26	0.32	0.00
Terrebonne	2.25	1.63	3.11	2.93	3.82	22.18	27.97	3.72	4.73	3.31	4.22	1.82
Union	0.76	0.25	1.44	0.55	3.29	3.24	9.51	0.32	2.49	0.33	1.18	0.45
Vermilion	1.34	1.10	1.93	9.40	11.69	10.05	15.14	3.52	3.96	1.72	2.15	1.46
Vernon	0.19	0.79	2.24	0.14	1.10	4.24	16.63	0.08	1.94	0.67	2.22	0.12
Washington	0.86	0.27	1.18	11.11	2.91	2.58	9.89	21.17	3.59	0.20	1.56	4.78
Webster	1.03	0.64	2.23	3.16	2.30	3.58	16.85	2.67	4.40	0.33	1.80	1.79
W Baton Rouge	1.33	1.60	1.21	2.17	6.38	6.71	8.89	6.28	4.41	0.78	0.81	1.65
West Carroll	0.37	0.38	0.49	2.38	7.20	1.14	3.76	0.23	1.19	0.09	0.54	0.06
West Feliciana	0.33	0.18	0.54	1.34	1.12	1.16	3.71	1.29	0.87	0.15	0.47	0.33
Winn	0.45	0.14	1.49	0.88	0.75	1.55	9.49	3.60	2.52	0.15	0.83	2.25
Total	101.65	122.32	157.94	450.81	360.00	585.42	1287.16	437.26	395.52	70.23	153.32	157.72

Table 7-4. Percent change in Louisiana emissions from 2010 to 2017. Empty entries indicate no emissions were reported or estimated in 2010 and 2017.

Parish	NOx				CO				VOC	TOG	TOG	VOC
	Area	Off-road	On-road	Points	Area	Off-road	On-road	Points	Area	Off-road	On-road	Points
Acadia	6.3	-30.7	-42.2	0.2	3.6	-15.3	-30.9	-8.4	4.4	-31.4	-32.3	-4.4
Allen	16.5	-32.9	-43.0	0.0	3.1	-15.3	-32.4	0.0	9.6	-31.5	-32.9	0.0
Ascension	7.9	-33.8	-40.6	0.0	10.7	-19.6	-25.8	0.0	11.5	-36.7	-29.5	0.0
Assumption	2.3	-31.0	-27.9	0.0	-0.3	-18.3	-26.0	0.0	-0.2	-38.7	-28.6	0.0
Avoyelles	3.8	-29.9	-41.4	0.0	-0.1	-17.6	-31.2	0.0	2.3	-35.0	-32.4	0.0
Beauregard	24.5	-32.1	-44.3	0.0	14.0	-9.9	-31.1	0.0	10.6	-28.4	-34.2	0.0
Bienville	0.2	-71.0	-46.6	0.0	0.4	-42.8	-33.3	0.0	3.8	-55.3	-36.5	0.0
Bossier	4.4	-58.0	-41.8	0.0	11.9	-22.2	-30.8	0.0	10.6	-39.7	-32.8	0.0
Caddo	0.8	-56.6	-42.7	-9.3	1.3	-18.2	-31.3	-8.9	9.9	-37.5	-34.0	-1.1
Calcasieu	25.2	-26.9	-43.7	8.8	11.2	-12.1	-28.3	24.3	16.0	-29.8	-31.8	7.4
Caldwell	-0.8	-32.8	-42.3	0.0	-4.5	-13.3	-31.7	0.0	-4.4	-32.4	-32.7	0.0
Cameron	7.7	-4.6	-45.5	488.3	0.1	-17.0	-32.0	1155.7	3.4	-38.6	-32.2	28.4
Catahoula	4.7	-29.8	-44.3		-0.3	-18.1	-32.7		2.2	-36.1	-33.1	
Claiborne	-3.8	-28.8	-44.6	0.0	-7.1	-9.1	-33.0	0.0	0.6	-27.3	-34.7	0.0
Concordia	5.0	-29.7	-44.0		2.4	-13.9	-32.7		6.1	-32.5	-33.8	
De Soto	21.9	-80.0	-46.2	-16.2	12.2	-66.9	-32.7	1.4	7.3	-67.7	-35.4	0.1
E Baton Rouge	6.2	-29.6	-44.0	-1.6	5.7	-14.4	-31.9	1.4	4.2	-31.4	-39.0	0.0
East Carroll	0.3	-27.0	-47.0	0.0	-0.3	-23.4	-34.7	0.0	-0.7	-36.0	-37.6	0.0
East Feliciana	2.7	-30.4	-42.0	0.0	-3.4	-9.2	-31.3	0.0	0.9	-27.4	-32.1	0.0
Evangeline	3.4	-29.5	-43.1	8.5	-0.1	-13.5	-32.0	-4.6	5.2	-30.1	-33.1	-11.4
Franklin	3.4	-30.6	-41.6	0.0	1.3	-18.2	-30.6	0.0	5.6	-33.3	-31.0	0.0
Grant	7.4	-31.4	-45.8	0.0	-0.7	-10.2	-30.7	0.0	4.4	-31.0	-33.3	0.0
Iberia	3.9	-30.8	-42.9	0.0	0.5	-16.8	-33.1	0.0	3.2	-36.0	-33.8	0.0
Iberville	3.6	-27.6	-42.7	-0.6	-0.3	-26.0	-26.8	-0.9	3.0	-41.6	-30.2	0.5
Jackson	4.3	-53.7	-43.2	0.0	3.1	-18.5	-32.0	0.0	0.9	-25.9	-32.5	0.0
Jefferson	5.2	-11.4	-38.3	-76.1	5.1	-13.6	-26.2	32.1	1.5	-32.7	-30.6	23.8
Jefferson Davis	5.3	-31.1	-45.5	0.0	0.7	-11.7	-32.4	0.0	5.1	-30.0	-34.8	0.0
Lafayette	6.6	-34.5	-42.1	-31.6	2.3	-12.1	-27.8	7.8	6.1	-29.8	-31.3	-10.7
Lafourche	2.0	-27.6	-42.6	0.0	1.6	-19.2	-28.7	0.0	8.3	-40.5	-31.5	0.0
La Salle	10.9	-36.5	-44.5	0.0	7.1	-16.0	-32.8	0.0	24.8	-35.5	-32.7	0.0
Lincoln	-1.1	-35.5	-45.6	0.0	0.9	-14.2	-32.5	0.0	2.1	-28.5	-35.7	0.0
Livingston	9.5	-38.3	-38.6	0.0	12.6	-15.7	-24.4	0.0	9.1	-33.2	-27.8	0.0
Madison	0.5	-29.2	-48.4	0.0	-0.2	-17.2	-33.3	0.0	2.1	-35.8	-40.0	0.0
Morehouse	2.0	-29.8	-42.7	0.0	-0.9	-20.3	-32.1	0.0	-0.5	-34.7	-33.4	0.0
Natchitoches	-1.8	-35.5	-45.8	0.0	-1.5	-21.2	-32.5	0.0	1.1	-37.2	-35.3	0.0
Orleans	9.0	-16.2	-45.1	-66.3	8.9	-13.9	-29.5	-28.2	21.2	-32.7	-34.6	-23.8
Ouachita	4.7	-33.5	-42.1	4.0	4.6	-14.0	-31.3	-0.2	6.2	-30.6	-33.0	-0.8
Plaquemines	6.0	-1.0	-34.3	0.0	5.9	-19.0	-28.0	0.0	7.1	-36.4	-28.2	0.0

Parish	NOx				CO				VOC	TOG	TOG	VOC
	Area	Off-road	On-road	Points	Area	Off-road	On-road	Points	Area	Off-road	On-road	Points
Pointe Coup	0.9	-30.0	-45.0	-34.7	-0.1	-15.7	-30.1	-2.3	0.2	-35.1	-33.0	0.4
Rapides	10.2	-31.7	-44.2	9.6	4.8	-13.2	-31.9	0.4	6.3	-31.3	-34.0	16.4
Red River	25.4	-80.0	-38.8	0.0	11.7	-66.8	-29.8	0.0	21.8	-64.7	-30.4	0.0
Richland	2.9	-30.7	-46.7	0.0	0.7	-18.3	-32.7	0.0	7.3	-36.2	-35.7	0.0
Sabine	0.2	-31.4	-43.7	0.0	4.2	-18.1	-32.5	0.0	4.0	-38.8	-32.8	0.0
St. Bernard	10.2	-9.0	-33.2	0.0	12.0	-21.4	-24.3	0.0	26.0	-40.5	-28.1	0.0
St. Charles	5.0	-19.5	-44.2	-25.4	3.8	-20.9	-28.2	0.3	3.5	-40.9	-32.1	-0.4
St. Helena	-0.7	-46.3	-42.9	0.0	-8.7	-17.3	-31.2	0.0	1.6	-23.8	-33.1	0.0
St. James	4.6	-24.9	-44.3	0.0	-0.6	-22.8	-28.6	0.0	1.6	-39.3	-32.2	0.0
St. J Baptist	4.3	-3.5	-43.9	7.9	1.3	-17.9	-30.9	10.7	1.4	-32.9	-33.9	11.3
St. Landry	4.4	-30.5	-43.0	0.0	0.9	-14.8	-31.2	0.0	2.8	-31.8	-33.0	0.0
St. Martin	4.5	-28.7	-42.3	0.0	2.4	-12.0	-30.7	0.0	4.8	-32.6	-32.0	0.0
St. Mary	4.7	-27.7	-43.0	-15.4	0.7	-19.5	-28.6	0.1	4.7	-39.7	-31.7	0.0
St. Tammany	7.2	-34.1	-40.7	0.0	9.2	-11.1	-30.1	0.0	5.3	-31.5	-32.4	0.0
Tangipahoa	7.2	-33.6	-43.8	0.0	8.1	-10.9	-31.1	0.0	5.8	-29.5	-33.7	0.0
Tensas	-1.9	-29.5	-47.7		-1.0	-21.4	-35.1		0.8	-36.9	-38.8	
Terrebonne	17.3	-29.0	-37.7	1.6	7.6	-14.6	-29.9	0.4	7.2	-35.4	-30.4	0.1
Union	3.6	-41.5	-44.2	0.0	0.9	-16.4	-32.8	0.0	-0.3	-30.4	-33.6	0.0
Vermilion	2.8	-25.0	-40.6	0.0	0.5	-13.6	-30.9	0.0	2.9	-33.1	-31.6	0.0
Vernon	2.4	-34.7	-42.6	0.0	-2.0	-10.5	-32.1	0.0	2.0	-28.3	-32.3	0.0
Washington	5.1	-40.0	-40.5	0.0	0.9	-19.4	-30.5	0.0	3.6	-34.4	-31.7	0.0
Webster	-1.2	-57.2	-44.5	0.0	0.5	-24.5	-32.3	0.0	2.5	-42.3	-34.5	0.0
W Baton Rouge	5.3	-15.0	-45.8	0.0	1.9	-12.8	-29.4	0.0	8.0	-29.0	-33.5	0.0
West Carroll	0.7	-30.9	-43.6	0.0	-0.1	-19.7	-31.3	0.0	0.9	-31.0	-31.4	0.0
West Feliciana	4.2	-39.7	-43.3	0.0	-3.4	-23.1	-32.1	0.0	0.4	-37.9	-33.0	0.0
Winn	10.0	-48.3	-47.0	0.0	-0.4	-18.7	-34.7	0.0	4.1	-28.9	-37.2	0.0
Total	6.0	-37.3	-42.8	-7.9	3.2	-17.6	-30.3	6.6	6.4	-36.0	-33.0	1.7

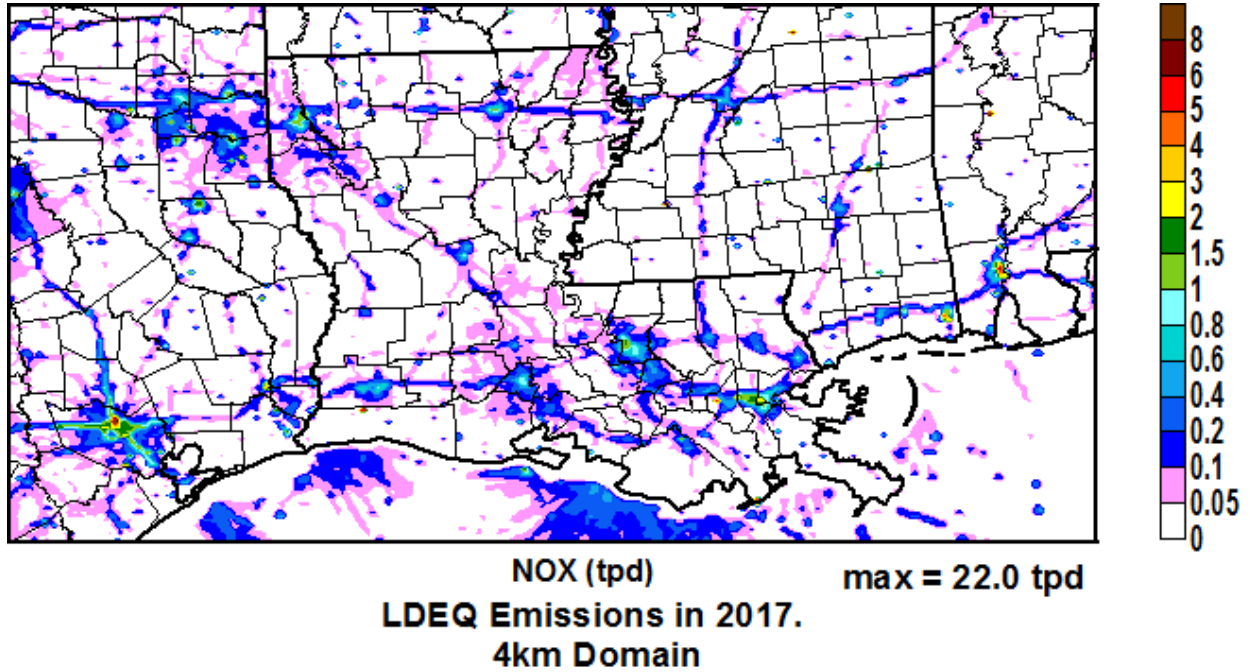


Figure 7-1. Spatial distribution of 2017 total (anthropogenic and biogenic) surface NOx emissions (tons/day).

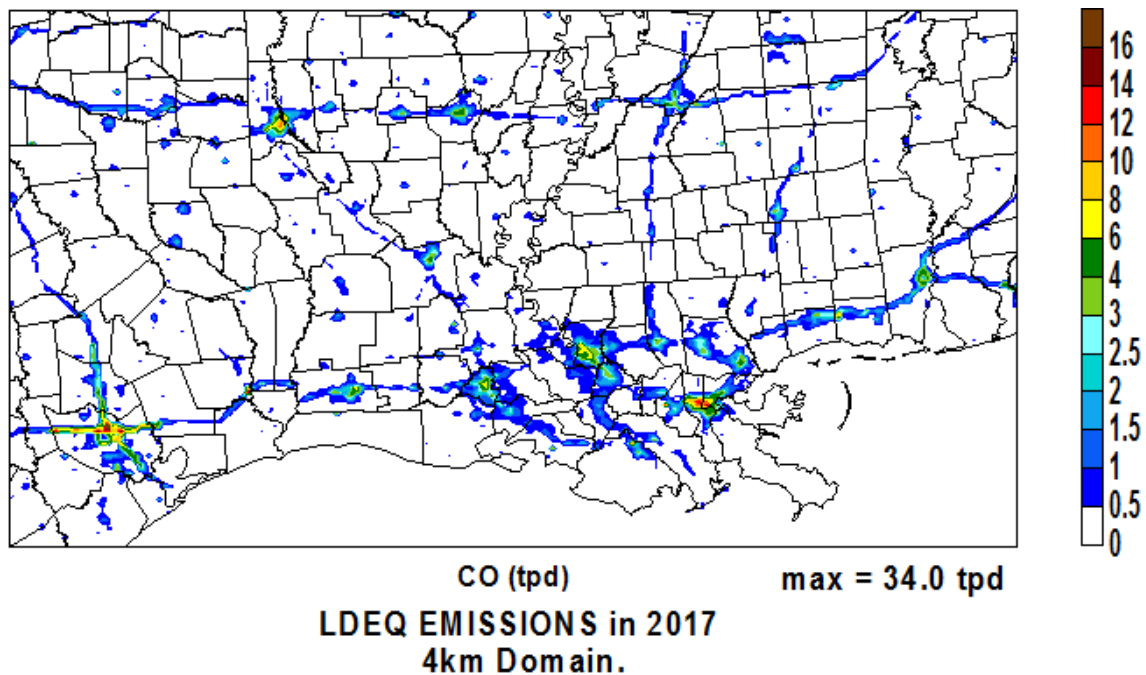


Figure 7-2. Spatial distribution of 2017 total surface CO emissions (tons/day).

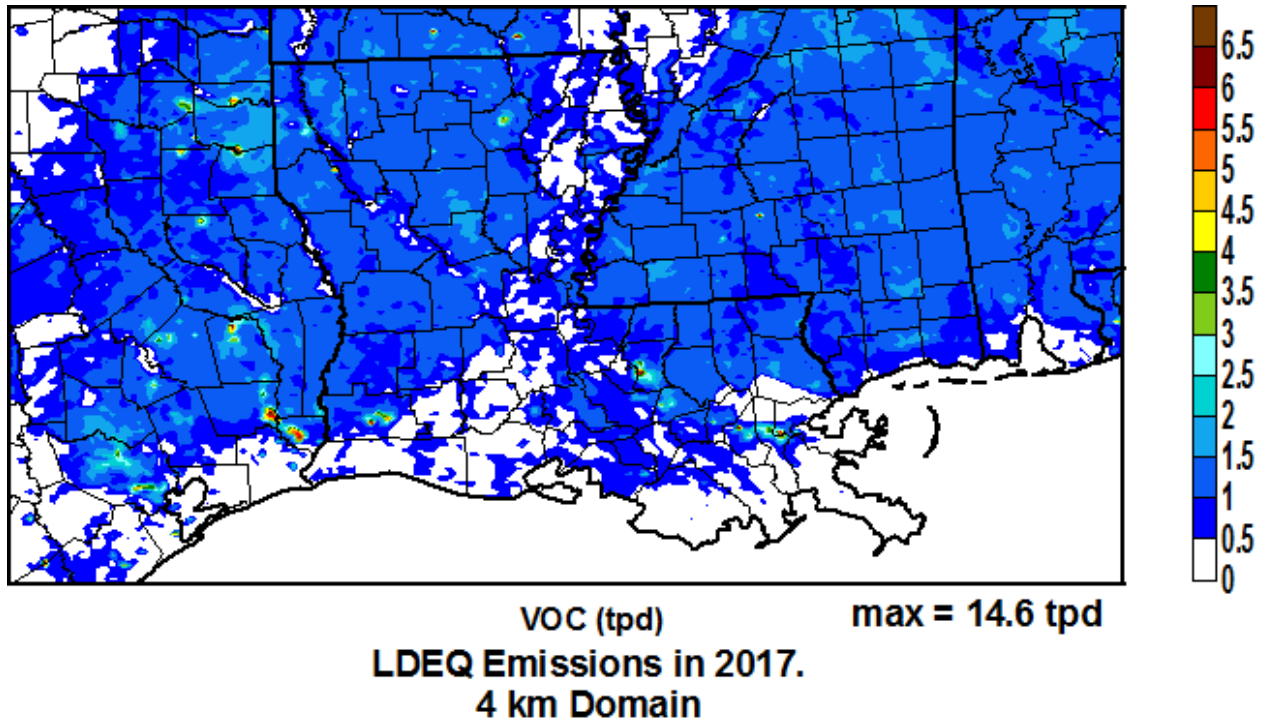


Figure 7-3. Spatial distribution of 2017 total (anthropogenic and biogenic) surface VOC emissions (tons/day).

7.2 Ozone Modeling and Attainment Test

CAMx was run using the final 2010 base year configuration (Run 17) described in Section 6.6, except that the 2010 “actual” emissions were exchanged with alternative inputs to yield two new runs: (1) “typical” 2010 base year emissions that reflect annual-averaged CAMD/ARP emissions (instead of day-specific); and (2) projected 2017 future year emissions as described above. Additionally, the 2017 emission estimates were converted to CB05 speciation to be consistent with the final base year configuration. Predicted daily maximum 8-hour ozone ($DM8O_3$) concentrations throughout the September-October modeling period were extracted from the CAMx results for both 2010 typical and 2017 future simulations. These modeled concentrations were supplied to the EPA Modeled Attainment Test Software (MATS) tool, which tabulated the change in $DM8O_3$ at each site, determined site-specific relative response factors (RRF) averaged over all high ozone days, and applied the RRFs to current design values (DV) to estimate the 2017 DV at each site. The steps in this procedure are outlined below.

7.2.1 Summary of the MATS Technique

EPA guidance (EPA, 2007) outlines the approach used by MATS to project base year DVs to a target attainment year. It begins by calculating the base year average DV for each monitoring site; in this case our base year is 2010. As exemplified below, the base year average DV is defined as a 3-year average of annual DVs centered on the base year, or more precisely, a weighted 5-year average of the annual 4th highest $DM8O_3$ at each site.

2010 DV: average of annual 4th highest DM8O₃ between 2008-2010

2011 DV: average of annual 4th highest DM8O₃ between 2009-2011

2012 DV: average of annual 4th highest MD8O₃ between 2010-2012

$$\begin{aligned}
 \text{2010 average DV} &= (2010 \text{ DV} + 2011 \text{ DV} + 2012 \text{ DV})/3 \\
 &= 1 \times (2008 \text{ 4th highest DM8O}_3)/9 + \\
 &\quad 2 \times (2009 \text{ 4th highest DM8O}_3)/9 + \\
 &\quad 3 \times (2010 \text{ 4th highest DM8O}_3)/9 + \\
 &\quad 2 \times (2011 \text{ 4th highest DM8O}_3)/9 + \\
 &\quad 1 \times (2012 \text{ 4th highest DM8O}_3)/9
 \end{aligned}$$

MATS is distributed with official DV data through 2008. We imported official DV data for the years 2009-2012 for the whole US.

Model results are then used to calculate 2010-2017 RRFs for each site. Hence, model results are not used in an absolute sense to determine attainment in 2017, but rather used in an episode-averaged relative sense to scale the observation-based average DV. For a given site, the RRF is defined as the ratio of the episode-mean 2017 DM8O₃ to the episode-mean 2010 DM8O₃. Episode means are determined over the days when the model predicts 2010 DM8O₃ above a minimum concentration threshold, preferably the current ozone standard (75 ppb in this case). The RRF is then applied directly to the 2010-2012 average DV to project a 2017 DV for each site.

MATS provides options to define how the DM8O₃ is chosen from the model grid output to represent simulated ozone at each monitor location. The user selects whether to search a 1x1, 3x3, 5x5, or 7x7 array of grid cells centered on the monitor. EPA guidance states that a larger array of grid cells should be used with finer resolution grids; 1x1 for 36-km grids, 3x3 for 12-km grids, or 7x7 for 4-km grids. Further, MATS allows the user to choose whether an average over the grid array is extracted, or the maximum value among all cells in the array is extracted. In our case using 4 km grids over Louisiana, we set the search array to 7x7 and selected the maximum predicted value in that array.

MATS then determines the number of days over the modeling period when simulated base year DM8O₃ is above a minimum concentration threshold from which to calculate the episode-average RRF at each site. We configured MATS to first find the number of days above 75 ppb, and MATS checks that at least 10 days meet this criterion. If 10 days are not found for a given site, then MATS lowers the critical value by 1 ppb successively until 10 days are found. We set the lower limit to 60 ppb; if 10 days are still not found at the lower limit, then MATS reduces the number of days successively until a minimum of 5 days are found. If at 60 ppb the minimum 5 days are not found, then an RRF is not calculated for that site. If at some point the minimum criteria for DM8O₃ concentration and number of days are met, then the RRF calculation proceeds.

Finally, MATS performs an “unmonitored area analysis” by extrapolating site-specific future year DVs to the entire modeling grid using modeled spatial gradients to help form the resulting DV surface. These fields are then plotted to indicate any areas expected to exceed the ozone standard in unmonitored areas of the State.

7.2.2 2017 DV Projection Results

Table 7-5 presents the 2010-2012 average DVs at each active monitoring site in Louisiana and the corresponding future year DVs projected by MATS. Missing values in the table indicate insufficient observation data from which to calculate a valid base year DV. All sites are projected to be below the 75 ppb ozone NAAQS in 2017.

Figure 7-4 displays the unmonitored area calculation for the portion of the 4 km grid covering the State of Louisiana. All projected DVs are below the 75 ppb NAAQS throughout the State. Areas contoured in white show locations where DVs are either estimated to be below 40 ppb, or are missing because they could not be extrapolated by MATS.

7.2.3 2017 Sensitivity Tests

Two emission sensitivity tests were run for the 2017 future year to quantify effects from simple across-the-board reductions in Louisiana anthropogenic NO_x and VOC emissions. An arbitrary reduction of 30% was applied first to NO_x (no change to VOC) and then to VOC (no change to NO_x). All 2017 model-ready anthropogenic emissions in grid cells covering the State were scaled downward, including all low-level (gridded) sources and point sources. Emissions outside the State were not affected, nor were biogenic and FINN fire sources throughout the 4 km grid.

Table 7-6 lists the site-specific 2017 DV projections for the NO_x test and Figure 7-5 displays the corresponding State-wide unmonitored analysis projected from the 2010-2012 average DV. No areas of the State exceed the 75 ppb ozone NAAQS.

Table 7-7 lists the site-specific 2017 DV projections for the VOC test and Figure 7-6 displays the corresponding unmonitored analysis. Again, no area exceed the 75 ppb standard. However, ozone reductions are not as large as the NO_x test by typically 2-3 ppb. This suggests that while both NO_x and VOC reductions are effective in reducing ozone throughout the State, ozone tends to be somewhat more responsive to NO_x reductions. This effect could be more quantitatively analyzed through the use of CAMx probing tools, such as the Ozone Source Apportionment Tool (OSAT) or the Decoupled Direct Method (DDM) of sensitivity analysis.

Table 7-5. Base year DM8O₃ design values at each active monitoring site in Louisiana for the 2010-2012 average and the 2017 projection. Values exceeding the current 75 ppb ozone NAAQS are highlighted in red. Blank entries indicate insufficient data from which to calculate the base year DV.

AIRS Site ID	Parish	Base Year	Future Year
		2010-12 DV	2017 DV
220050004	Ascension	76	70
220110002	Beauregard		
220150008	Bossier	77	68
220170001	Caddo	74	70
220190002	Calcasieu	74	68
220190008	Calcasieu	66	61
220190009	Calcasieu	73	67
220330003	E Baton Rouge	79	73
220330009	E Baton Rouge	75	69
220330013	E Baton Rouge	72	66
220331001	E Baton Rouge	72	66
220430001	Grant		
220470007	Iberville	71	64
220470009	Iberville	74	67
220470012	Iberville	75	68
220511001	Jefferson	75	68
220550005	Lafayette		
220550007	Lafayette	72	64
220570004	Lafourche	72	66
220630002	Livingston	75	69
220710012	Orleans	70	63
220730004	Ouachita	64	58
220770001	Pointe Coupee	75	70
220870002	St. Bernard		
220870009	St. Bernard	69	63
220890003	St. Charles	71	65
220930002	St. James	68	64
220950002	St. J. Baptist	74	69
221010003	St. Mary		
221030002	St. Tammany	74	65
221210001	W Baton Rouge	71	65

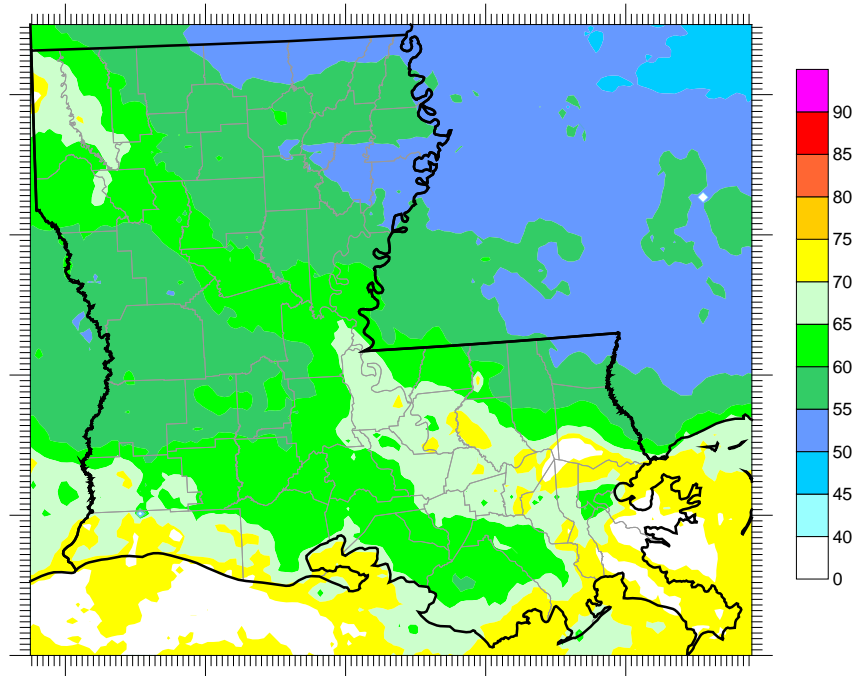


Figure 7-4. MATS-derived 2017 DM8O₃ design value projection from the 2010-2012 average design value for un-monitored areas in Louisiana.

Table 7-6. Base year DM8O₃ design values at each active monitoring site in Louisiana for the 2010-2012 average and the 2017 projection in response to an additional 30% across-the-board anthropogenic NO_x reduction in Louisiana. Values exceeding the current 75 ppb ozone NAAQS are highlighted in red. Blank entries indicate insufficient data from which to calculate the base year DV.

AIRS Site ID	Parish	Base Year	Future Year
		2010-12 DV	2017 DV
220050004	Ascension	76	66
220110002	Beauregard		
220150008	Bossier	77	65
220170001	Caddo	74	69
220190002	Calcasieu	74	66
220190008	Calcasieu	66	60
220190009	Calcasieu	73	64
220330003	E Baton Rouge	79	70
220330009	E Baton Rouge	75	66
220330013	E Baton Rouge	72	63
220331001	E Baton Rouge	72	63
220430001	Grant		
220470007	Iberville	71	60
220470009	Iberville	74	63
220470012	Iberville	75	65
220511001	Jefferson	75	64
220550005	Lafayette		
220550007	Lafayette	72	61
220570004	Lafourche	72	62
220630002	Livingston	75	65
220710012	Orleans	70	60
220730004	Ouachita	64	54
220770001	Pointe Coupee	75	66
220870002	St. Bernard		
220870009	St. Bernard	69	60
220890003	St. Charles	71	62
220930002	St. James	68	60
220950002	St. J. Baptist	74	65
221010003	St. Mary		
221030002	St. Tammany	74	61
221210001	W Baton Rouge	71	63

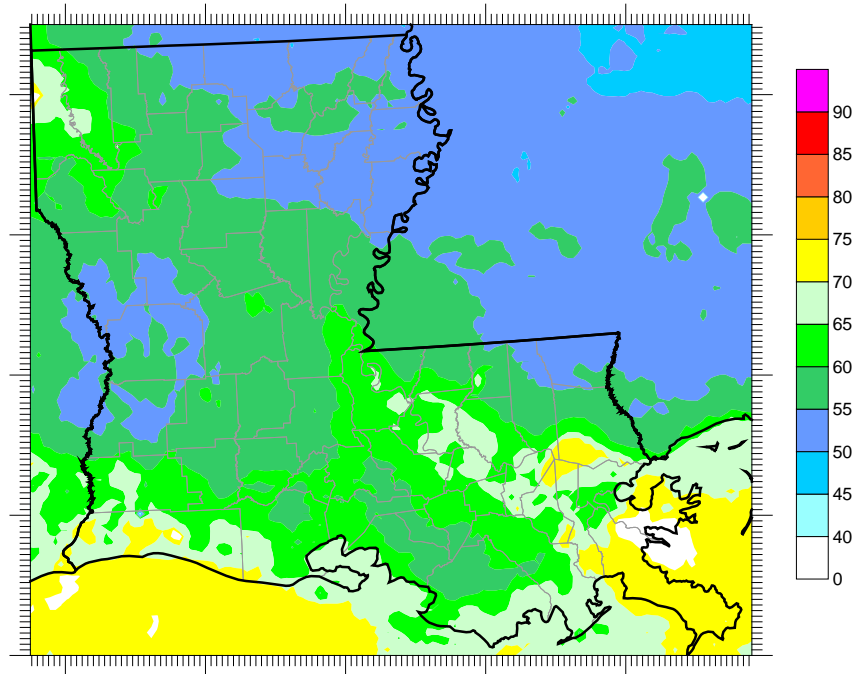


Figure 7-5. MATS-derived 2017 DM8O₃ design value projection from the 2010-2012 average design value for un-monitored areas in Louisiana; response to an additional 30% across-the-board anthropogenic NO_x reduction in Louisiana.

Table 7-7. Base year DM8O₃ design values at each active monitoring site in Louisiana for the 2010-2012 average and the 2017 projection in response to an additional 30% across-the-board anthropogenic VOC reduction in Louisiana. Values exceeding the current 75 ppb ozone NAAQS are highlighted in red. Blank entries indicate insufficient data from which to calculate the base year DV.

AIRS Site ID	Parish	Base Year	Future Year
		2010-12 DV	2017 DV
220050004	Ascension	76	69
220110002	Beauregard		
220150008	Bossier	77	68
220170001	Caddo	74	70
220190002	Calcasieu	74	67
220190008	Calcasieu	66	61
220190009	Calcasieu	73	67
220330003	E Baton Rouge	79	72
220330009	E Baton Rouge	75	68
220330013	E Baton Rouge	72	66
220331001	E Baton Rouge	72	66
220430001	Grant		
220470007	Iberville	71	63
220470009	Iberville	74	66
220470012	Iberville	75	68
220511001	Jefferson	75	67
220550005	Lafayette		
220550007	Lafayette	72	64
220570004	Lafourche	72	65
220630002	Livingston	75	68
220710012	Orleans	70	62
220730004	Ouachita	64	57
220770001	Pointe Coupee	75	69
220870002	St. Bernard		
220870009	St. Bernard	69	62
220890003	St. Charles	71	64
220930002	St. James	68	63
220950002	St. J. Baptist	74	68
221010003	St. Mary		
221030002	St. Tammany	74	64
221210001	W Baton Rouge	71	65

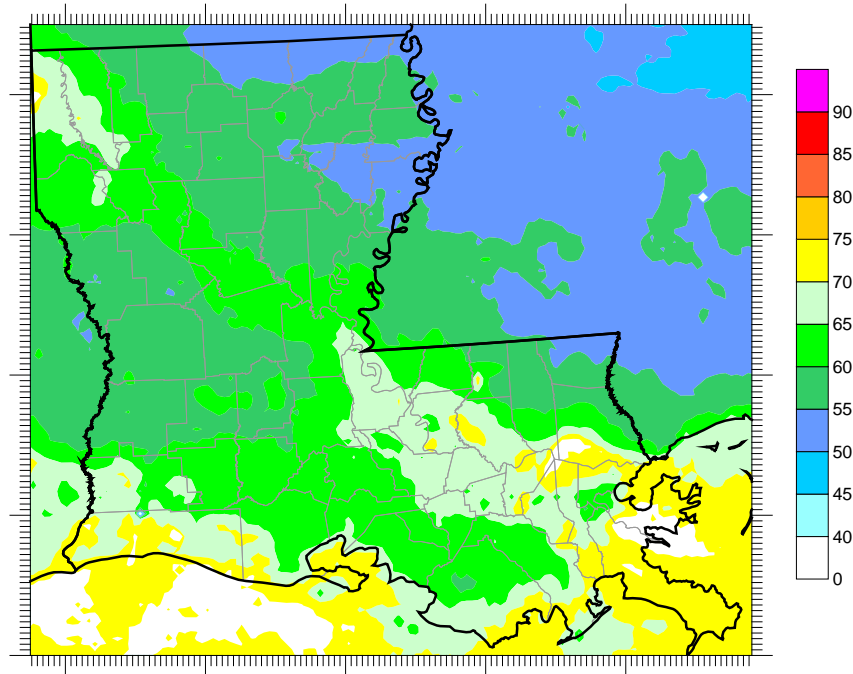


Figure 7-6. MATS-derived 2017 DM8O₃ design value projection from the 2010-2012 average design value for un-monitored areas in Louisiana; response to an additional 30% across-the-board anthropogenic VOC reduction in Louisiana.

8.0 REFERENCES

- Alpine Geophysics. 2012. "Application and Evaluation of WRF For August through October 2010." Prepared for the Louisiana Foundation for Excellence in Science, Technology and Education, Baton Rouge, LA. Prepared by Alpine Geophysics, LLC, Arvada, Colorado (August 10, 2012).
- Alvarado, M.J., et al. 2010. Nitrogen oxides and PAN in plumes from boreal fires during ARCTAS-B and their impact on ozone: an integrated analysis of aircraft and satellite observations. *Atmospheric Chemistry and Physics*, **10**, 9739-9760, doi:10.5194/acp-10-9739-2010.
- BOEM. 2010. Year 2008 Gulfwide Emission Inventory Study. US Department of the Interior; Bureau of Ocean Energy Management, Regulation and Enforcement; Gulf of Mexico OCS Region (December 2010). <http://www.boem.gov/Environmental-Stewardship/Environmental-Studies/Gulf-of-Mexico-Region/Air-Quality/2008-Gulfwide-Emission-Inventory.aspx>.
- BOEM. 2012. 2008 and 2010 Lease-Specific Oil and Gas Production Quantities. US Department of the Interior; Bureau of Ocean Energy Management, Regulation and Enforcement; Gulf of Mexico OCS Region (May 8).
- EIA. 2012. 2013 Annual Energy Outlook – Early Release. US Department of Energy, Energy Information Administration (December 5).
- ENVIRON. 2010. Updated commercial marine shipping emissions for the State of Louisiana. Memorandum to LDEQ, Contract CFMS #670411, Work Order #6 (September 17, 2010).
- ENVIRON. 2011. User's Guide, Comprehensive Air quality Model with extensions (CAMx), Version 5.40. ENVIRON International Corporation, Novato, CA (September 2011) www.camx.com.
- ENVIRON. 2012. Improved Biogenic Emission Inventories across the West – Final Report (March 2012). http://www.wrapair2.org/pdf/WGA_BiogEmisInv_FinalReport_March20_2012.pdf.
- ENVIRON and ERG. 2009. Technical Support Document: Modeling to Support the Baton Rouge, Louisiana 8-Hour Ozone State Implementation Plan. Prepared for the Louisiana Department of Environmental Quality, Office of Environmental Assessment, Air Quality Assessment Division, Baton Rouge, Louisiana. Prepared by ENVIRON International Corporation, Novato, CA, and Eastern Research Group, Inc., Sacramento, CA (November 20, 2009).
- ENVIRON and ERG. 2012. Modeling Protocol: Photochemical Modeling for the Louisiana 8-Hour Ozone State Implementation Plan. Prepared for the Louisiana Department of Environmental Quality, Office of Environmental Services, Air Permits Division, Baton Rouge, LA. Prepared by ENVIRON International Corporation, Novato, CA and Eastern Research Group, Inc., Rancho Cordova, CA (March 8, 2012).

- EPA. 2007. Guidance on the Use of Models and Other Analyses for Demonstrating Attainment of Air Quality Goals for Ozone, PM_{2.5} and Regional Haze. US Environmental Protection Agency, Research Triangle Park, NC. EPA-454/B-07-002. April.
(<http://www.epa.gov/ttn/scram/guidance/guide/final-03-pm-rh-guidance.pdf>).
- EPA. 2010. Technical Guidance on the Use of MOVES2010 for Emission Inventory Preparation in State Implementation Plans and Transportation Conformity. Transportation and Regional Programs Division, Office of Transportation and Air Quality, United States Environmental Protection Agency. Document number EPA-420-B-10-023 (April).
- EPA. 2012. Louisiana 2010 Acid Rain Program (ARP) Unit Emissions. US Environmental Protection Agency, Air Markets Program Data: : <http://ampd.epa.gov/ampd/>.
- Federal Register. 2011. Approval and Promulgation of Implementation Plans and Designation of Areas for Air Quality Planning; Louisiana; Baton Rouge Area: Redesignation to Attainment for the 1997 8-Hour Ozone Standard. Environmental Protection Agency, 40 CFR Parts 52 and 81 [EPA-R06-OAR-2010-0776; FRL-9498-2], Vol. 76, No. 230 (Wednesday, November 30, 2011).
- Grant, J., Parker, L., Bar-Ilan, A., Kembell-Cook, S., Yarwood, G. 2009. Development of Emissions Inventories for Natural Gas Exploration and Production Activity in the Haynesville Shale. Prepared by ENVIRON International Corporation, Novato, CA for the East Texas Council of Governments (August 2009).
- Guenther, A., Karl, T., Harley, P., Wiedinmyer, C., Palmer, P. I., Geron, C. 2006. Estimates of global terrestrial isoprene emissions using MEGAN (Model of Emissions of Gases and Aerosols from Nature). *Atmospheric Chemistry and Physics*, **6**, 3181-3210.
- Latifovic, R., Z.-L. Zhu, J. Cihlar and C. Giri. 2002. Land cover of North America 2000. Natural Resources Canada, Canada Centre for Remote Sensing, US Geological Service EROS Data Center.
- LDEQ. 2012a. Louisiana 2010 Point Source Inventory. Provided by John Babin, Louisiana Department of Environmental Quality (March 13).
- LDEQ. 2012b. Louisiana 2009 Attainment Demonstration Area Source Emission Estimates - NO_x, CO, and VOC. Provided by Tim Bergeron, Louisiana Department of Environmental Quality (March 12).
- LDEQ. 2013a. Louisiana Future New Facilities and Expansion Projects. Provided by Michael Vince and Bryan Johnston, Louisiana Department of Environmental Quality (March 4).
- LDEQ. 2013b. Big Cajun 2 Plantwide Applicability Limitations. Provided by Bryan Johnston, Louisiana Department of Environmental Quality (March 18).
- LWC. 2013. Industry Employment Projections (2010 – 2020). Louisiana Workforce Commission: http://www.laworks.net/LaborMarketInfo/LMI_OcclIndustryProj.asp?years=20102020.
- O'Brien, J. 1970. "A Note on the Vertical Structure of the Eddy Exchange Coefficient in the Planetary Boundary Layer." *Journal of the Atmospheric Sciences*, **27**, 1213-1215.

Parikh, R., Grant, J., Bhat, S., Bar-Ilan, A., Kemball-Cook, S., Yarwood, G. 2013. Emissions From Natural Gas Exploration And Production Activity In The Haynesville Shale. Prepared by ENVIRON International Corporation, Novato, CA for the East Texas Council of Governments (January 2013).

Sakulyanontvittaya, T., Duhi, T., Wiedinmyer, C., Helmig, D., Matsunaga, S., Potosnak, M., Milford, J., Guenther, A. 2008. Monoterpene and sesquiterpene emission estimates for the United States. *Environmental Science & Technology*, **42** (5), 1623-1629.

Starcrest Consulting Group, LLC, and LSU Center for Energy Studies. 2010. Port Fourchon Ozone Day Port-Related Emissions Inventory Study (July 2010).

US Census. 2012. Annual Estimates of the Resident Population for Parishes: April 1, 2010 to July 1, 2011. US Census Bureau (April: CO-EST 2011-01-22): <http://www.census.gov/popest/data/parishes/totals/2011/CO-EST2011-01.html>.